Inherited retinal diseases

Studies on genotype, phenotype and treatment

Sanne K. Verbakel

Inherited retinal diseases

Studies on genotype, phenotype and treatment

Sanne K. Verbakel

Inherited retinal diseases
Studies on genotype, phenotype and treatment

Proefschrift

ter verkrijging van de graad van doctor
aan de Radboud Universiteit Nijmegen
op gezag van de rector magnificus prof. dr. J.H.J.M. van Krieken,
volgens besluit van het college van decanen
in het openbaar te verdedigen op
vrijdag 13 december om 12:30 uur precies

door

Sanne Kirsten Verbakel

geboren op 7 maart 1991
te Tilburg

Promotoren

Prof. dr. B. Jeroen Klevering

Prof. dr. Carel B. Hoyng

Copromotoren

Dr. Ramon A.C. van Huet

Dr. Susanne Roosing

Manuscriptcommissie

Prof. dr. Baziel G.M. van Engelen

Prof. dr. Isabelle Audo (Institut de la Vision, Frankrijk)

Dr. Mary J. van Schooneveld (Bartiméus Zeist en Amsterdam UMC)

Table of Contents

List of abbreviations

AAVs	Adeno-associated viruses
adRP	Autosomal dominant retinitis pigmentosa
AOFD	Adult-onset foveomacular dystrophy
AONs	Antisense oligonucleotides
AOSLO	Adaptive optics scanning laser ophthalmoscopy
AOVMD	Adult-onset vitelliform macular dystrophy
arCRD	Autosomal recessive cone-rod dystrophy
arMD	Autosomal recessive macular dystrophy
arRP	Autosomal recessive retinitis pigmentosa
BBS	Bardet-Biedl syndrome
BCAMD	Benign concentric annular macular dystrophy
BDNF	Brain-derived neurotrophic factor
bFGF	Basic fibroblast growth factor
CAI	Carbonic anhydrase inhibitors
CD	Cone dystrophy
cDNA	Complementary deoxyribonucleic acid
cGMP	Cyclic guanosine monophosphate
CME	Cystoid macular edema
CNTF	Ciliary neurotrophic factor
CNV	Copy number variation
CRD	Cone-rod dystrophy
cSLO	Confocal scanning laser ophthalmoscopy
CSNB	Congenital stationary night blindness
DCX	Doublecortin
DNA	Deoxyribonucleic acid
EOG	Electrooculography
ERG	Electroretinography
ESCs	Embryotic stem cells
ESE	Exonic splice enhancer
ESS	Exonic splice silencer
FAF	Fundus autofluorescence
ffERG	Full-field electroretinography
FZT	Foveal zone thickness
GDNF	Glial cell–derived neurotrophic factor
GTP	Guanosine triphosphate
IFT	Interflagellar transport
iPSCs	Induced pluripotent stem cells
IRD	Inherited retinal disease

JBTS	Joubert syndrome
LCA	Leber congenital amaurosis
logMAR	Logarithm of the minimal angle of resolution
MD	Macular dystrophy
mfERG	Multifocal electroretinography
MKS	Meckel syndrome
NGF	Nerve growth factor
NIR-FAF	Near-infrared fundusautofluorescence
NPHP	Nephronophthisis
OCT	Optical coherence tomography
OCTA	Optical coherence angiography
PPCs	Photoreceptor progenitor cells
PPR	Pericentral pigmentary retinopathy
PPRCA	Pigmented paravenous retinochoroidal atrophy
RCD	Rod-cone dystrophy
rdCVF	Rod-derived cone viability factor
RP	Retinitis pigmentosa
RPC	Retinal progenitor cells
RPE	Retinal pigment epithelium
SD-OCT	Spectral-domain optical coherence tomography
siRNA	Small interfering ribonucleic acid
SW-FAF	Short-wavelength fundus autofluorescence
TES	Transcorneal electrical stimulation
VA	Visual acuity
VEGF	Vascular endothelial growth factor
WES	Whole exome sequencing
WGS	Whole genome sequencing
XLRS	X-linked juvenile retinoschisis

Gene names are not included in this list. Information regarding gene names is available on the Retinal Information Network (RetNet, available at https://sph.uth.edu/retnet/).

General introduction

Approximately three-quarters of what we learn during our life is information that is presented visually.[1] This information, however, comes at a price. During evolution our visual system has evolved to a state in which approximately 50% of our cerebral cortex is in one way or another devoted to processing visual information. These areas and pathways rank amongst the highest energy-consuming systems within the brain.[2-4] This large percentage is remarkable considering the fact that the highly complex human eye has an average diameter of only 23-24 mm and weighing no more than 7 grams.[5-7] Needless to say that the visual system as a whole is highly complex. This complexity, unfortunately, means that disturbances in the visual system are relatively common and can occur at many levels and in many degrees of severity. Naturally, the scope of the ophthalmologist mainly lies at the level of ocular tissues, although there are many ophthalmic diseases that have to do with surrounding structures and/or functionally connected tissues including the eyelids, the orbit and the brain. In this thesis, however, we will focus on ocular disorders and more specifically the subgroup of hereditary eye diseases that affect the retina. In order to understand the etiology and consequences of these rare diseases that have great impact on the affected individuals, we first have to understand the anatomy and function of the retina.

Anatomy of the human eye

(Adapted from http://lilfreds.net/netter-eye-anatomy/)
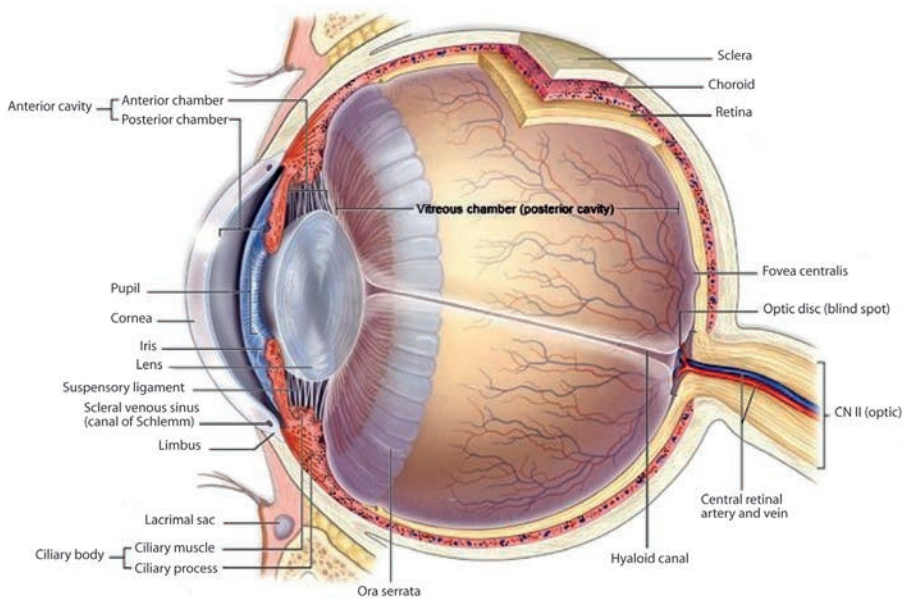
Figure 1. Histologic and schematic overview of the retinal layers. Most of the highly organized layers contain either cell bodies or synapses. For example, the outer nuclear layer contains the cell bodies of the photoreceptor cells, the inner nuclear layer of the bipolar, amacrine, horizontal and Müller cells, and the ganglion cell layer of the ganglion cells. The two plexiform layers, the inner and outer plexiform layer, are formed by the synapses between these cells. Other layers represent the inner and outer segments of the photoreceptors, the transition between the inner segment and the cell body of the photoreceptor (i.e., the external limiting membrane), the axons of the ganglion cells (i.e., the nerve fiber layer), and the boundary between the retina and the vitreous formed by the endfeet of Müller cells (i.e., the inner limiting membrane).[8]
(Adapted from: © 2018 American Academy of Ophthalmology (http://www.aao.org) and Hartong DT et al.,2006[9])
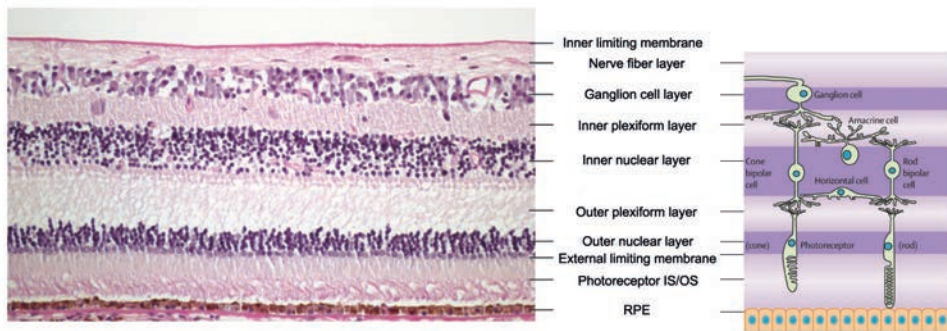
The retina

The retina is an incredibly thin and fragile layer—comparable to a wet paper towel—that covers the inside lining of the eye. It contains photosensitive cells, the photoreceptors at its base, which convert the light signal into an electrical impulse that is transmitted and modulated through the retinal neural circuit, and finally transmitted through the optic nerve fibers to the brain where the visual information is interpreted and an image of the outside world is created. Despite a thickness of no more than 100–250 micrometers, the retina can be further subdivided into 10 separate layers: the neuroretina, consisting of the nine inner layers of the retina, and the retinal pigment epithelium (RPE) (see Figure 1).

The neurosensory retina consists of nine transparent layers of neurons and supporting cells that are connected via synapses (Figure 1).[10] Incoming light crosses eight layers of the neuroretina before it reaches the outermost layer, the outer segments of the photoreceptors. Here, the process takes place by which light is converted into an electrical impulse (i.e., the phototransduction cascade; explained in more detail in Chapter 2.1). Subsequently, the impulse is transmitted via the bipolar and ganglion cells to the visual cortex.

The retina contains approximately 126 million photoreceptors: 120 million rods and 6 million cones, which are unevenly distributes across the retina.[11] Rods are far more numerous in the periphery of the retina, whereas the fovea at the absolute center of the retina only contains cones (Figure 2). The cone to rod ratio at the macula, the center 15-20 degrees of visual field, is higher than in the periphery. Rod photoreceptors are approximately 100 times more sensitive to light compared to cone photoreceptors, and are therefore responsible for vision in dim light conditions and allow the detection of motion.[12] In contrast, cones are important for discriminating colors and facilitate high spatial resolution.[12] Color discrimination is possible
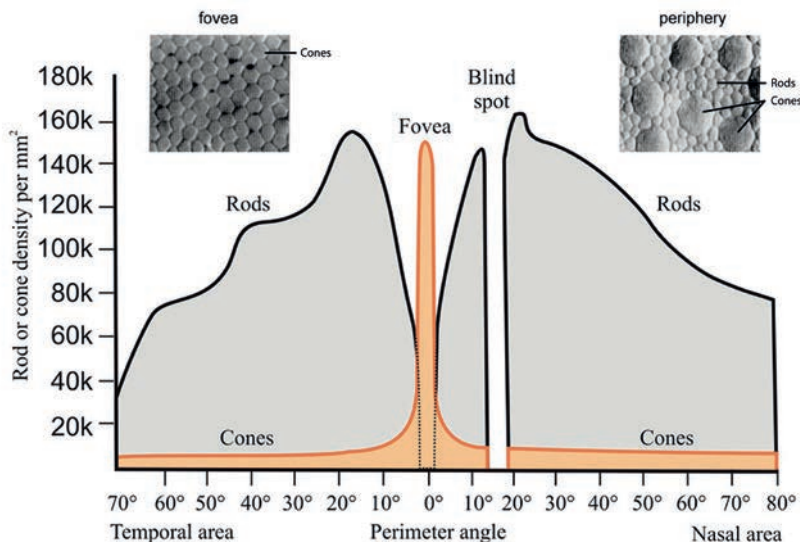
Figure 2. Distribution of photoreceptors across the retina. (Adapted from http://www.rags-int-inc.com/phototechstuff/cameraeye/)

because of the presence of three types of cones: the long (red), medium (green) and short-wavelength (blue) sensitive cones. Combining this knowledge about the distribution and function of the photoreceptor cells, we can explain why patients with peripheral retinal abnormalities complain about night blindness, and macular disease results in loss of color vision and visual acuity.

The RPE is the outermost layer of the retina and forms a functional unit with the overlying photoreceptor cells. This pigment epithelium consists of a monolayer of cuboidal, pigmented cells that are laterally connected via cellular junctions (i.e., tight, adherens and gap junctions).[13,14] These cellular junctions form the outer blood-retina barrier, as they prevent the transport of molecules and ions from the choroid to the subretinal space, which extends from the external limiting membrane to the apical surface of the RPE cells. In addition to forming the blood-retina barrier, the RPE has several functions, which are crucial to normal photoreceptor functioning.[14] For example, the RPE plays a vital role in the visual cycle by regenerating 11-*cis*-retinal from all-*trans*-retinal produced in the phototransduction cascade in the photoreceptors (see Chapter 2.1). Other functions involve the phagocytosis of photoreceptor outer segments, ion and fluid transport control between the subretinal space and the underlying permeable choriocapillaris, the supply of nutrients to the photoreceptors, and the secretion of several (growth) factors and signaling molecules. The pigment, particularly melanin in the melanosomes, has a function in warmth regulation and the absorption of scattered light and therefore helps to improve vision and reduce oxidative stress.[15] It has been estimated that over the course of a 70-year lifetime, an RPE cell phagocytizes 3 billion photoreceptor outer segment discs.[16] However, not all outer segment material is phagocytized completely and residual molecules accumulate in lysosomes

under the collective term lipofuscin, the principal fluorophore in RPE cells. Since RPE cells are post-mitotic, the amount of lipofuscin steadily accumulates with age.

Inherited retinal diseases

Hereditary retinal diseases encompass a group of disorders caused by a large range of genetic alterations. All types of retinal dystrophy are rare, yet together they account for more than 3 million affected individuals worldwide, and cause severe visual loss and blindness. This group is highly heterogeneous and shows large variation in, for example, age of onset (ranging from birth to adulthood) and type of complaints (predominantly problems with central vision or visual field defects). However, what all of them have in common is the immense impact on a person's daily life and his or her family. A retinal disease usually affects young individuals with normal vision who start to notice a gradual decline in visual function. What may start with a problem such as reading the blackboard, cycling in the dark or losing the cursor of the computer, can eventually progress to complete loss of central vision and/or peripheral vision and even blindness. Needless to say this has great social consequences as it will affect patients' daily living, study or career choice, or their desire to have children. To date, only a specific subgroup of patients is eligible for genetic treatment, namely patients with a mutation in the *RPE65* gene.[17] All that remains for the other patients is the hope for new treatment options to arrive soon enough to be able to halt or even reverse the detrimental progression of their retinal disorder.

Classification of inherited retinal diseases
Historically, retinal dystrophies have been categorized into stationary and progressive retinal disease. These can be further subdivided based on the mode of inheritance or the primary site of retinal dysfunction. Progressive dystrophies may remain confined to the posterior pole (e.g., macular dystrophy; MD), or become more generalized. Generalized dystrophies may be classified based on the photoreceptor system that is primarily affected: cone dystrophy (CD), cone-rod dystrophy (CRD; i.e. cone degeneration that precedes rod degeneration) and rod-cone dystrophy (RCD; i.e. rod degeneration preceding cone degeneration). However, these subdivisions are not always straightforward and can be subject of heated discussions (see Chapter 2.1).

Clinical examination in inherited retinal diseases

Retinal imaging

Since retinal dystrophies display large clinical variability, patients may present with various complaints and the fundus abnormalities that ophthalmologists encounter may also vary greatly (Figure 3). It is challenging to accurately describe the abnormalities observed during the ophthalmic examination. Imaging, more specific retinal imaging, offers a more objective approach, and may therefore be of great value in the follow-up of patients with a retinal disease. An additional advantage is that these images can be used for educational purposes to train ophthalmologists to recognize rare hereditary diseases. Currently, many of the ophthalmic imaging methods are quick, without evident discomfort to the patient. Here, two types of imaging modalities are explained in more detail.

Optical coherence tomography

Optical coherence tomography (OCT) is a noninvasive imaging modality that provides high resolution cross-sectional images of the retinal architecture. This technique measures differences in light reflectance from different layers of the retina, comparable to the ultrasonic sound waves used by ultrasound devices. Multiple one-dimensional depth scans can be combined to form two or even three-dimensional images of the retina, which can show subtle structural abnormalities (Figure 4). In patients with a retinal dystrophy, these images can be valuable in, for example, the identification and follow-up of cystoid macular edema, macular thickness, and the identification of affected retinal layers that are disorganized or even no longer visible, such as the photoreceptor layer and RPE.

Fundus autofluorescence imaging

Conventional (short-wavelength) fundus autofluorescence (FAF) enables evaluation of the RPE function in that it reflects the amount of lipofuscin (a waste product) in the RPE cell. It may show a decline in retinal health not yet visible with conventional examination of the fundus. Besides short-wavelength FAF imaging there is also near-infrared autofluorescence, which, as the name already implies, uses a much longer wavelength. Near-infrared FAF is much less frequently used, but gains in popularity. It displays the autofluorescence signal that originates from melanin in the RPE and, to a lesser extent, choroidal melanin or related fluorophores.[18]

Altered FAF levels may be found in a high variety of retinal disorders. High FAF levels may be indicative of increased or disrupted phagocytosis of photoreceptor outer segments, where low- or absent levels of FAF depict loss of RPE cells or blockage of the autofluorescence signal, as is observed at blood vessels or with bone spicules (Figure 5).[19] In inherited retinal diseases, FAF imaging can provide important additional information for the differential diagnosis, for example in macular dystrophies by visualization of hyperautofluorescent flecks in early stage Stargardt disease that are not yet visible with ophthalmoscopy.[20] FAF can also be used to delineate areas with RPE atrophy and may therefore play a role in monitoring disease progression over time,
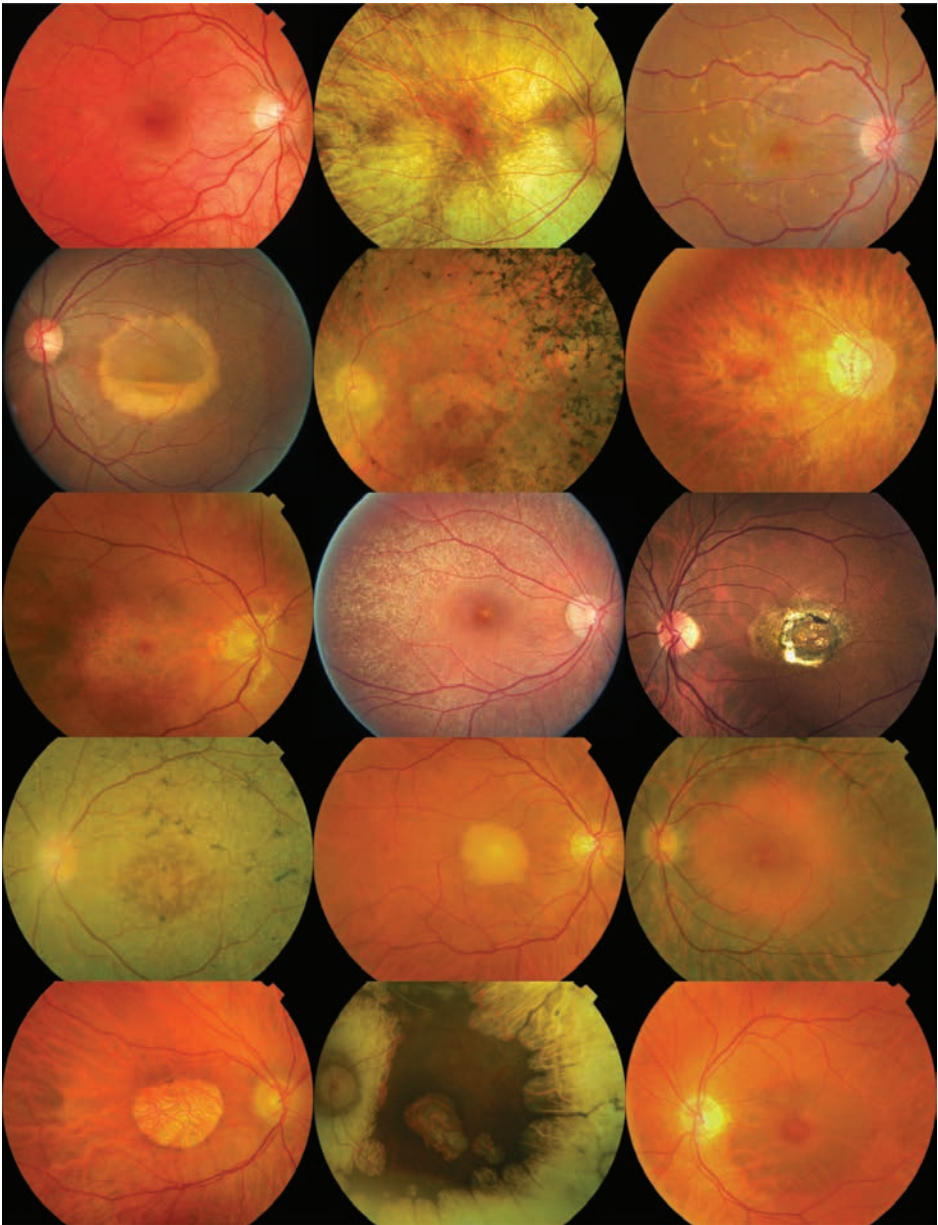
Figure 3. Multiple fundus photographs of inherited retinal diseases that show the great diversity of this group of disorders. The top left image is a fundus photograph of a healthy right eye.

possibly as a clinical endpoint in therapeutic trials.[21] Figure 5 provides an impression of the wide range of abnormalities that may be observed using short-wavelength FAF.
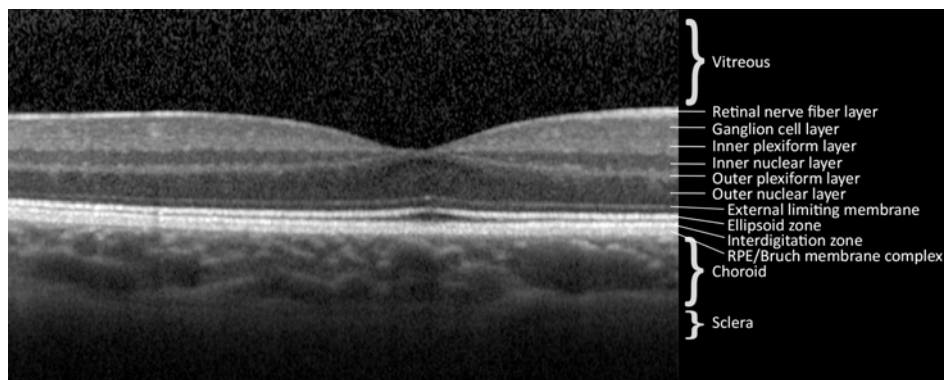
Figure 4. Optical coherence tomography image of a healthy person showing the layers of the retina at the fovea.

Functional assessment

More than 5,000 years ago, the Egyptians tested the visual acuity by testing someone's ability to distinguish the double star of the Big Dipper in the constellation Ursa Major (Figure 6).[22,23] The second star from the end of the handle of the Big Dipper is an optical double star. Nowadays, visual acuity is still an important parameter, also tested during daytime under standardized conditions with the use of the well-known letter chart. The visual acuity is measured each visit, but additional functional tests may be indicated based on the patient's complaints and fundus abnormalities. Here, two additional tests, perimetry and electrophysiological examination are further explained.

Perimetry

For the general public, visual acuity is synonymous with eye function. Visual acuity, however, is a function of the macula (not considering the ocular media and optic nerve) and does not relate to the peripheral visual field. This is a gross underestimation of the importance of the peripheral visual field. In tunnel vision, the visual field is almost completely lost with exception of a central island of 5-10 degrees. This occurs in end stage glaucoma and RP and these patients may still have a visual acuity of 20/20. Nevertheless, these patients with 20/20 visio encounter significantly more problems in daily life than patients with a very low visual acuity but with intact peripheral vision, like in end stage age-related macular degeneration. It is for good reason that patients with a visual field of 20 degrees or less in the better eye are considered legally blind. In patients with inherited retinal disease where large areas of the retina can be affected—resulting in central and/or peripheral field loss—visual field testing or perimetry provides a map of the residual visual field and successive testing provides reliable information on the progression of visual field loss.

Two types of perimetry can be distinguished: static perimetry, kinetic perimetry. Static perimetry measures the sensitivity of specific points in the visual field by determining the minimum brightness required for detection of the light stimulus by the patient. This test is generally
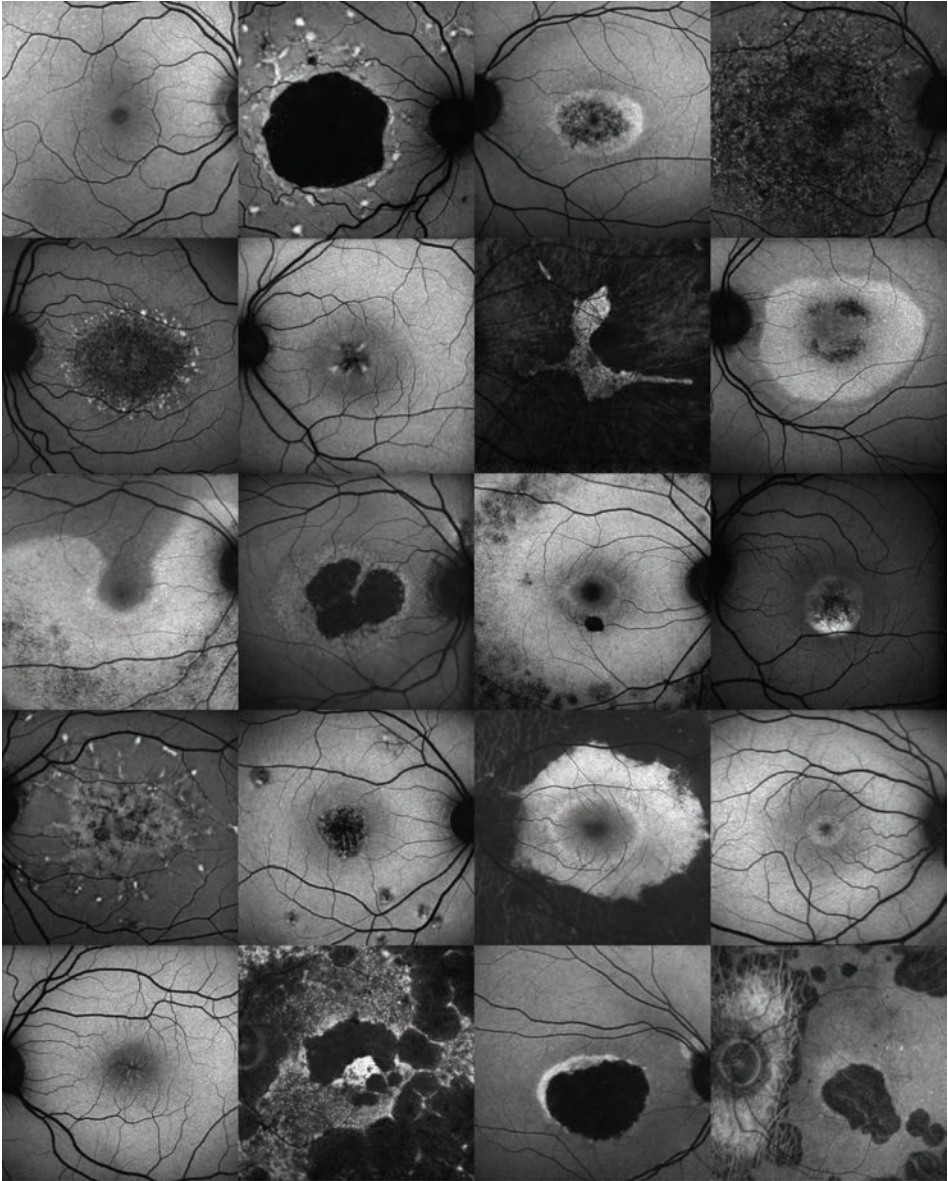
Figure 5. Multiple FAF images that illustrate the wide range of possible hyper-and hypoautofluorescent abnormalities. The top left image is an image of a healthy right eye.

restricted to the central 10, 24 or 30 degrees of the visual field, and is therefore important to detect visual field defects in glaucoma but also for central field defects in inherited retinal disease such as macular dystrophies or the remaining central island in more generalized disorders. However, full-field automated perimetry is also an option. Kinetic perimetry is
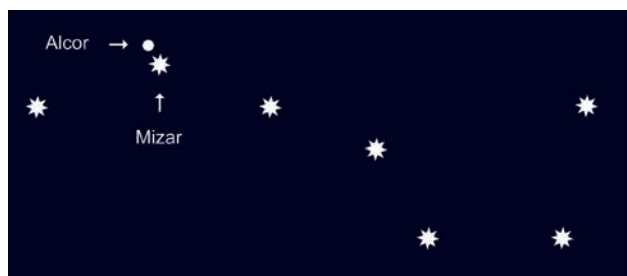
Figure 6. Mizar and Alcor, the double star of the Big Dipper.
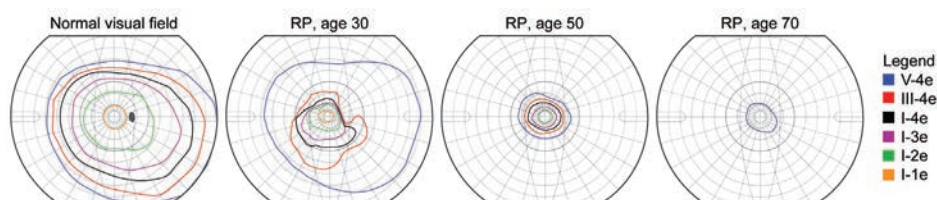
Figure 7. Illustration of the visual field loss as detected by Goldmann kinetic perimetry. Over an interval of 40 years, the visual field loss of the right eye of a patient with RP gradually progresses to blindness.

particularly used to assess the peripheral visual field in patients with a generalized retinal dystrophy (Figure 7). Kinetic perimetry, such as the ubiquitous Goldmann perimeter, uses light stimuli of descending intensity and size that are projected from the periphery to the center. The moment of detection is noted for each stimulus intensity leading to different isopters (i.e. stimuli with different brightness and size). On the downside, this manual technique is difficult to standardize and highly dependent on the experience of the perimetrist. Recently, semi-automated kinetic perimetry devices have been introduced that provide more precise control of the stimulus motion and seem promising successors, which is necessary since the Goldmann perimeter is no longer produced as of 2007.[24] Finally, microperimetry (also known as fundus-perimetry) is a relatively novel technique to assess the sensitivity threshold of multiple predefined points within the central 45 degrees of the retina.[25] This technique uses precise eye tracking throughout the examination, and enables direct structure-function correlations by providing an annotated en face image of the posterior pole.

Electrophysiological examination
The clinical classification of retinal disease is based on the affected photoreceptor type (rods and/or cones) and the order in which they become affected. The visual symptoms as reported by the patients often provides clues as to which photoreceptor system is primarily affected. For instance, night blindness versus photophobia and/or visual acuity loss in respectively rod versus cone function loss. However, this may not always be as straightforward, for example in young patients or patients were several symptoms present more or less simultaneously. Also, loss of visual acuity is more apparent than night blindness, especially in a well-lit urban environment.

Dark-adapted 0.01 ERG
(rod response)

Dark-adapted 3.0 ERG
(combined rod-cone response)

Dark-adapted 10.0 ERG

peak time
(t)

a

b

a

b

100 µV
20 ms

t

t

Dark-adapted 3.0
oscillatory potentials

Light-adapted 3.0 ERG
(cone response)

Light-adapted 3.0 flicker

b

a

t

30 µV
10 ms

100 µV
20 ms
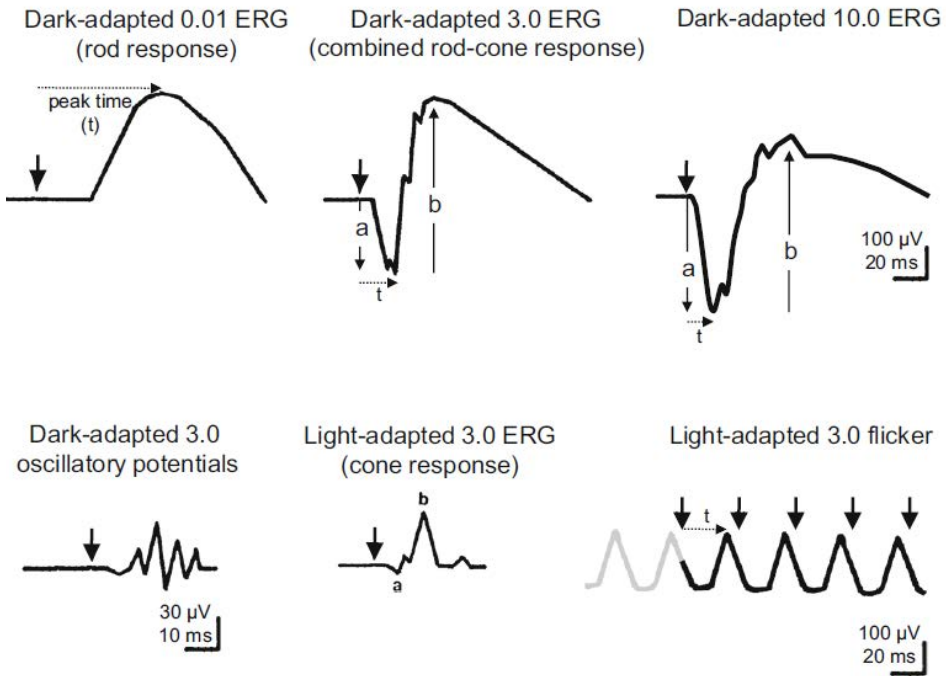
Figure 8. Diagram of the six basic ERGs defined by the ISCEV Standard. These waveforms are exemplary only and are not intended to indicate minimum, maximum or typical values. Bold arrowheads indicate the stimulus flash, solid arrows illustrate a-wave and b-wave amplitudes, and dotted arrows exemplify how to measure time-to-peak (t, implicit time or peak time) (Source: McCulloch D.L. et al. 2015[26])

Finally, rod involvement in patients with abnormalities that seem to be restricted to the macular area, might be underestimated. The electroretinogram (ERG) objectively records the rod and cone responses to specific stimuli allowing for precise analysis and follow-up of photoreceptor dysfunction.

The full-field ERG is a recording of the mass electrical response of the retina after light flash stimulation and provides objective data on retinal function that can help to provide an adequate diagnosis, assess the disease severity, and monitor disease progression. Historically, the ERG has often been used to exclude retinal disease in individuals with a positive family history, because ERG abnormalities precede symptomatic disease. To date, however, molecular testing has largely taken over this role.

Full-field ERG measurements are performed under standardized conditions with varying light and stimulus intensities, which enables a distinction between first-order neuron function (a-wave from the photoreceptors and OFF-bipolar cells) and second-order neuron function (b-wave from Müller cells and ON-bipolar cells). [26] The examination is divided into scotopic (i.e., dark-adapted) and photopic (i.e., light adapted) measurements that differentiate between rod and cone photoreceptor responses.26 The scotopic ERG is typically performed after at least 20 minutes of dark adaptation when a weak stimulus (i.e., a stimulus with an intensity below the

sensitivity threshold of cones) is presented to elicit a rod response (Figure 8). By using a brighter flash, both rod and cone photoreceptors are stimulated. Isolated cone responses can be elicited with the light-adapted 30 Hz flicker ERG, this high frequency exceeds the regenerative capacity of the rod and thus only measures the cone system. Four of the six basic ERG measurements are performed under scotopic conditions. The remaining two are performed under photopic conditions, which causes the rods to be bleached out.

The full-field ERG provides information on the rod and cone systems and can differentiate between, for example, a cone-rod pattern (i.e., the cone pathway is more severely affected than the rod pathway, as in CRD). Conversely, in RP, the ERG will typically demonstrate a rod-cone pattern. In advanced disease, both rod and cone responses can be severely reduced or even non-recordable, which impedes the differentiation between CRD and RP. For this reason, it is important to always consider the course of the disease in its entirety and not focus solely on present findings.

The full-field ERG may also show highly specific patterns associated with certain disorders. For example, an electronegative ffERG, caused by a reduced b-wave with preservation of the a-wave, is typically for pathologic processes in the inner retina such as X-linked retinoschisis (XLRS) and congenital stationary night blindness.[27] Patients with the enhanced S-cone syndrome (Goldmann-Favre) are born with an overabundance of blue cones, a reduced number of red and green cones, and few, if any, functional rods. In this case, the ERG shows supernormal short-wavelength cone responses.[28]

In contrast to the panretinal response of the full-field ERG, multifocal electroretinography allows detection of localized electrical activity in the macula and thus isolates macular function.[29] In this manner, a precise overview of the macular function is provided, and can identify localized retinal damage, which is often invisible on full-field ERG.

Electro-oculography (EOG) is a technique that provides information on the function of the outer retina and RPE by measuring the standing potential of the eye (i.e., the difference in electrical potential between the front and back of the eye), and its change after dark and light adaptation.[30] The difference in electrical potential between scotopic and photopic conditions is displayed as the ratio between the light peak and the dark trough (i.e., the light peak-to-dark trough ratio, formerly known as Arden ratio). EOG abnormalities are generally proportional to the severity of rod-mediated ERG abnormalities. An exception is Best disease, in which the full-field ERG usually remains normal but the EOG is abnormal. In these patients, the EOG may differentiate between Best disease and other types of vitelliform macular dystrophy.[30]

Genetic testing in inherited retinal diseases

DNA is the blue print of every complex living organism (at least on earth..). DNA provides the information for building proteins, which are large, complex molecules that play many critical roles in the body. Proteins are required for the structure, function, and regulation of the body's

tissues and organs. The unique code of human DNA is composed of 6 billion building blocks, called nucleotides that are divided over two complementary strands.[34] Each nucleotide is composed of a sugar molecule, a phosphate molecule and comprises one of the four bases: a purine base such as guanine (G) and adenine (A) or a pyrimidine base such as cytosine (C) and thymine (T). Nucleotides present themselves in base pairs linked by hydrogen bonds: guanine in one strand always pairs with cytosine in the other strand, and adenine always pairs with thymine. However, from these 3 billion base pairs merely 3% account for one of the 20,000 protein-coding genes. Excluding the parts of the gene that are not used to encode protein (i.e., the introns), only 1% of the DNA consists of protein-coding regions (i.e., the exons).[35] The exact function of the remaining base pairs, previously referred to as 'junk-DNA', remains to be discovered, but it is hypothesized that the vast majority is involved in the regulation of gene expression or maintaining the DNA structure.[36] Surprisingly, the amount of bases is seemingly not correlated with a species complexity, unless we completely misunderstand the physical and mental capacity of a crop like wheat that contains more than 15 million bases accounting for more than 108,000 genes.[37]

The discovery of the DNA

In 1869, the Swiss chemist Friedrich Miescher first described the presence of nuclein (later changed to deoxyribonucleic acid; DNA) inside the nuclei of human white blood cells.[31] However, more than 80 years passed before James Watson and Francis Crick discovered the double-helical structure of the DNA molecule in 1953.[32] Since then, significant progress in understanding the genetic structure has been made, such as mapping of the nucleotide sequence of the entire human genome in 2003.[33]

Inherited diseases are caused by damaging alterations or variants in our DNA. To fully appreciate the consequences of an alteration in our DNA, we first need to understand how the genetic code is converted into a protein. This conversion takes place in two consecutive steps: transcription and translation (Figure 9). First, the genetic information stored in the double-stranded DNA is transcribed to a single-stranded precursor messenger RNA. Subsequently, the pre-messenger RNA undergoes several modifications such as 5'capping, polyadenylation, and splicing, before it becomes messenger RNA and leaves the nucleus. The splicing step removes the non-coding intronic regions from the pre-messenger RNA and connects the exons. The cleavage sites at the boundary between the introns and exons, the splice sites, generally consist of conserved sequences (Figure 10). The 5' end of the intron (i.e., the splice donor site) consists of a GT dinucleotide, and the 3' end of the intron (i.e., the splice acceptor site) consist of a AG dinucleotide (Figure 10).[39] The spliceosome, the splicing machinery composed of proteins and small nuclear RNAs, recognizes these and other specific sequences and facilitates intron splicing. The canonical GT and AG sequences are important and alterations in these sequences will prevent the process of splicing.
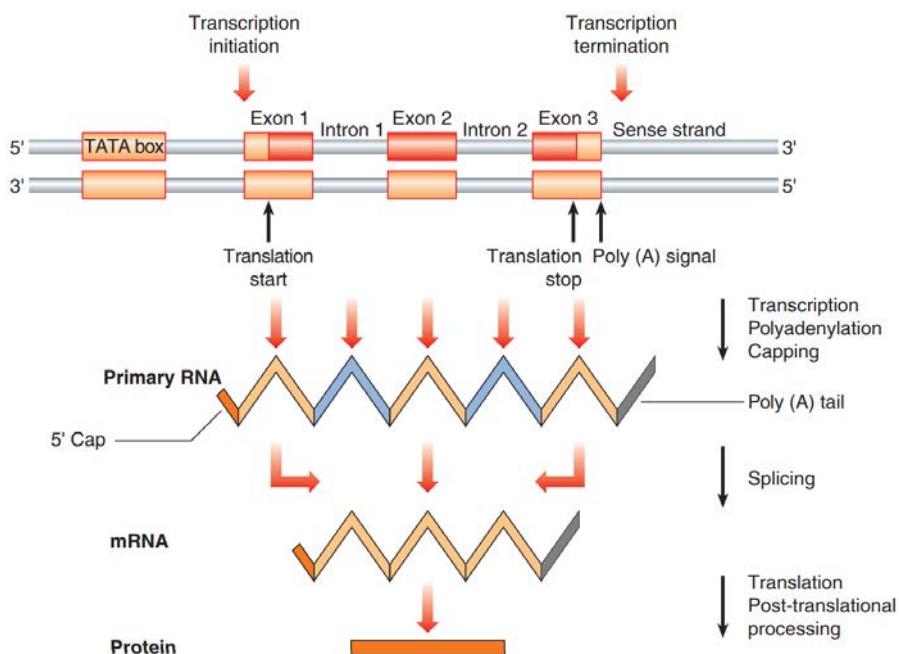
Figure 9. Schematic illustration of translation, splicing and translation processes. (Source: Turnpenny and Ellard. Emery's elements of medical genetics, 14th edition, Elsevier, 2012[38])

Moreover, when pathogenic variants occur in the non-canonical splice region or in a deep-intronic region they may influence splicing by creating or removing putative splice sites or give rise to a newly inserted (pseudo)exon. However, the pre-messenger RNA is not always spliced in the same manner; alternative splicing has been reported in over 90% of multiexon genes.[40] In alternative splicing, particular exons are removed from the pre-messenger RNA and are therefore not present in the final messenger RNA. Consequently, multiple protein subtypes or isoforms can result from a single gene. These isoforms can be ubiquitously expressed, or tissue-specific and may have a unique function. The production of alternative messenger RNAs is regulated by splice regulatory elements and proteins, among which exonic splice enhancers and silencers (i.e., DNA sequence motifs to which splice enhancer and splice silencer proteins bind).[41] An optimal ratio between these splice enhancers and splice silencers is essential for correct splicing in the human cells and a imbalance may cause disease (see Chapter 3.2).

Once the process of splicing is finished, the messenger RNA is transported from the nucleus to the cytoplasm, where the ribosomes decode the messenger RNA and link amino acids to form a stretch of amino acids, a process called translation. Finally, the polypeptide chain may undergo post-translational modification, such as protein folding, to obtain their desired structure and function in the human body.
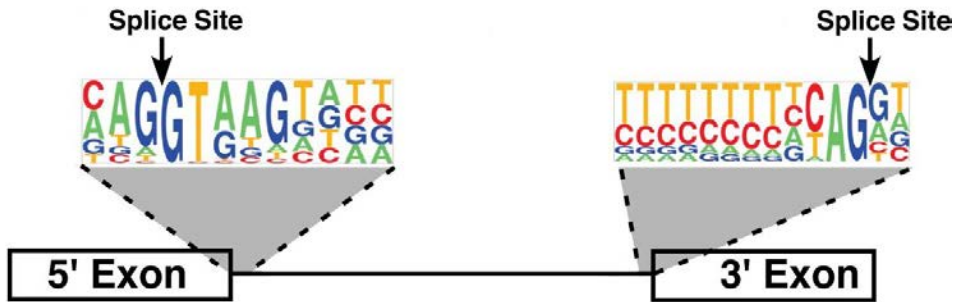
Figure 10. Schematic illustration of the splice consensus at the splice donor and splice acceptor site. The colored letters represent the nucleotides, and the height of the colored nucleotides indicates the relative frequency of nucleotides in that position. The more frequent a specific nucleotide, the more likely an alterations of this particular nucleotide will result in aberrant splicing (Adapted from Padgett et al., 2012.[42]).

Disease gene identification

Humans share approximately 99.9% of their DNA. The remaining 0.1%, includes 20 million bases that vary between individuals.[35] Among all possible genetic differences between humans there are damaging variants that can cause an inherited disease of any kind. To assign the causative DNA variant causing disease is looking for a needle in a haystack. Nevertheless, over the past decades, molecular sequencing techniques have evolved and have claimed their position in the diagnostic process of retinal diseases.

In 1984, the first disease locus for an inherited retinal disease was identified by Bhattacharya and colleagues, who discovered a locus on the X-chromosome in patients with X-linked RP.[43] Several years later, in 1990, Dryja et al. reported rhodopsin (*RHO*) as the first identified gene involved in autosomal dominant RP.[44] In the same year, Cremers et al. discovered that pathogenic variants in the *CHM* gene cause choroideraemia.[45] Since then, over 250 genes have been associated with inherited retinal dystrophies (Retnet, available at https://sph.uth.edu/retnet/ https://sph.uth.edu/retnet/). Key in the identification of many of these genes was the introduction of next-generation sequencing technologies in 2005. Whole exome sequencing (WES), one of the currently most commonly used techniques, allows screening for all coding region and the intron-exon boundaries and thereby enables analysis for all types of inherited retinal dystrophies in a single test.[46] Still, the variant may not have been detected using WES because it resides in a GC-rich region, concerns a structural variant, or WES lacked coverage for the specific variant.[46,47] Whole genome sequencing (WGS) may largely overcome these limitations by covering these non-coding regions and enabling detection of structural variants, and may therefore be implemented in the daily clinical practice in the near future.

Genetic heterogeneity

Besides their clinical heterogeneity, inherited retinal dystrophies also display an immense genetic heterogeneity. Not only are there more than 80 genes implicated in RP (see Chapter 2.1), there are also numerous different causal variants—many of which have still not been

found—within these genes. Both the high number of genes and the different variants within these genes attribute to the plethora of clinical manifestations in inherited retinal disease. For example, variants in *PRPH2* have been associated with MD, CD, CRD and RP,[48] and variants in *RP1* can cause a CRD, MD, and RP phenotype (see Chapter 4.1).

Examples of inherited retinal diseases

This section provides a description of the features of the inherited retinal dystrophies that are included in this thesis: namely, RP, Leber congenital amaurosis (LCA), CRD, MD, and XLRS.

Retinitis pigmentosa

The term 'RP' encompasses a group of progressive inherited retinal dystrophies characterized by the degeneration of photoreceptors in a rod-cone pattern, and is, with a worldwide prevalence of 1:4,000, the most common inherited retinal dystrophy. RP shows remarkable clinical and genetic heterogeneity. An extensive overview of the clinical characteristics, the large number of associated genes, and management of RP patients is provided in Chapter 2.1.

Leber congenital amaurosis

LCA is considered the most severe retinal dystrophy with an onset before infancy (variably defined as age one or two). One could consider LCA to be a very early onset form of RP. The loss of visual function early in life results in a specific set of symptoms, including nystagmus, abnormal or absent pupillary responses, high hyperopia, and oculo-digital signs (i.e., poking, pressing, and rubbing the eyes). Although the retinal aspect may appear normal initially, the ERG shows severely reduced or even absent responses of the photoreceptor pathways. Eventually, various abnormalities such as bone spicule pigmentation, optic disc abnormalities and profound atrophy may develop.[49] LCA is generally inherited in an autosomal recessive manner, although dominant inheritance has been described in *CRX*-associated LCA cases.[50-53] To date, 25 genes have been associated with LCA (Retnet; available at https://sph.uth.edu/retnet/).[49]

Cone-rod dystrophy

Cone-rod dystrophies comprises a group of inherited retinal dystrophies in which cone degeneration precedes rod degeneration. CRD is less frequent compared with RP, with an estimated prevalence of 1:40,000.[54,55] Patients generally experience loss of visual acuity in the first decade, sometimes accompanied by photophobia and/or color vision disturbances, whereas night blindness may develop later in life as the rods become involved.[54,56] The macular appearance can range from normal to bull's eye maculopathy or RPE atrophy, and the optic nerve may show temporal pallor. In later stages, bone spicule pigmentation and attenuation of the retinal vessels can be observed.[54,55] Goldmann perimetry shows central

sensitivity loss or a central scotoma and may eventually reveal constriction of the peripheral visual field. Particularly in the early stages, the ERG is typically reduced in a cone-rod pattern, which is important in the differentiation between RP and CRD. In advanced disease, both rod and cone responses can become severely reduced differentiation between CRD and RP may be difficult.

Like RP, CRD can follow all modes of Mendelian inheritance, i.e. autosomal dominant, autosomal recessive and X-linked. Thirty-five genes have been implicated in CRD (RetNet, available at https://sph.uth.edu/retnet/).

Macular dystrophies

The group of macular dystrophies is a highly heterogeneous group of disorders characterized by central visual loss, and relative symmetric fundus abnormalities, that include chorioretinal atrophy, and accumulation of lipofuscin and/or pigmentation, predominantly limited to the macular region.[57] Some of these macular dystrophies may evolve to become panretinal photoreceptors dystrophies during the course of the disease. Even more than RP and CRD, the clinical manifestation of MDs varies wildly. This is matched by a large genetic heterogeneity with genes encoding proteins involved in a variety of vital processes in the retina. Although the underlying molecular defect is often expressed throughout the entire retina, the retinal abnormalities are more or less limited to the macular region, which appears to be more susceptible to pathologic changes in these cases. MD has been associated with 22 genes (RetNet, available at https://sph.uth.edu/retnet/). One of the most recently discovered genes is the *RP1* gene, mutations in this gene were already known to cause RP. This new genotype-phenotype association is described in Chapter 4.1 of this thesis.

X-linked juvenile retinoschisis (XLRS)

XLRS is the leading cause of hereditary juvenile macular degeneration in males with an estimated prevalence ranging from 1 in 5,000 to 1 in 25,000.[58] XLRS is caused by mutations in the *RS1* gene, which encodes the retinoschisin protein that is involved in cellular adhesion and cell-cell interactions, and thereby plays a role in maintaining the normal retinal integrity.[59,60] Consequently, reduced or malfunctioning of retinoschisin causes splitting or 'schisis' of the neuroretinal layers.

Patients generally present in the first decade of life with a decrease in visual acuity, although an earlier onset during infancy has also been reported.[61,62] The hallmark finding is a bilateral foveoschisis, in young patients visible as a spoke-wheel pattern in the macula (Figure 11-B).[62] In addition, a peripheral retinoschisis is present in up to 50% of patients and patients are often hypermetropic.[27,63] The best diagnostic tool to detect the retinoschisis is an OCT scan that visualizes the cystoid macular lesions, which can be present throughout different retinal layers (i.e. from the nerve fiber layer tot the outer nuclear layer).[27] The full-field ERG typically shows a characteristic electronegative ERG, caused by a reduced b-wave with preservation of the a-wave. With progression of the disease, the cystoid macular lesions diminish and chorioretinal macular
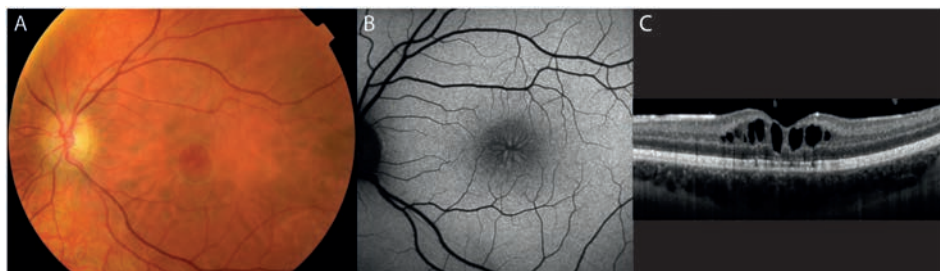
Figure 11. Images of the left eye of a 15-year old patient with X-linked juvenile retinoschisis. (A) Fundus photograph and (B) fundus autofluorescence image showing a macular spoke-wheel pattern. (C) Optical coherence tomography image showing cystic macular lesions in the inner nuclear layer.

atrophy occurs accompanied by permanent loss of central vision.[64] Other vision-threatening complications that may occur include retinal detachment, vitreous hemorrhage and progression of the retinoschisis towards the centre. To reduce the amount of cystoid macular lesions and improve vision, XLRS patients may be treated with carbonic anhydrase inhibitors, as discussed in Chapter 5.1.

Aims and outlines of this thesis

Our knowledge of retinal dystrophies has rapidly increased since the discovery of the first gene (rhodopsin) implicated in retinal dystrophies in 1990 by Drya and co-workers.[44] However, much remains to be elucidated about these disorders. For example, we still cannot determine a molecular diagnosis in approximately one third of all patients.[46,65,66] The pathogenesis underlying the large variation in clinical presentation is also currently unknown. This knowledge is important to accurately predict the individual disease course and to counsel patients and their families. It is also important in the selection of patients for upcoming therapeutic trials and in the evaluation of the effects of these novel treatments.

Knowledge on the clinical findings of inherited retinal disease is scattered throughout many publications in the scientific literature. The objective of this thesis is two-fold: the first aim is to provide a synthesis of all the clinical, genetic and therapeutic information currently available for RP. Second, our goal is to increase knowledge of RP and other retinal dystrophies. This thesis describes the disease spectrum associated with variants in the *RP1* gene. In addition, four specific retinal dystrophies: XLRS, and three RP subtypes caused by variants in respectively the *IMPG1*, *KIAA1549*, and *TULP1* gene are discussed.

Non-syndromic retinitis pigmentosa
Chapter 2.1 provides a detailed overview of the clinical, genetic and therapeutic aspects of non-syndromic RP, as well as the specific features of all genetically defined RP subtypes. This

chapter contains a unique atlas that covers 75 of the 87 known genetic subtypes of RP, and contains images of all the genetic subtypes that have been published over the years. Additionally, this chapter shows a schematic representation of human photoreceptor cells, the RPE and the interphotoreceptor matrix, and demonstrates the vital processes affected in RP (e.g. the phototransduction cascade, the visual cycle, etc.), as well as the genes involved. The final part of this chapter is devoted to current and future therapeutic options.

Genotype

Chapter 3 focuses on the description of two new genetic associations. Chapter 3.1 provides additional evidence supporting the hypothesis that variants in the *KIAA1549* gene are associated with RP. Moreover, it includes additional information on the function of KIAA1549, and describes the clinical findings in *KIAA1549*-associated RP. Chapter 3.2 describes the identification of the first near exon RNA splice variant that is not present in a consensus splice site sequence in *TULP1* in two siblings with early-onset retinitis pigmentosa, and highlights the importance of genetic tests that include the non-coding regions.

Phenotype

The emphasis in Chapter 4 is on the phenotypic characteristics of certain RP subtypes. Chapter 4.1 describes the clinical spectrum of diseases caused by mutations in the *RP1* gene, which ranges from macular dystrophy to phenotypes that encompass the entire retina such as CRD and RP. This chapter also discusses possible genotype-phenotype correlations. Chapter 4.2 provides additional evidence on the causal role of the p.Leu579Pro missense change in *IMPG1* in a large Dutch family with autosomal dominant RP. Additionally, new clinical information is presented, among which composite fundus photographs and OCT images.

Treatment

Little is known regarding the therapeutic effect of carbonic anhydrase inhibitors in the management of cystic macular lesions in children with XLRS, despite the fact that this disease often manifests during childhood. Therefore, Chapter 5 evaluates the effect of treatment with carbonic anhydrase inhibitors in children with XLRS.

General discussion

Chapter 6 further discusses the studies described in this thesis and places the gained knowledge and novel hypotheses into a wider context.

References

1. Shabiralyani G, Hasan KS, Hamad N, Iqbal N. Impact of Visual Aids in Enhancing the Learning Process Case Research: District Dera Ghazi Khan. *Journal of Education and Practice.* 2015;6(19):226-233.
2. Niven JE, Laughlin SB. Energy limitation as a selective pressure on the evolution of sensory systems. *J Exp Biol.* 2008;211(Pt 11):1792-1804.
3. Laughlin SB. Energy as a constraint on the coding and processing of sensory information. *Curr Opin Neurobiol.* 2001;11(4):475-480.
4. Felleman DJ, Van DE. Distributed hierarchical processing in the primate cerebral cortex. *Cerebral cortex (New York, NY: 1991).* 1991;1(1):1-47.
5. Fotedar R, Wang JJ, Burlutsky G, et al. Distribution of axial length and ocular biometry measured using partial coherence laser interferometry (IOL Master) in an older white population. *Ophthalmology.* 2010;117(3):417-423.
6. Heymsfield S, Gonzalez M, Thomas D, Murray K, Jia G. Adult Human Ocular Volume: Scaling to Body Size and Composition. *Anat Physiol.* 2016;6(239):2161-0940.1000239.
7. Tideman JW, Snabel MC, Tedja MS, et al. Association of Axial Length With Risk of Uncorrectable Visual Impairment for Europeans With Myopia. *JAMA Ophthalmol.* 2016;134(12):1355-1363.
8. Kolb H. Simple Anatomy of the Retina. In: Kolb H, Fernandez E, Nelson R, eds. *Webvision: The Organization of the Retina and Visual System.* Salt Lake City (UT): University of Utah Health Sciences Center, Copyright: (c) 2018 Webvision.; 1995.
9. Hartong DT, Berson EL, Dryja TP. Retinitis pigmentosa. *Lancet.* 2006;368(9549):1795-1809.
10. Marc RE. *Functional neuroanatomy of the retina.* 3rd ed. New York: Elsevier; 2008.
11. Stilma JS, Voorn TB. *Oogheelkunde.* Bohn Stafleu van Loghum; 2008.
12. Purves D, Augustine GJ, Fitzpatrick D, et al. *Neuroscience.* 2nd edition ed. Sunderland (MA): Sinauer Associates; 2001. Functional Specialization of the Rod and Cone Systems.
13. Bonilha VL. Retinal pigment epithelium (RPE) cytoskeleton in vivo and in vitro. *Exp Eye Res.* 2014;126:38-45.
14. Sparrow JR, Hicks D, Hamel CP. The retinal pigment epithelium in health and disease. *Curr Mol Med.* 2010;10(9):802-823.
15. Strauss O. The retinal pigment epithelium in visual function. *Physiol Rev.* 2005;85(3):845-881.
16. Schmitz-Valckenberg S, Holz FG, Bird AC, Spaide RF. Fundus autofluorescence imaging: review and perspectives. *Retina (Philadelphia, Pa).* 2008;28(3):385-409.
17. Bainbridge JW, Smith AJ, Barker SS, et al. Effect of gene therapy on visual function in Leber's congenital amaurosis. *N Engl J Med.* 2008;358(21):2231-2239.
18. Keilhauer CN, Delori FC. Near-infrared autofluorescence imaging of the fundus: visualization of ocular melanin. *Invest Ophthalmol Vis Sci.* 2006;47(8):3556-3564.
19. Kennedy CJ, Rakoczy PE, Constable IJ. Lipofuscin of the retinal pigment epithelium: a review. *Eye (Lond).* 1995;9 (Pt 6):763-771.
20. Boon CJ, Jeroen Klevering B, Keunen JE, Hoyng CB, Theelen T. Fundus autofluorescence imaging of retinal dystrophies. *Vision Res.* 2008;48(26):2569-2577.
21. Lambertus S, Bax NM, Fakin A, et al. Highly sensitive measurements of disease progression in rare disorders: Developing and validating a multimodal model of retinal degeneration in Stargardt disease. *PLoS One.* 2017;12(3):e0174020.
22. Wade NJ. Image, eye, and retina (invited review). *Journal of the Optical Society of America A, Optics, Image Science, and Vision.* 2007;24(5):1229-1249.
23. Bohigian GM. An ancient eye test--using the stars. *Surv Ophthalmol.* 2008;53(5):536-539.
24. Bevers C, Blanckaert G, Van Keer K, Fils JF, Vandewalle E, Stalmans I. Semi-automated kinetic perimetry: Comparison of the Octopus 900 and Humphrey visual field analyzer 3 versus Goldmann perimetry. *Acta Ophthalmol.* 2018.
25. Markowitz SN, Reyes SV. Microperimetry and clinical practice: an evidence-based review. *Can J Ophthalmol.* 2013;48(5):350-357.
26. McCulloch DL, Marmor MF, Brigell MG, et al. ISCEV Standard for full-field clinical electroretinography (2015 update). *Doc Ophthalmol.* 2015;130(1):1-12.
27. Molday RS, Kellner U, Weber BH. X-linked juvenile retinoschisis: clinical diagnosis, genetic analysis, and molecular mechanisms. *Prog Retin Eye Res.* 2012;31(3):195-212.
28. Yzer S, Barbazetto I, Allikmets R, et al. Expanded clinical spectrum of enhanced S-cone syndrome. *JAMA Ophthalmol.* 2013;131(10):1324-1330.
29. Hood DC, Bach M, Brigell M, et al. ISCEV standard for clinical multifocal electroretinography (mfERG) (2011 edition). *Doc Ophthalmol.* 2012;124(1):1-13.
30. Constable PA, Bach M, Frishman LJ, Jeffrey BG, Robson AG, International Society for Clinical Electrophysiology of V. ISCEV Standard for clinical electro-oculography (2017 update). *Doc Ophthalmol.* 2017;134(1):1-9.
31. Pray L. Discovery of DNA structure and function: Watson and Crick. *Nature Education.* 2008;1(1):100.
32. Turnpenny PD, Ellard S. *Emery's elements of medical genetics.* Churchill Livingstone Elsevier; 2009.
33. Collins FS, Green ED, Guttmacher AE, Guyer MS. A vision for the future of genomics research. *Nature.* 2003;422:835.
34. Pray L. Eukaryotic genome complexity. *Nature Education.* 2008;1(1):96.
35. Genomes Project C, Auton A, Brooks LD, et al. A global reference for human genetic variation. *Nature.* 2015;526(7571):68-74.

36. Consortium EP, Bernstein BE, Birney E, et al. An integrated encyclopedia of DNA elements in the human genome. *Nature.* 2012;489(7414):57-74.
37. Appels R, Eversole K, Feuillet C, et al. Shifting the limits in wheat research and breeding using a fully annotated reference genome. *Science.* 2018;361(6403).
38. Turnpenny PD, Ellard S. Emery's Elements of Medical Genetics. In: Elsevier 2012:19.
39. Clancy S. RNA Splicing: Introns, Exons and Spliceosome. *Nature Education.* 2008;1(1).
40. Pan Q, Shai O, Lee LJ, Frey BJ, Blencowe BJ. Deep surveying of alternative splicing complexity in the human transcriptome by high-throughput sequencing. *Nat Genet.* 2008;40:1413.
41. Fairbrother WG, Chasin LA. Human genomic sequences that inhibit splicing. *Mol Cell Biol.* 2000;20(18):6816-6825.
42. Padgett RA. New connections between splicing and human disease. *Trends Genet.* 2012;28(4):147-154.
43. Bhattacharya SS, Wright AF, Clayton JF, et al. Close genetic linkage between X-linked retinitis pigmentosa and a restriction fragment length polymorphism identified by recombinant DNA probe L1.28. *Nature.* 1984;309(5965):253-255.
44. Dryja TP, McGee TL, Reichel E, et al. A point mutation of the rhodopsin gene in one form of retinitis pigmentosa. *Nature.* 1990;343(6256):364-366.
45. Cremers FP, van de Pol DJ, van Kerkhoff LP, Wieringa B, Ropers HH. Cloning of a gene that is rearranged in patients with choroideraemia. *Nature.* 1990;347(6294):674-677.
46. Haer-Wigman L, van Zelst-Stams WA, Pfundt R, et al. Diagnostic exome sequencing in 266 Dutch patients with visual impairment. *Eur J Hum Genet.* 2017;25(5):591-599.
47. Carss KJ, Arno G, Erwood M, et al. Comprehensive Rare Variant Analysis via Whole-Genome Sequencing to Determine the Molecular Pathology of Inherited Retinal Disease. *Am J Hum Genet.* 2017;100(1):75-90.
48. Boon CJ, den Hollander AI, Hoyng CB, Cremers FP, Klevering BJ, Keunen JE. The spectrum of retinal dystrophies caused by mutations in the peripherin/RDS gene. *Prog Retin Eye Res.* 2008;27(2):213-235.
49. Kumaran N, Moore AT, Weleber RG, Michaelides M. Leber congenital amaurosis/early-onset severe retinal dystrophy: clinical features, molecular genetics and therapeutic interventions. *Br J Ophthalmol.* 2017;101(9):1147-1154.
50. den Hollander AI, Lopez I, Yzer S, et al. Identification of novel mutations in patients with Leber congenital amaurosis and juvenile RP by genome-wide homozygosity mapping with SNP microarrays. *Invest Ophthalmol Vis Sci.* 2007;48(12):5690-5698.
51. Weleber RG, Francis PJ, Trzupek KM, Beattie C. Leber Congenital Amaurosis. In: Adam MP, Ardinger HH, Pagon RA, et al., eds. *GeneReviews((R)).* Seattle (WA)1993.
52. Rivolta C, Berson EL, Dryja TP. Dominant Leber congenital amaurosis, cone-rod degeneration, and retinitis pigmentosa caused by mutant versions of the transcription factor CRX. *Hum Mutat.* 2001;18(6):488-498.
53. Perrault I, Hanein S, Gerber S, et al. Evidence of autosomal dominant Leber congenital amaurosis (LCA) underlain by a CRX heterozygous null allele. *J Med Genet.* 2003;40(7):e90.
54. Hamel CP. Cone rod dystrophies. *Orphanet J Rare Dis.* 2007;2:7.
55. Roosing S, Thiadens AA, Hoyng CB, Klaver CC, den Hollander AI, Cremers FP. Causes and consequences of inherited cone disorders. *Prog Retin Eye Res.* 2014;42:1-26.
56. Thiadens AA, Phan TM, Zekveld-Vroon RC, et al. Clinical course, genetic etiology, and visual outcome in cone and cone-rod dystrophy. *Ophthalmology.* 2012;119(4):819-826.
57. Michaelides M, Hunt DM, Moore AT. The genetics of inherited macular dystrophies. *J Med Genet.* 2003;40(9):641-650.
58. Mooy CM, Van Den Born LI, Baarsma S, et al. Hereditary X-linked juvenile retinoschisis: a review of the role of Muller cells. *Arch Ophthalmol.* 2002;120(7):979-984.
59. Sauer CG, Gehrig A, Warneke-Wittstock R, et al. Positional cloning of the gene associated with X-linked juvenile retinoschisis. *Nat Genet.* 1997;17(2):164-170.
60. Molday LL, Hicks D, Sauer CG, Weber BH, Molday RS. Expression of X-linked retinoschisis protein RS1 in photoreceptor and bipolar cells. *Invest Ophthalmol Vis Sci.* 2001;42(3):816-825.
61. George ND, Yates JR, Bradshaw K, Moore AT. Infantile presentation of X linked retinoschisis. *Br J Ophthalmol.* 1995;79(7):653-657.
62. Deutman AF. Sex-linked juvenile retinoschisis. In: Deutman A, ed. *The hereditary dystrophies of the posterior pole of the eye.* Assen: Van Gorcum; 1971.
63. Kato K, Miyake Y, Kachi S, et al. Axial length and refractive error in X-linked retinoschisis. *Am J Ophthalmol.* 2001;131(6):812-814.
64. George ND, Yates JR, Moore AT. Clinical features in affected males with X-linked retinoschisis. *Arch Ophthalmol.* 1996;114(3):274-280.
65. Tiwari A, Bahr A, Bahr L, et al. Next generation sequencing based identification of disease-associated mutations in Swiss patients with retinal dystrophies. *Sci Rep.* 2016;6:28755.
66. Abu-Safieh L, Alrashed M, Anazi S, et al. Autozygome-guided exome sequencing in retinal dystrophy patients reveals pathogenetic mutations and novel candidate disease genes. *Genome Res.* 2013;23(2):236-247.

Non-syndromic retinitis pigmentosa

Non-syndromic retinitis pigmentosa

Sanne K. Verbakel, Ramon A.C. van Huet, Camiel J.F. Boon, Anneke I. den Hollander,
Rob W.J. Collin, Caroline C.W. Klaver, Carel B. Hoyng, Ronald Roepman, B. Jeroen Klevering

Abstract

Retinitis pigmentosa (RP) encompasses a group of inherited retinal dystrophies characterized by the primary degeneration of rod and cone photoreceptors. RP is a leading cause of visual disability, with a worldwide prevalence of 1:4000. Although the majority of RP cases are non-syndromic, 20-30% of patients with RP also have an associated non-ocular condition. RP typically manifests with night blindness in adolescence, followed by concentric visual field loss, reflecting the principal dysfunction of rod photoreceptors; central vision loss occurs later in life due to cone dysfunction. Photoreceptor function measured with an electroretinogram is markedly reduced or even absent. Optical coherence tomography (OCT) and fundus autofluorescence (FAF) imaging show a progressive loss of outer retinal layers and altered lipofuscin distribution in a characteristic pattern. Over the past three decades, a vast number of disease-causing variants in more than 80 genes have been associated with non-syndromic RP. The wide heterogeneity of RP makes it challenging to describe the clinical findings and pathogenesis. In this review, we provide a comprehensive overview of the clinical characteristics of RP specific to genetically defined patient subsets. We supply a unique atlas with color fundus photographs of most RP subtypes, and we discuss the relevant considerations with respect to differential diagnoses. In addition, we discuss the genes involved in the pathogenesis of RP, as well as the retinal processes that are affected by pathogenic mutations in these genes. Finally, we review management strategies for patients with RP, including counseling, visual rehabilitation, and current and emerging therapeutic options.

Introduction

Retinitis pigmentosa (RP) is a major cause of visual disability and blindness, affecting more than 1.5 million patients worldwide. RP is the most common inherited retinal dystrophy (IRD), with a worldwide prevalence of approximately 1:4000,[1] although reports vary from 1:9000[2] to as high as 1:750,[3] depending on the geographic location. The term "retinitis pigmentosa" was first coined by the famous Dutch ophthalmologist F.C. Donders in 1857,[4] although his colleague A.C. van Trigt provided the first description of RP viewed through an ophthalmoscope four years earlier.[5] Even in those early days, certain forms of retinal degenerations had already been reported. For example, in 1744 R.F. Ovelgün described a form of familial night blindness closely resembling RP.[6] In the early 19th century, both M. Schon and F.A. von Ammon reported patients with poor vision and pigmented retinal lesions.[7,8]

RP encompasses a group of progressive IRDs characterized by the primary degeneration of rod photoreceptors, followed by the loss of cone photoreceptors. The initial symptom is reduced night vision, which is followed by a progressive loss of the visual field in a concentric pattern. Function at the macula is usually relatively well preserved until later stages of the disease. Fundus abnormalities typically include bone spicule pigmentation predominantly in the periphery and/or mid-periphery, attenuation of retinal vessels, and a waxy pallor of the optic nerve head. An electroretinogram can help in the diagnosis and reveals the characteristic loss of photoreceptor function, primarily among rod photoreceptors rather than cones in early stages of the disease.

RP is clinically distinct from other IRDs, including IRDs that manifest at birth or within the first few months of life (e.g., Leber congenital amaurosis, or LCA), dystrophies in which cone degeneration precedes rod degeneration (e.g., cone-rod dystrophy), macular dystrophies, and disorders that are generally not progressive such as achromatopsia and congenital stationary night blindness (CSNB). In addition, 20-30% of patients with RP present with a syndromic form of RP associated with extra-ocular abnormalities. Together, all of these disorders form a continuum of retinal dystrophies with partially overlapping clinical and/or genetic findings (Figure 1). This overlap can complicate the classification of an individual IRD and is subject to discussion. Moreover, few therapeutic options are currently available in daily clinical practice. Therefore, the practitioner's focus should be to provide the patient with the best possible information regarding the expected clinical course and inheritance pattern. In this respect, developing a classification system that combines the clinical diagnosis with the underlying genetic factors can provide valuable prognostic information regarding the rate of progression and long-term outcome.

The wide heterogeneity among RP patients is best illustrated by the large number of genetic defects associated with RP. In 1990, Dryja et al. reported the first identified gene involved in autosomal dominant RP: the rhodopsin (*RHO*) gene.[9] Since then, mutations in more than 80 genes have been implicated in non-syndromic RP,[10] and each year new genes are added to this list. Each of these genes corresponds to a gene-specific subtype of RP with a specific age of onset, visual impairment, retinal appearance, and/or rate of progression. Moreover, several
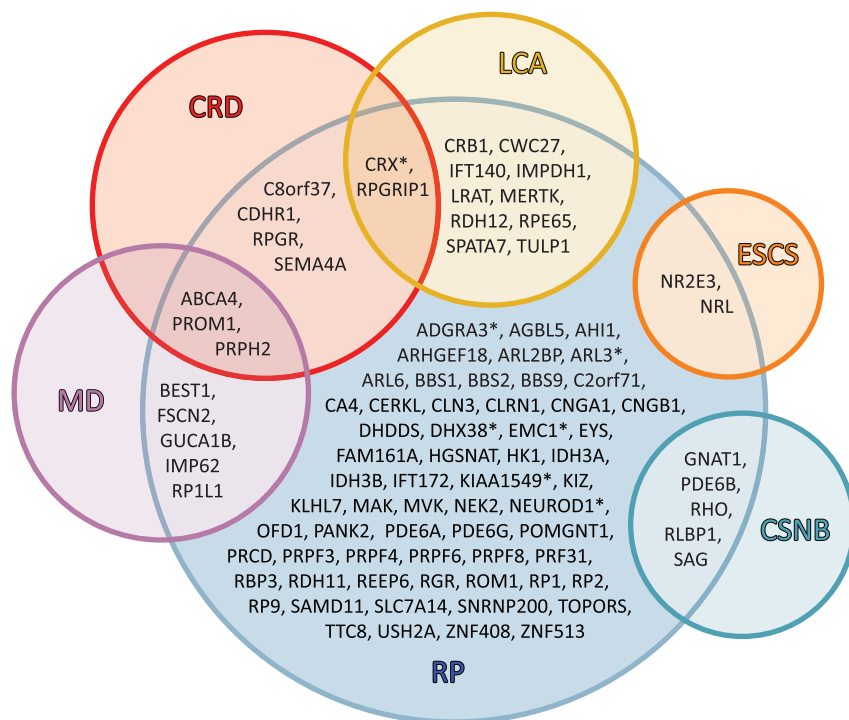
Figure 1. Venn diagram summarizing the genetic overlap between RP and other inherited retinal dystrophies. Each circle represents a specific clinical diagnosis. The gene names listed in the overlapping areas indicate that mutations in these genes can lead to different phenotypes. Genes marked with an asterisk are candidate genes for non-syndromic RP.
Abbreviations: CRD: cone-rod dystrophy, CSNB: congenital stationary night blindness, ESCS: enhanced S-cone syndrome, LCA: Leber congenital amaurosis, MD: macular dystrophy, RP: retinitis pigmentosa.

factors can vary widely within each of these gene-specific subtypes, even between affected family members, suggesting the presence of unidentified genetic and/or environmental factors that can influence the RP phenotype.

Information regarding the clinical course of various RP subtypes is spread across numerous reports that often describe only limited numbers of patients. In this review, we provide a comprehensive overview of the clinical features associated with the various genetic subtypes of non-syndromic RP. A related—yet equally complicated—subject is the functional role of the many proteins encoded by their respective RP genes. To better appreciate the effect of mutations in RP genes, we also discuss the role of these proteins in the structure and function of the retina. Finally, we discuss the current therapeutic options and future perspectives for non-syndromic RP.

Clinical findings in RP

RP is characterized by the progressive degeneration of photoreceptors and retinal pigment epithelium (RPE), leading to night blindness, tunnel vision, and a gradual reduction of central vision. However, the clinical findings in RP vary widely due to the large number of genes involved, each of which can have several alleles. In this chapter, we discuss the clinical features that are generally considered to be characteristic of RP. A comprehensive overview of the features specific to the various genetic subtypes of RP is provided in Chapter 4.

Age of onset and rate of progression
In the "classic" presentation of RP, difficulty with dark adaptation begins in adolescence, and visual loss in the mid-peripheral field becomes apparent in young adulthood. However, the age at onset among patients with RP varies widely; thus, some patients develop symptomatic visual loss in early childhood, whereas others can remain relatively asymptomatic until mid-adulthood. The exact age of onset is often difficult to determine, as many patients—particularly children— are able to compensate for peripheral visual loss. In addition, difficulties with dark adaptation can remain unnoticed by the patient due to our artificially illuminated nighttime environment. In general, RP subtypes that manifest early in life tend to progress more rapidly. Moreover, the severity of the disease is correlated with the disease's Mendelian pattern of inheritance. In general, patients with X-linked RP (5-15% of RP patients) have a more severe disease course compared to patients with autosomal recessive RP (50-60% of RP patients), whereas patients with an autosomal dominant form of RP (30-40% of RP patients)[11,12] have the best long-term prognosis with respect to retaining central vision.[13,14]

Symptoms
The initial symptoms of RP include night blindness (nyctalopia) and difficulty with dark adaptation. In some cases, RP can also present with loss of the mid-peripheral visual field, although this is rarely reported as an early symptom. The central retina remains relatively preserved until the final stages of the disease, although anatomical abnormalities in the central retina can appear early in the course of the disease. Eventually, and typically when the patient reaches middle age, central cone degeneration leads to a decline in visual acuity. Most patients with RP retain the ability to perceive light due to residual macular function and/or the presence of a preserved peripheral temporal retinal island.[13] Photopsia is a common but often-neglected symptom[15] that can be highly disturbing to patients. This phenomenon may be caused by a lack of afferent nerve impulses in response to photoreceptor degeneration[16] or spontaneous self-signaling activity as a result of inner retina remodeling.[17] Photopsia can occur in the early stages of RP,[18] but is most striking—and particularly disturbing—in patients with more advanced stages of the disease.[19] In advanced RP, the visual hallucinations can take animate forms, which corresponds with the diagnosis Charles Bonnet syndrome.[20] Patients with RP can also experience photophobia and dyschromatopsia.[13,21]

Family history

A thorough family history is very important in any patient suspected for RP and we recommend drawing a pedigree for each proband. A pedigree is useful in several ways, it helps assessing the mode of inheritance and may also have diagnostic consequences. For example, if an X-linked inheritance is suspected, the *RPGR* gene should be sequenced prior to whole exome sequencing (see section 6.1). A pedigree may also illustrate which family members are at risk for developing RP and/or indicate subjects where non-penetrance should be suspected, for instance when mutations in *PRPF31* and *HK1* are involved (see Chapter 4).

Ophthalmic examination

The classic RP triad

Three clinical features—bone spicule pigmentation, attenuation of retinal vessels, and a waxy pallor of the optic nerve—are the hallmark signs of RP. In the early stages of RP, a fundus examination may appear normal, as bone spicule–shaped pigment deposits are either absent or sparse, vascular attenuation is minimal, and the optic disc is normal in appearance. Prior to the typical RP abnormalities, some patients may present with aspecific abnormalities such as irregular reflexes from the internal limiting membrane, broadening of the foveal reflex, and discrete local whithish lesions at the level of the RPE. Not all RP patients develop typical bone spicules; some develop dust-like pigmentation, whereas others develop nummular hyperpigmentation. The degree of hyperpigmentation can vary among patients and does not necessarily reflect the severity of the disease. Bone spicule pigmentation consists of RPE cells that detach from Bruch membrane following photoreceptor degeneration and migrate to intraretinal perivascular sites, where they form melanin pigment deposits.[22] These bone spicules often arise in the mid-periphery, where the concentration of rod cells is highest.[23] Precisely what triggers RPE migration is unknown, given the high level of interdependence between the choriocapillaris, RPE, and photoreceptors. However, the RPE migration might be triggered by the reduced distance between the inner retinal vessels and the RPE, due to the degeneration of photoreceptors in *RHO* knock-out mice.[24]

The etiology underlying the attenuation of retinal vessels in RP remains unclear. Initially, this clinical feature was attributed to reduced metabolic demand following ganglion cell degeneration secondary to photoreceptor cell loss. An alternative hypothesis attributes the loss of oxygen-consuming photoreceptors to a hyperoxic state of the remaining inner retina, which leads to vasoconstriction and reduced blood flow in retinal vessels.[25-28] Additionally, Li et al. found that thickening of the extracellular matrix between the retinal vessels and the migrated RPE cells causes narrowing of the vessels.[22] Finally, Stone et al. suggested that a loss of synaptic input secondary to photoreceptor cell death—and the resulting decline in trophic factors— causes reduced metabolism of the inner retinal layers, which may induce vascular remodeling and subsequent vessel attenuation.[29] On the other hand, Cellini et al. found that ocular blood flow was reduced more than would be expected due to retinal atrophy, which raises the question of whether vascular changes in RP patients are merely secondary to neuroretinal remodeling,

or whether they play a more pivotal role in the development of RP.[30] In addition, a role for the vasoconstrictor endothelin-1 has been suggested, although both increased and decreased plasma levels of endothelin-1 have been reported among RP patients, thus indicating the need for further study.[30-33] Given that most of the genes linked to RP play a role in either the photoreceptor-RPE complex or the interphotoreceptor matrix, a secondary cause of these vascular changes is likely.

The optic disc typically develops a waxy pallor as the disease progresses; this feature is likely caused by the formation of glial cells both on the surface and inside the optic disc, resulting in increased light reflectance.[34,35]

Ocular findings associated with RP

Several other ocular conditions—some of which are amenable to treatment—are often associated with RP. For example, patients with early-onset RP can also present with nystagmus, and disease-associated refractive error is also common. Macular complications can include cystoid macular edema (CME), macular hole, and epiretinal membrane formation. CME has been reported to occur in up to 50% of patients with RP.[36] Although the etiology remains unknown, Strong et al. recently proposed several mechanisms that may contribute to the formation of CME, including *i*) breakdown of the blood-retina barrier, *ii*) impaired function of the RPE pumping mechanism, *iii*) Müller cell edema and dysfunction, *iv*) anti-retinal antibodies, and *v*) vitreomacular traction.[36] Up to 36% of RP patients present with epiretinal membrane formation,[37-41] which may be the result of idiopathic preretinal glial cell proliferation[35] or—as suggested recently—may occur secondary to an inflammatory process.[38] The notion of an inflammatory component in RP is not new, as evidenced by the word "retinitis" in the name, and is generally believed to be secondary to photoreceptor cell death. Recent evidence, however, suggests that inflammatory cells contribute to retinal degeneration via their cytotoxic effect on bystander cells such as photoreceptors.[42,43] Posterior subcapsular cataract may significantly affect vision and occurs in approximately 45% of RP patients;[44-46] visually significant cataract can be removed even when there is macular involvement. The underlying mechanism in posterior subcapsular cataract is currently unknown, although a possible association with inflammation was recently suggested.[47] Another vitreous abnormality that can occur in RP is the presence of vitreous cysts, which have been reported to occur in 6% of RP patients.[48] In addition, optic nerve head drusen and/or optic nerve fiber layer drusen were reported in 9% of a cohort of 262 RP patients,[49] and later studies were able to link these drusen to specific subtypes of RP (see section 4.9). Finally, RP appears to be one of the most commonly underlying diseases in patients with secondary retinal vasoproliferative tumors.[50]

Retinal function

Perimetry

Progressive loss of the visual field is a characteristic feature of RP. This visual field loss has high bilateral symmetry[51] and typically begins with isolated scotomas in the mid-peripheral areas, which gradually coalesce to form a partial or complete ring scotoma. As the disease progresses,

this annular scotoma extends both outward and—albeit more slowly—inward. In addition to ring scotomas, other patterns of visual field progression have been reported, including concentric visual field loss without a preceding ring scotoma and visual field loss progressing from the superior to inferior retina in an arcuate pattern.[52] Kinetic perimetry is best suitable for assessment of peripheral visual field loss; the annual rate of decline for target V4e of the Goldmann perimeter ranges from 2-12% and varies among gene-specific subtypes.[53-58] Progression of central visual field loss is usually determined using static perimetry. A relatively novel technique to assess the central visual field is fundus-driven perimetry (i.e., microperimetry), which uses precise eye tracking throughout the examination, and enables direct structure-function correlations by providing an annotated en face image of the posterior pole.

Color vision

Initially, color vision may be normal; however, dyschromatopsia—particularly blue-yellow color vision defects where patients principally experience difficulty distinguishing shades of blue from green and yellow-green from violet—can occur in advanced stages of the disease. These so-called type III (blue) acquired color vision defects are more prevalent then type I (red-green) color vision defects.[21] Blue cone dysfunction has been attributed to the scarcity of these short-wavelength cones at the fovea.[59] Due to this uneven distribution, loss of pericentral retinal function may lead to tritanopia (blue-yellow color blindness). Loss of visual acuity—together with the associated degeneration of central photoreceptors—increases the likelihood of developing a type I color defect.[60] On the other hand, vision loss due to CME seems to have little effect on color vision.[21]

Dark adaptometry

An abnormal dark-adapted threshold is a hallmark feature of RP. Rod threshold is often increased due to decreased rod sensitivity and prolonged recovery of rod sensitivity.[61] Studies regarding dark adaptation in RP revealed increases in both cone and rod thresholds, a delay in reaching the asymptotic rod threshold, or the complete loss of rod photoreceptor function.[62]

Electroretinography

Full-field electrophysiological testing—according to the ISCEV guidelines (http://www.iscev.org/standards)—helps in the diagnosis and is essential in the quantitative assessment of the severity of the disease, as well as monitoring disease progression.[63] Electroretinogram (ERG) abnormalities occur early and precede the night blindness symptoms and fundus abnormalities (Figure 2). On the dark-adapted, bright flash (combined rod-cone) ERG, the a-wave is subnormal. In addition, isolated rod responses to a dark-adapted (scotopic) dim flash are delayed, diminished, or absent in a full-field ERG recording. Cone responses may also be affected in the early phases of RP, but this typically lags behind the onset of rod dysfunction. When present, cone dysfunction manifests in the light-adapted (photopic) ERG as a delayed and reduced response to a bright flash and 30-Hz flicker stimuli.[64] Oscillatory potentials may also be reduced
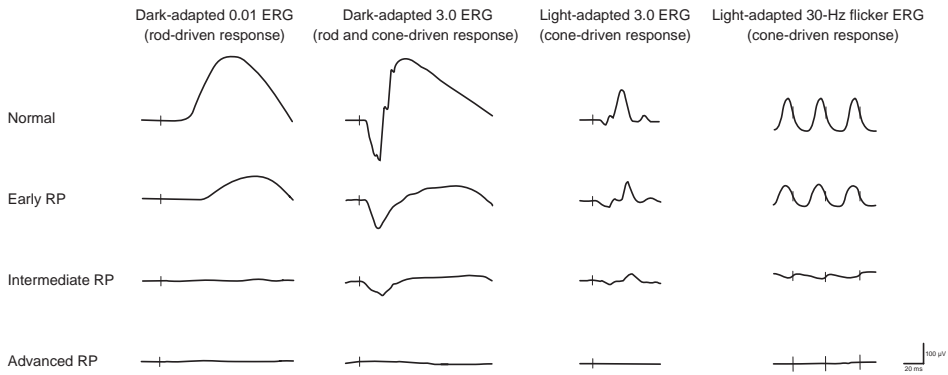
Figure 2. Schematic representation of ERG recordings in different stages of RP (i.e. early, intermediate and advanced RP). Vertical lines indicate the moment of stimulus flash. As the RP progresses, the amplitude of responses decreases, and the implicit time may increase. Cone dysfunction typically lags behind the onset of rod dysfunction. Eventually, the ERG—under both scotopic and photopic conditions—is extinguished.

2.6 Retinal imaging

in RP patients.[65] The annual rate of decay in the full-field ERG among RP patients ranges from 9-11%.[66] The decay in central cone functional is slower;[67,68] in a heterogeneous patient cohort including all three inheritance patterns (autosomal dominant, autosomal recessive, and X-linked) and syndromic subtypes, the annual rate of decay in central cone function was estimated at 4-7%.[69] As the disease progresses, the full-field ERG may become non-recordable despite a residual visual field. Under these circumstances, full-field stimulus threshold (FST), a fast test that does not require patients' fixation, or a multifocal ERG (mfERG) may still be able to elicit responses and may therefore be used to follow the disease progression.[68,70] Delayed responses in the mfERG may be used to predict visual field loss in a healthy-appearing retina.[71]

Fundus imaging

In a single capture, conventional fundus photography covers a field of view of 30-50 degrees of the retina. The peripheral retinal is generally covered rather poorly, even with 7-field fundus photography. Conventional color fundus photography is limited by media opacities and inadequate pupillary dilation, and patient cooperation is important. A better alternative may be found in ultra-wide field imaging, which uses confocal scanning laser ophthalmoscopy (cSLO) with green and red laser light. Ultra-wide field imaging depicts up to 200 degrees of retina in a single capture.[72,73] This technique, however, also has its disadvantages: the colors are artificial, the peripheral image is distorted caused by the two dimensional image of the three dimensional globe, and structures anterior to the retina (e.g. eyelashes and vitreous opacities) can cause artefacts.[72] Multicolor imaging is a technique that uses the reflectance of three lasers with a particular wavelength, to provide information about different layers of the retina.[74] The eventual multicolor image is composed of the reflectance images from the individual lasers, and the coloring is also artificial. In patients with RP, multicolor imaging is better at defining the borders of the intact macular area compared to conventional fundus photography.[75]
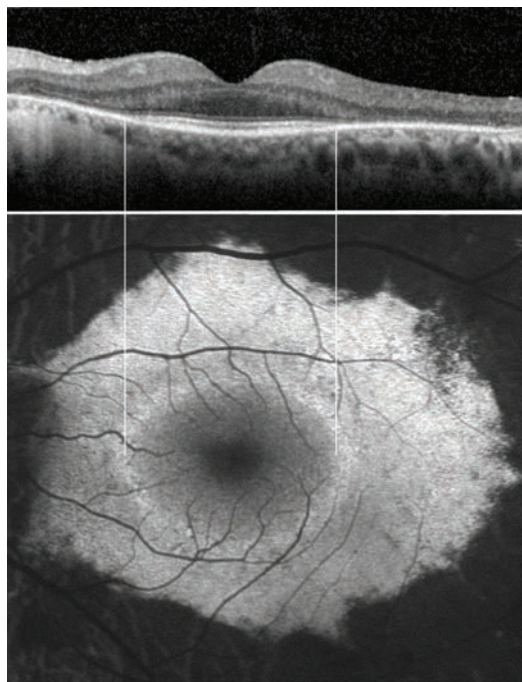
Figure 3. Horizontal spectral-domain optical coherence tomography (SD-OCT; top panel) and fundus autofluorescence (FAF) images of the left eye of a patient with RP. The OCT image shows the perifoveal loss of the outer retinal layers. The central preservation of the ellipsoid zone corresponds to the internal edges of the hyperautofluorescent ring visible on FAF.

Optical coherence tomography

The earliest histopathological change in RP is shortening of the photoreceptor outer segments.[76] This change is reflected in a spectral-domain optical coherence tomography (SD-OCT) image as disorganization of the outer retinal layers, initially at the interdigitation zone, followed by the ellipsoid zone, and finally at the external limiting membrane (Figure 3 and Figure 4).[77] As RP progresses, thinning of the outer segments is accompanied by a decrease in the thickness of the outer nuclear layer, which contains the nuclei of the photoreceptor cells. The late stages of RP are characterized by the complete loss of both the outer segment and the outer nuclear layer.[78] In contrast, the inner retinal layers—including the inner nuclear layer and the ganglion cell layer—remain relatively well preserved. In fact, a decrease in the thickness of the photoreceptor outer segments may even be accompanied by *thickening* of the inner retinal layers; although the underlying cause of this thickening is not entirely clear, it may be related to edema formation in the retinal nerve fiber layer and/or neuronal-glial retinal remodeling in response to thinning of the outer retina.[79] In patients with advanced disease and atrophy of the outer retinal layers, SD-OCT imaging may reveal outer retinal tabulations.[80] Hyperreflective foci are a common finding in the inner nuclear layer, the outer nuclear layer, and/or the subretinal space. These hyperreflective foci may represent migrating RPE cells and seem to be correlated with the condition of the RPE layer, the condition of the ellipsoid zone, and—in some cases— fundoscopically visible hyperpigmentation. Interestingly, an absence of hyperreflective foci in the outer nuclear layer has been associated with better visual acuity.[81] Several studies also
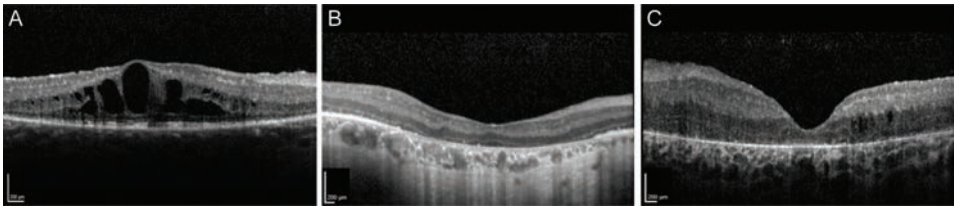
Figure 4. Horizontal spectral-domain optical coherence tomography (SD-OCT) images of three patients with RP. (A) SD-OCT image of a 27-year-old female with *PDE6B*-associated RP, showing cystoid macular edema and central loss of the ellipsoid zone band (B) SD-OCT image of a 46-year-old male with *CDHR1*-associated RP, showing profound loss of photoreceptor outer segments, with central loss of the RPE and increased visibility of the choroidal vasculature. (C) SD-OCT image of a 9-year-old female with *CRB1*-associated RP, showing minimal intraretinal cysts, irregular foveal architecture and an increased retinal thickness—despite a generalized loss of the outer retinal layers—with loss of the retinal laminations.

revealed a correlation between the visual acuity in RP patients and the condition of the ellipsoid zone line.[82-84] In addition, the width of the ellipsoid zone line is associated with a decrease in visual field sensitivity. Another study found a linear correlation between a decrease in the visual field and thinning of the outer segments.[77]

OCT imaging may also be valuable in diagnosing other macular abnormalities present in up to half of all RP patients.[85] For example, CME is the most common finding, followed by epiretinal membrane formation, vitreomacular traction syndrome, and macular hole.[77] In RP patients with CME, cystoid spaces are found primarily in the inner nuclear layer, but they can also occur in the outer nuclear layer, the outer plexiform layer, and/or the ganglion cell layer.[85]

Fundus autofluorescence imaging

Fundus autofluorescence (FAF) can reveal an otherwise undetectable disruption in RPE metabolism. With short-wavelength (SW)-FAF, using blue or green light, the signal emanates principally from lipofuscin molecules present in the RPE.[86] In contrast, near-infrared (NIR)-FAF displays the autofluorescence signal that originates from RPE and—to a lesser extent—choroidal melanin or related fluorophores.[87] FAF is increasingly used in evaluating and monitoring the progression of RP; however, sufficient data is lacking regarding the increased susceptibility to light toxicity of retinas with retinal dystrophies characterized by the accumulation of photosensitizers such as lipofuscin.[88,89]

An abnormal foveal ring or curvilinear arc of increased autofluorescence (Figure 3), not visible on ophthalmoscopy, is present in 50-60% of RP patients.[90] This ring can be visualized using both SW-FAF and NIR-FAF. The diameter of the ring ranges from 3-20 degrees and usually has a relatively high level of interocular symmetry.[91] This hyperautofluorescent ring represents a transition zone between abnormal and normal retinal function; thus, function is relatively normal within the ring and absent outside of the ring. The level of autofluorescence immediately outside of the ring is relatively preserved, despite severely impaired retinal function. Moreover, the degeneration of photoreceptor cells outside of the ring is reflected in a loss of the ellipsoid zone and the external limiting membrane, as well as a thinning or absence of the outer nuclear

layer in an SD-OCT scan (Figure 3).[92] The autofluorescent ring itself corresponds to an area of outer segment dysgenesis and lipofuscin production, with progressive retinal thinning, usually accompanied by loss of the ellipsoid zone at—or close to—the internal edge of the ring.[92-95] In the majority of patients, the autofluorescence measured inside the ring is quantitatively similar to autofluorescence in a healthy eye.[96] Over time, the diameter of the hyperautofluorescent ring grows smaller; although the rate of this reduction in diameter varies, relatively large rings tend to reduce in size more rapidly than small rings. The inner edge of the constricting ring generally matches the progression of cone system dysfunction; in contrast, the loss of rod sensitivity is more widespread and includes the parafoveal area within the ring.[97] Eventually, the ring may disperse, and this phenomenon is correlated with a widespread loss of sensitivity and visual acuity.[97-99] Microperimetry in RP patients shows that visual sensitivity is relatively preserved within the ring, reduced in the ring zone itself, and decreased or non-recordable in the region outside of the ring.[100]

Besides the hyperfluorescent ring, other autofluorescence patterns can be observed (see Figure 5, and section 4.9). In nearly all adult patients with RP, wide-field FAF imaging shows patchy and/or reduced autofluorescence in the mid-periphery, which appears to be related to a loss of peripheral vision.[101] In addition, an abnormal pattern of increased autofluorescence maybe observed at the central macula and is associated with central visual impairment.[98,99,102]

Fluorescein angiography

These days, fluorescein angiography is not commonly used in RP. On the angiogram, chorioretinal atrophy can be readily observed, initially in the periphery and/or mid-periphery, and later at the posterior pole. Although there is usually no delay in the filling of the retinal vessels, the vessels themselves are attenuated, and some leakage of dye may be present. The presence and extent of CME is also easily depicted with fluorescein angiography. Choroidal neovascularization—although not common in RP—can be visualized with fluorescein angiography and, more recently, with optical coherence tomography angiography (OCTA), a non-invasive alternative.[103,104]

Adaptive optics scanning laser ophthalmoscopy

Adaptive optics scanning laser ophthalmoscopy (AOSLO) is a relatively new, non-invasive imaging modality that enables the visualization of photoreceptors at a microscopic level by correcting for ocular aberrations.[105] In patients with RP, the high resolution of AOSLO allows early detection of photoreceptor damage, even when the outer retinal architecture on OCT appears intact.[106] In addition, it can reveal a decrease in cone density before the visual acuity is reduced, since a significant cone reduction is possible before the visual acuity becomes affected.[107] AOSLO is a highly sensitive imaging modality that may be of additional value in monitoring disease progression, and evaluating treatment safety and efficacy in clinical trials.
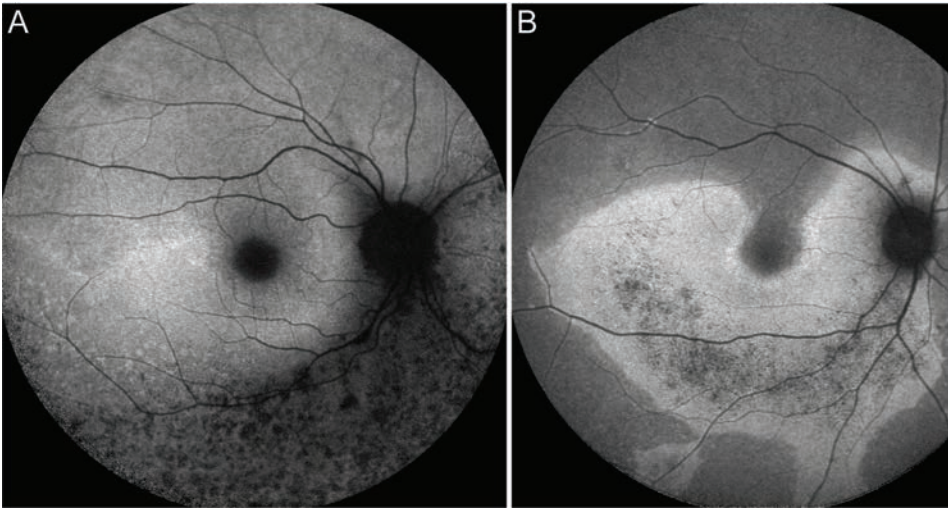
Figure 5. Fifty-five-degree fundus autofluorescence (FAF) images of two RP patients that illustrate the diversity of autofluorescence patterns in RP. (A) FAF image of 27-year-old female with *FAM161A*-associated RP, showing a curvilinear arc of hyperautofluorescence surrounding the macula, in combination with sectoral peripheral hypoautofluorescence in the inferior quadrants. (B) FAF image of a 55-year-old female with *EYS*-associated RP, showing a well demarcated hyperautofluorescent area along the inferior vascular arcade, partially surrounding the fovea.

Differential diagnosis for non-syndromic retinitis pigmentosa

The spectrum of IRDs is broad and includes disorders that primarily affect the macula (e.g., Stargardt disease and Best vitelliform macular dystrophy) and stationary disorders such as achromatopsia and CSNB. Precisely where RP lies within this spectrum is based on both relatively objective criteria such as symptoms, fundus abnormalities, and ERG findings, as well as seemingly arbitrary criteria such as the patient's age at onset and even historical factors. Finally, when classifying an IRD, it is important to take the entire disease course into consideration, as some phenotypes tend to overlap in late stages. An overview of the considerations for differential diagnoses in RP is given in Table 1 (See Appendix 1 for a more comprehensive overview, including clinical features).

Other inherited retinal dystrophies
Early-onset RP has both clinical and genetic overlap with LCA, and both disorders represent a continuum of retinal dystrophies divided by indistinct criteria based on the age of onset. Most often, patients who present at birth or within the first few months of life are classified as having LCA.[108] The lower age limit for diagnosing RP has been set by some after infancy (variably defined as age one or two), resulting in a gray area where both disorders overlap.[108] In LCA, the extremely early loss of visual function leads to a set of symptoms that include nystagmus, sluggish or near-absent pupillary response, photophobia, and oculo-digital signs such as poking, pressing, and

Table 1. Differential diagnoses for non-syndromic retinitis pigmentosa.

inherited retinal diseases	Syndromic forms of retinitis pigmentosa	Pseudoretinitis pigmentosa
Progressive retinal disease • Cone-rod dystrophy • Cone dystrophy • Leber congenital amaurosis • Bietti crystalline corneoretinal dystrophy • Late-onset retinal degeneration • Macular dystrophy (Stargardt disease, Sorsby fundus dystrophy) **Stationary retinal disease** • Congenital stationary night blindness (including fundus albipunctatus and Oguchi disease) **Inherited vitreoretinopathies** • X-linked juvenile retinoschisis • Enhanced S-cone syndrome/ Goldmann-Favre syndrome • Wagner syndrome/erosive vitreoretinopathy • Snowflake vitreoretinopathy **Chorioretinal dystrophies** • Choroideremia • Gyrate atrophy • Helicoid peripapillary chorioretinal degeneration (Sveinsson chorioretinal atrophy) • Progressive bifocal chorioretinal atrophy **Female carriers of inherited retinal diseases** • Retinitis pigmentosa • Choroideremia • Ocular albinism	**Ciliopathies** • Usher syndrome • Bardet-Biedl syndrome • Cohen syndrome • Joubert syndrome • Senior-Løken syndrome • Sensenbrenner syndrome (cranioectodermal dysplasia) • Short-rib thoracic dysplasia with or without polydactyly (includes Jeune, Mainzer-Saldino, Ellis-van Creveld, and short-rib polydactyly syndrome) **Metabolic disorders** • Alfa-tocopherol transfer protein deficiency (familial isolated vitamin E deficiency) • Bassen-Kornzweig syndrome (abetalipoproteinemia) • Mucopolysaccharidoses • Neuronal ceroid-lipofuscinoses, childhood onset (Batten disease) • Refsum disease (phytanic acid oxidase deficiency) • Mevalonate kinase deficiency • HARP syndrome (hypoprebetalipoproteinemia, acanthocytosis, RP and pallidal degeneration) • PHARC syndrome (polyneuropathy, hearing loss, ataxia, RP, and cataract) **Mitochondrial disorders** • Kearns-Sayre syndrome • NARP syndrome (neuropathy, ataxia, and RP)	**Drug-induced** • Thioridazine and chlorpromazine • Quinolines (e.g. (Hydroxy) chloroquine) **Chorioretinal infections** • Syphilis, Lyme disease, acute retinal necrosis and other viral infections (rubella, chicken pox, measles, cytomegalovirus) **Sequela of inflammatory disease** • Sarcoidosis • Acute posterior multifocal placoid pigment epitheliopathy • Birdshot chorioretinopathy • Serpiginous choroidopathy • Diffuse unilateral subacute neuroretinitis • Systemic lupus erythematosus **Miscellaneous** • Vitamin A deficiency • Paraneoplastic • Trauma • Siderosis bulbi • Old retinal detachment • Pigmented paravenous retinochoroidal atrophy • Acute zonal occult outer retinopathy

rubbing the eyes. Visual acuity is rarely better than 20/400, and the aspect of the fundus can range from normal to an extensive atrophic RP-like pigmentary retinopathy. Scotopic and photopic ERG recordings are generally non-recordable or—at the very least—severely reduced. As shown in Table 2, early-onset RP can present with many of these symptoms, and this overlap with LCA is clearly reflected in the number of genes associated with both disorders (see Figure 1).

Cone-rod dystrophy is another IRD that has both clinical and genetic overlap with RP. An ERG recording is not always conclusive with respect to determining which photoreceptors are primarily affected, particularly in the later stages of the disease. However, the early symptoms of cone-rod dystrophy, which include early loss of visual acuity, intense photophobia, variable achromatopsia, and the initial absence of night blindness, can help the practitioner differentiate between cone-rod dystrophy and RP.[109]

Certain retinal dystrophies demonstrate degeneration in a rod-cone pattern; however, based on their highly specific phenotype, they have historically been differentiated from RP. Examples are choroideremia (patchy chorioretinal atrophy and normal appearing retinal vessels), gyrate atrophy (well demarcated circular chorioretinal atrophy with elevated ornithine levels), and late-onset retinal degeneration (perimacular drusen-like lesions and long anterior lens zonules).[110,111] Retinitis punctata albescens also has a very specific phenotype; nevertheless, this entity has been considered an RP subtype throughout most of the literature.

CSNB is an example of a stationary disorder characterized predominantly by rod dysfunction. With the exception of two subtypes of CSNB—namely, Oguchi disease and fundus albipunctatus—CSNB patients generally have a normal fundus. However, CSNB has considerable overlap with RP with respect to the genes involved; thus mutations in the *PDE6B*, *RDH5, RHO, RLBP1,* and *SAG* genes can lead to either RP or CSNB.112

Syndromic RP

Mutations in genes involved in ciliary function often—but not always—result in a syndromic form of RP. Arguably, the most common ciliopathy is Usher syndrome, which presents with a variable degree of neurosensory hearing loss.[113] Another well recognized syndromic form of RP is Bardet-Biedl syndrome; in addition to retinopathy, patients with this syndrome can also present with obesity, postaxial polydactyly, hypogonadism, renal dysfunction, and/or cognitive impairment.[114] The type and extent of these extra-ocular features in Bardet-Biedl can vary widely and depend—for the most part—on the specific gene involved and the specific mutation within that gene. Syndromic RP is also associated with systemic metabolic and mitochondrial disorders. The extra-ocular features in syndromic RP can be extremely subtle (for example, an impaired sense of smell) and/or easily overlooked by the examining ophthalmologist (for example, in the case of cardiovascular and/or renal disease); on the other hand, some features can be surgically corrected at an early age (e.g., polydactyly). Therefore, obtaining a careful, thorough history that includes these various extra-ocular abnormalities is extremely important for obtaining a diagnosis. However, genetic analysis may reveal mutations in a gene that is associated with syndromic forms of RP, when the initial clinical assessment did not indicate extra-ocular abnormalities. In such cases, it is important to reexamine the patient for the presence of systemic manifestations. For example, patients with *TRNT1*-associated RP all demonstrate a mild erythrocytic microcytosis that is only discovered after analysis of the blood count parameters.[115] Keep in mind, however, that not all extra-ocular abnormalities indicate syndromic disease: these abnormalities should match with the gene involved. A number of genes associated with non-syndromic RP (e.g. *BBS1*, *CLRN1* and *USH2A*) may also cause syndromic RP (see Table 2). Correctly diagnosing a patient with syndromic RP can have sight-saving—or even life-saving—implications, particularly in patients with a metabolic disorder such as Refsum disease or Kearns-Sayre syndrome, a mitochondrial disorder that often includes cardiac dysfunction.

Pseudoretinitis pigmentosa

Several conditions can mimic the clinical features of RP (phenocopy) and are classified as pseudoretinitis pigmentosa (Table 1, Appendix 2). It is important to distinguish these entities from RP, as several forms of pseudoretinitis pigmentosa are treatable and do not have an underlying genetic component. A thorough history, including current and past medications, lack of interocular symmetry, and lack of disease progression, may indicate a diagnosis other than RP. Indeed, many patients who were diagnosed with "unilateral RP" fall in this category, although a germline mutation in the *RP1* gene was reported in a patient with strictly unilateral RP.[116]

Clinical findings in genetic subtypes of RP

In Chapter 2, we discussed the typical features attributed to RP in general. However, the heterogeneous presentation of these conditions warrants a closer look at the clinical findings that have been reported for genetic subtypes of RP. Many early studies used non-genotyped RP cohorts and occasionally subdivided the patients according to their inheritance pattern. More recently, however, the phenotype for a specific causative gene is described, albeit with limited numbers of patients and/or a lack of clinical details. Obtaining a clear picture regarding the phenotypes associated with genetic subtypes of RP is therefore challenging. In Tables 2 and 3 and Figure 6, we provide a comprehensive overview of the specific clinical features attributed to various subtypes in order to help the clinician identify the subtype and predict the clinical course. In addition, a unique atlas containing color fundus photographs of most RP subtypes is available in Appendix 3. Nevertheless, it is important to realize that even within a specific subtype, considerable phenotypic variation can occur due to the variable effects of mutations, genetic modifiers, and—in some cases—environmental factors.

Figure 6. Fundus photographs of patients with various non-syndromic RP subtypes. ▶
(A) Composite fundus photograph of a 47-year-old male patient with *USH2A*-associated RP, showing bone spicule pigmentation in the mid-periphery, and attenuated vessels. (B) Composite fundus photograph of a 59-year-old female patient with *IMPG2*-associated RP, showing marked bone spicule pigmentation in the mid-periphery, waxy pallor of the optic disc, attenuated vessels, and macular atrophy. (C) Composite fundus photograph of a 27-year-old female patient with *PDE6B*-associated RP, showing bone spicule pigmentation in the mid-periphery, vessel attenuation, and CME. (D) Composite fundus photograph of a 46-year-old male patient with *CDHR1*-associated RP, showing vessel attenuation, bone spicule like pigmentation, and patchy atrophy in the periphery and macula. (E) Composite fundus photograph of a 67-year-old male patient with *CNGB1*-assocated RP, showing attenuated vessels, RPE atrophy, and mid-peripheral pigment clumping. (F) Composite fundus photograph of a 21-year-old male RP patient carrying a mutation in the *CRB1* gene, showing dense pigment migration with para-arteriolar absence of pigmentation. (G) Fundus photograph of a 42-year-old female patient with *CA4*-associated RP, showing the classical triad of bone spicule pigmentation in the mid-periphery, attenuated vessels, and waxy pallor of the optic disc. (H) Fundus photograph of a 46-year-old female *RPGR* carrier, showing a tapetal-like fundus reflex.

51
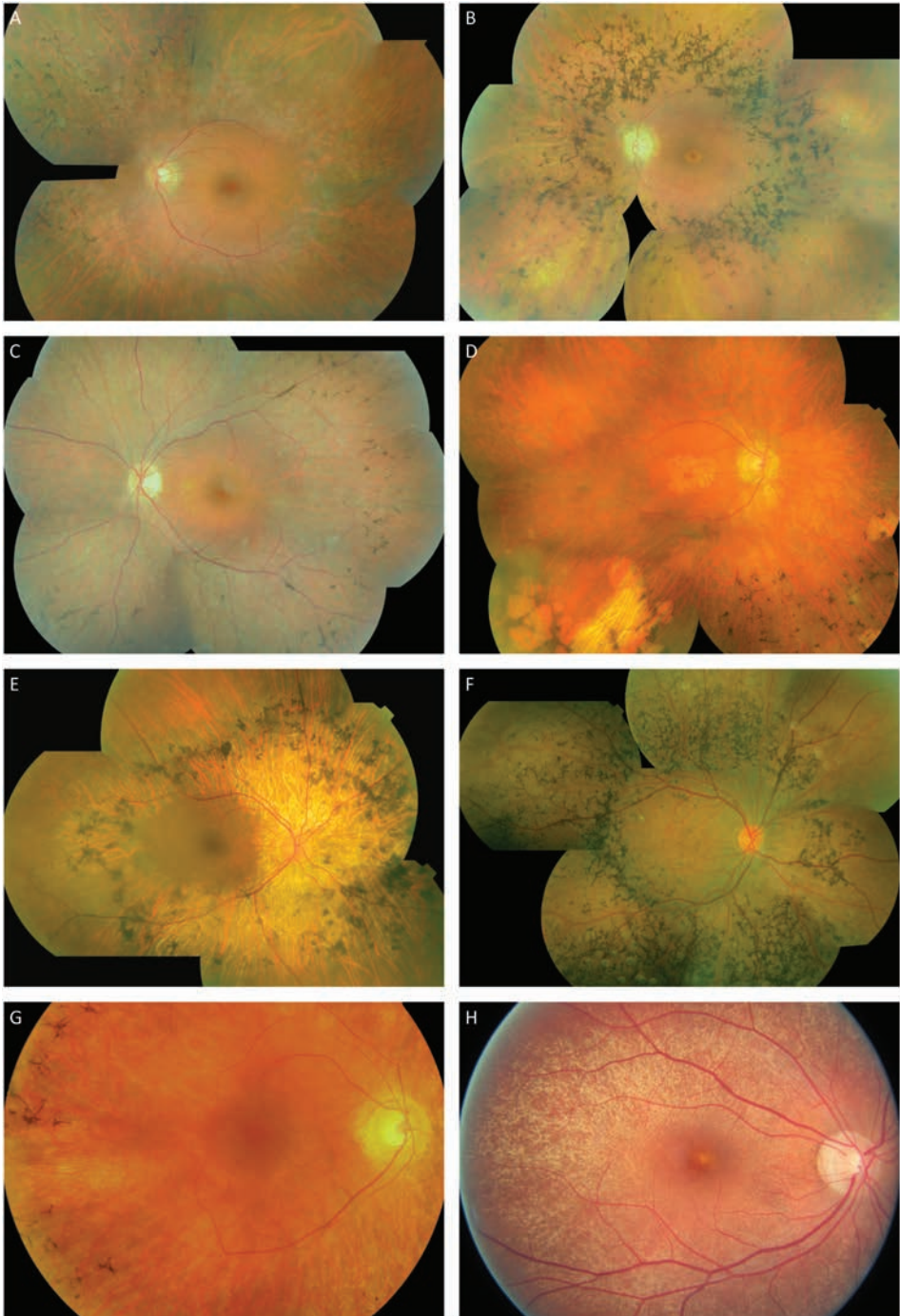
Table 2. Genetic subtypes of non-syndromic RP and their specific characteristics.

Gene/locus	RP type	Inheritance pattern	Decade of onset	Visual function
ABCA4[1a]	19	AR	1	VA is severely affected: FC to NLP at higher age.
AGBL5[2b]	75	AR	1-2	VA loss is highly variable. At 40-50 years, VA may range from 20/40 to NLP.
AHI1[2a]	NA	AR	3-4	VA in 3rd decade can range from 20/32 to HM or even LP.
ARHGEF18[2a]	78	AR	3-4	VA: 20/30-20/60 in 4th decade, but may decrease to CF in the 6th decade. Photopsias.
ARL2BP[2b]	66[§]	AR	3	Relative early loss of VA: HM (or even LP) in the 4th decade of life. Yet, other patients may retain a VA of 20/40 up to the 6th decade of life.
ARL6[3a]	55	AR	NA	No information on the visual function available.
BBS1[2a]	NA	AR	1-2, (earliest:1y)	Severe visual loss, may reach LP by 5th - 6th decade of life. Severe constriction of VFs up to 5˚-10˚ in the 4th decade.
BBS2[2a]	74	AR	1-2	Severe, relative early visual loss: HM or LP before the age 60. VFs are severely constricted.
BBS9[2a]	NA	AR	NA	No further information available.
BEST1[2a]	50	AD AR (1 family)	1-2, (5)	Nightblindness may be absent. Loss of VA is a prominent symptom.
C2orf71[1a]	54	AR	1-2 (2 cases <5y)	Night blindness may be absent. Ring scotomas in 4th -5th decade of life. Photophobia may occur.
C8orf37[1a]	64	AR	1-2	Severe visual loss to HM/LP in the 4th decade. The VF is constricted to 5˚. Sometimes photophobia.
CA4[2b]	17*	AD	2-3	VA levels of 20/200 (age 11) and LP (58 years).
CDHR1[2a]	65	AR	2	VA loss to HM by the 4th or 5th decade of life. Severe color vision defects and VF constriction to 5-10˚, sometimes with mid-peripheral residue. Photophobia (3rd decade).
CERKL[1a]	26	AR	2-3 (mean: 23y)	VA generally severely affected and may decrease to LP around the 5th decade. Photophobia.
CLN3[a]	NA	AR	1-5	VA loss to HM by the 5th decade reported. Severe constriction of VFs up to 5˚-10˚ in the 6th decade.
CLRN1[3a]	61	AR	NA	Classic RP phenotype.
CNGA1[1a]	49	AR	1	A gradual decrease in VA may occur from the 4th decade onwards. Concentric constriction of the VF during the 3rd decade of life.
CNGB1[1a]	45	AR	1-2	Macular involvement with VA loss to LP. VF loss from a mean age of 33 years (13-40). Sometimes photophobia.
CRB1[1a]	12	AR	1-5 (median: 4y)	50% of patients have a VA <20/200 at age 35 years.
CWC27[3a]	NA	AR	1	VF is severely constricted early in the disease course.
DHDDS[1a]	59	AR	2-3	VA is generally mildly affected, although in some eyes VA decreases to LP levels.

Ophthalmic features	ERG	Syndromic associations	Other IRD phenotypes	Ref
Bone spicule-like pigmentation may reach into the macular region. Severe chorioretinal atrophy.	Rod-cone pattern, later both responses NR	-	STGD, CRD (may occur simultaneously in RP families)	126-131
Macular involvement: macular atrophy, CME. PSC.	Rod-cone pattern	Mental retardation (correlation with *AGBL5* unknown)	-	132-134
Macular involvement. PSC.	Rod-cone pattern	JS type 3	-	135-138
Nummular pigment clumping, CME. Vitreous opacities (in 1 patient)	Rod-cone pattern	-	-	139
Marked macular atrophy, PSC, ERM.	NR	Situs inversus, primary ciliary dyskinesia (respiratory failure), otitis media	-	140,141
No information on the retinal phenotype available.	No further information available	BBS type 3	-	142-144
Nystagmus, possible macular atrophy, cataract (PSC and cortical).	Generally NR, severely disturbed in rod-cone pattern in 2nd decade	BBS type 1	-	145,146
Macular atrophy, bull's eye maculopathy, PSC, ERM.	NR	BBS type 2	-	147,148
No information on the retinal phenotype available.	No further information available	BBS type 9	-	149,150
Yellow fundus flecks in the mid-periphery, pigmentation in far periphery, CME, ERM. Macula relatively spared unless serous macular detachments.	NR scotopic responses, residual photopic responses	-	BVMD, AVMD, ARB, ADVIRC	151-153
Foveal atrophy. Early onset associated with severe chorioretinal atrophy.	Rod-cone pattern, often NR	Hearing loss, ataxia and cerebellar atrophy (digenic with RP1L1)	-	154-160
High myopia, cataract. Marked geographic macular atrophy.	Generally NR	BBS type 21	CRD	161-164
Pigment clumping at the level of the RPE has been described (in 1 patient).	Reduced or NR photopic and scotopic responses	-	-	165-167
In early stage: sparse bone spicule pigment migration. Later stages: dense pigment migration, macular atrophy.	Generally NR, although ERG may show recordable rod- and cone-driven responses	-	CRD	168-170
Early macular involvement, sometimes with hyperpigmentation. Pericentral localization of bone spicules. Normal appearance of optic disc.	Responses are SR in a rod-cone pattern, may be NR in the 3rd decade	-	-	171-176
Sparce bone spicule pigmentation, macular atrophy, CME	NR or rod-cone pattern	JNCL	CRD	177,178
Typical RP features.	Rod-cone pattern	USH type 3	-	179-181
Sometimes macular atrophy. Pericentral RP (described once).	NR	-	-	182-188
Macular atrophy, pericentral RP (described once).	Rod-cone pattern	-	-	154,188-193
Nystagmus (±40%), hyperopia, CME (50%), PPRPE, Coats-like vasculopathy, optic disc drusen, retinal vascular sheathing, asteroid hyalosis, thickened retina with loss of the retinal laminations, bull's eye maculopathy and yellow round deposits in the posterior pole. Occasional dense pigmentation.	NR from 2nd – 3rd decade	Nanophthalmos	LCA, PPRCA	55,194-201
No information on the retinal phenotype available.	No further information available	Brachydactyly, craniofacial abnormalities, short stature, neurologic defects	LCA	202
Occasional CME. Parafoveal atrophy of the RPE. Pericentral localization of pigmentation (reported once).	SR or NR rod- and cone-driven responses from the 2nd decade.	-	-	175,203-205

Gene/locus	RP type	Inheritance pattern	Decade of onset	Visual function
EYS[1a]	25	AR	2-3 (range 8-62y)	VA loss from the 4th decade to levels of 20/200 to NLP in the 7th decade.
FAM161A[1a]	28	AR	2-3	Legally blind in 6th – 7th decade. Constriction of to 10˚.
FSCN2[2a]	30	AD	1	VA and VF relatively spared until the 4th decade, then VA loss to levels of HM.
				Unclear if *FSCN2* is involved in RP, because the c.72delG mutation does not segregate in Chinese families
GNAT1[3a]	NA	AR	2	Variable VA: 20/20 (80 years) to 20/80 (32 years).
GUCA1B[2b]	48	AD	NA	Variable visual function: 20/20 (62 years) – 20/100 (47 years).
HGSNAT[2b]	73	AR	1-2 5-6	Severe VA loss to CF at age 60 years. VA is more preserved in case of late disease onset.
HK1[1b]	79	AD, NP ≤15%	1-4 (range 4y-mid-30s)	Highly variable VA loss. VA loss to CF in 3rd decade reported. Photophobia.
IDH3A[2b]	NA	AR	1-2 (range 1-11y)	VA loss dependent on the presence of macular pseudocoloboma.
IDH3B[3b]	46	AR	NA	Classic RP phenotype.
IFT140[1a]	NA	AR	1-4 (range 2y-early-30s)	Vision loss from 3rd - 5th decade, VA may eventually reduce to LP.
IFT172[3a]	71	AR	1-2	Night blindness is the initial symptom. Further symptoms have not been specified.
IMPDH1[1a]	10	AD AR: (Asp226Asn)	1-3	*AD disease*: variable degrees of VA loss. Legal blindness before the age of 40 has been described.
				AR disease: no information on the visual function available.
IMPG2[1b]	56	AR	1-2	Central vision generally affected.
KIZ[2b]	69	AR	2	Classic RP phenotype.
KLHL7[1b]	42	AD	3	VA remains (near) normal up to the 5th or 6th decade. VF loss usually is the initial symptom.
LRAT[1a]	NA	AR	1 (earliest: 2y)	Severe, early VA loss to 20/100-20/200 and VF constriction to 30˚- 60˚ before the age of 10 years. Photophobia.
MAK[1b]	62	AR	2-5	May show initial preservation of nasal VF.
MERTK[1a]	38	AR	1-2 (earliest: 3y)	VA loss to ≤20/200 in the 2nd decade. Variable VF loss: normal VF (3rd decade) – 5˚ (2nd decade). Legal blindness: ±40 years. Impaired color discrimination.
MVK[3b]	NA	AR	3	VF loss may be the initial symptom.
NEK2[3a]	67	AR	NA	No information on the visual function available.
NR2E3[1a]	37	AD, AR	1-3 (earliest: 3y)	*AD disease*: VF loss from the 2nd– 3rd decade.
				AR disease: early VA loss.

Ophthalmic features	ERG	Syndromic associations	Other IRD phenotypes	Ref
Variable levels of bone spicule pigmentation and macular atrophy. PSC.	Rod-cone pattern, but often NR	-	-	206-209
Limited number of bone spicules. Macular atrophy. PSC.	NR	Hearing problems, hyposmia	-	210-215
Early vessel attenuation. Incidental macular atrophy.	SR at early ages, generally NR from the 4th decade	-	MD	216-219
				220,221
Round pigment clumps and typical bone spicules. ERM.	Rod-cone pattern or NR	-	CSNB	222-224
Highly variable retinal expression in Japanese patients: normal fundi, sector RP with macular involvement, only macular atrophy or diffuse RP.	NR in patients with diffuse RP. Sector RP with macular atrophy leads to reduced scotopic and photopic responses	-	MD	225
CME, ERM, pericentral RP (described once).	Reduced or NR rod- and cone-driven responses	MPS type IIIC	-	226,227
Bull's eye maculopathy, pericentral RP.	Rod-cone pattern	HMSN, nonspherocytic hemolytic anemia	-	228-230
Macular pseudocoloboma, CME.	SR or NR rod-drive responses, cone-responses SR	-	-	231
Typical RP features, PSC.	SR amplitudes of both scotopic and photopic responses	-	-	232
Macular atrophy, CME, ERM, early cataract or white dots. Dense pigmentation in 7th decade reported.	SR in a rod-cone pattern	SRTD type 9	LCA	233-237
Variable macular involvement: macular atrophy, CME, ERM.	No further information available	SRTD type 10, BBS type 20	-	238-240
AD disease: CME, significant vitreous disturbances, PSC.	*AD disease*: SR or NR rod and cone responses	-	LCA	241-245
AR disease: macular involvement.	*AR disease*: NR			
Macular atrophy and bull's eye maculopathy. Sheathing of peripheral vessels.	SR in a rod-cone pattern or NR	-	VMD	246,247
Macular thinning (in 1 patient).	NR at the age of 35 years	Obesity, hearing problems (correlation with *KIZ* unknown)	-	248
Fundus appearance can be normal up to the 4th decade. Later: CME and parafoveal atrophy.	Rod-cone pattern, eventually NR. The mean (SD) decline in light-adapted 31-Hz flicker response is 3.0% (3.0) per year.	CISS	-	249-252
High hyperopia, nystagmus, poorly reactive pupils. Sparse or absent bone spicules (age 9 years). RPA. Reduced FAF signal.	SR in a rod-cone pattern or NR	-	LCA	118,253-256
Macula generally not involved, but sometimes CME (in 1 patient) or macular atrophy.	Reduced in a rod-cone pattern, but often NR	-	-	205,257-260
Nystagmus, bull's eye maculopathy, macular atrophy. Pallor of the optic disc may be absent.	Photopic responses become NR during the 1st decade. Scotopic responses are NR	-	LCA	261-266
Arterial tortuosity, PSC, ERM, thickening of the nerve fiber layer on OCT, CME (described once).	SR in a rod-cone pattern	MKD (MEVA or HIDS)	-	267,268
No information on the retinal phenotype available.	No further information available	-	-	269
AD disease: nummular and spicular pigmentation. Early-onset cataract. FAF: 2 or 3 hyperfluorescent rings may be visible. Pericentral RP.	*AD disease*: rod-cone pattern. Rod responses are SR, and become NR in advanced disease. Cone-driven responses are affected relatively late.	-	ESCS	119,270-275
AR disease: clumped pigment	*AR disease*: rod-cone pattern			

Gene/locus	RP type	Inheritance pattern	Decade of onset	Visual function
NRL[1a]	27	AD, AR	1 (earliest: 1y)	*AD disease*: VA loss from the 4th decade: 20/20 – 20/00. VF diameters: 50-60˚ in the 3rd decade and decrease up to 10˚ in the 8th decade.
				AR disease: visual function is more severely affected compared to AD disease.
OFD1[2a]	23	XL	1 (<2y)	Early loss of central vision. Only temporal and inferior VF residues.
PANK2[3a]	NA	AR	5	VA reduction to HM in the 6th decade.
PDE6A[1]	43	AR	1	Marked peripheral VF loss.
PDE6B[1a]	40	AR	1	Loss of peripheral VF is a prominent symptom that occurs during the 2nd-3rd decade.
PDE6G[3a]	57	AR	1	Marked constriction of the VF up to 5-10˚.
POMGNT1[1a]	76	AR	1-2 (3-4)	Variable VA loss, may decrease to LP. VF constriction to 5˚ in the 6th-7th decade.
PRCD[1a]	36	AR	1-3	Relative early visual loss.
PROM1[1a]	41	AR	1	Visual loss during the 1st decade.
PRPF3[1a]	18	AD, full penetrance	1 (4, once)	Classic RP phenotype.
PRPF4[2a]	70	AD	2-3	Variable visual loss, may reach HM. VF constriction to 5-10˚ in the 6th decade.
PRPF6[3b]	60	AD	2-4	VA initially spared, but may decrease to LP. Constriction of VFs to 30-40˚ (4th decade) and ±10˚ (6th decade).
PRPF8[1a]	13	AD	1-2	VA may remain normal up to the 3rd – 4th decade, with progression to 20/200 in the 7th decade. VF constriction to ±10° in 4th decade.
PRPF31[1a]	11	AD NP ≤10%	1-2	Variable presentation. Incomplete penetrance suggested in asymptomatic patients. Mean annual VF loss: 6.9%. Legal blindness: 4th decade.
PRPH2[1a] (formerly known as RDS)	7	AD digenic with ROM1	2-6	VA usually spared, but dependent on the degree of macular involvement.
RBP3[2a]	66[§]	AR	*Early onset*: 1	*Early-onset disease*: early visual loss. Strabismus.
			Late-onset: 4-6	*Late-onset disease*: blurred vision is an early symptom; night blindness may be absent.

Ophthalmic features	ERG	Syndromic associations	Other IRD phenotypes	Ref
AD disease: nystagmus, minimal or absent hyperpigmentation in 2nd decade. Round pigment clumps. Chorioretinal atrophy, macular atrophy, bull's eye maculopathy, PSC. Peripheral retinal telangiectasis (which may cause serous retinal detachment).	NR	-	-	276-281
AR disease: peripheral pigment clumps. Retinal features are similar to NR2E3-associated enhanced S-cone syndrome.				
Grayish spots at the level of the RPE. Granularity of macular RPE.	NR	JS, OFDS type 1, SGBS type 2	-	282-284
No information on the retinal phenotype available.	No further information available	HARP syndrome, NBIA1 (also termed HSS)	-	233,285, 286
CME, PSC and dense pigmentation.	Rod-cone pattern	-	-	287-290
CME, PSC, dense pigmentation at high age (80 years), pericentral RP.	Rod-cone pattern *Carriers*: rod-driven responses may be reduced	-	CSNB	188,291-298
Normal vessels and optic discs in young patients. CME in all patients (1 family).	Both rod- and cone-driven responses are NR within the 1st decade of life.	-	-	299,300
Macular involvement, CME.	NR	MEB	-	301-303
Various macular involvement: bull's eye maculopathy, macular atrophy, CME. ERM, PSC. Fairly normal-colored optic disc.	Scotopically and photopically NR in an early stage of disease (earliest described: age 6 years)	-	-	233,304-307
Large inter- and intrafamilial variability: from isolated (bull's eye) maculopathy to pericentral RP and severe RCD. Nystagmus.	NR	Polydactyly	CRD, AD MD	188,308-313
Classic RP phenotype.	Rod-cone pattern Rod-driven responses are abolished from the 2nd decade, cone-driven responses are SR by then	-	-	314-319
Variable degree of macular atrophy.	Generally NR	-	-	320,321
Macular atrophy in later stages. Optic nerve heads may initially be normal. PSC.	SR responses in the earlier phases of the disease. Scotopic responses become NR over time, photopic responses tend to diminish more slowly.	-	-	322
Dense intraretinal pigment migration (in 1 patient).	NR	-	-	314,319, 323,324
Macular atrophy, CME, PSC. May present with para-arteriolar absence of pigmentation or pericentral RP (described once). No abnormalities observed in patients that lack penetrance.	The mean (SD) decline in light-adapted 30-Hz flicker response is 9.2% per year. Responses may be normal in patients that lack penetrance	-	-	188,314, 319, 325-327
Variable macular involvement, CME, RPA, pericentral RP (described once).	Rod-cone pattern, will become NR during 6th decade	-	MD, PD, CRD, LCA	175, 328-333
Early-onset disease: (high) myopia, PSC.	*Early-onset disease*: SR responses, most often in a rod-cone pattern, although cone-rod patterns also occur.	-	-	123,334, 335
Late-onset disease: PSC, (high) myopia.	*Late-onset disease*: SR rod- and cone-driven responses, often NR			

Gene/locus	RP type	Inheritance pattern	Decade of onset	Visual function
RDH12[1a]	53	AD, AR	*AD disease*: 2-5	*AD disease*: classic RP phenotype.
			AR disease: 1-3	*AR disease*: VA at presentation: 20/40-20/200, may reach HM-LP. VF constriction to <5˚ in the 2nd – 3rd decade. Central scotoma may occur. Photophobia.
REEP6[2a]	77	AR	1-2	Gradual VA loss, although a decline to 20/400 at the age of 32 has been described.
RGR[1b]	44	AR	NA	VA loss to ≤20/200. Severe VF constriction.
	Unclear if *RGR* is involved in RP, or due to parallel occurrence of *CDHR1* mutation			
RHO[1a]	4	AD, AR	1-2, (4)	Highly variable clinical course (also intrafamilial). Annual VA decline: 1.6%. Annual VF loss: 2.6%. Legal blindness: 6th – 8th decade.
RLBP1[1a]	NA	AR	2	Variable VF loss from the 3rd decade, to <5° residues.
ROM1[1a]	NA	Digenic (*ROM1*: Leu185Pro + *PRPH2*)	NA	No information on the visual function available.
RP1[1a]	1	AD, AR	*AD disease*: 2-3	*AD disease*: moderate decrease in VA in 4-5th decade.
			AR disease: 1	*AR disease*: relative early loss of VA to CF or HM in the 5th decade. VF constriction to 10˚ in the 3rd decade.
RP1L1[3a]	NA	AR	4-5	Moderate decrease in VA to ±20/80. VF constriction to 5˚ in the 8th decade.
RP2[1a]	2	XL	1	Early loss of central vision. Central scotoma in 50% of patients. Severe VF constriction in 2nd decade. Large intrafamilial differences.
			Female carriers: can be affected as well. Presentation highly variable.	
RP9[3b]	9	AD NP	1-2	Highly variable presentation. Incomplete penetrance suggested in asymptomatic patients. Relative early VF constriction: <20˚ in 3rd decade.
RPE65[1a]	20	AD (NP described), AR	*AD disease*: 2-5	*AD disease*: incomplete penetrance suggested in asymptomatic patients. Early loss of central vision.
			AR disease: 1	*AR disease*: severely, relative early visual loss: CF or HM in the 1st decade. Photophobia is generally absent.
RPGR[1a]	3	XL	1-2	Early loss of central vision. Annual VF loss: 4.7-9%. Mean age legally blind: 45 years.
			Females carriers: can be affected as well. Presentation highly variable.	
RPGRIP1[2a]	NA	AR	1-2	Relative early VA loss to levels of 20/200-CF in 3rd decade.
SAG[1a]	47	AD, AR	2	*AD disease*: VF constriction to 10°.
			AR disease: VA loss may precede NB.	
SAMD11[3b]	NA	AR	3-4	Loss of VA from the 6th decade, may eventually reach HM. VF constriction to <10°. Incidental photophobia.
SEMA4A[2a]	35	AD	NA	No information on the visual function available.
SLC7A14[2a]	68	AR	1-2	Visual loss, may reach HM in the 4th decade.

	Ophthalmic features	ERG	Syndromic associations	Other IRD phenotypes	Ref
	AD disease: typical RP features.	*AD disease*: no further information available	-	LCA	233, 336-341
	AR disease: nystagmus, macular atrophy, dense intraretinal pigment migration with para-arteriolar sparing. Hyperpigmentation may reach into the macular region. Preservation of peripapillary RPE. CME, PSC.	*AR disease*: NR or SR in both scotopic and photopic conditions.			
	CME, PSC, vascular sheathing.	SR in a rod-cone pattern or NR	Anosmia	-	342
	Macular atrophy in patients with severely affected VA.	Responses are reduced in a rod-cone pattern	-	-	343,344
					344
	Sector RP, and to a lesser extent pericentral RP. CME. Late-onset chorioretinal atrophy in patients with p.Met207Lys mutation.	Rod-cone pattern. Mean annual decline: 7.7 - 8.7%.	-	CSNB	57,175, 345-349
	Minimal or absent bone spicules, RPA.	Rod-cone pattern	-	BRD, NFRCD, FA	154,350, 351
	No information on the retinal phenotype available.	SR scotopic and photopic responses	-	-	352-354
	AD disease: PSC. RP sine pigmento (described once).	Rod-cone pattern	-	-	122, 355-362
	AR disease: macular atrophy, CME, myopia.				
	Typical RP features.	NA	Hearing loss, ataxia, cerebellar atrophy (digenic with C2orf71)	OMD	158,363
	Myopia. Bull's eye maculopathy, macular atrophy, sometimes choroideremia-like degeneration. A tapetal-like reflex (reported once).	Rod-cone pattern	-	-	364-369
	PSC, CME, macular atrophy. Early stage: regional (or 'patchy') loss of rod and cone function.	Highly variable, varying from normal to NR responses.	-	-	370-372
	AD disease: (sparce) nummular and spicular pigmentation. Extensive chorioretinal atrophy, macular atrophy. PSC.	Scotopic responses are generally NR, residual photopic responses may be present, but often NR.	-	LCA	373-378
	AR disease: nystagmus, macular atrophy. Bone spicule pigmentation is often sparse. Lack of FAF.				
	Variable macular involvement: from no abnormalities to atrophic lesions. Coats-like vasculopathy (1 patient). OCT: Ellipsoid zone width constriction ±175 μm/year; ONL thinning ±2,50 μm/year.	Rod-cone pattern, but often NR. Annual decline in cone ERG amplitude: 7.1%	Hearing loss, respiratory infections	CRD, CD, MD	53,368, 379-385
	Female carriers: tapetal-like reflex possible.				
	Nystagmus, macular atrophy, pigmentary changes may be sparse or absent.	NR	-	LCA, CRD	386-388
	AD disease: typical RP features, hyperreflective foci on OCT.	Rod-cone pattern	-	Oguchi disease, (can occur simultaneously within families)	389-392
	AR disease: macular atrophy, CME Golden-yellow fundus reflex with Mizuo-Nakamura phenomenon.				
	Foveal atrophy, ERM, PSC. Incidental: CME, corneal guttata.	NR	-	-	393
	No information on the retinal phenotype available.	No further information available	-	CRD	394,395
	Extensive chorioretinal atrophy, including macular atrophy.	NR	-	-	396

Chapter 2.1

Gene/locus	RP type	Inheritance pattern	Decade of onset	Visual function
SNRNP200[1a]	33	AD, NP described	1-4 (mainly 2)	Variable progression. Generally slow VA loss to HM in the 8th decade. VF constriction to 10˚.
SPATA7[1a]	NA	AR	1	Considerable VA loss in case of macular involvement. Severe VF constriction.
TOPORS[1a]	31	AD	2-5	VA is maintained in most patients. Constriction of VF to 10°.
TTC8[3a]	51	AR	1-2	NB and photophobia are early symptoms. Early VA loss to 20/200.
TULP1[1a]	14	AR	1 (onset <5y possible)	Rapid progression. VA: 20/200 at age 20, may decrease to HM or even LP. VF loss to 10˚.
USH2A[1a]	39	AR	3 (mean: 25y)	VA relatively intact to 3rd to 4th decade, then annual VA decline: 2.6%. Annual loss V4e VF area: 7.0% Legal blindness (based on VA): 6th - 7th decade.
ZNF408[2a]	72	AR	2-4	VA generally remains ≥20/40 in the 5th decade VF constriction to 10° at age 50 years. Photophobia is common.
ZNF513[3a]	58	AR	1	Visual loss to 20/200 - LP.
Candidate genes				
ADGRA3[3b] (formerly GPR125)	NA	AR	NA	No information on the visual function available.
ARL3[3a]	NA	AD	3	Photopsias.
CRX[3a]	NA	AD	6-7	VA may decrease to CF in the 8th.
DHX38[3b]	NA	AR	1	VA severely affected by macular colobomas. Early loss of LP.
EMC1[3b]	NA	AR	NA	No information on the visual function available.
KIAA1549[3b]	NA	AR	NA	No information on the visual function available.
NEUROD1[3a]	NA	AR	2	VA loss from the 3rd decade.
Loci				
RP6 locus[3]	6	XL	1-2 (generally <13)	Classic RP phenotype.
RP17 locus[3]	17*	AD	NA	VA in 3rd decade can range from 20/20 to 20/200. Variable VF constriction: from pericentral scotoma to 10˚ residue.
RP22 locus[3]	22	AR	1	Rapidly progressive decline in VA, leading to severe visual impairment at the age of 40.
RP24 locus[3]	24	XL	1	Peripheral VF loss in 4th decade. *Female carriers*: asymptomatic, although perimetry reveals sensitivity losses.
RP29 locus[3]	29	AR	2-3	Onset VA loss: 3rd decade. VA may decrease to NLP in 5th decade.

Ophthalmic features	ERG	Syndromic associations	Other IRD phenotypes	Ref
Macular atrophy, CME. May present with heavy pigment clumping. PSC (patients >45 years).	SR or NR	-	-	397-402
Nystagmus, maculopathy, PSC.	NR, although a cone-rod pattern has been described in early disease	LCA with fertility- or auditory dysfunction	LCA	403-406
Pericentral RPE atrophy in young patients, which progresses to a diffuse pigmentary retinopathy with choroidal sclerosis.	Rod-cone pattern	-	-	407-409
May include macular atrophy, sparse bone spicule pigmentation.	NR	BBS type 8	-	410-413
Nystagmus, hyperopia, PSC, macular atrophy; yellow perifoveal annular ring, pericentral RP (described once).	Scotopic and photopic responses are SR or NR	-	LCA	188, 414-419
CME can be observed. FAF: distinctive pattern of diffuse and homogeneous peripheral hypoautofluorescence. RP sine pigmento (reported once), pericentral RP.	Photopic responses are SR early in disease course, and become NR as the disease progresses. Mean annual decline in amplitude to 30 Hz flashes is 13.2%.	USH type 2A	-	54, 420-426
High myopia. Vitreous condensations, PSC, ERM, CME (in 1 patient).	SR in a rod-cone pattern or NR	-	FEVR	124,125, 427
Macular atrophy in all patients, sometimes with hyperpigmentation.	Loss of both rod- and cone-driven responses.	-	-	428,429
No information on the retinal phenotype available.	No further information available	-	-	430
CME, PSC.	No further information available	-	-	431
Early macular involvement, pericentral pigmentation.	Reduced photopic and scotopic responses	-	LCA, CRD	175, 432-434
Macular colobomas.	SR rod- and cone driven responses	-	-	435
No information on the retinal phenotype available.	No further information available	Cerebellar atrophy, psychomotor retardation	-	430,436
No information on the retinal phenotype available.	No further information available	-	-	430
PSC has been reported.	Reduced or NR rod and cone responses	MODY/late-onset diabetes, neurological abnormalities	-	437-439
Female carriers: tapetal-like reflex.	Reduced scotopic and photopic responses	CGD, McLeod phenotype, mental retardation	-	440-443
Atrophic patches, pigment dispersion, granular aspect of the RPE.	MR scotopic and photopic responses.	-	-	444
Absence of pigmentation has been described. *Female carriers:* rod-driven responses may be reduced	NR.	Obesity, mental retardation, hypogonadism, hexadactyly.	-	445
Typical RP features.	SR or NR rod-driven responses in 2nd decade. Cone-driven responses: initially normal, average annual decline: 0.1 log unit during 1st and 2nd decade.	-	-	446
Anterior and posterior polar cataracts, vitreous cells, obliteration of peripheral blood vessels.	No further information available	-	-	447

Gene/locus	RP type	Inheritance pattern	Decade of onset	Visual function
RP32 locus[3]	32	AR	1	Severely, relatively early visual loss: HM in 3rd decade to LP or worse in 4th-5th decade.
RP34 locus[3]	34	XL	2	Nyctalopia is the initial symptom, despite a cone-rod pattern on ERG. Early impaired color vision.
RP63 locus[3]	63	AD	2-5	Blurred vision is an early symptom. Yet, VA generally is normal or near normal.

Withdrawn RP subtypes

- 5 Second *RHO* (RP4) locus

- 8 Initially described in an Irish family with RP and sensorineural hearing loss that was not linked to the known RP loci. Later the genetic defect in this family was mapped to 9q, and finally the causative gene, the mitochondrial *MT-TS2* gene, was identified. Same subtype as the former RP21 subtype.

- 5 Remapped to the RP3 locus (current RPGR gene).

- 16 -

- 21 Appeared to be the same subtype as the former RP8 subtype.

- 52 -

A gene is considered a candidate for causality if it has been described in association with non-syndromic RP in only one patient or family. However, this does not include a single family with non-syndromic RP caused by a gene known to be associated with syndromic RP. The caveat should be entered that some clinical characteristics are based on limited numbers of patients. The number of times a gene has been described in association with non-syndromic RP: [1] = more than 5 families described, [2] = 3-5 families described, [3] = 1 or 2 families described, [a] = animal model that displays a retinal phenotype have been described, [b] = no animal models have been described.

* possible second locus, [§] second RP 66 gene, - none.

Abbreviations: AD: autosomal dominant, ADVIRC: autosomal dominant vitreoretinochoroidopathy, ARB: autosomal recessive bestrophinopathy, AVMD: adult onset vitelliform macular dystrophy, AR: autosomal recessive, BBS: Bardet-Biedl syndrome, BRD: Bothnia retinal dystrophy, BVMD: Best vitelliform macular dystrophy, CACD: central areolar choroidal dystrophy, CD: cone dystrophy, CGD: Chronic granulomatous disease, CISS: Cold-induced sweating syndrome, CF: counting fingers, CRD: cone-rod dystrophy, CSNB: congenital stationary night blindness, DG: digenic, ERM: epiretinal membrane, ESCS: enhanced S-cone syndrome, FA: fundus albipunctatus, FAF: fundus autofluorescence, HARP: hypoprebetalipoproteinemia, acanthocytosis, RP and pallidal degeneration, HIDS: hyper-immunoglobulin D and periodic fever syndrome, HM: hand movements, HMSN: hereditary motor and sensory neuropathy, HSS: Hallervorden-Spatz syndrome, IP: inheritance pattern, IRD: inherited retinal dystrophy, JNCL: juvenile neuronal ceroid-lipofuscinoses, JS: Joubert syndrome, LCA: Leber congenital amaurosis, LP: light perception, MD: macular dystrophy, MEB: muscle-eye-brain disease, MEVA: mevalonic aciduria, MODY: maturity-onset diabetes of the young, MPS: mucopolysaccharidosis, MR: moderately reduced, MRCS; microcornea, rod-cone dystrophy, cataract, posterior staphyloma, MVK: mevalonate kinase deficiency, NA: not available, NB: night blindness, NBIA1: neurodegeneration with brain iron accumulation 1, NFRCD: Newfoundland rod-cone dystrophy, NLP: no light perception, NP: non-penetrance, NR: nonrecordable, OCT: optical coherence tomography, OFDS: orofaciodigital syndrome, OMD: occult macular dystrophy, PD: pattern dystrophy, PPRPE: preserved para-arteriolar retinal pigment epithelium, PSC: posterior subcapsular cataracts, RPA: retinitis punctata albescens, RPE: retinal pigment epithelium, SGBS: Simpson-Golabi-Behmel syndrome, SIFD: sideroblastic anemia, B-cell immunodeficiency, recurrent fevers and developmental delay, SR: severely reduced, SRTD: Short-rib thoracic dysplasia, STGD: Stargardt disease, USH: Usher syndrome, VA: visual acuity, VF: visual field, VMD: vitelliform macular dystrophy.

Ophthalmic features	ERG	Syndromic associations	Other IRD phenotypes	Ref
Generalized grayish carpet-like retinal degeneration. Bull's eye maculopathy, macular atrophy.	SR responses in 1st-2nd decade, later NR.	-	-	448
Typical RP features.	Cone-rod pattern	-	-	449
Macular atrophy in some patients.	Both rod- and cone-driven responses are generally only MR	-	-	450
				451
				452-454
				455

Chapter 2.1

Nomenclature

To understand the relatively confusing nomenclature used for RP subtypes, one must consider its origins. In the early days of genetic research on RP, subtypes were numbered according to the order in which the RP-linked loci were discovered; thus, the RP1 locus at chromosome 1 was the first RP locus discovered. Unfortunately, the order in which various RP-associated genes were identified differs from this locus-based numbering system. For example, the rhodopsin (*RHO*) gene was the first RP-linked gene identified; however, the RP subtype caused by mutations in the *RHO* gene is actually called RP4, as the *RHO* locus was the fourth RP locus identified. Over the years, the list of RP subtypes has undergone numerous changes; for example, the RP1 locus was re-defined from chromosome 1 to chromosome 4, and subtypes RP5, RP8, RP15, RP16, RP21, and RP52 have been withdrawn. The RP subtypes are listed in Table 2 and are organized according to the underlying gene (or locus if the causative gene has not been identified), rather than the traditional classification for RP subtypes, as a classification system based on the underlying gene is more informative, less subject to change, and provides a direct link to the underlying mechanism as well as possible therapeutic options.

Age of onset

In most RP cases, the disease manifests in adolescence; however, the age of onset for RP varies widely. Table 3 summarizes the genes associated with early-onset and late-onset RP. Early forms of RP and LCA have many causative genes in common; these common genes—with the exceptions of the *CWC27*, *IMPDH1*, and *CRX* genes—are all associated with an onset of RP before the age of five years. *HGSNAT*-linked RP can manifest either early or later in life, ranging from well under the age of 10 years to after the fifth decade; this wide range in onset is likely due to a large genetic-modifying effect. In addition to *HGSNAT*, two other RP genes—*CRX* and *RBP3*—have also been associated with late-onset RP. In patients who develop symptoms at a later age, one must always consider the possibility of a pseudoretinitis (see Table 1).

Refractive errors

Both myopia and hyperopia—particularly high myopia (odds ratio 10.1) and high hyperopia (odds ratio 9.7) —are more prevalent in RP patients compared to the general population.[117] Hyperopia is typical among RP patients with mutations in the *CRB1,*[55] *LRAT,*[118] or the *NR2E3*[119] gene. Interestingly, hyperopia is frequently associated with LCA, particularly among patients with a mutation in the *GUCY2D*, *RPGRIP1*, *CRX*, or *CEP290* gene.[120] Myopia is associated with Usher syndrome and the following five genetic subtypes of RP: *RP1, RBP3*, and *ZNF408* in autosomal recessive RP, and *RPGR* and *RP2* in X-linked RP.[117,121-125]

Pigmentary abnormalities

Peripheral retinal pigmentation

In addition to the typical bone spicule pigmentation that originates in the mid-periphery of the retina and has an apparent predilection for the perivascular area, other shapes and/or

Table 3. Common clinical characteristics of the genetic subtypes of non-syndromic RP.

Clinical feature	Associated genes
Age of onset <5 years	*BBS1, C2orf71, C8orf37, CRB1, CNGA1, DHX38, FSCN2, IDH3A, IFT140, LRAT, MERTK, NR2E3, NRL, OFD1, PDE6G, PRPF3, PRPF31, RBP3, RDH12, RP2,* RP32 locus, *RPE65, RPGR, RPGRIP1, SNRNP200, SPATA7, TTC8, TULP1*
Age of onset <10 years	*ABCA4, AGBL5, BBS2, BEST1, CLN3, CNGB1, CWC27, HGSNAT, IFT172, IMPDH1, IMGP2, PDE6A, PDE6B, POMGNT1, PRCD, PROM1, PRPF8, REEP6, RHO, RLBP1, RP9, SLC7A14, ZNF513,* RP6 locus, RP22 locus, RP24 locus
Age of onset >50 years	*CRX, RBP3, HGSNAT*
Early macular atrophy	*C2orf71, C8orf37, CDHR1, CERKL, CRX, DHX38, FSCN2, GUCA1B, HK1, IDH3A, IFT140, IMPG2, MERTK, PROM1, PRPF6, RDH12, RP2, RPGR, RPGRIP1, SAG, SPATA7, TTC8, ZNF513*
Bull's eye maculopathy	*BBS2, CDHR1, CRB1, IMPG2, HK1, MERTK, NRL, PRCD, PROM1, RP2,* RP32 locus
Dense pigment migration	*BEST1, CDHR1, CRB1, EYS, IFTA140, PDE6A, PDE6B, PRPF8, RDH12, SNRNP200*
Absence/scarcity of retinal hyperpigmentation	*CDHR1, CLN3, FAM161A, HGSNAT, LRAT, NRL, OFD1, RLBP1, RP1, RPE65, RPGRIP1, TTC8, USH2A*
Pericentral pigmentary retinopathy	*CERKL, CNGA1*, CNGB1*, CRX*, DHDDS*, HGSNAT, HK1, NR2E3, PDE6B, PRPF31*, PROM1*, PRPH2, RHO, TOPORS, TULP1*, USH2A*

For references, see Table 2. * phenotype described once.

localizations have also been reported. Round clumps of pigment are common in patients carrying mutations in the *ARHGEF18,*[139] *GNAT1,*[222] *NR2E3,*[119] or *NRL*[278] gene. In *BEST1*-associated RP, these pigments are typically located in the outermost periphery of the retina.[151] Para-arteriolar absence of pigmentation is a feature of RP in patients with mutations in the *CRB1,*[55,197] *PRPF31* (Appendix 3) or *RDH12*[340] gene.

Absence of retinal hyperpigmentation
An absence or scarcity of typical RP-related hyperpigmentation—known as RP sine pigmento—has been described in several RP subtypes (see Table 3), although this finding may also be related to the fact that pigmentation is sometimes absent in the early stages of RP.[456] The absence of pigmentation in RP patients over 20 years of age has been reported in patients with mutations in the *RLBP1,*[154,350] *RP1,*[457] *RPGRIP1,*[386,388] and *USH2A*[426] genes; it is important to note, however, that only the patient with *RP1*-associated RP was over 30 years of age. The reason for this lack of retinal hyperpigmentation is unclear, although myopic degeneration may be a factor in some RP patients.[210] Nevertheless, an absence of pigmentation should not be used to exclude a diagnosis of RP, particularly in young patients, although other disorders (Table 1) should also be considered. Minimal pigmentary changes have also been associated with mutations in the BBS genes; however, with the exception of *TTC8 (BBS8),* this only concerns syndromic cases.[458,459]

Pigmentary abnormalities in the macula
In certain RP subtypes, central RPE alterations and atrophy occur relatively early in the disease course (i.e., earlier than one would expect based on the degree of visual field constriction). These subtypes are associated with a more rapid decline in visual acuity[460] and can be difficult

to distinguish from a cone-rod dystrophy. The genes associated with early macular atrophy are listed in Table 3. In patients with the *DHX38*[435] or *IDH3A*[231] subtype, the macular atrophy is often referred to as macular pseudocoloboma, which is a rather unfortunate term, as a pseudocoloboma should not be confused with a "true" coloboma, which results from a closure defect in the embryonic fissure during development and is often accompanied by other closure defects. In contrast to a loss of pigmentation due to RPE atrophy, deposits of macular pigments have been described in early-onset RP subtypes due to mutations in either the *ABCA4* or *RDH12*[128,339] gene. In these subtypes, the pigment deposits extend from the periphery/mid-periphery to the macular region; in other subtypes, the macula usually remains free of pigment clumping.

Cystoid macular edema
CME is a common finding among RP patients and is prevalent in all age groups (Table 2).[461] The reported prevalence among patients with an autosomal dominant form of RP is relatively high,[39,462] although this finding has not been widely confirmed by other groups.[85,461,463] One report also suggested an association between CME and female patients.[39] The relatively high prevalence of CME among RP patients suggests that it may not be subtype-specific. A combination of CME and cells in the vitreous body has been reported in children with variants in the *CRB1* or *RP1* gene, as well as in young adults with mutations in the *PRPF31* or *USH2A* gene.[464,465] This combination of clinical findings can lead to an incorrect diagnosis of intermediate uveitis, particularly in children with RP in which retinal abnormalities are subtle or even absent.[466,467] The therapeutic opticons for CME are discussed in section 6.3.

Vascular abnormalities
Coats-like exudative retinopathy, which is characterized by retinal telangiectasia, lipid deposits, and exudative retinal detachment, has been reported in 7-15% of patients with *CRB1*-associated RP[55,199,201,468] and in one patient with a mutation in exon ORF15 in the *RPGR* gene.[385] Unlike Coats' disease, which is usually unilateral, the Coats-like phenotype in RP patients is frequently bilateral.[469] However, not all affected siblings present with the Coats-like phenotype, which suggests the presence of non-genetic factors.[195] Finally, vascular sheathing has been reported in some patients with mutations in the *CRB1* gene,[197] *IMPG2*,[247] or *REEP6* gene (Appendix 3).

Localized forms of RP
Sector RP
Although RP is considered a generalized photoreceptor dystrophy, in some patients the retinal abnormalities are limited to a specific region of the retina. In 1937, Bietti was the first to describe a form of RP in which the pigmentary alterations were limited to the inferonasal quadrant of both eyes.[470] This so-called sector RP is an atypical form of RP characterized by symmetrical areas of regional pigmentary alterations, usually restricted to the inferior quadrants of the retina.[471] Visual field defects often correspond to the boundaries of these retinal pigmentary

alterations, although the abnormalities visible on fluorescein angiography and ERG can extend beyond the affected areas seen with ophthalmoscopy.[472,473] Sector RP usually progresses slowly, but can evolve to a panretinal RP phenotype.[474,475] Sector RP has been described primarily in patients with an autosomal dominant form of RP caused by pathogenic mutations in the *RHO* gene.[474,476,477] Other groups have reported sector RP in *GUCA1B*-associated autosomal dominant[225] and *RPGR*-associated X-linked forms of RP.[478,479] Nevertheless, why the atrophic pigmentary abnormalities are initially limited to a specific region—despite the fact that the underlying molecular defects are most likely expressed ubiquitously throughout the retina—remains unclear. Localized differences in the retina's exposure to light have been suggested as a possible explanation in RP patients with mutations in the *RHO* gene.[474]

Pericentral pigmentary retinopathy

Several RP genes have been associated with pigmentary alterations and annular chorioretinal atrophy that extends temporal from the optic disc along or adjacent to the vascular arcade and tends to spare the far periphery (Table 3).[175,188,229,407] The clinical findings reported in this pericentral pigmentary retinopathy (PPR) vary among patients, including both slow progression and stationary forms of the disease.[175,480,481] PPR can be considered part of the RP spectrum, particularly in patients with progressive disease, a history of night blindness, an annular scotoma, and reduced rod activity measured on ERG. This clinical picture corresponds with reports that family members of PPR patients can present with a more typical RP phenotype.[175] PPR can resemble pigmented paravenous retinochoroidal atrophy (PPRCA) and postinflammatory changes in retinal pigmentation.

Retinitis punctata albescens

Some RP patients can present with white punctate deposits that are distributed diffusely throughout the retina and often decrease in number before the onset of atrophy. Although this clinical phenomenon has been described as a distinct form of retinal dystrophy called retinitis punctata albescens, it can also be considered a descriptive subtype of non-syndromic RP. Retinitis punctata albescens can be caused by mutations in the *LRAT*,[254] *PRPH2*,[482] *RHO*,[483] or *RLBP1*[484] genes. Mutations in the *RLBP1* gene have also been associated with Bothnia retinal dystrophy[485] and Newfoundland rod-cone dystrophy,[486] two specific RP subtypes characterized by the same white punctate deposits present in retinitis punctata albescens.[487] These white deposits have been attributed to the accumulation of all-*trans*-retinyl esters in the RPE;[351] however, given that retinitis punctata albescens patients with *LRAT* mutations produce little to no retinyl esters, the precise composition of these deposits remains unclear.[488]

Miscellaneous

Optic disc drusen are a common finding in RP patients, particularly patients with mutations in the *CRB1* gene, in which the prevalence approaches 1 in 3 patients.[55,199] A tapetal-like fundus reflex is a yellow-golden sheen similar to the Mizuo-Nakamura phenomenon observed in Oguchi

disease, although this sheen typically does not disappear after dark adaption. This reflex is best visualized using red-free or near-infrared reflectance.[489] Originally, this finding was believed to be pathognomonic for female carriers of *RPGR*-associated RP; however, it has also been reported in female carriers of X-linked *RP2*.[367] Besides the well-recognized hyperautofluorescent ring, other FAF characteristics have been reported in certain genetic subtypes. For example, mutations in the *RPE65* or *LRAT* gene, which are both involved in the visual cycle, can lead to a reduced or even absent signal on FAF imaging.[255,490] The presence of 2 or 3 hyperautofluorescent rings has been associated with mutations in the *NR2E3* gene.[270,274]

Genes and proteins involved in RP

To date, 84 genes (Figure 7) and 7 candidate genes have been linked to non-syndromic RP. Each of these genes encodes a protein that plays a role in vital processes within the neuroretina and/ or RPE (e.g., the phototransduction cascade and the visual cycle) or an underlying structure (e.g., the connecting cilium). Therefore, a mutation in a gene within a specific pathway can cause the whole pathway to become impaired or even disrupted entirely. In principle, a certain degree of clinical overlap is to be expected among RP subtypes that are caused by mutations in genes associated with a common pathway. In practice, however, genetic variants that modify a pathway's activity can increase the clinical and/or genetic heterogeneity of diseases that involve a common pathway. Identifying the pathways affected in non-syndromic RP is therefore important for understanding the underlying pathogenesis. In this chapter, we provide an overview of the principal pathways that are affected in RP, and we discuss the location and function of the genes/proteins involved in RP (Figure 8, Table S3). Specifically, we focus on the phototransduction cascade (with 10 RP genes involved), the visual cycle (7 RP genes), ciliary structure and transport (35 RP genes), and the interphotoreceptor matrix (1 RP gene); the remaining 38 RP genes and their function are listed in Table S3.

The phototransduction cascade

The phototransduction pathway is a cascade of successive reactions triggered by excitation of the opsin molecule by a photon, resulting in an electrical signal that is transmitted via the optic nerve to the visual cortex, leading to the perception of an image (see panel 3 in Figure 8). This cascade is largely similar between rods and cones, with slight differences due to their different functions in dim light versus bright light.

In rod cells, rhodopsin (encoded by the *RHO* gene) consists of the apoprotein opsin and the chromophore 11-*cis*-retinal. Upon capturing a photon, 11-*cis*-retinal converts to the all-*trans*-retinal isomer, which changes the structure of rhodopsin into that of the photoactive metarhodopsin II.[491] Metarhodopsin II activates the G protein transducin (encoded by the *GNAT1* gene), which then activates the cyclic guanosine monophosphate (cGMP) phosphodiesterase (with subunits encoded by the *PDE6A*, *PDE6B*, and *PDE6G* genes), which hydrolyzes cGMP to
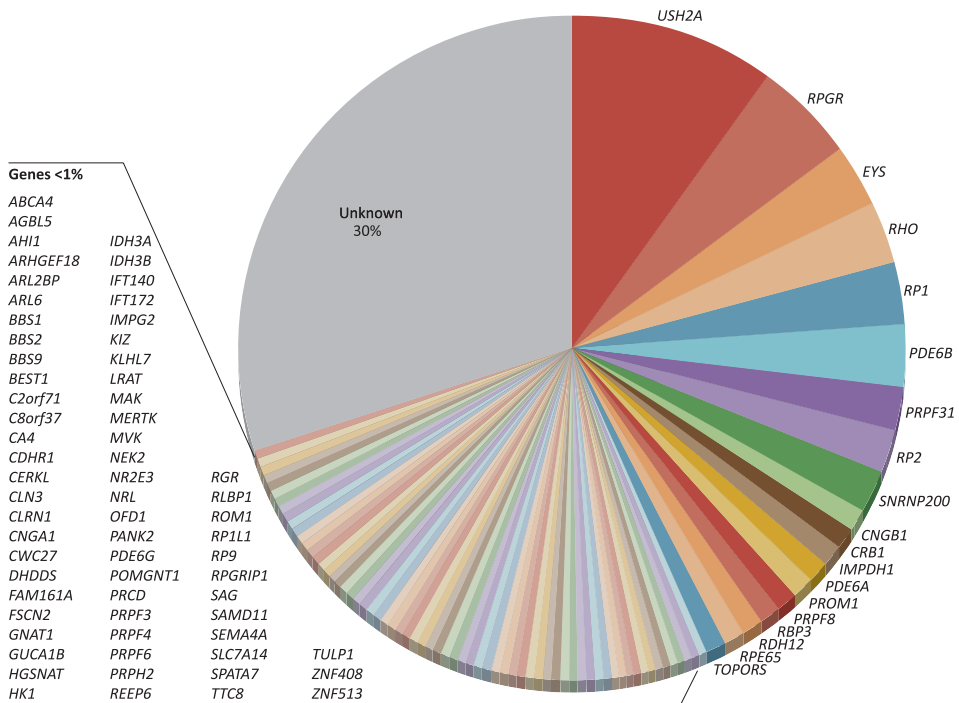
Figure 7. Estimated relative contribution of genes to non-syndromic retinitis pigmentosa. The estimates are based on personal experience and a search of the literature. It is important to realize that the frequency may vary depending on the geographic region.

form 5'-GMP.[492] This process decreases the concentration of cGMP in the photoreceptor's cytoplasm, which closes cGMP-gated cation channels (with subunits encoded by the *CNGA1* and *CNGB1* genes) in the plasma membrane. This in turn hyperpolarizes the plasma membrane due to a large decrease in intracellular calcium concentration; this hyperpolarization of the plasma membrane leads to decreased glutamate release at the photoreceptor's synapse.

After phototransduction, the system returns to the pre-photoactivation state via the following steps: *i*) phosphorylation of metarhodopsin II by rhodopsin kinase and the subsequent binding of arrestin (encoded by the *SAG* gene), which deactivates transducin;[493,494] *ii*) dissociation of all-*trans*-retinal from the visual pigment and conversion to 11-*cis*-retinal via the visual (retinoid) cycle (see below); *iii*) inactivation of transducin by GTPase-accelerating proteins (in particular, RGS9), thereby inactivating the phosphodiesterase;[495,496] and *iv*) the return of intracellular cGMP to normal levels by guanylate cyclase (encoded by the *GUCY2D* gene) which is activated by guanylate cyclase–activating protein (encoded by the *GUCA1A GUCA1B*, and *GUCA1C* genes).[497,498] After all-*trans*-retinal has dissociated from opsin, 11-*cis*-retinal binds to opsin to produce rhodopsin, which then dissociates from arrestin. Rhodopsin is then de-phosphorylated by protein phosphatase 2A. Thus, in the dark, rhodopsin is predominantly in the non-phosphorylated state.
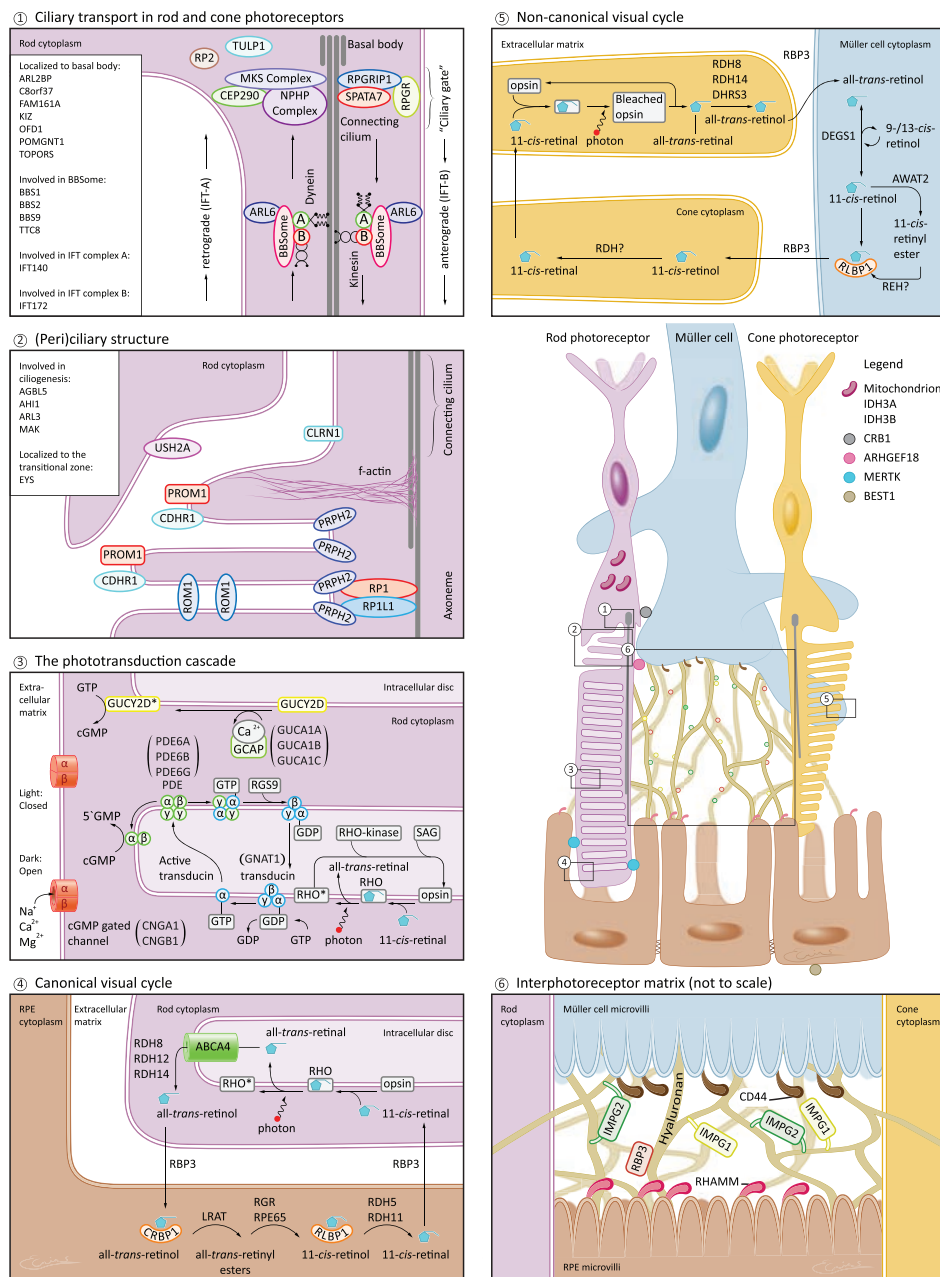
Figure 8. Schematic representation of a human rod photoreceptor (purple), cone photoreceptor (orange), Müller cell (blue), RPE cells (brown), and the interphotoreceptor matrix (beige). The six separate panels provide detailed information regarding the genes involved in four key processes (panels 1, 3, 4, and 5) and two structures (panels 2 and 6). Note that genes are not shown in italics. These processes are described in detail in sections 5.1-5.5.

Abbreviations: cGMP: cyclic guanosine monophosphate; GCAP: guanylate cyclase-activating protein; GDP: guanosine diphosphate; GTP: guanosine triphosphate; PDE: phosphodiesterase; RHAMM: receptor for hyaluronic acid-mediated mobility; RHO*: activated rhodopsin; RPE: retinal pigment epithelium.

The majority of molecules in the rod phototransduction cascade have a homolog that performs a similar function in cone cells. There are two principal differences between rods and cones with respect to phototransduction. First, cone cells express three different opsins, each of which is specific—albeit less sensitive—to a given wavelength. Second, opsins in cone cells have faster kinetics than rod opsins and are nearly unsaturable. Although the functional consequence of this difference in kinetics is not completely clear, most research suggests that the faster kinetics in cones translates to a shorter recovery phase. This may be due to the more rapid phosphorylation of activated cone pigments, a faster dissociation rate of all-*trans*-retinal, and/or faster inactivation kinetics of transducin.[499,500] Hydrolysis of transducin-bound GTP is the rate-limiting reaction in rod cells; however, compared to rods, cones contain ten-fold higher concentrations of the GTPase-accelerating protein complex.

The visual cycle

The vitamin A derivative 11-*cis*-retinal is an essential component in the phototransduction cascade. Dietary vitamin A (all-*trans*-retinol) is absorbed from the blood, enters the RPE, and is converted to 11-*cis*-retinal. The visual cycle is a complex process that focuses on regenerating 11-*cis*-retinal from all-*trans*-retinal produced in the phototransduction cascade (see panel 4 in Figure 8) and occurs simultaneously with phototransduction.

Upon photoactivation, all-*trans*-retinal is released from the activated visual pigment into the lumen of the outer segment discs, where it reacts with phosphatidylethanolamine to form *N*-retinylidene-phosphatidylethanolamine.[501] Via the flippase activity of the ABC (ATP-binding cassette) transporter ABCR (encoded by the *ABCA4* gene), all-*trans*-retinal is released into the cytoplasm of the photoreceptor, where it is reduced to all-*trans*-retinol by the enzyme all-*trans*-retinal dehydrogenase (encoded by the *RDH8*, *RDH12*, and *RDH14* genes).[502,503] All-*trans*-retinol is then transported into the subretinal space, where it binds to interphotoreceptor retinoid–binding protein (IRBP, encoded by the *RBP3* gene) and is transported to the RPE.[504] In the cytoplasm of the RPE cell, all-*trans*-retinol binds to cellular retinol–binding protein (encoded by the *CRBP1* gene) and is re-isomerized via a cascade involving lecithin-retinol acyltransferase (LRAT), RPE65 (also known as retinoid isomerohydrolase), retinal G protein-coupled receptor (RGR), and 11-*cis*-retinol dehydrogenase (encoded by the *RDH5* and *RDH11* genes).[351,505-508] The resulting 11-*cis*-retinal is then transported into the interphotoreceptor matrix by cellular retinaldehyde–binding protein (CRALBP, encoded by the *RLBP1* gene) and is subsequently transported back into the photoreceptor's cytoplasm by IRBP. Once back in the photoreceptor, 11-*cis*-retinal binds to opsin to form a new rhodopsin molecule. This pathway, known as the canonical visual cycle, catalyzes the re-isomerization of retinal in rod cells.

Recent studies have shown that in addition to the above-mentioned visual cycle, cones also have a second, non-canonical visual cycle that operates in cone outer segments and Müller cells (see panel 5 in Figure 8); this cycle regenerates 11-*cis*-retinal at a 20-fold faster rate,[509,510] although all of the proteins in this cycle have not yet been identified. This cycle is initiated when cone-specific opsin is photobleached and releases all-*trans*-retinal into the cell's cytosol, where

it is then reduced to all-*trans*-retinol by retinol dehydrogenases (encoded by the *RDH8* and *RDH14* genes) and the cone-specific enzyme retSDR1 (encoded by the *DHRS3* gene).[511] All-*trans*--retinol then binds to IRBP and is transported into Müller cells, where dihydroceramide desaturase-1 (DES1, encoded by the *DEGS1* gene) catalyzes the direct isomerization of all-*trans*-retinol to produce 11-*cis*-retinol, as well as 9-*cis*-retinol and 13-*cis*-retinol.[510,512] Because the isomerization reaction catalyzed by DES1 is reversible,[512] the newly formed 11-*cis*-retinol is susceptible to re-isomerization. The cell uses two mechanisms to reduce this susceptibility to re-isomerization. First, 11-*cis*-retinol can be esterified by multifunctional *O*-acyltransferase (MFAT, encoded by the *AWAT2* gene) to form 11-*cis*-retinyl-ester, and secondly, newly formed 11-*cis*-retinol can be captured by CRALBP.[513] A currently undefined 11-*cis*-retinol-ester hydrolase (labeled "REH?" in Figure 8) hydrolyzes 11-*cis*-retinyl-ester to form 11-*cis*-retinol; this occurs only when CRALBP is available to bind 11-*cis*-retinol and prevent re-isomerization by DES1.[514] When bound to CRALBP, 11-*cis*-retinol is released into the interphotoreceptor matrix, where it binds IRBP and is taken up by the cone outer segment.[515] There, an unknown RDH (labeled "RDH?" in Figure 8) oxidizes 11-*cis*-retinol to form 11-*cis*-retinal, which then binds to opsin, forming a new pigment molecule. This final oxidation reaction can occur in cone outer segments, but not in rod outer segments;[510] thus, the non-canonical visual cycle is specific to cone cells.

Ciliary transport

Cilia are slender, longitudinal, microtubule-based projections that extend from the surface of most mammalian cells and vary in both shape and size depending on the cell type.[516] Cilia can be divided in two main categories: motile cilia and non-motile (primary) cilia. Motile cilia are used in specific organs and processes that require the movement of ciliary fluid; examples include the establishment of left-right asymmetry of viscera in the developing embryo, the clearance of mucus from the airways, and sperm motility. In contrast, primary cilia are present on the vast majority of non-motile eukaryotic cells and serve as sensory "antennae" in most sensory organs.[517,518] Given the nearly ubiquitous presence of cilia throughout the body, mutations in genes encoding ciliary proteins can lead to so-called ciliopathies, which often involve a syndromic phenotype with multiple affected organs and cellular processes.[519,520]

Photoreceptor cells contain a highly specialized sensory cilium that consists of the connecting cilium and associated basal body, as well as an apical outer segment, a highly specialized structure in which phototransduction takes place.[521] Because the outer segment lacks biosynthetic machinery, all of its components are synthesized and partially pre-assembled in the inner segment and then transported to the outer segment via the connecting cilium, a process facilitated by intraflagellar transport (IFT). IFT is also used to assemble and maintain the cilia.[522-526] To date, mutations in more than 30 ciliary protein–encoding genes have been linked to non-syndromic retinal diseases (Table S3).[527,528] The functions of these ciliary proteins in the connecting cilium have been identified, and most of these proteins are involved in either IFT function/regulation or ciliary structure.

IFT is a bidirectional transport system that uses microtubule-based motor molecules to

transport cargo both from the cilia's base to the tip (i.e., anterograde transport, which is driven by kinesin motor proteins) and from the tip to the base (i.e., retrograde transport, which is driven by dynein motor proteins).[529-531] This transport system is capable of moving thousands of molecules per second in each photoreceptor cell, including the anterograde transport of RHO and the light-dependent transport of arrestin and transducin.[532-535]

Many genes associated with non-syndromic RP encode proteins that are involved in various aspects of ciliary transport (Table S3). For example, ARL3 and RP2 mediate the localization of motor units at the ciliary tip.[536] In addition, IFT is mediated by the so-called IFT proteins (e.g., IFT140 and IFT172) that form two complexes (complex A and complex B), which bind and transport ciliary cargo.[537,538] Moreover, the BBSome complex (in which BBS stands for Bardet-Biedl syndrome) serves as an adaptor between cargo and the IFT complex.[539,540] The BBSome complex consists of eight protein subunits (BBS1, -2, -4, -5, -7, -8 (TTC8), -9, and -18).[540] Mutations in BBSome subunits generally give rise to Bardet-Biedl syndrome;[114] however, four of the genes that encode BBSome subunits (*BBS1*, *BBS2*, *BBS9*, and *TTC8*), as well as the gene that encodes ARL6 (a protein that recruits the BBSome complex to the membrane), are associated with non-syndromic RP.[145,147,149,410-412,541-543]

The entry and exit of cargo on the ciliary IFT machinery is regulated by the "ciliary gate", a specialized ciliary structure located at the base of the primary cilium; this structure forms a general barrier against periciliary particle diffusion and therefore regulates transport to and from the structurally isolated outer segment.[529,544-548] The gate's function is mediated by transition fibers and the transition zone. Transition fibers (also known as distal appendages) anchor the cilium to the plasma membrane, and the transition zone is a modular structure containing Y-shaped linkers that are believed to act as a "molecular sieve" in order to restrict and select the entry and exit of ciliary cargo. The photoreceptor-connecting cilium is both structurally and functionally analogous to a prototypical transition zone. However, the elongated shape of this cilium is likely required to achieve the high trafficking rate for transporting biosynthetic material, as approximately 10% of the outer segment is renewed each day through shedding and replacement of materials at the tip.[549] In addition, a ciliary pore complex, which is homologous to the nuclear pore complex, functions as an active molecule gate at the base of the cilium.[550] Two interacting protein modules—namely, the Meckel/Joubert syndrome (MKS/JBTS) and nephronophthisis (NPHP) associated modules—assemble the transition zone and control its gating function.[551-553] These modules consist of several ciliopathy-associated proteins and interact with nearby transition zone components (e.g., the BBSome complex) and a complex that contains the protein encoded by the *RPGR* gene, which accounts for 70-90% of X-linked RP cases and 10-20% of all RP cases.[548,554] The RPGR protein is anchored to the connecting cilium by RPGR interacting protein 1 (RPGRIP1), the localization of which requires another ciliary protein, spermatogenesis-associated protein 7 (SPATA7). Defects in the RPGR-RPGRIP1-SPATA7 complex lead to the aberrant localization of specific opsins; therefore, this complex is believed to play a role in the transport of specific opsins.[555] For a thorough overview of the interactions between RPGR and other ciliary proteins such as centrosomal protein 290 (CEP290),

Chapter 2.1

phosphodiesterase 6D (PDE6D), nephrocystin 1 (NPHP1), nephrocystin 4 (NPHP4), and Whirlin (WHRN), the reader is referred to a recent review by Megaw and colleagues.[554]

Outer segment structure

The cilium of the photoreceptor cell consists of the connecting cilium and the outer segment, the latter of which contains a highly specialized compartment consisting of stacks of intracellular discs (in rod cells) or lamellae (in cone cells).[556,557] Goldberg et al. recently reviewed the morphogenesis and architecture of intracellular discs in the ouster segment.[558] Some subtypes of non-syndromic RP are associated with proteins that are involved in the development and/or orientation of outer segment discs (Table S3 and Figure 8), and their genes are discussed below.

Outer segment discs develop from the connecting cilium as evaginations in the plasma membrane that are subsequently internalized to form a stack of intracellular discs.[559] F-actin microfilaments located at basal axonemal microtubules are required for the initiation of new disc evagination.[558] The RP-associated gene *FSCN2* encodes retinal fascin homolog 2 (FSCN2), which crosslinks and bundles F-actin filaments.[560,561] Peripherin-2 (PRPH2) plays a role in the formation of the outer segment disc rim, and loss of PRPH2 leads to the absence of outer segment discs.[558,562] PRPH2 has also been suggested to play a role in disc stability and disc shedding.[558,563] Recently, Salinas et al. reported that the photoreceptor cilium can release large numbers of ectosomes,[564] similar to the process recently described in primary cilia, in which ciliary G protein–coupled receptors are dispatched in extracellular signaling–competent vesicles via actin-mediated ectocytosis.[565] PRPH2 maintains this process at the appropriate level, enabling retained ectosomes to morph into outer segment discs.[564] The formation of PRPH2 is regulated by the rod outer segment membrane protein-1 (ROM1) protein, thereby regulating the process of disc internalization.[566] The initiation of outer segment disc formation requires the membrane-bound protein prominin-1 (PROM1), which is localized to the nascent disc edge.[558] PROM1 also appears to link outer segment disc rims, thereby helping to stabilize the stack.[567] Cadherin-related family member 1 (also known as protocadherin-21 and encoded by the *CDHR1* gene) has also been implicated in disc rim formation and has been suggested to function cooperatively with PROM1, as it also resides at the nascent disc edge.[568] The photoreceptor-specific cytosolic protein RP1 is associated with the ciliary axoneme and is required for outer segment disc morphogenesis.[359] Thus, RP1 plays a role in outer segment disc orientation and has been suggested to serve as the link between outer segment discs and the axoneme.[569] Finally, RP1 has a synergistic interaction with RP1L1, a protein that has a similar localization pattern and is also required for outer segment morphogenesis.[570]

The interphotoreceptor matrix

The interphotoreceptor matrix fills the subretinal space, which extends from the external limiting membrane (i.e., the basal ends of the Müller cells) to the apical surface of the RPE; the inner and outer segments of photoreceptor cells are also embedded in this space.[571] For many years,

the interphotoreceptor matrix was believed to simply provide support to the retinal tissue, with no other significant functions. However, we now know that the interphotoreceptor matrix plays an important role in many key processes, including: *i*) retinal (retinoid) metabolism; *ii*) retinal adhesion to the RPE;[572-575] *iii*) intercellular communication in terms of outer segment shedding and phagocytosis by the RPE; *iv*) matrix turnover; *v*) photoreceptor alignment; *vi*) growth factor presentation;[576] and *vii*) regulation of the transport of oxygen and nutrients to photoreceptor cells.[577,578] In addition, this extracellular matrix may also play a key role in the clinical presentation of progressive retinal degeneration.[579]

The interphotoreceptor matrix is composed of proteins and carbohydrates that are secreted by photoreceptors and RPE cells.[580] The principal components of this matrix are proteoglycans, hyaluronic acid, collagen and elastin fibers, and other proteins such as fibronectin, fibrillin, laminins, and fibulins. Hyaluronic acid polymers form extremely large (100-10,000 kDa) polysaccharides that interconnect to produce a three-dimensional mesh network.[571] This network is connected to Müller cells via CD44 and to the RPE via proteins containing RHAMM (receptor for hyaluronic acid-mediated motility)-type binding motifs. In addition, other extracellular matrix components such as SPACR, SPACRCAN, pigment epithelium-derived factor (PEDF), and IRBP also contain RHAMM-binding motifs and are also linked to the hyaluronic acid network.[571,581]

Three genes (*IMPG2*, *RBP3*, and *EYS*) associated with non-syndromic RP encode proteins that bind to the hyaluronic acid network.[206,207,246,247,334,582,583] SPACRCAN (encoded by the *IMPG2* gene) is a proteoglycan that binds both hyaluronic acid and chondroitin sulfate and plays several functional roles, including organizing the interphotoreceptor matrix and regulating the growth and maintenance of the photoreceptor outer segment.[584,585] IRBP (encoded by the *RBP3* gene) is the primary soluble protein in the interphotoreceptor matrix and—as discussed above—plays a role in the visual cycle (see section 4.2).

In humans, the *EYS* gene encodes the human ortholog of the *Drosophila* eyes shut protein and is one of the largest genes expressed in the retina. The resulting protein contains several sites for the attachment of glycosaminoglycans side chains; in *Drosophila*, this protein is an extracellular protein.[586,587] The high degree of homology between the human and *Drosophila* orthologs suggests that the human protein also functions in the extracellular matrix. In humans, however, this protein, which has four isoforms,[588] can localize to subcellular compartments in the cytoplasm and to the axoneme of the connecting cilium; moreover, deleting EYS expression in zebrafish causes mislocalization of outer segment proteins, suggesting a functional role in ciliary transport.[589] In addition, posttranslational modifications may allow the protein to target to specific locations.[588] Finally, the RP1 protein also contains hyaluronic acid–binding motifs and may interact with the hyaluronic acid scaffold if it associates with the photoreceptor's plasma membrane.[571]

Management of RP

Retinitis pigmentosa can profoundly impact the physical and emotional lives of patients and their families. Therefore, providing adequate support to patients and their relatives is an essential component in managing RP. In this chapter, we discuss ophthalmic and genetic counseling, we describe the current options for genetic testing, we emphasize the importance of regular visits to the clinic, and we discuss both current and future therapeutic options.

Ophthalmic and genetic counseling

A multidisciplinary approach that combines ophthalmic and genetic counseling services can optimize both the diagnostic process and the long-term management of RP.[590] In recent years, the field has witnessed significant advances in the methods used to identify genes. For example, some centers have switched from using targeted panel sequencing tests for diagnostics and now perform exome sequencing using a vision-related gene filter.[591] In exome sequencing, all coding regions (i.e., exons) within the entire human genome are sequenced. The addition of a gene filter containing all known IRD genes can limit the risk of incidental findings in genes that are not necessarily related to the disease. The advantage of exome sequencing is that if the causative gene is not identified in any of the known RP genes, the search can be readily expanded to include other genes, thereby potentially identifying novel RP-related genes. On the other hand, exome sequencing is not usually the first choice for obvious cases of X-linked forms of RP. Although mutations in the *RPGR* gene account for 70-75% of all patients with an X-linked form of RP, this gene is not suitable for exome sequencing,[592] particularly due to the highly repetitive, purine-rich ORF15 region. Therefore, this region is better suited to direct sequencing. Currently, exome sequencing provides a molecular diagnosis in 60-80% of RP patients;[430,591] the remaining patients likely have a variant that cannot be detected using exome sequencing, which can include structural rearrangements, mutations in non-coding and/or GC-rich regions, and mutations in genes that have not yet been associated with retinal dystrophy.[269,593] The introduction of whole-genome sequencing in routine diagnostics will likely further increase our ability to obtain molecular diagnoses, although determining the functional role of many of these putative causative variants will remain a challenge.

Genetic testing often raises a wide range of questions, and patients are usually referred for genetic counseling, where questions regarding the reliability of the test results and the implications to the patient and his/her relatives can be addressed. Performing presymptomatic and/or predictive testing at too early an age may increase the likelihood of an unfavorable impact on quality of life; therefore, the ideal age for undergoing genetic testing is currently under debate.[594] To help ensure their future autonomy, children rarely undergo presymptomatic testing; however, the availability of new treatment options, which ideally are applied in the earliest possible stage of the disease, may warrant testing at a younger age.

Genotyping usually improves the outcome of ophthalmic counseling; however, the number of well described phenotypes for a given genetic subtype is usually limited, and the phenotypes

can vary widely within a subtype and even between family members who share identical mutations. Nevertheless, the information discussed in Chapter 4 can provide the clinician with an overview of the clinical aspects associated with the various genetic subtypes. For example, central visual function often deteriorates rapidly in RP patients with a mutation in the *CERKL* gene, whereas visual acuity is generally preserved much longer in RP patients with a mutation in the *TOPORS* gene. Therefore, understanding the underlying genetic profile and other modifiers that can influence the phenotype will help provide a more reliable clinical prognosis. In anticipation of such an in-depth genetic analysis, thorough follow-up examinations that include visual field analysis, SD-OCT, and FAF will serve to monitor the clinical progression of the retinal dystrophy, as well as to predict the decline in visual function. In addition, other ocular pathologies such as cataract and CME may also be identified at an early stage and treated accordingly.

Visual rehabilitation

In recent years, visual rehabilitation for RP patients with low visual acuity has evolved into a multidisciplinary approach that focuses on the patient's functional abilities and needs,[595] thereby providing high value to patients with RP. Vision rehabilitation centers provide support and training, including orientation and mobility training combined with low-vision aids such as flashlights, night-vision goggles, and/or reverse telescopes in order to optimize residual visual function. In advanced disease, the patient's independence and functional quality of life can be improved using text-to-speech software to allow the patient to interpret text, and a guide dog can further increase the patient's mobility and independence. However, the social impact of the gradual deterioration of the visual field should not be underestimated.

Treatment of associated ocular abnormalities

The visual gain realized following cataract surgery in RP patients depends largely on the amount of residual macular function. The likelihood of visual recovery is highest in RP patients who have an intact—or only slightly disrupted—foveal ellipsoid zone.[596,597]

Some reports indicate that RP patients may have an increased risk of developing complications during and following cataract surgery; these complications can include zonular insufficiency (in 19% of cases),[598] posterior capsular opacification (44-95% of cases),[596,599,600] and anterior capsule contraction (10-38% of cases).[596,601,602] Although the scientific evidence is absent, some surgeons report a more severe post-operative inflammation in RP patients. In general, pre-operative treatment with steroids may be useful in patients with RP to prevent this inflammation as well as CME. There is currently no indication that surgery accelerates the progression of RP.[599]

On the other hand, the subjective visual gain following cataract surgery in RP patients is often considerable. Therefore, cataract extraction should be seriously considered in visually significant cataracts, even in the presence of advanced RP.

To date, no large randomized controlled clinical trial has been performed to evaluate the effect of treating CME in RP patients. The treatment of choice for CME is carbonic anhydrase inhibitors.[36]

A meta-analysis conducted by Huang et al. showed a mean reduction in central retinal thickness of 46%.[603] However, often there is no correlation between anatomical and functional improvement.[603] Prescribed dosages for oral acetazolamide vary between 125-500mg daily, and topical carbonic anhydrase inhibitors like 1-2% dorzolamide or brinzolamide are typically administered three times a day. Since the optimal therapeutic dose for the individual is still unknown, a trial and error approach is advised. Recurrence of CME can occur after cessation of carbonic anhydrase inhibitor treatment,[603] and efficacy may diminish during prolonged treatment.[604] Retreatment with carbonic anhydrase inhibitors after a period of discontinued use, may again have a favorable effect.[605] Refractory CME can be treated with intravitreal steroids.[604] The use of intravitreal anti-VEGF (vascular endothelial growth factor) in RP patients remains unclear, as studies do not agree with respect to the beneficial effects; moreover, VEGF levels are markedly lower in the aqueous humor of RP patients.[36] It is important to note that the amount of CME can fluctuate over time—particularly in children—even without intervention; this should be taken into account during treatment.[604]

Although epiretinal membranes are prevalent among RP patients, few reports address the effects of membrane peeling in RP patients. Ikeda et al. recently reported morphological improvement following epiretinal membrane peeling in 9 out of 11 eyes, although only three of these eyes—two of which underwent concomitant cataract extraction surgery—had long-term improvement in visual acuity.[606] This relatively limited rate of success, together with the potential toxicity associated with direct intraocular illumination, suggests that epiretinal membrane peeling should be used with caution in patients with RP.

Treatment options for RP

Significant advances in our knowledge regarding the genetic causes of RP have been paralleled by significant progress in the development of novel strategies for treating this disease.[607] These strategies can be subdivided into two general categories: i) approaches that are gene-specific or even mutation-specific, and ii) approaches that exert a therapeutic effect independent of the underlying genetic defect. Below, we discuss the main features of the various therapeutic approaches, including their potential advantages and limitations with respect to treating patients with RP.

Gene-specific and mutation-specific approaches

The majority of genes mutated in RP encode proteins that are expressed either in photoreceptor cells or in the RPE. Therefore, to be effective, gene-specific and/or mutation-specific approaches require the presence of the cells that will be targeted; as a result, these approaches are most successful in the early stages of the disease, before cell degeneration. With gene augmentation therapy–based approaches, a construct driving the expression of a wild-type copy of the cDNA corresponding to the mutated gene is introduced into the target cells, with the goal of restoring wild-type expression in these cells. In the case of RP and allied diseases, virus-based vectors such as adeno-associated viruses (AAVs) are often used to deliver the genetic cargo to target

cells in the retina; the virus is usually administered via intravitreal or subretinal injection. In 2008, the first studies to test the safety and efficacy of using *RPE65* gene augmentation therapy in patients with LCA or early-onset RP due to bi-allelic *RPE65* mutations were reported.[608-610] The promising results obtained from these studies provided an enormous boost to the field and led to phase I/II clinical trials designed to test gene therapy–based approaches for treating several other genetic subtypes of retinal disease, including choroideraemia,[611] *MERTK*-associated RP,[612] and—more recently—*CNGA3*-associated achromatopsia, *PDE6A*-associated RP, *RPGR*-associated X-linked RP, retinoschisis, and Stargardt disease (see www.clinicaltrials.gov). The recent phase 3 study in patients with a *RPE65*-mediated inherited retinal dystrophy who were treated with voretigene neparvovec, confirmed treatment safety and efficacy; patients showed improved light sensitivity, visual fields and navigational ability under dim light conditions.[613] Subsequently, this led to the first US FDA approved gene therapy for retinal disease. Despite these initial advances, however, important challenges must be overcome before gene augmentation therapy can be widely implemented. For example, it is unclear whether one-time administration of a therapeutic vector can provide long-term, long-lasting clinical benefits. The cargo capacity of the most commonly used viral vectors is also relatively limited and is therefore not suitable for delivering the large cDNAs corresponding to several of the genes that are mutated in many patients with RP (for example, the *EYS* and *USH2A* genes). Other challenges include controlled expression levels, dominant-negative mechanisms, the relative small number of patients for the genetic subtypes as well as the financial costs of the highly individualized forms of treatment.

Other emerging therapeutic strategies involve antisense oligonucleotides (AONs), which are small, versatile RNA molecules that can modify pre-mRNA splicing by specifically binding to a target region in the pre-mRNA, thereby suppressing aberrant splicing events caused by certain mutations,[614] and genome editing, for example using the CRISPR/Cas9 system. This latter technique introduces a highly precise double-strand break in the genomic DNA at the site of the mutation, and can be used to repair a primary genetic defect directly within the patient's genome.[615]

Another class of highly versatile therapeutic compounds that can act in a gene-specific and/or mutation-specific manner are the small-molecule compounds. In early-onset retinal degeneration in patients with a mutation in the *LRAT* or *RPE65* gene, the visual cycle—in which all-*trans*-retinal is converted back into 11-*cis*-retinal via several enzymatic reactions—is disrupted. Oral treatment with 9-*cis*-retinoid, an analog of 11-*cis*-retinal, was well tolerated and moderately effective in early-phase clinical trials in patients with a mutation in the aforementioned genes; moreover, treatment efficacy was correlated with residual retinal integrity.[616]

Although beyond the scope of this review, it is important to note that diet-based treatment can prevent or reduce disease progression in the following three syndromic forms of RP: adult Refsum disease, Bassen-Kornzweig syndrome, and α-tocopherol transfer protein deficiency (also known as familial isolated vitamin E deficiency).

Mutation-independent approaches

In recent years, several dietary changes and dietary supplements (e.g., vitamin A) have been recommended for the treatment of RP.[617] However, a Cochrane systematic review conducted by Rayapudi et al.[618] found no clear evidence that vitamin A and/or the fish oil docosahexaenoic acid has beneficial effects in RP patients in general.

Cell replacement therapy is the administration of ocular-derived retinal progenitor cells (RPCs) or non–ocular-derived stem cells such as embryotic stem cells (ESCs) and induced pluripotent stem cells (iPSCs) into the vitreous body or subretinal space. Each of these cell types has specific advantages and disadvantages.[619] For example, RPCs are relatively easy to process, and the recipient does not require immunosuppression therapy; however, obtaining sufficient donor cells is problematic. In contrast, stem cells require a more extensive manufacturing process. The key difference between ESCs and iPSCs is that iPSCs can be derived from the patient, thereby allowing the autologous transplantation of iPSC-derived RPE or photoreceptor cells, thus avoiding immunosuppressive treatment; moreover, the underlying genetic defect can even be corrected prior to transplantation using genome editing.[620] However, such highly individualized treatments are associated with extremely high costs. Therefore, options for using human leukocyte antigen (HLA)-matched iPSCs from a databank are receiving increasing attention.[621,622] Various transplantation approaches are currently used, including transplantation of stem cell–derived RPE cells and/or photoreceptor cells.[623] Phase I/II trials using RPCs are currently being performed in RP patients in order to assess the *in vivo* safety, long-term survival, and function of the graft (see www.clinicaltrials.gov). Although clinical applications are still in their infancy, stem/progenitor cell–based therapeutic approaches represent a promising future for patients with advanced RP.

Another emerging approach is the use of electronic retinal implants for end-stage RP patients with little or no light perception. Two retinal implants are currently available on the market. The Argus II epiretinal implant (produced by Second Sight Medical Products Inc. in Sylmar, CA) has received both European CE certification and US FDA approval, and the Alpha AMS subretinal implant (produced by Retina Implant AG in Reutlingen, Germany) has received CE certification.[624] Both of these implants function by stimulating the inner retinal layers and therefore require an intact inner retinal architecture. An epiretinal implant is connected to a miniature camera mounted on eyeglasses; the implant then stimulates the residual retinal ganglion cells directly. In contrast, a subretinal implant consists of a light-sensitive micro-photodiode array that stimulates the bipolar cell layer. Retinal implants can restore basic visual function, improve performance in vision-related tests, and increase the daily mobility of patients with RP.[625-627] For example, improvement in visual acuity from light perception without projection to 20/546 was recently reported in a patient who received an Alpha AMS implant.[627] Despite these promising results, visual rehabilitation for patients with these prostheses is complex, and several challenges must still be overcome, including adverse effects, device longevity, and resolution.[628,629]

Yet another relatively new approach that can provide therapeutic benefits in patients who have lost photoreceptor and/or RPE cells is optogenetics, which uses gene therapy to express light-

activated ion channels in the residual retinal neurons, thereby restoring photosensitivity.[630] Despite promising results in both cell-based models and animal models, the true potential of this approach needs to be tested fully in a clinical setting.

Finally, several neuroprotective factors have been shown to slow photoreceptor loss in numerous animal models, including brain-derived neurotrophic factor (BDNF),[631] basic fibroblast growth factor (bFGF),[632] ciliary neurotrophic factor (CNTF),[633] glial cell–derived neurotrophic factor (GDNF),[634] nerve growth factor (NGF),[635] and rod-derived cone viability factor (rdCVF).[636] However, there is currently no evidence that these compounds are beneficial in treating RP.[637] Transcorneal electrical stimulation (TES), a novel therapeutic approach for retina disease and optic neuropathy, also seems to exert its effect through the release of neurotrophic factors after corneal electrostimulation. Proof of principle of TES has been established in animal models[638] and treatment appears to be safe in patients,[639-641] although larger studies are needed to provide treatment efficacy over a prolonged time.

Conclusions

In this review, we provided an overview of the clinical characteristics of RP in general, as well as the specific features of genetically defined RP subtypes. This information can help the clinician identify the clinical RP entity and better predict the disease course, ultimately providing the patient with the best possible information regarding prognosis. In addition, we discussed the main pathways affected in RP, as well as the location and function of the proteins involved, thereby revealing high genetic and clinical similarity between RP and other IRDs, including LCA and cone-rod dystrophies. Together, these disorders are currently considered to represent a continuum of retinal dystrophies with significant clinical and genetic overlap.

Our rapidly increasing knowledge of affected biological pathways has shifted attention to the individual genetic subtypes of RP. This is paralleled by various treatment strategies exploring the applications of gene and cell-based therapies, retinal implants or transplantation. The nature of the genetic defect, the resulting molecular pathogenesis and the extent of the degeneration will determine which therapeutic modality will be the most appropriate in the individual RP patient.

References

1. Pagon RA. Retinitis pigmentosa. *Surv Ophthalmol.* 1988;33(3):137-177.
2. Na KH, Kim HJ, Kim KH, et al. Prevalence, Age at Diagnosis, Mortality and Cause of Death in Retinitis Pigmentosa in Korea - A Nationwide Population-based Study. *Am J Ophthalmol.* 2017;176:157-165.
3. Nangia V, Jonas JB, Khare A, Sinha A. Prevalence of retinitis pigmentosa in India: the Central India Eye and Medical Study. *Acta Ophthalmol.* 2012;90(8):e649-650.
4. Donders F. Beiträge zur pathologischen Anatomie des Auges. *Graefe's Archive for Clinical and Experimental Ophthalmology.* 1857;3(1):139-165.
5. Van Trigt A. De oogspiegel. *Nederlandisch Lancet, third series, Utrecht.* 1853:417-509.
6. Ovelgün RF. Nyctalopia haereditaria. *Acta physico-medica Academiae Caesareae Leopoldino-Carolinae (Norimbergae).* 1744;7:76-77.
7. Schon M. *Handbuch der pathologischen Anatomie des menschliches Auges.* Hamburg, West Germany1828.
8. Von Ammon FA. *Klinische Darstellungen der Krankheiten und Bildungsfehler des menschlichen Auges.* Vol 1. Berlin: G Reimer; 1838.
9. Dryja TP, McGee TL, Reichel E, et al. A point mutation of the rhodopsin gene in one form of retinitis pigmentosa. *Nature.* 1990;343(6256):364-366.
10. Daiger SP, Sullivan LS, Bowne SJ. RetNet, the Retinal Information Network. 2016; http://www.sph.uth.tmc.edu/RetNet/. Accessed 28-11-2016, 2016.
11. Novak-Lauš K, Kukulj S, Zorić-Geber M, Bastaić O. Primary tapetoretinal dystrophies as the cause of blindness and impaired vision in the republic of croatia. *Acta Clin Croat.* 2002;41:23-27.
12. Bunker CH, Berson EL, Bromley WC, Hayes RP, Roderick TH. Prevalence of retinitis pigmentosa in Maine. *Am J Ophthalmol.* 1984;97(3):357-365.
13. Hamel C. Retinitis pigmentosa. *Orphanet J Rare Dis.* 2006;1:40.
14. Grover S, Fishman GA, Alexander KR, Anderson RJ, Derlacki DJ. Visual acuity impairment in patients with retinitis pigmentosa. *Ophthalmology.* 1996;103(10):1593-1600.
15. Heckenlively JR, Yoser SL, Friedman LH, Oversier JJ. Clinical findings and common symptoms in retinitis pigmentosa. *Am J Ophthalmol.* 1988;105(5):504-511.
16. Kolmel HW. Visual illusions and hallucinations. *Baillieres Clin Neurol.* 1993;2(2):243-264.
17. Marc RE, Jones BW, Watt CB, Strettoi E. Neural remodeling in retinal degeneration. *Prog Retin Eye Res.* 2003;22(5):607-655.
18. Bittner AK, Diener-West M, Dagnelie G. A Survey of Photopsias in Self-reported Retinitis Pigmentosa: Location of Photopsias is related to Disease Severity. *Retina (Philadelphia, Pa).* 2009;29(10):1513-1521.
19. Bittner AK, Diener-West M, Dagnelie G. Characteristics and possible visual consequences of photopsias as vision measures are reduced in retinitis pigmentosa. *Invest Ophthalmol Vis Sci.* 2011;52(9):6370-6376.
20. O'Hare F, Bentley SA, Wu Z, Guymer RH, Luu CD, Ayton LN. Charles Bonnet Syndrome in Advanced Retinitis Pigmentosa. *Ophthalmology.* 2015;122(9):1951-1953.
21. Pinckers A, van Aarem A, Keunen JE. Colour vision in retinitis pigmentosa. Influence of cystoid macular edema. *Int Ophthalmol.* 1993;17(3):143-146.
22. Li ZY, Possin DE, Milam AH. Histopathology of bone spicule pigmentation in retinitis pigmentosa. *Ophthalmology.* 1995;102(5):805-816.
23. Berson EL. Retinitis pigmentosa. The Friedenwald Lecture. *Invest Ophthalmol Vis Sci.* 1993;34(5):1659-1676.
24. Jaissle GB, May CA, van de Pavert SA, et al. Bone spicule pigment formation in retinitis pigmentosa: insights from a mouse model. *Graefes Arch Clin Exp Ophthalmol.* 2010;248(8):1063-1070.
25. Grunwald JE, Maguire AM, Dupont J. Retinal hemodynamics in retinitis pigmentosa. *Am J Ophthalmol.* 1996;122(4):502-508.
26. Padnick-Silver L, Kang Derwent JJ, Giuliano E, Narfstrom K, Linsenmeier RA. Retinal oxygenation and oxygen metabolism in Abyssinian cats with a hereditary retinal degeneration. *Invest Ophthalmol Vis Sci.* 2006;47(8):3683-3689.
27. Penn JS, Li S, Naash MI. Ambient hypoxia reverses retinal vascular attenuation in a transgenic mouse model of autosomal dominant retinitis pigmentosa. *Invest Ophthalmol Vis Sci.* 2000;41(12):4007-4013.
28. Yu DY, Cringle SJ. Retinal degeneration and local oxygen metabolism. *Exp Eye Res.* 2005;80(6):745-751.
29. Stone JL, Barlow WE, Humayun MS, de Juan E, Jr., Milam AH. Morphometric analysis of macular photoreceptors and ganglion cells in retinas with retinitis pigmentosa. *Arch Ophthalmol.* 1992;110(11):1634-1639.
30. Cellini M, Strobbe E, Gizzi C, Campos EC. ET-1 plasma levels and ocular blood flow in retinitis pigmentosa. *Can J Physiol Pharmacol.* 2010;88(6):630-635.
31. Strobbe E, Cellini M, Fresina M, Campos EC. ET-1 Plasma Levels, Aqueous Flare, and Choroidal Thickness in Patients with Retinitis Pigmentosa. *J Ophthalmol.* 2015;2015:292615.
32. Ohguro H, Mashima Y, Nakazawa M. Low levels of plasma endothelin-1 in patients with retinitis pigmentosa. *Clin Ophthalmol.* 2010;4:569-573.
33. Sorrentino FS, Bonifazzi C, Perri P. The Role of the Endothelin System in the Vascular Dysregulation Involved in Retinitis Pigmentosa. *J Ophthalmol.* 2015;2015:405234.

34. Hwang YH, Kim SW, Kim YY, Na JH, Kim HK, Sohn YH. Optic nerve head, retinal nerve fiber layer, and macular thickness measurements in young patients with retinitis pigmentosa. *Curr Eye Res.* 2012;37(10):914-920.
35. Szamier RB. Ultrastructure of the preretinal membrane in retinitis pigmentosa. *Invest Ophthalmol Vis Sci.* 1981;21(2):227-236.
36. Strong S, Liew G, Michaelides M. Retinitis pigmentosa-associated cystoid macular oedema: pathogenesis and avenues of intervention. *Br J Ophthalmol.* 2017;101(1):31-37.
37. Hagiwara A, Yamamoto S, Ogata K, et al. Macular abnormalities in patients with retinitis pigmentosa: prevalence on OCT examination and outcomes of vitreoretinal surgery. *Acta Ophthalmol.* 2011;89(2):e122-125.
38. Fujiwara K, Ikeda Y, Murakami Y, et al. Association Between Aqueous Flare and Epiretinal Membrane in Retinitis Pigmentosa. *Invest Ophthalmol Vis Sci.* 2016;57(10):4282-4286.
39. Testa F, Rossi S, Colucci R, et al. Macular abnormalities in Italian patients with retinitis pigmentosa. *Br J Ophthalmol.* 2014;98(7):946-950.
40. Chebil A, Touati S, Maamouri R, Kort F, El Matri L. Spectral Domain optical coherence tomography findings in patients with retinitis pigmentosa. *Tunis Med.* 2016;94(4):265-271.
41. Triolo G, Pierro L, Parodi MB, et al. Spectral domain optical coherence tomography findings in patients with retinitis pigmentosa. *Ophthalmic Res.* 2013;50(3):160-164.
42. Peng B, Xiao J, Wang K, So KF, Tipoe GL, Lin B. Suppression of microglial activation is neuroprotective in a mouse model of human retinitis pigmentosa. *J Neurosci.* 2014;34(24):8139-8150.
43. Zhao L, Zabel MK, Wang X, et al. Microglial phagocytosis of living photoreceptors contributes to inherited retinal degeneration. *EMBO Mol Med.* 2015;7(9):1179-1197.
44. Auffarth GU, Tetz MR, Krastel H, Blankenagel A, Volcker HE. [Complicated cataracts in various forms of retinitis pigmentosa. Type and incidence]. *Ophthalmologe.* 1997;94(9):642-646.
45. Pruett RC. Retinitis pigmentosa: clinical observations and correlations. *Trans Am Ophthalmol Soc.* 1983;81:693-735.
46. Heckenlively J. The frequency of posterior subcapsular cataract in the hereditary retinal degenerations. *Am J Ophthalmol.* 1982;93(6):733-738.
47. Fujiwara K, Ikeda Y, Murakami Y, et al. Risk Factors for Posterior Subcapsular Cataract in Retinitis Pigmentosa. *Invest Ophthalmol Vis Sci.* 2017;58(5):2534-2537.
48. Yoshida N, Ikeda Y, Murakami Y, et al. Vitreous cysts in patients with retinitis pigmentosa. *Jpn J Ophthalmol.* 2015;59(6):373-377.
49. Grover S, Fishman GA, Brown J, Jr. Frequency of optic disc or parapapillary nerve fiber layer drusen in retinitis pigmentosa. *Ophthalmology.* 1997;104(2):295-298.
50. Shields CL, Kaliki S, Al-Dahmash S, et al. Retinal vasoproliferative tumors: comparative clinical features of primary vs secondary tumors in 334 cases. *JAMA Ophthalmol.* 2013;131(3):328-334.
51. Massof RW, Finkelstein D, Starr SJ, Kenyon KR, Fleischman JA, Maumenee IH. Bilateral symmetry of vision disorders in typical retinitis pigmentosa. *Br J Ophthalmol.* 1979;63(2):90-96.
52. Grover S, Fishman GA, Brown J, Jr. Patterns of visual field progression in patients with retinitis pigmentosa. *Ophthalmology.* 1998;105(6):1069-1075.
53. Sandberg MA, Rosner B, Weigel-DiFranco C, Dryja TP, Berson EL. Disease course of patients with X-linked retinitis pigmentosa due to RPGR gene mutations. *Invest Ophthalmol Vis Sci.* 2007;48(3):1298-1304.
54. Sandberg MA, Rosner B, Weigel-DiFranco C, McGee TL, Dryja TP, Berson EL. Disease course in patients with autosomal recessive retinitis pigmentosa due to the USH2A gene. *Invest Ophthalmol Vis Sci.* 2008;49(12):5532-5539.
55. Talib M, van Schooneveld MJ, van Genderen MM, et al. Genotypic and Phenotypic Characteristics of CRB1-Associated Retinal Dystrophies: A Long-Term Follow-up Study. *Ophthalmology.* 2017;124(6):884-895.
56. Hafler BP, Comander J, Weigel DiFranco C, Place EM, Pierce EA. Course of Ocular Function in PRPF31 Retinitis Pigmentosa. *Semin Ophthalmol.* 2016;31(1-2):49-52.
57. Berson EL, Rosner B, Weigel-DiFranco C, Dryja TP, Sandberg MA. Disease progression in patients with dominant retinitis pigmentosa and rhodopsin mutations. *Invest Ophthalmol Vis Sci.* 2002;43(9):3027-3036.
58. Holopigian K, Greenstein V, Seiple W, Carr RE. Rates of change differ among measures of visual function in patients with retinitis pigmentosa. *Ophthalmology.* 1996;103(3):398-405.
59. Kolb H. S-Cone Pathways. In: Kolb H, Fernandez E, Nelson R, eds. *Webvision: The Organization of the Retina and Visual System.* Salt Lake City (UT)1995.
60. Pokorny J, Smith V, Verriest G, Pinckers A. *Congenital and a Acquired Color Vision Defects.* New York: Grune & Stratton; 1979.
61. Alexander KR, Fishman GA. Prolonged rod dark adaptation in retinitis pigmentosa. *Br J Ophthalmol.* 1984;68(8):561-569.
62. Mantyjarvi M, Tuppurainen K. Clinical symptoms at different ages in autosomal dominant retinitis pigmentosa. A family study in three generations. *Ophthalmologica.* 1994;208(1):23-28.
63. McCulloch DL, Marmor MF, Brigell MG, et al. ISCEV Standard for full-field clinical electroretinography (2015 update). *Doc Ophthalmol.* 2015;130(1):1-12.
64. Berson EL. Retinitis pigmentosa and allied diseases: applications of electroretinographic testing. *Int Ophthalmol.* 1981;4(1-2):7-22.
65. Wachtmeister L. Oscillatory potentials in the retina: what do they reveal. *Prog Retin Eye Res.* 1998;17(4):485-521.
66. Berson EL, Rosner B, Sandberg MA, et al. A randomized trial of vitamin A and vitamin E supplementation for retinitis

pigmentosa. *Arch Ophthalmol.* 1993;111(6):761-772.

67. Berson EL, Sandberg MA, Rosner B, Birch DG, Hanson AH. Natural course of retinitis pigmentosa over a three-year interval. *Am J Ophthalmol.* 1985;99(3):240-251.

68. Nagy D, Schonfisch B, Zrenner E, Jagle H. Long-term follow-up of retinitis pigmentosa patients with multifocal electroretinography. *Invest Ophthalmol Vis Sci.* 2008;49(10):4664-4671.

69. Falsini B, Galli-Resta L, Fadda A, et al. Long-term decline of central cone function in retinitis pigmentosa evaluated by focal electroretinogram. *Invest Ophthalmol Vis Sci.* 2012;53(12):7701-7709.

70. Messias K, Jagle H, Saran R, et al. Psychophysically determined full-field stimulus thresholds (FST) in retinitis pigmentosa: relationships with electroretinography and visual field outcomes. *Doc Ophthalmol.* 2013;127(2):123-129.

71. Hood DC. Assessing retinal function with the multifocal technique. *Prog Retin Eye Res.* 2000;19(5):607-646.

72. Witmer MT, Kiss S. Wide-field imaging of the retina. *Surv Ophthalmol.* 2013;58(2):143-154.

73. Shoughy SS, Arevalo JF, Kozak I. Update on wide- and ultra-widefield retinal imaging. *Indian J Ophthalmol.* 2015;63(7):575-581.

74. Sergott RC. Retinal segmentation using multicolor laser imaging. *J Neuroophthalmol.* 2014;34 Suppl:S24-28.

75. Liu G, Du Q, Keyal K, Wang F. Morphologic characteristics and clinical significance of the macular-sparing area in patients with retinitis pigmentosa as revealed by multicolor imaging. *Exp Ther Med.* 2017;14(6):5387-5394.

76. Milam AH, Li ZY, Fariss RN. Histopathology of the human retina in retinitis pigmentosa. *Prog Retin Eye Res.* 1998;17(2):175-205.

77. Liu G, Liu X, Li H, Du Q, Wang F. Optical Coherence Tomographic Analysis of Retina in Retinitis Pigmentosa Patients. *Ophthalmic Res.* 2016;56(3):111-122.

78. Hood DC, Lazow MA, Locke KG, Greenstein VC, Birch DG. The transition zone between healthy and diseased retina in patients with retinitis pigmentosa. *Invest Ophthalmol Vis Sci.* 2011;52(1):101-108.

79. Aleman TS, Cideciyan AV, Sumaroka A, et al. Inner retinal abnormalities in X-linked retinitis pigmentosa with RPGR mutations. *Invest Ophthalmol Vis Sci.* 2007;48(10):4759-4765.

80. Goldberg NR, Greenberg JP, Laud K, Tsang S, Freund KB. Outer retinal tubulation in degenerative retinal disorders. *Retina.* 2013;33(9):1871-1876.

81. Kuroda M, Hirami Y, Hata M, Mandai M, Takahashi M, Kurimoto Y. Intraretinal hyperreflective foci on spectral-domain optical coherence tomographic images of patients with retinitis pigmentosa. *Clin Ophthalmol.* 2014;8:435-440.

82. Aizawa S, Mitamura Y, Baba T, Hagiwara A, Ogata K, Yamamoto S. Correlation between visual function and photoreceptor inner/outer segment junction in patients with retinitis pigmentosa. *Eye (Lond).* 2009;23(2):304-308.

83. Witkin AJ, Ko TH, Fujimoto JG, et al. Ultra-high resolution optical coherence tomography assessment of photoreceptors in retinitis pigmentosa and related diseases. *Am J Ophthalmol.* 2006;142(6):945-952.

84. Tamaki M, Matsuo T. Optical coherence tomographic parameters as objective signs for visual acuity in patients with retinitis pigmentosa, future candidates for retinal prostheses. *J Artif Organs.* 2011;14(2):140-150.

85. Makiyama Y, Oishi A, Otani A, et al. Prevalence and spatial distribution of cystoid spaces in retinitis pigmentosa: investigation with spectral domain optical coherence tomography. *Retina.* 2014;34(5):981-988.

86. Delori FC, Dorey CK, Staurenghi G, Arend O, Goger DG, Weiter JJ. In vivo fluorescence of the ocular fundus exhibits retinal pigment epithelium lipofuscin characteristics. *Invest Ophthalmol Vis Sci.* 1995;36(3):718-729.

87. Keilhauer CN, Delori FC. Near-infrared autofluorescence imaging of the fundus: visualization of ocular melanin. *Invest Ophthalmol Vis Sci.* 2006;47(8):3556-3564.

88. Teussink MM, Lambertus S, de Mul FF, et al. Lipofuscin-associated photo-oxidative stress during fundus autofluorescence imaging. *PLoS One.* 2017;12(2):e0172635.

89. Hunter JJ, Morgan JI, Merigan WH, Sliney DH, Sparrow JR, Williams DR. The susceptibility of the retina to photochemical damage from visible light. *Prog Retin Eye Res.* 2012;31(1):28-42.

90. Lois N, Forrester JV. *Fundus Autofluorescence.* Second ed: Wolters Kluwer; 2015.

91. Sujirakul T, Davis R, Erol D, et al. Bilateral Concordance of the Fundus Hyperautofluorescent Ring in Typical Retinitis Pigmentosa Patients. *Ophthalmic Genet.* 2015;36(2):113-122.

92. Lima LH, Cella W, Greenstein VC, et al. Structural assessment of hyperautofluorescent ring in patients with retinitis pigmentosa. *Retina.* 2009;29(7):1025-1031.

93. Murakami T, Akimoto M, Ooto S, et al. Association between abnormal autofluorescence and photoreceptor disorganization in retinitis pigmentosa. *Am J Ophthalmol.* 2008;145(4):687-694.

94. Lenassi E, Troeger E, Wilke R, Hawlina M. Correlation between macular morphology and sensitivity in patients with retinitis pigmentosa and hyperautofluorescent ring. *Invest Ophthalmol Vis Sci.* 2012;53(1):47-52.

95. Greenstein VC, Duncker T, Holopigian K, et al. Structural and functional changes associated with normal and abnormal fundus autofluorescence in patients with retinitis pigmentosa. *Retina.* 2012;32(2):349-357.

96. Schuerch K, Woods RL, Lee W, et al. Quantifying Fundus Autofluorescence in Patients With Retinitis Pigmentosa. *Invest Ophthalmol Vis Sci.* 2017;58(3):1843-1855.

97. Robson AG, Lenassi E, Saihan Z, et al. Comparison of fundus autofluorescence with photopic and scotopic fine matrix mapping in patients with retinitis pigmentosa: 4- to 8-year follow-up. *Invest Ophthalmol Vis Sci.* 2012;53(10):6187-6195.

98. Wakabayashi T, Sawa M, Gomi F, Tsujikawa M. Correlation of fundus autofluorescence with photoreceptor morphology and functional changes in eyes with retinitis pigmentosa. *Acta Ophthalmol.* 2010;88(5):e177-183.

99. Robson AG, Tufail A, Fitzke F, et al. Serial imaging and structure-function correlates of high-density rings of fundus autofluorescence in retinitis pigmentosa. *Retina.* 2011;31(8):1670-1679.

100. Duncker T, Tabacaru MR, Lee W, Tsang SH, Sparrow JR, Greenstein VC. Comparison of near-infrared and short-wavelength autofluorescence in retinitis pigmentosa. *Invest Ophthalmol Vis Sci.* 2013;54(1):585-591.

101. Oishi A, Ogino K, Makiyama Y, Nakagawa S, Kurimoto M, Yoshimura N. Wide-field fundus autofluorescence imaging of retinitis pigmentosa. *Ophthalmology.* 2013;120(9):1827-1834.

102. von Ruckmann A, Fitzke FW, Bird AC. Distribution of pigment epithelium autofluorescence in retinal disease state recorded in vivo and its change over time. *Graefes Arch Clin Exp Ophthalmol.* 1999;237(1):1-9.

103. Kashani AH, Chen CL, Gahm JK, et al. Optical coherence tomography angiography: A comprehensive review of current methods and clinical applications. *Prog Retin Eye Res.* 2017;60:66-100.

104. Sayadi J, Miere A, Souied EH, Cohen SY. Type 3 Neovascularization Associated with Retinitis Pigmentosa. *Case Rep Ophthalmol.* 2017;8(1):245-249.

105. Georgiou M, Kalitzeos A, Patterson EJ, Dubra A, Carroll J, Michaelides M. Adaptive optics imaging of inherited retinal diseases. *Br J Ophthalmol.* 2017.

106. Sun LW, Johnson RD, Langlo CS, et al. Assessing Photoreceptor Structure in Retinitis Pigmentosa and Usher Syndrome. *Invest Ophthalmol Vis Sci.* 2016;57(6):2428-2442.

107. Ratnam K, Carroll J, Porco TC, Duncan JL, Roorda A. Relationship between foveal cone structure and clinical measures of visual function in patients with inherited retinal degenerations. *Invest Ophthalmol Vis Sci.* 2013;54(8):5836-5847.

108. Kumaran N, Moore AT, Weleber RG, Michaelides M. Leber congenital amaurosis/early-onset severe retinal dystrophy: clinical features, molecular genetics and therapeutic interventions. *Br J Ophthalmol.* 2017;101(9):1147-1154.

109. Hamel CP. Cone rod dystrophies. *Orphanet J Rare Dis.* 2007;2(1):7.

110. Mauthner L. Ein Fall von Choroideremia. *Berl Natur-med Ver Innsbruck.* 1872;2:191.

111. Borooah S, Collins C, Wright A, Dhillon B. Late-onset retinal macular degeneration: clinical insights into an inherited retinal degeneration. *Br J Ophthalmol.* 2009;93(3):284-289.

112. Zeitz C, Robson AG, Audo I. Congenital stationary night blindness: an analysis and update of genotype-phenotype correlations and pathogenic mechanisms. *Prog Retin Eye Res.* 2015;45:58-110.

113. Boughman JA, Vernon M, Shaver KA. Usher syndrome: definition and estimate of prevalence from two high-risk populations. *J Chronic Dis.* 1983;36(8):595-603.

114. Mockel A, Perdomo Y, Stutzmann F, Letsch J, Marion V, Dollfus H. Retinal dystrophy in Bardet-Biedl syndrome and related syndromic ciliopathies. *Prog Retin Eye Res.* 2011;30(4):258-274.

115. DeLuca AP, Whitmore SS, Barnes J, et al. Hypomorphic mutations in TRNT1 cause retinitis pigmentosa with erythrocytic microcytosis. *Hum Mol Genet.* 2016;25(1):44-56.

116. Mukhopadhyay R, Holder GE, Moore AT, Webster AR. Unilateral retinitis pigmentosa occurring in an individual with a germline mutation in the RP1 gene. *Arch Ophthalmol.* 2011;129(7):954-956.

117. Hendriks M, Verhoeven VJM, Buitendijk GHS, et al. Development of refractive errors - what can we learn from inherited retinal dystrophies? *Am J Ophthalmol.* 2017;182:81-89.

118. den Hollander AI, Lopez I, Yzer S, et al. Identification of novel mutations in patients with Leber congenital amaurosis and juvenile RP by genome-wide homozygosity mapping with SNP microarrays. *Invest Ophthalmol Vis Sci.* 2007;48(12):5690-5698.

119. Bandah D, Merin S, Ashhab M, Banin E, Sharon D. The spectrum of retinal diseases caused by NR2E3 mutations in Israeli and Palestinian patients. *Arch Ophthalmol.* 2009;127(3):297-302.

120. Hanein S, Perrault I, Gerber S, Tanguy G, Rozet JM, Kaplan J. Leber congenital amaurosis: survey of the genetic heterogeneity, refinement of the clinical definition and phenotype-genotype correlations as a strategy for molecular diagnosis. Clinical and molecular survey in LCA. *Adv Exp Med Biol.* 2006;572:15-20.

121. Krantz EM, Cruickshanks KJ, Klein BE, Klein R, Huang GH, Nieto FJ. Measuring refraction in adults in epidemiological studies. *Arch Ophthalmol.* 2010;128(1):88-92.

122. Chassine T, Bocquet B, Daien V, et al. Autosomal recessive retinitis pigmentosa with RP1 mutations is associated with myopia. *Br J Ophthalmol.* 2015;99(10):1360-1365.

123. Arno G, Hull S, Robson AG, et al. Lack of Interphotoreceptor Retinoid Binding Protein Caused by Homozygous Mutation of RBP3 Is Associated With High Myopia and Retinal Dystrophy. *Invest Ophthalmol Vis Sci.* 2015;56(4):2358-2365.

124. Habibi I, Chebil A, Kort F, Schorderet DF, El Matri L. Exome sequencing confirms ZNF408 mutations as a cause of familial retinitis pigmentosa. *Ophthalmic Genet.* 2017:1-4.

125. Avila-Fernandez A, Perez-Carro R, Corton M, et al. Whole-exome sequencing reveals ZNF408 as a new gene associated with autosomal recessive retinitis pigmentosa with vitreal alterations. *Hum Mol Genet.* 2015;24(14):4037-4048.

126. Allikmets R, Singh N, Sun H, et al. A photoreceptor cell-specific ATP-binding transporter gene (ABCR) is mutated in recessive Stargardt macular dystrophy. *Nat Genet.* 1997;15(3):236-246.

127. Martinez-Mir A, Bayes M, Vilageliu L, et al. A new locus for autosomal recessive retinitis pigmentosa (RP19) maps to 1p13-1p21. *Genomics.* 1997;40(1):142-146.

128. Cremers FP, van de Pol DJ, van Driel M, et al. Autosomal recessive retinitis pigmentosa and cone-rod dystrophy caused by splice site mutations in the Stargardt's disease gene ABCR. *Hum Mol Genet.* 1998;7(3):355-362.

129. Klevering BJ, Deutman AF, Maugeri A, Cremers FP, Hoyng CB. The spectrum of retinal phenotypes caused by mutations in

the ABCA4 gene. *Graefes Arch Clin Exp Ophthalmol.* 2005;243(2):90-100.

130. Mullins RF, Kuehn MH, Radu RA, et al. Autosomal recessive retinitis pigmentosa due to ABCA4 mutations: clinical, pathologic, and molecular characterization. *Invest Ophthalmol Vis Sci.* 2012;53(4):1883-1894.

131. Weng J, Mata NL, Azarian SM, Tzekov RT, Birch DG, Travis GH. Insights into the function of Rim protein in photoreceptors and etiology of Stargardt's disease from the phenotype in abcr knockout mice. *Cell.* 1999;98(1):13-23.

132. Astuti GD, Arno G, Hull S, et al. Mutations in AGBL5, Encoding alpha-Tubulin Deglutamylase, Are Associated With Autosomal Recessive Retinitis Pigmentosa. *Invest Ophthalmol Vis Sci.* 2016;57(14):6180-6187.

133. Branham K, Matsui H, Biswas P, et al. Establishing the involvement of the novel gene AGBL5 in retinitis pigmentosa by whole genome sequencing. *Physiol Genomics.* 2016:physiolgenomics.00101.02016.

134. Kastner S, Thiemann IJ, Dekomien G, et al. Exome Sequencing Reveals AGBL5 as Novel Candidate Gene and Additional Variants for Retinitis Pigmentosa in Five Turkish Families. *Invest Ophthalmol Vis Sci.* 2015;56(13):8045-8053.

135. Huang XF, Huang F, Wu KC, et al. Genotype-phenotype correlation and mutation spectrum in a large cohort of patients with inherited retinal dystrophy revealed by next-generation sequencing. *Genet Med.* 2015;17(4):271-278.

136. Nguyen TT, Hull S, Roepman R, et al. Missense mutations in the WD40 domain of AHI1 cause non-syndromic retinitis pigmentosa. *J Med Genet.* 2017.

137. Dixon-Salazar T, Silhavy JL, Marsh SE, et al. Mutations in the AHI1 gene, encoding jouberin, cause Joubert syndrome with cortical polymicrogyria. *Am J Hum Genet.* 2004;75(6):979-987.

138. Elsayed SM, Phillips JB, Heller R, et al. Non-manifesting AHI1 truncations indicate localized loss-of-function tolerance in a severe Mendelian disease gene. *Hum Mol Genet.* 2015;24(9):2594-2603.

139. Arno G, Carss KJ, Hull S, et al. Biallelic Mutation of ARHGEF18, Involved in the Determination of Epithelial Apicobasal Polarity, Causes Adult-Onset Retinal Degeneration. *Am J Hum Genet.* 2017;100(2):334-342.

140. Davidson AE, Schwarz N, Zelinger L, et al. Mutations in ARL2BP, Encoding ADP-Ribosylation-Factor-Like 2 Binding Protein, Cause Autosomal-Recessive Retinitis Pigmentosa. *Am J Hum Genet.* 2013.

141. Audo I, El Shamieh S, Mejecase C, et al. ARL2BP mutations account for 0.1% of autosomal recessive rod-cone dystrophies with the report of a novel splice variant. *Clin Genet.* 2017;92(1):109-111.

142. Abu Safieh L, Aldahmesh MA, Shamseldin H, et al. Clinical and molecular characterisation of Bardet-Biedl syndrome in consanguineous populations: the power of homozygosity mapping. *J Med Genet.* 2010;47(4):236-241.

143. Aldahmesh MA, Safieh LA, Alkuraya H, et al. Molecular characterization of retinitis pigmentosa in Saudi Arabia. *Mol Vis.* 2009;15:2464-2469.

144. Pretorius PR, Baye LM, Nishimura DY, et al. Identification and functional analysis of the vision-specific BBS3 (ARL6) long isoform. *PLoS genetics.* 2010;6(3):e1000884.

145. Estrada-Cuzcano A, Koenekoop RK, Senechal A, et al. BBS1 mutations in a wide spectrum of phenotypes ranging from nonsyndromic retinitis pigmentosa to Bardet-Biedl syndrome. *Arch Ophthalmol.* 2012;130(11):1425-1432.

146. Davis RE, Swiderski RE, Rahmouni K, et al. A knockin mouse model of the Bardet-Biedl syndrome 1 M390R mutation has cilia defects, ventriculomegaly, retinopathy, and obesity. *Proc Natl Acad Sci U S A.* 2007;104(49):19422-19427.

147. Shevach E, Ali M, Mizrahi-Meissonnier L, et al. Association between missense mutations in the BBS2 gene and nonsyndromic retinitis pigmentosa. *JAMA Ophthalmol.* 2015;133(3):312-318.

148. Nishimura DY, Fath M, Mullins RF, et al. Bbs2-null mice have neurosensory deficits, a defect in social dominance, and retinopathy associated with mislocalization of rhodopsin. *Proc Natl Acad Sci U S A.* 2004;101(47):16588-16593.

149. Abu-Safieh L, Al-Anazi S, Al-Abdi L, et al. In search of triallelism in Bardet-Biedl syndrome. *Eur J Hum Genet.* 2012;20(4):420-427.

150. Veleri S, Bishop K, Dalle Nogare DE, et al. Knockdown of Bardet-Biedl syndrome gene BBS9/PTHB1 leads to cilia defects. *PLoS One.* 2012;7(3):e34389.

151. Davidson AE, Millar ID, Urquhart JE, et al. Missense mutations in a retinal pigment epithelium protein, bestrophin-1, cause retinitis pigmentosa. *Am J Hum Genet.* 2009;85(5):581-592.

152. Boon CJ, Klevering BJ, Leroy BP, Hoyng CB, Keunen JE, den Hollander AI. The spectrum of ocular phenotypes caused by mutations in the BEST1 gene. *Prog Retin Eye Res.* 2009;28(3):187-205.

153. Dalvin LA, Chehade JEA, Chiang J, Fuchs J, Iezzi R, Marmorstein AD. Retinitis pigmentosa associated with a mutation in BEST1. *Am J Ophthalmol Case Reports.* 2016;2:11-17.

154. Bocquet B, Marzouka NA, Hebrard M, et al. Homozygosity mapping in autosomal recessive retinitis pigmentosa families detects novel mutations. *Mol Vis.* 2013;19:2487-2500.

155. Collin RW, Safieh C, Littink KW, et al. Mutations in C2ORF71 cause autosomal-recessive retinitis pigmentosa. *Am J Hum Genet.* 2010;86(5):783-788.

156. Hebrard M, Manes G, Bocquet B, et al. Combining gene mapping and phenotype assessment for fast mutation finding in non-consanguineous autosomal recessive retinitis pigmentosa families. *Eur J Hum Genet.* 2011;19(12):1256-1263.

157. Audo I, Lancelot ME, Mohand-Said S, et al. Novel C2orf71 mutations account for approximately 1% of cases in a large French arRP cohort. *Hum Mutat.* 2011;32(4):E2091-2103.

158. Liu YP, Bosch DG, Siemiatkowska AM, et al. Putative digenic inheritance of heterozygous RP1L1 and C2orf71 null mutations in syndromic retinal dystrophy. *Ophthalmic Genet.* 2017;38(2):127-132.

159. Kevany BM, Zhang N, Jastrzebska B, Palczewski K. Animals deficient in C2Orf71, an autosomal recessive retinitis pigmentosa-

associated locus, develop severe early-onset retinal degeneration. *Hum Mol Genet.* 2015;24(9):2627-2640.

160. Gerth-Kahlert C, Tiwari A, Hanson JVM, et al. C2orf71 Mutations as a Frequent Cause of Autosomal-Recessive Retinitis Pigmentosa: Clinical Analysis and Presentation of 8 Novel Mutations. *Invest Ophthalmol Vis Sci.* 2017;58(10):3840-3850.

161. Estrada-Cuzcano A, Neveling K, Kohl S, et al. Mutations in C8orf37, encoding a ciliary protein, are associated with autosomal-recessive retinal dystrophies with early macular involvement. *Am J Hum Genet.* 2012;90(1):102-109.

162. van Huet RA, Estrada-Cuzcano A, Banin E, et al. Clinical characteristics of rod and cone photoreceptor dystrophies in patients with mutations in the C8orf37 gene. *Invest Ophthalmol Vis Sci.* 2013;54(7):4683-4690.

163. Katagiri S, Hayashi T, Yoshitake K, et al. Novel C8orf37 Mutations in Patients with Early-onset Retinal Dystrophy, Macular Atrophy, Cataracts, and High Myopia. *Ophthalmic Genet.* 2015:1-8.

164. Heon E, Kim G, Qin S, et al. Mutations in C8ORF37 cause Bardet Biedl syndrome (BBS21). *Hum Mol Genet.* 2016;25(11):2283-2294.

165. Yang Z, Alvarez BV, Chakarova C, et al. Mutant carbonic anhydrase 4 impairs pH regulation and causes retinal photoreceptor degeneration. *Hum Mol Genet.* 2005;14(2):255-265.

166. Alvarez BV, Vithana EN, Yang Z, et al. Identification and characterization of a novel mutation in the carbonic anhydrase IV gene that causes retinitis pigmentosa. *Invest Ophthalmol Vis Sci.* 2007;48(8):3459-3468.

167. Rebello G, Ramesar R, Vorster A, et al. Apoptosis-inducing signal sequence mutation in carbonic anhydrase IV identified in patients with the RP17 form of retinitis pigmentosa. *Proc Natl Acad Sci U S A.* 2004;101(17):6617-6622.

168. Henderson RH, Li Z, Abd El Aziz MM, et al. Biallelic mutation of protocadherin-21 (PCDH21) causes retinal degeneration in humans. *Mol Vis.* 2010;16:46-52.

169. Duncan JL, Roorda A, Navani M, et al. Identification of a novel mutation in the CDHR1 gene in a family with recessive retinal degeneration. *Arch Ophthalmol.* 2012;130(10):1301-1308.

170. Rattner A, Smallwood PM, Williams J, et al. A photoreceptor-specific cadherin is essential for the structural integrity of the outer segment and for photoreceptor survival. *Neuron.* 2001;32(5):775-786.

171. Bayes M, Goldaracena B, Martinez-Mir A, et al. A new autosomal recessive retinitis pigmentosa locus maps on chromosome 2q31-q33. *J Med Genet.* 1998;35(2):141-145.

172. Avila-Fernandez A, Riveiro-Alvarez R, Vallespin E, et al. CERKL mutations and associated phenotypes in seven Spanish families with autosomal recessive retinitis pigmentosa. *Invest Ophthalmol Vis Sci.* 2008;49(6):2709-2713.

173. Tang Z, Wang Z, Ke T, Wang QK, Liu M. Novel compound heterozygous mutations in CERKL cause autosomal recessive retinitis pigmentosa in a nonconsanguineous Chinese family. *Arch Ophthalmol.* 2009;127(8):1077-1078.

174. Auslender N, Sharon D, Abbasi AH, Garzozi HJ, Banin E, Ben-Yosef T. A common founder mutation of CERKL underlies autosomal recessive retinal degeneration with early macular involvement among Yemenite Jews. *Invest Ophthalmol Vis Sci.* 2007;48(12):5431-5438.

175. Matsui R, Cideciyan AV, Schwartz SB, et al. Molecular Heterogeneity Within the Clinical Diagnosis of Pericentral Retinal Degeneration. *Invest Ophthalmol Vis Sci.* 2015;56(10):6007-6018.

176. Garanto A, Vicente-Tejedor J, Riera M, et al. Targeted knockdown of Cerkl, a retinal dystrophy gene, causes mild affectation of the retinal ganglion cell layer. *Biochim Biophys Acta.* 2012;1822(8):1258-1269.

177. Wang F, Wang H, Tuan HF, et al. Next generation sequencing-based molecular diagnosis of retinitis pigmentosa: identification of a novel genotype-phenotype correlation and clinical refinements. *Hum Genet.* 2014;133(3):331-345.

178. Ku CA, Hull S, Arno G, et al. Detailed Clinical Phenotype and Molecular Genetic Findings in CLN3-Associated Isolated Retinal Degeneration. *JAMA Ophthalmol.* 2017;135(7):749-760.

179. Joensuu T, Hamalainen R, Yuan B, et al. Mutations in a novel gene with transmembrane domains underlie Usher syndrome type 3. *Am J Hum Genet.* 2001;69(4):673-684.

180. Khan MI, Kersten FF, Azam M, et al. CLRN1 mutations cause nonsyndromic retinitis pigmentosa. *Ophthalmology.* 2011;118(7):1444-1448.

181. Geng R, Geller SF, Hayashi T, et al. Usher syndrome IIIA gene clarin-1 is essential for hair cell function and associated neural activation. *Hum Mol Genet.* 2009;18(15):2748-2760.

182. Jin X, Qu LH, Hou BK, et al. Novel compound heterozygous mutation in the CNGA1 gene underlie autosomal recessive retinitis pigmentosa in a Chinese family. *Biosci Rep.* 2016;36(1):e00289.

183. Katagiri S, Akahori M, Sergeev Y, et al. Whole exome analysis identifies frequent CNGA1 mutations in Japanese population with autosomal recessive retinitis pigmentosa. *PLoS One.* 2014;9(9):e108721.

184. Paloma E, Martinez-Mir A, Garcia-Sandoval B, et al. Novel homozygous mutation in the alpha subunit of the rod cGMP gated channel (CNGA1) in two Spanish sibs affected with autosomal recessive retinitis pigmentosa. *J Med Genet.* 2002;39(10):E66.

185. Wang M, Gan D, Huang X, Xu G. Novel compound heterozygous mutations in CNGA1in a Chinese family affected with autosomal recessive retinitis pigmentosa by targeted sequencing. *BMC Ophthalmol.* 2016;16:101.

186. Zhang Q, Zulfiqar F, Riazuddin SA, et al. Autosomal recessive retinitis pigmentosa in a Pakistani family mapped to CNGA1 with identification of a novel mutation. *Mol Vis.* 2004;10:884-889.

187. Wiik AC, Ropstad EO, Ekesten B, Karlstam L, Wade CM, Lingaas F. Progressive retinal atrophy in Shetland sheepdog is associated with a mutation in the CNGA1 gene. *Anim Genet.* 2015;46(5):515-521.

188. Comander J, Weigel-DiFranco C, Maher M, et al. The Genetic Basis of Pericentral Retinitis Pigmentosa-A Form of Mild Retinitis Pigmentosa. *Genes (Basel).* 2017;8(10).

Chapter 2.1

189. Bareil C, Hamel CP, Delague V, Arnaud B, Demaille J, Claustres M. Segregation of a mutation in CNGB1 encoding the beta-subunit of the rod cGMP-gated channel in a family with autosomal recessive retinitis pigmentosa. *Hum Genet.* 2001;108(4):328-334.
190. Kondo H, Qin M, Mizota A, et al. A homozygosity-based search for mutations in patients with autosomal recessive retinitis pigmentosa, using microsatellite markers. *Invest Ophthalmol Vis Sci.* 2004;45(12):4433-4439.
191. Hull S, Attanasio M, Arno G, et al. Clinical Characterization of CNGB1-Related Autosomal Recessive Retinitis Pigmentosa. *JAMA Ophthalmol.* 2017.
192. Fradin M, Colin E, Hannouche-Bared D, et al. Run of homozygosity analysis reveals a novel nonsense variant of the CNGB1 gene involved in retinitis pigmentosa 45. *Ophthalmic Genet.* 2016;37(3):357-359.
193. Winkler PA, Ekenstedt KJ, Occelli LM, et al. A large animal model for CNGB1 autosomal recessive retinitis pigmentosa. *PLoS One.* 2013;8(8):e72229.
194. Ehrenberg M, Pierce EA, Cox GF, Fulton AB. CRB1: one gene, many phenotypes. *Semin Ophthalmol.* 2013;28(5-6):397-405.
195. den Hollander AI, Heckenlively JR, van den Born LI, et al. Leber congenital amaurosis and retinitis pigmentosa with Coats-like exudative vasculopathy are associated with mutations in the crumbs homologue 1 (CRB1) gene. *Am J Hum Genet.* 2001;69(1):198-203.
196. Lotery AJ, Malik A, Shami SA, et al. CRB1 mutations may result in retinitis pigmentosa without para-arteriolar RPE preservation. *Ophthalmic Genet.* 2001;22(3):163-169.
197. van den Born LI, van Soest S, van Schooneveld MJ, Riemslag FC, de Jong PT, Bleeker-Wagemakers EM. Autosomal recessive retinitis pigmentosa with preserved para-arteriolar retinal pigment epithelium. *Am J Ophthalmol.* 1994;118(4):430-439.
198. Zenteno JC, Buentello-Volante B, Ayala-Ramirez R, Villanueva-Mendoza C. Homozygosity mapping identifies the Crumbs homologue 1 (Crb1) gene as responsible for a recessive syndrome of retinitis pigmentosa and nanophthalmos. *Am J Med Genet A.* 2011;155a(5):1001-1006.
199. Mathijssen IB, Florijn RJ, van den Born LI, et al. Long-term follow-up of patients with retinitis pigmentosa type 12 caused by CRB1 mutations: a severe phenotype with considerable interindividual variability. *Retina.* 2017;37(1):161-172.
200. Mehalow AK, Kameya S, Smith RS, et al. CRB1 is essential for external limiting membrane integrity and photoreceptor morphogenesis in the mammalian retina. *Hum Mol Genet.* 2003;12(17):2179-2189.
201. Aleman TS, Cideciyan AV, Aguirre GK, et al. Human CRB1-associated retinal degeneration: comparison with the rd8 Crb1-mutant mouse model. *Invest Ophthalmol Vis Sci.* 2011;52(9):6898-6910.
202. Xu M, Xie YA, Abouzeid H, et al. Mutations in the Spliceosome Component CWC27 Cause Retinal Degeneration with or without Additional Developmental Anomalies. *Am J Hum Genet.* 2017;100(4):592-604.
203. Zelinger L, Banin E, Obolensky A, et al. A missense mutation in DHDDS, encoding dehydrodolichyl diphosphate synthase, is associated with autosomal-recessive retinitis pigmentosa in Ashkenazi Jews. *Am J Hum Genet.* 2011;88(2):207-215.
204. Zuchner S, Dallman J, Wen R, et al. Whole-exome sequencing links a variant in DHDDS to retinitis pigmentosa. *Am J Hum Genet.* 2011;88(2):201-206.
205. Venturini G, Koskiniemi-Kuendig H, Harper S, Berson EL, Rivolta C. Two specific mutations are prevalent causes of recessive retinitis pigmentosa in North American patients of Jewish ancestry. *Genet Med.* 2015;17(4):285-290.
206. Collin RW, Littink KW, Klevering BJ, et al. Identification of a 2 Mb human ortholog of Drosophila eyes shut/spacemaker that is mutated in patients with retinitis pigmentosa. *Am J Hum Genet.* 2008;83(5):594-603.
207. Littink KW, van den Born LI, Koenekoop RK, et al. Mutations in the EYS gene account for approximately 5% of autosomal recessive retinitis pigmentosa and cause a fairly homogeneous phenotype. *Ophthalmology.* 2010;117(10):2026-2033, 2033 e2021-2027.
208. Bandah-Rozenfeld D, Littink KW, Ben-Yosef T, et al. Novel null mutations in the EYS gene are a frequent cause of autosomal recessive retinitis pigmentosa in the Israeli population. *Invest Ophthalmol Vis Sci.* 2010;51(9):4387-4394.
209. Iwanami M, Oshikawa M, Nishida T, Nakadomari S, Kato S. High prevalence of mutations in the EYS gene in Japanese patients with autosomal recessive retinitis pigmentosa. *Invest Ophthalmol Vis Sci.* 2012;53(2):1033-1040.
210. Bandah-Rozenfeld D, Mizrahi-Meissonnier L, Farhy C, et al. Homozygosity mapping reveals null mutations in FAM161A as a cause of autosomal-recessive retinitis pigmentosa. *Am J Hum Genet.* 2010;87(3):382-391.
211. Langmann T, Di Gioia SA, Rau I, et al. Nonsense mutations in FAM161A cause RP28-associated recessive retinitis pigmentosa. *Am J Hum Genet.* 2010;87(3):376-381.
212. Venturini G, Di Gioia SA, Harper S, Weigel-DiFranco C, Rivolta C, Berson EL. Molecular genetics of FAM161A in North American patients with early-onset retinitis pigmentosa. *PLoS One.* 2014;9(3):e92479.
213. Rose AM, Sergouniotis P, Alfano G, et al. Diverse clinical phenotypes associated with a nonsense mutation in FAM161A. *Eye (Lond).* 2015;29(9):1226-1232.
214. Van Schil K, Klevering BJ, Leroy BP, et al. A Nonsense Mutation in FAM161A Is a Recurrent Founder Allele in Dutch and Belgian Individuals With Autosomal Recessive Retinitis Pigmentosa. *Invest Ophthalmol Vis Sci.* 2015;56(12):7418-7426.
215. Karlstetter M, Sorusch N, Caramoy A, et al. Disruption of the retinitis pigmentosa 28 gene Fam161a in mice affects photoreceptor ciliary structure and leads to progressive retinal degeneration. *Hum Mol Genet.* 2014;23(19):5197-5210.
216. Wada Y, Abe T, Takeshita T, Sato H, Yanashima K, Tamai M. Mutation of human retinal fascin gene (FSCN2) causes autosomal dominant retinitis pigmentosa. *Invest Ophthalmol Vis Sci.* 2001;42(10):2395-2400.
217. Wada Y, Abe T, Itabashi T, Sato H, Kawamura M, Tamai M. Autosomal dominant macular degeneration associated with

208delG mutation in the FSCN2 gene. *Arch Ophthalmol.* 2003;121(11):1613-1620.

218. Jinda W, Taylor TD, Suzuki Y, et al. Whole exome sequencing in Thai patients with retinitis pigmentosa reveals novel mutations in six genes. *Invest Ophthalmol Vis Sci.* 2014;55(4):2259-2268.

219. Yokokura S, Wada Y, Nakai S, et al. Targeted disruption of FSCN2 gene induces retinopathy in mice. *Invest Ophthalmol Vis Sci.* 2005;46(8):2905-2915.

220. Zhang Q, Li S, Xiao X, Jia X, Guo X. The 208delG mutation in FSCN2 does not associate with retinal degeneration in Chinese individuals. *Invest Ophthalmol Vis Sci.* 2007;48(2):530-533.

221. Jin ZB, Mandai M, Homma K, et al. Allelic copy number variation in FSCN2 detected using allele-specific genotyping and multiplex real-time PCRs. *Invest Ophthalmol Vis Sci.* 2008;49(9):3799-3805.

222. Carrigan M, Duignan E, Humphries P, Palfi A, Kenna PF, Farrar GJ. A novel homozygous truncating GNAT1 mutation implicated in retinal degeneration. *Br J Ophthalmol.* 2016;100(4):495-500.

223. Mejecase C, Laurent-Coriat C, Mayer C, et al. Identification of a Novel Homozygous Nonsense Mutation Confirms the Implication of GNAT1 in Rod-Cone Dystrophy. *PLoS One.* 2016;11(12):e0168271.

224. Calvert PD, Krasnoperova NV, Lyubarsky AL, et al. Phototransduction in transgenic mice after targeted deletion of the rod transducin alpha -subunit. *Proc Natl Acad Sci U S A.* 2000;97(25):13913-13918.

225. Sato M, Nakazawa M, Usui T, Tanimoto N, Abe H, Ohguro H. Mutations in the gene coding for guanylate cyclase-activating protein 2 (GUCA1B gene) in patients with autosomal dominant retinal dystrophies. *Graefes Arch Clin Exp Ophthalmol.* 2005;243(3):235-242.

226. Haer-Wigman L, Newman H, Leibu R, et al. Non-syndromic retinitis pigmentosa due to mutations in the mucopolysaccharidosis type IIIC gene, heparan-alpha-glucosaminide N-acetyltransferase (HGSNAT). *Hum Mol Genet.* 2015;24(13):3742-3751.

227. Van Cauwenbergh C, Van Schil K, Cannoodt R, et al. arrEYE: a customized platform for high-resolution copy number analysis of coding and noncoding regions of known and candidate retinal dystrophy genes and retinal noncoding RNAs. *Genet Med.* 2017;19(4):457-466.

228. Wang F, Wang Y, Zhang B, et al. A missense mutation in HK1 leads to autosomal dominant retinitis pigmentosa. *Invest Ophthalmol Vis Sci.* 2014;55(11):7159-7164.

229. Sullivan LS, Koboldt DC, Bowne SJ, et al. A dominant mutation in hexokinase 1 (HK1) causes retinitis pigmentosa. *Invest Ophthalmol Vis Sci.* 2014;55(11):7147-7158.

230. Daiger SP, Sullivan LS, Bowne SJ, et al. Identification of a Novel Gene on 10q22.1 Causing Autosomal Dominant Retinitis Pigmentosa (adRP). *Adv Exp Med Biol.* 2016;854:193-200.

231. Pierrache LHM, Kimchi A, Ratnapriya R, et al. Whole-Exome Sequencing Identifies Biallelic IDH3A Variants as a Cause of Retinitis Pigmentosa Accompanied by Pseudocoloboma. *Ophthalmology.* 2017;124(7):992-1003.

232. Hartong DT, Dange M, McGee TL, Berson EL, Dryja TP, Colman RF. Insights from retinitis pigmentosa into the roles of isocitrate dehydrogenases in the Krebs cycle. *Nat Genet.* 2008;40(10):1230-1234.

233. Beheshtian M, Saee Rad S, Babanejad M, et al. Impact of whole exome sequencing among Iranian patients with autosomal recessive retinitis pigmentosa. *Arch Iran Med.* 2015;18(11):776-785.

234. Xu M, Yang L, Wang F, et al. Mutations in human IFT140 cause non-syndromic retinal degeneration. *Hum Genet.* 2015;134(10):1069-1078.

235. Hull S, Owen N, Islam F, et al. Nonsyndromic Retinal Dystrophy due to Bi-Allelic Mutations in the Ciliary Transport Gene IFT140. *Invest Ophthalmol Vis Sci.* 2016;57(3):1053-1062.

236. Perrault I, Saunier S, Hanein S, et al. Mainzer-Saldino syndrome is a ciliopathy caused by IFT140 mutations. *Am J Hum Genet.* 2012;90(5):864-870.

237. Miller KA, Ah-Cann CJ, Welfare MF, et al. Cauli: a mouse strain with an Ift140 mutation that results in a skeletal ciliopathy modelling Jeune syndrome. *PLoS genetics.* 2013;9(8):e1003746.

238. Halbritter J, Bizet AA, Schmidts M, et al. Defects in the IFT-B component IFT172 cause Jeune and Mainzer-Saldino syndromes in humans. *Am J Hum Genet.* 2013;93(5):915-925.

239. Bujakowska KM, Zhang Q, Siemiatkowska AM, et al. Mutations in IFT172 cause isolated retinal degeneration and Bardet-Biedl syndrome. *Hum Mol Genet.* 2015;24(1):230-242.

240. Schaefer E, Stoetzel C, Scheidecker S, et al. Identification of a novel mutation confirms the implication of IFT172 (BBS20) in Bardet-Biedl syndrome. *J Hum Genet.* 2016;61(5):447-450.

241. Bowne SJ, Sullivan LS, Blanton SH, et al. Mutations in the inosine monophosphate dehydrogenase 1 gene (IMPDH1) cause the RP10 form of autosomal dominant retinitis pigmentosa. *Hum Mol Genet.* 2002;11(5):559-568.

242. Bowne SJ, Sullivan LS, Mortimer SE, et al. Spectrum and frequency of mutations in IMPDH1 associated with autosomal dominant retinitis pigmentosa and leber congenital amaurosis. *Invest Ophthalmol Vis Sci.* 2006;47(1):34-42.

243. Kozma P, Hughbanks-Wheaton DK, Locke KG, et al. Phenotypic characterization of a large family with RP10 autosomal-dominant retinitis pigmentosa: an Asp226Asn mutation in the IMPDH1 gene. *Am J Ophthalmol.* 2005;140(5):858-867.

244. Ali S, Khan SY, Naeem MA, et al. Phenotypic variability associated with the D226N allele of IMPDH1. *Ophthalmology.* 2015;122(2):429-431.

245. Aherne A, Kennan A, Kenna PF, et al. On the molecular pathology of neurodegeneration in IMPDH1-based retinitis pigmentosa. *Hum Mol Genet.* 2004;13(6):641-650.

Chapter 2.1

246. Bandah-Rozenfeld D, Collin RW, Banin E, et al. Mutations in IMPG2, encoding interphotoreceptor matrix proteoglycan 2, cause autosomal-recessive retinitis pigmentosa. *Am J Hum Genet.* 2010;87(2):199-208.

247. van Huet RA, Collin RW, Siemiatkowska AM, et al. IMPG2-associated retinitis pigmentosa displays relatively early macular involvement. *Invest Ophthalmol Vis Sci.* 2014;55(6):3939-3953.

248. El Shamieh S, Neuille M, Terray A, et al. Whole-exome sequencing identifies KIZ as a ciliary gene associated with autosomal-recessive rod-cone dystrophy. *Am J Hum Genet.* 2014;94(4):625-633.

249. Friedman JS, Ray JW, Waseem N, et al. Mutations in a BTB-Kelch protein, KLHL7, cause autosomal-dominant retinitis pigmentosa. *Am J Hum Genet.* 2009;84(6):792-800.

250. Hugosson T, Friedman JS, Ponjavic V, Abrahamson M, Swaroop A, Andreasson S. Phenotype associated with mutation in the recently identified autosomal dominant retinitis pigmentosa KLHL7 gene. *Arch Ophthalmol.* 2010;128(6):772-778.

251. Wen Y, Locke KG, Klein M, et al. Phenotypic characterization of 3 families with autosomal dominant retinitis pigmentosa due to mutations in KLHL7. *Arch Ophthalmol.* 2011;129(11):1475-1482.

252. Angius A, Uva P, Buers I, et al. Bi-allelic Mutations in KLHL7 Cause a Crisponi/CISS1-like Phenotype Associated with Early-Onset Retinitis Pigmentosa. *Am J Hum Genet.* 2016;99(1):236-245.

253. Thompson DA, Li Y, McHenry CL, et al. Mutations in the gene encoding lecithin retinol acyltransferase are associated with early-onset severe retinal dystrophy. *Nat Genet.* 2001;28(2):123-124.

254. Littink KW, van Genderen MM, van Schooneveld MJ, et al. A homozygous frameshift mutation in LRAT causes retinitis punctata albescens. *Ophthalmology.* 2012;119(9):1899-1906.

255. Dev Borman A, Ocaka LA, Mackay DS, et al. Early onset retinal dystrophy due to mutations in LRAT: molecular analysis and detailed phenotypic study. *Invest Ophthalmol Vis Sci.* 2012;53(7):3927-3938.

256. Batten ML, Imanishi Y, Maeda T, et al. Lecithin-retinol acyltransferase is essential for accumulation of all-trans-retinyl esters in the eye and in the liver. *J Biol Chem.* 2004;279(11):10422-10432.

257. Ozgul RK, Siemiatkowska AM, Yucel D, et al. Exome sequencing and cis-regulatory mapping identify mutations in MAK, a gene encoding a regulator of ciliary length, as a cause of retinitis pigmentosa. *Am J Hum Genet.* 2011;89(2):253-264.

258. Stone EM, Luo X, Heon E, et al. Autosomal recessive retinitis pigmentosa caused by mutations in the MAK gene. *Invest Ophthalmol Vis Sci.* 2011;52(13):9665-9673.

259. van Huet RA, Siemiatkowska AM, Ozgul RK, et al. Retinitis pigmentosa caused by mutations in the ciliary MAK gene is relatively mild and is not associated with apparent extra-ocular features. *Acta Ophthalmol.* 2015;93(1):83-94.

260. Lai YH, Capasso JE, Kaiser R, Levin AV. Intraretinal cystoid spaces in a patient with retinitis pigmentosa due to mutation in the MAK gene. *Ophthalmic Genet.* 2016;37(4):424-426.

261. Charbel Issa P, Bolz HJ, Ebermann I, Domeier E, Holz FG, Scholl HP. Characterisation of severe rod-cone dystrophy in a consanguineous family with a splice site mutation in the MERTK gene. *Br J Ophthalmol.* 2009;93(7):920-925.

262. Mackay DS, Henderson RH, Sergouniotis PI, et al. Novel mutations in MERTK associated with childhood onset rod-cone dystrophy. *Mol Vis.* 2010;16:369-377.

263. Ostergaard E, Duno M, Batbayli M, Vilhelmsen K, Rosenberg T. A novel MERTK deletion is a common founder mutation in the Faroe Islands and is responsible for a high proportion of retinitis pigmentosa cases. *Mol Vis.* 2011;17:1485-1492.

264. Ksantini M, Lafont E, Bocquet B, Meunier I, Hamel CP. Homozygous mutation in MERTK causes severe autosomal recessive retinitis pigmentosa. *Eur J Ophthalmol.* 2012;22(4):647-653.

265. Shahzadi A, Riazuddin SA, Ali S, et al. Nonsense mutation in MERTK causes autosomal recessive retinitis pigmentosa in a consanguineous Pakistani family. *Br J Ophthalmol.* 2010;94(8):1094-1099.

266. D'Cruz PM, Yasumura D, Weir J, et al. Mutation of the receptor tyrosine kinase gene Mertk in the retinal dystrophic RCS rat. *Hum Mol Genet.* 2000;9(4):645-651.

267. Siemiatkowska AM, van den Born LI, van Hagen PM, et al. Mutations in the mevalonate kinase (MVK) gene cause nonsyndromic retinitis pigmentosa. *Ophthalmology.* 2013;120(12):2697-2705.

268. Kellner U, Stohr H, Weinitz S, Farmand G, Weber BH. Mevalonate kinase deficiency associated with ataxia and retinitis pigmentosa in two brothers with MVK gene mutations. *Ophthalmic Genet.* 2017:1-5.

269. Nishiguchi KM, Tearle RG, Liu YP, et al. Whole genome sequencing in patients with retinitis pigmentosa reveals pathogenic DNA structural changes and NEK2 as a new disease gene. *Proc Natl Acad Sci U S A.* 2013;110(40):16139-16144.

270. Coppieters F, Leroy BP, Beysen D, et al. Recurrent mutation in the first zinc finger of the orphan nuclear receptor NR2E3 causes autosomal dominant retinitis pigmentosa. *Am J Hum Genet.* 2007;81(1):147-157.

271. Escher P, Gouras P, Roduit R, et al. Mutations in NR2E3 can cause dominant or recessive retinal degenerations in the same family. *Hum Mutat.* 2009;30(3):342-351.

272. Gire AI, Sullivan LS, Bowne SJ, et al. The Gly56Arg mutation in NR2E3 accounts for 1-2% of autosomal dominant retinitis pigmentosa. *Mol Vis.* 2007;13:1970-1975.

273. Gerber S, Rozet JM, Takezawa SI, et al. The photoreceptor cell-specific nuclear receptor gene (PNR) accounts for retinitis pigmentosa in the Crypto-Jews from Portugal (Marranos), survivors from the Spanish Inquisition. *Hum Genet.* 2000;107(3):276-284.

274. Escher P, Tran HV, Vaclavik V, Borruat FX, Schorderet DF, Munier FL. Double concentric autofluorescence ring in NR2E3-p. G56R-linked autosomal dominant retinitis pigmentosa. *Invest Ophthalmol Vis Sci.* 2012;53(8):4754-4764.

275. Blanco-Kelly F, Garcia Hoyos M, Lopez Martinez MA, et al. Dominant Retinitis Pigmentosa, p.Gly56Arg Mutation in NR2E3:

Phenotype in a Large Cohort of 24 Cases. *PLoS One.* 2016;11(2):e0149473.

276. Martinez-Gimeno M, Maseras M, Baiget M, et al. Mutations P51U and G122E in retinal transcription factor NRL associated with autosomal dominant and sporadic retinitis pigmentosa. *Hum Mutat.* 2001;17(6):520.

277. DeAngelis MM, Grimsby JL, Sandberg MA, Berson EL, Dryja TP. Novel mutations in the NRL gene and associated clinical findings in patients with dominant retinitis pigmentosa. *Arch Ophthalmol.* 2002;120(3):369-375.

278. Bessant DA, Holder GE, Fitzke FW, Payne AM, Bhattacharya SS, Bird AC. Phenotype of retinitis pigmentosa associated with the Ser50Thr mutation in the NRL gene. *Arch Ophthalmol.* 2003;121(6):793-802.

279. Nishiguchi KM, Friedman JS, Sandberg MA, Swaroop A, Berson EL, Dryja TP. Recessive NRL mutations in patients with clumped pigmentary retinal degeneration and relative preservation of blue cone function. *Proc Natl Acad Sci U S A.* 2004;101(51):17819-17824.

280. Newman H, Blumen SC, Braverman I, et al. Homozygosity for a Recessive Loss-of-Function Mutation of the NRL Gene Is Associated With a Variant of Enhanced S-Cone Syndrome. *Invest Ophthalmol Vis Sci.* 2016;57(13):5361-5371.

281. Yu W, Mookherjee S, Chaitankar V, et al. Nrl knockdown by AAV-delivered CRISPR/Cas9 prevents retinal degeneration in mice. *Nat Commun.* 2017;8:14716.

282. Hardcastle AJ, Thiselton DL, Zito I, et al. Evidence for a new locus for X-linked retinitis pigmentosa (RP23). *Invest Ophthalmol Vis Sci.* 2000;41(8):2080-2086.

283. Coene KL, Roepman R, Doherty D, et al. OFD1 is mutated in X-linked Joubert syndrome and interacts with LCA5-encoded lebercilin. *Am J Hum Genet.* 2009;85(4):465-481.

284. Ferrante MI, Romio L, Castro S, et al. Convergent extension movements and ciliary function are mediated by ofd1, a zebrafish orthologue of the human oral-facial-digital type 1 syndrome gene. *Hum Mol Genet.* 2009;18(2):289-303.

285. Orrell RW, Amrolia PJ, Heald A, et al. Acanthocytosis, retinitis pigmentosa, and pallidal degeneration: a report of three patients, including the second reported case with hypoprebetalipoproteinemia (HARP syndrome). *Neurology.* 1995;45(3 Pt 1):487-492.

286. Kuo YM, Duncan JL, Westaway SK, et al. Deficiency of pantothenate kinase 2 (Pank2) in mice leads to retinal degeneration and azoospermia. *Hum Mol Genet.* 2005;14(1):49-57.

287. Huang SH, Pittler SJ, Huang X, Oliveira L, Berson EL, Dryja TP. Autosomal recessive retinitis pigmentosa caused by mutations in the alpha subunit of rod cGMP phosphodiesterase. *Nat Genet.* 1995;11(4):468-471.

288. Riazuddin SA, Zulfiqar F, Zhang Q, et al. Mutations in the gene encoding the alpha-subunit of rod phosphodiesterase in consanguineous Pakistani families. *Mol Vis.* 2006;12:1283-1291.

289. Khan SY, Ali S, Naeem MA, et al. Splice-site mutations identified in PDE6A responsible for retinitis pigmentosa in consanguineous Pakistani families. *Mol Vis.* 2015;21:871-882.

290. Kjellstrom U, Veiga-Crespo P, Andreasson S, Ekstrom P. Increased Plasma cGMP in a Family With Autosomal Recessive Retinitis Pigmentosa Due to Homozygous Mutations in the PDE6A Gene. *Invest Ophthalmol Vis Sci.* 2016;57(14):6048-6057.

291. McLaughlin ME, Sandberg MA, Berson EL, Dryja TP. Recessive mutations in the gene encoding the beta-subunit of rod phosphodiesterase in patients with retinitis pigmentosa. *Nat Genet.* 1993;4(2):130-134.

292. Jacobson SG, Sumaroka A, Aleman TS, Cideciyan AV, Danciger M, Farber DB. Evidence for retinal remodelling in retinitis pigmentosa caused by PDE6B mutation. *Br J Ophthalmol.* 2007;91(5):699-701.

293. Ali S, Riazuddin SA, Shahzadi A, et al. Mutations in the beta-subunit of rod phosphodiesterase identified in consanguineous Pakistani families with autosomal recessive retinitis pigmentosa. *Mol Vis.* 2011;17:1373-1380.

294. Shen S, Sujirakul T, Tsang SH. Next-generation sequencing revealed a novel mutation in the gene encoding the beta subunit of rod phosphodiesterase. *Ophthalmic Genet.* 2014;35(3):142-150.

295. Kuniyoshi K, Sakuramoto H, Yoshitake K, et al. Reduced rod electroretinograms in carrier parents of two Japanese siblings with autosomal recessive retinitis pigmentosa associated with PDE6B gene mutations. *Doc Ophthalmol.* 2015.

296. Ullah I, Kabir F, Gottsch CB, et al. Mutations in phosphodiesterase 6 identified in familial cases of retinitis pigmentosa. *Hum Genome Var.* 2016;3:16036.

297. Gal A, Orth U, Baehr W, Schwinger E, Rosenberg T. Heterozygous missense mutation in the rod cGMP phosphodiesterase beta-subunit gene in autosomal dominant stationary night blindness. *Nat Genet.* 1994;7(1):64-68.

298. Bowes C, Li T, Danciger M, Baxter LC, Applebury ML, Farber DB. Retinal degeneration in the rd mouse is caused by a defect in the beta subunit of rod cGMP-phosphodiesterase. *Nature.* 1990;347(6294):677-680.

299. Dvir L, Srour G, Abu-Ras R, Miller B, Shalev SA, Ben-Yosef T. Autosomal-recessive early-onset retinitis pigmentosa caused by a mutation in PDE6G, the gene encoding the gamma subunit of rod cGMP phosphodiesterase. *Am J Hum Genet.* 2010;87(2):258-264.

300. Tsang SH, Gouras P, Yamashita CK, et al. Retinal degeneration in mice lacking the gamma subunit of the rod cGMP phosphodiesterase. *Science.* 1996;272(5264):1026-1029.

301. Xu M, Yamada T, Sun Z, et al. Mutations in POMGNT1 cause non-syndromic retinitis pigmentosa. *Hum Mol Genet.* 2016;25(8):1479-1488.

302. Wang NH, Chen SJ, Yang CF, et al. Homozygosity Mapping and Whole-Genome Sequencing Links a Missense Mutation in POMGNT1 to Autosomal Recessive Retinitis Pigmentosa. *Invest Ophthalmol Vis Sci.* 2016;57(8):3601-3609.

303. Hu H, Candiello J, Zhang P, Ball SL, Cameron DA, Halfter W. Retinal ectopias and mechanically weakened basement membrane in a mouse model of muscle-eye-brain (MEB) disease congenital muscular dystrophy. *Mol Vis.* 2010;16:1415-1428.

Chapter 2.1

304. Nevet MJ, Shalev SA, Zlotogora J, Mazzawi N, Ben-Yosef T. Identification of a prevalent founder mutation in an Israeli Muslim Arab village confirms the role of PRCD in the aetiology of retinitis pigmentosa in humans. *J Med Genet.* 2010;47(8):533-537.

305. Pach J, Kohl S, Gekeler F, Zobor D. Identification of a novel mutation in the PRCD gene causing autosomal recessive retinitis pigmentosa in a Turkish family. *Mol Vis.* 2013;19:1350-1355.

306. Remez L, Zobor D, Kohl S, Ben-Yosef T. The progressive rod-cone degeneration (PRCD) protein is secreted through the conventional ER/Golgi-dependent pathway. *Exp Eye Res.* 2014;125:217-225.

307. Zangerl B, Goldstein O, Philp AR, et al. Identical mutation in a novel retinal gene causes progressive rod-cone degeneration in dogs and retinitis pigmentosa in humans. *Genomics.* 2006;88(5):551-563.

308. Zhang Q, Zulfiqar F, Xiao X, et al. Severe retinitis pigmentosa mapped to 4p15 and associated with a novel mutation in the PROM1 gene. *Hum Genet.* 2007;122(3-4):293-299.

309. Maw MA, Corbeil D, Koch J, et al. A frameshift mutation in prominin (mouse)-like 1 causes human retinal degeneration. *Hum Mol Genet.* 2000;9(1):27-34.

310. Permanyer J, Navarro R, Friedman J, et al. Autosomal recessive retinitis pigmentosa with early macular affectation caused by premature truncation in PROM1. *Invest Ophthalmol Vis Sci.* 2010;51(5):2656-2663.

311. Michaelides M, Gaillard MC, Escher P, et al. The PROM1 mutation p.R373C causes an autosomal dominant bull's eye maculopathy associated with rod, rod-cone, and macular dystrophy. *Invest Ophthalmol Vis Sci.* 2010;51(9):4771-4780.

312. Liu S, Xie L, Yue J, et al. Whole-exome sequencing identifies a novel homozygous frameshift mutation in the PROM1 gene as a causative mutation in two patients with sporadic retinitis pigmentosa. *Int J Mol Med.* 2016;37(6):1528-1534.

313. Dellett M, Sasai N, Nishide K, et al. Genetic background and light-dependent progression of photoreceptor cell degeneration in Prominin-1 knockout mice. *Invest Ophthalmol Vis Sci.* 2014;56(1):164-176.

314. Martinez-Gimeno M, Gamundi MJ, Hernan I, et al. Mutations in the pre-mRNA splicing-factor genes PRPF3, PRPF8, and PRPF31 in Spanish families with autosomal dominant retinitis pigmentosa. *Invest Ophthalmol Vis Sci.* 2003;44(5):2171-2177.

315. Inglehearn CF, Tarttelin EE, Keen TJ, et al. A new dominant retinitis pigmentosa family mapping to the RP18 locus on chromosome 1q11-21. *J Med Genet.* 1998;35(9):788-789.

316. Xu SY, Schwartz M, Rosenberg T, Gal A. A ninth locus (RP18) for autosomal dominant retinitis pigmentosa maps in the pericentromeric region of chromosome 1. *Hum Mol Genet.* 1996;5(8):1193-1197.

317. Vaclavik V, Gaillard MC, Tiab L, Schorderet DF, Munier FL. Variable phenotypic expressivity in a Swiss family with autosomal dominant retinitis pigmentosa due to a T494M mutation in the PRPF3 gene. *Mol Vis.* 2010;16:467-475.

318. Zhong Z, Yan M, Sun W, et al. Two novel mutations in PRPF3 causing autosomal dominant retinitis pigmentosa. *Sci Rep.* 2016;6:37840.

319. Graziotto JJ, Farkas MH, Bujakowska K, et al. Three gene-targeted mouse models of RNA splicing factor RP show late-onset RPE and retinal degeneration. *Invest Ophthalmol Vis Sci.* 2011;52(1):190-198.

320. Chen X, Liu Y, Sheng X, et al. PRPF4 mutations cause autosomal dominant retinitis pigmentosa. *Hum Mol Genet.* 2014;23(11):2926-2939.

321. Linder B, Hirmer A, Gal A, et al. Identification of a PRPF4 loss-of-function variant that abrogates U4/U6.U5 tri-snRNP integration and is associated with retinitis pigmentosa. *PLoS One.* 2014;9(11):e111754.

322. Tanackovic G, Ransijn A, Ayuso C, Harper S, Berson EL, Rivolta C. A missense mutation in PRPF6 causes impairment of pre-mRNA splicing and autosomal-dominant retinitis pigmentosa. *Am J Hum Genet.* 2011;88(5):643-649.

323. van Lith-Verhoeven JJ, van der Velde-Visser SD, Sohocki MM, et al. Clinical characterization, linkage analysis, and PRPC8 mutation analysis of a family with autosomal dominant retinitis pigmentosa type 13 (RP13). *Ophthalmic Genet.* 2002;23(1):1-12.

324. Ezquerra-Inchausti M, Barandika O, Anasagasti A, Irigoyen C, Lopez de Munain A, Ruiz-Ederra J. High prevalence of mutations affecting the splicing process in a Spanish cohort with autosomal dominant retinitis pigmentosa. *Sci Rep.* 2017;7:39652.

325. Evans K, al-Maghtheh M, Fitzke FW, et al. Bimodal expressivity in dominant retinitis pigmentosa genetically linked to chromosome 19q. *Br J Ophthalmol.* 1995;79(9):841-846.

326. Sullivan LS, Bowne SJ, Seaman CR, et al. Genomic rearrangements of the PRPF31 gene account for 2.5% of autosomal dominant retinitis pigmentosa. *Invest Ophthalmol Vis Sci.* 2006;47(10):4579-4588.

327. Martin-Merida I, Sanchez-Alcudia R, Fernandez-San Jose P, et al. Analysis of the PRPF31 Gene in Spanish Autosomal Dominant Retinitis Pigmentosa Patients: A Novel Genomic Rearrangement. *Invest Ophthalmol Vis Sci.* 2017;58(2):1045-1053.

328. Dryja TP, Hahn LB, Kajiwara K, Berson EL. Dominant and digenic mutations in the peripherin/RDS and ROM1 genes in retinitis pigmentosa. *Invest Ophthalmol Vis Sci.* 1997;38(10):1972-1982.

329. Renner AB, Fiebig BS, Weber BH, et al. Phenotypic variability and long-term follow-up of patients with known and novel PRPH2/RDS gene mutations. *Am J Ophthalmol.* 2009;147(3):518-530 e511.

330. Boon CJ, den Hollander AI, Hoyng CB, Cremers FP, Klevering BJ, Keunen JE. The spectrum of retinal dystrophies caused by mutations in the peripherin/RDS gene. *Prog Retin Eye Res.* 2008;27(2):213-235.

331. Manes G, Guillaumie T, Vos WL, et al. High prevalence of PRPH2 in autosomal dominant retinitis pigmentosa in france and characterization of biochemical and clinical features. *Am J Ophthalmol.* 2015;159(2):302-314.

332. Wang X, Wang H, Sun V, et al. Comprehensive molecular diagnosis of 179 Leber congenital amaurosis and juvenile retinitis pigmentosa patients by targeted next generation sequencing. *J Med Genet.* 2013;50(10):674-688.

333. Travis GH, Sutcliffe JG, Bok D. The retinal degeneration slow (rds) gene product is a photoreceptor disc membrane-associated glycoprotein. *Neuron.* 1991;6(1):61-70.

334. den Hollander AI, McGee TL, Ziviello C, et al. A homozygous missense mutation in the IRBP gene (RBP3) associated with autosomal recessive retinitis pigmentosa. *Invest Ophthalmol Vis Sci.* 2009;50(4):1864-1872.

335. Liou GI, Fei Y, Peachey NS, et al. Early onset photoreceptor abnormalities induced by targeted disruption of the interphotoreceptor retinoid-binding protein gene. *J Neurosci.* 1998;18(12):4511-4520.

336. Fingert JH, Oh K, Chung M, et al. Association of a novel mutation in the retinol dehydrogenase 12 (RDH12) gene with autosomal dominant retinitis pigmentosa. *Arch Ophthalmol.* 2008;126(9):1301-1307.

337. Chacon-Camacho OF, Jitskii S, Buentello-Volante B, Quevedo-Martinez J, Zenteno JC. Exome sequencing identifies RDH12 compound heterozygous mutations in a family with severe retinitis pigmentosa. *Gene.* 2013;528(2):178-182.

338. Janecke AR, Thompson DA, Utermann G, et al. Mutations in RDH12 encoding a photoreceptor cell retinol dehydrogenase cause childhood-onset severe retinal dystrophy. *Nat Genet.* 2004;36(8):850-854.

339. Schuster A, Janecke AR, Wilke R, et al. The phenotype of early-onset retinal degeneration in persons with RDH12 mutations. *Invest Ophthalmol Vis Sci.* 2007;48(4):1824-1831.

340. Mackay DS, Dev Borman A, Moradi P, et al. RDH12 retinopathy: novel mutations and phenotypic description. *Mol Vis.* 2011;17:2706-2716.

341. Garg A, Lee W, Sengillo JD, Allikmets R, Garg K, Tsang SH. Peripapillary sparing in RDH12-associated Leber congenital amaurosis. *Ophthalmic Genet.* 2017;38(6):575-579.

342. Arno G, Agrawal SA, Eblimit A, et al. Mutations in REEP6 Cause Autosomal-Recessive Retinitis Pigmentosa. *Am J Hum Genet.* 2016;99(6):1305-1315.

343. Morimura H, Saindelle-Ribeaudeau F, Berson EL, Dryja TP. Mutations in RGR, encoding a light-sensitive opsin homologue, in patients with retinitis pigmentosa. *Nat Genet.* 1999;23(4):393-394.

344. Arno G, Hull S, Carss K, et al. Reevaluation of the Retinal Dystrophy Due to Recessive Alleles of RGR With the Discovery of a Cis-Acting Mutation in CDHR1. *Invest Ophthalmol Vis Sci.* 2016;57(11):4806-4813.

345. Sandberg MA, Weigel-DiFranco C, Dryja TP, Berson EL. Clinical expression correlates with location of rhodopsin mutation in dominant retinitis pigmentosa. *Invest Ophthalmol Vis Sci.* 1995;36(9):1934-1942.

346. Dryja TP. Doyne Lecture. Rhodopsin and autosomal dominant retinitis pigmentosa. *Eye (Lond).* 1992;6 (Pt 1):1-10.

347. Zeitz C, Gross AK, Leifert D, et al. Identification and functional characterization of a novel rhodopsin mutation associated with autosomal dominant CSNB. *Invest Ophthalmol Vis Sci.* 2008;49(9):4105-4114.

348. Audo I, Friedrich A, Mohand-Said S, et al. An unusual retinal phenotype associated with a novel mutation in RHO. *Arch Ophthalmol.* 2010;128(8):1036-1045.

349. Kijas JW, Cideciyan AV, Aleman TS, et al. Naturally occurring rhodopsin mutation in the dog causes retinal dysfunction and degeneration mimicking human dominant retinitis pigmentosa. *Proc Natl Acad Sci U S A.* 2002;99(9):6328-6333.

350. Hipp S, Zobor G, Glockle N, et al. Phenotype variations of retinal dystrophies caused by mutations in the RLBP1 gene. *Acta Ophthalmol.* 2015;93(4):e281-286.

351. Saari JC, Nawrot M, Kennedy BN, et al. Visual cycle impairment in cellular retinaldehyde binding protein (CRALBP) knockout mice results in delayed dark adaptation. *Neuron.* 2001;29(3):739-748.

352. Sakuma H, Inana G, Murakami A, et al. A heterozygous putative null mutation in ROM1 without a mutation in peripherin/RDS in a family with retinitis pigmentosa. *Genomics.* 1995;27(2):384-386.

353. Stuck MW, Conley SM, Naash MI. PRPH2/RDS and ROM-1: Historical context, current views and future considerations. *Prog Retin Eye Res.* 2016;52:47-63.

354. Kajiwara K, Berson EL, Dryja TP. Digenic retinitis pigmentosa due to mutations at the unlinked peripherin/RDS and ROM1 loci. *Science.* 1994;264(5165):1604-1608.

355. Jacobson SG, Cideciyan AV, Iannaccone A, et al. Disease expression of RP1 mutations causing autosomal dominant retinitis pigmentosa. *Invest Ophthalmol Vis Sci.* 2000;41(7):1898-1908.

356. Audo I, Mohand-Said S, Dhaenens CM, et al. RP1 and autosomal dominant rod-cone dystrophy: novel mutations, a review of published variants, and genotype-phenotype correlation. *Hum Mutat.* 2012;33(1):73-80.

357. Avila-Fernandez A, Corton M, Nishiguchi KM, et al. Identification of an RP1 prevalent founder mutation and related phenotype in Spanish patients with early-onset autosomal recessive retinitis. *Ophthalmology.* 2012;119(12):2616-2621.

358. Liu Q, Zhou J, Daiger SP, et al. Identification and subcellular localization of the RP1 protein in human and mouse photoreceptors. *Invest Ophthalmol Vis Sci.* 2002;43(1):22-32.

359. Liu Q, Zuo J, Pierce EA. The retinitis pigmentosa 1 protein is a photoreceptor microtubule-associated protein. *J Neurosci.* 2004;24(29):6427-6436.

360. Pierce EA, Quinn T, Meehan T, McGee TL, Berson EL, Dryja TP. Mutations in a gene encoding a new oxygen-regulated photoreceptor protein cause dominant retinitis pigmentosa. *Nat Genet.* 1999;22(3):248-254.

361. El Shamieh S, Boulanger-Scemama E, Lancelot ME, et al. Targeted next generation sequencing identifies novel mutations in RP1 as a relatively common cause of autosomal recessive rod-cone dystrophy. *Biomed Res Int.* 2015;2015:485624.

362. Gao J, Cheon K, Nusinowitz S, et al. Progressive photoreceptor degeneration, outer segment dysplasia, and rhodopsin mislocalization in mice with targeted disruption of the retinitis pigmentosa-1 (Rp1) gene. *Proc Natl Acad Sci U S A.* 2002;99(8):5698-5703.

363. Davidson AE, Sergouniotis PI, Mackay DS, et al. RP1L1 variants are associated with a spectrum of inherited retinal diseases including retinitis pigmentosa and occult macular dystrophy. *Hum Mutat.* 2013;34(3):506-514.

Chapter 2.1

364. Ponjavic V, Andreasson S, Abrahamson M, et al. Clinical expression of X-linked retinitis pigmentosa in a Swedish family with the RP2 genotype. *Ophthalmic Genet.* 1998;19(4):187-196.
365. Jayasundera T, Branham KE, Othman M, et al. RP2 phenotype and pathogenetic correlations in X-linked retinitis pigmentosa. *Arch Ophthalmol.* 2010;128(7):915-923.
366. Rosenberg T, Schwahn U, Feil S, Berger W. Genotype-phenotype correlation in X-linked retinitis pigmentosa 2 (RP2). *Ophthalmic Genet.* 1999;20(3):161-172.
367. Flaxel CJ, Jay M, Thiselton DL, et al. Difference between RP2 and RP3 phenotypes in X linked retinitis pigmentosa. *Br J Ophthalmol.* 1999;83(10):1144-1148.
368. Jiang J, Wu X, Shen D, et al. Analysis of RP2 and RPGR Mutations in Five X-Linked Chinese Families with Retinitis Pigmentosa. *Sci Rep.* 2017;7:44465.
369. Li L, Khan N, Hurd T, et al. Ablation of the X-linked retinitis pigmentosa 2 (Rp2) gene in mice results in opsin mislocalization and photoreceptor degeneration. *Invest Ophthalmol Vis Sci.* 2013;54(7):4503-4511.
370. Keen TJ, Hims MM, McKie AB, et al. Mutations in a protein target of the Pim-1 kinase associated with the RP9 form of autosomal dominant retinitis pigmentosa. *Eur J Hum Genet.* 2002;10(4):245-249.
371. Kim RY, Fitzke FW, Moore AT, et al. Autosomal dominant retinitis pigmentosa mapping to chromosome 7p exhibits variable expression. *Br J Ophthalmol.* 1995;79(1):23-27.
372. Moore AT, Fitzke F, Jay M, et al. Autosomal dominant retinitis pigmentosa with apparent incomplete penetrance: a clinical, electrophysiological, psychophysical, and molecular genetic study. *Br J Ophthalmol.* 1993;77(8):473-479.
373. Gu SM, Thompson DA, Srikumari CR, et al. Mutations in RPE65 cause autosomal recessive childhood-onset severe retinal dystrophy. *Nat Genet.* 1997;17(2):194-197.
374. Hamel CP, Griffoin JM, Lasquellec L, Bazalgette C, Arnaud B. Retinal dystrophies caused by mutations in RPE65: assessment of visual functions. *Br J Ophthalmol.* 2001;85(4):424-427.
375. Lorenz B, Gyurus P, Preising M, et al. Early-onset severe rod-cone dystrophy in young children with RPE65 mutations. *Invest Ophthalmol Vis Sci.* 2000;41(9):2735-2742.
376. Thompson DA, Gyurus P, Fleischer LL, et al. Genetics and phenotypes of RPE65 mutations in inherited retinal degeneration. *Invest Ophthalmol Vis Sci.* 2000;41(13):4293-4299.
377. Bowne SJ, Humphries MM, Sullivan LS, et al. A dominant mutation in RPE65 identified by whole-exome sequencing causes retinitis pigmentosa with choroidal involvement. *Eur J Hum Genet.* 2011;19(10):1074-1081.
378. Hull S, Mukherjee R, Holder GE, Moore AT, Webster AR. The clinical features of retinal disease due to a dominant mutation in RPE65. *Mol Vis.* 2016;22:626-635.
379. Fishman GA, Grover S, Jacobson SG, et al. X-linked retinitis pigmentosa in two families with a missense mutation in the RPGR gene and putative change of glycine to valine at codon 60. *Ophthalmology.* 1998;105(12):2286-2296.
380. Iannaccone A, Breuer DK, Wang XF, et al. Clinical and immunohistochemical evidence for an X linked retinitis pigmentosa syndrome with recurrent infections and hearing loss in association with an RPGR mutation. *J Med Genet.* 2003;40(11):e118.
381. Moore A, Escudier E, Roger G, et al. RPGR is mutated in patients with a complex X linked phenotype combining primary ciliary dyskinesia and retinitis pigmentosa. *J Med Genet.* 2006;43(4):326-333.
382. Yang L, Yin X, Feng L, et al. Novel mutations of RPGR in Chinese retinitis pigmentosa patients and the genotype-phenotype correlation. *PLoS One.* 2014;9(1):e85752.
383. Tee JJ, Smith AJ, Hardcastle AJ, Michaelides M. RPGR-associated retinopathy: clinical features, molecular genetics, animal models and therapeutic options. *Br J Ophthalmol.* 2016;100(8):1022-1027.
384. Tee JJL, Carroll J, Webster AR, Michaelides M. Quantitative Analysis of Retinal Structure Using Spectral-Domain Optical Coherence Tomography in RPGR-Associated Retinopathy. *Am J Ophthalmol.* 2017;178:18-26.
385. Demirci FY, Rigatti BW, Mah TS, Gorin MB. A novel RPGR exon ORF15 mutation in a family with X-linked retinitis pigmentosa and Coats'-like exudative vasculopathy. *Am J Ophthalmol.* 2006;141(1):208-210.
386. Booij JC, Florijn RJ, ten Brink JB, et al. Identification of mutations in the AIPL1, CRB1, GUCY2D, RPE65, and RPGRIP1 genes in patients with juvenile retinitis pigmentosa. *J Med Genet.* 2005;42(11):e67.
387. Hameed A, Abid A, Aziz A, Ismail M, Mehdi SQ, Khaliq S. Evidence of RPGRIP1 gene mutations associated with recessive cone-rod dystrophy. *J Med Genet.* 2003;40(8):616-619.
388. Huang H, Wang Y, Chen H, et al. Targeted next generation sequencing identified novel mutations in RPGRIP1 associated with both retinitis pigmentosa and Leber's congenital amaurosis in unrelated Chinese patients. *Oncotarget.* 2017;8(21):35176-35183.
389. Nakazawa M, Wada Y, Tamai M. Arrestin gene mutations in autosomal recessive retinitis pigmentosa. *Arch Ophthalmol.* 1998;116(4):498-501.
390. Chan S, Rubin WW, Mendez A, et al. Functional comparisons of visual arrestins in rod photoreceptors of transgenic mice. *Invest Ophthalmol Vis Sci.* 2007;48(5):1968-1975.
391. Sullivan LS, Bowne SJ, Koboldt DC, et al. A Novel Dominant Mutation in SAG, the Arrestin-1 Gene, Is a Common Cause of Retinitis Pigmentosa in Hispanic Families in the Southwestern United States. *Invest Ophthalmol Vis Sci.* 2017;58(5):2774-2784.
392. Sonoyama H, Shinoda K, Ishigami C, et al. Oguchi disease masked by retinitis pigmentosa. *Doc Ophthalmol.* 2011;123(2):127-133.
393. Corton M, Avila-Fernandez A, Campello L, et al. Identification of the Photoreceptor Transcriptional Co-Repressor SAMD11

as Novel Cause of Autosomal Recessive Retinitis Pigmentosa. *Sci Rep.* 2016;6:35370.

394. Abid A, Ismail M, Mehdi SQ, Khaliq S. Identification of novel mutations in the SEMA4A gene associated with retinal degenerative diseases. *J Med Genet.* 2006;43(4):378-381.

395. Rice DS, Huang W, Jones HA, et al. Severe retinal degeneration associated with disruption of semaphorin 4A. *Invest Ophthalmol Vis Sci.* 2004;45(8):2767-2777.

396. Jin ZB, Huang XF, Lv JN, et al. SLC7A14 linked to autosomal recessive retinitis pigmentosa. *Nature communications.* 2014;5:3517.

397. Zhao C, Lu S, Zhou X, Zhang X, Zhao K, Larsson C. A novel locus (RP33) for autosomal dominant retinitis pigmentosa mapping to chromosomal region 2cen-q12.1. *Hum Genet.* 2006;119(6):617-623.

398. Zhao C, Bellur DL, Lu S, et al. Autosomal-dominant retinitis pigmentosa caused by a mutation in SNRNP200, a gene required for unwinding of U4/U6 snRNAs. *Am J Hum Genet.* 2009;85(5):617-627.

399. Liu T, Jin X, Zhang X, et al. A novel missense SNRNP200 mutation associated with autosomal dominant retinitis pigmentosa in a Chinese family. *PLoS One.* 2012;7(9):e45464.

400. Zhang X, Lai TY, Chiang SW, et al. Contribution of SNRNP200 sequence variations to retinitis pigmentosa. *Eye (Lond).* 2013;27(10):1204-1213.

401. Liu Y, Chen X, Qin N, et al. Knocking Down Snrnp200 Initiates Demorphogenesis of Rod Photoreceptors in Zebrafish. *J Ophthalmol.* 2015;2015:816329.

402. Bowne SJ, Sullivan LS, Avery CE, et al. Mutations in the small nuclear riboprotein 200 kDa gene (SNRNP200) cause 1.6% of autosomal dominant retinitis pigmentosa. *Mol Vis.* 2013;19:2407-2417.

403. Wang H, den Hollander AI, Moayedi Y, et al. Mutations in SPATA7 cause Leber congenital amaurosis and juvenile retinitis pigmentosa. *Am J Hum Genet.* 2009;84(3):380-387.

404. Mayer AK, Mahajnah M, Zobor D, Bonin M, Sharkia R, Wissinger B. Novel homozygous large deletion including the 5' part of the SPATA7 gene in a consanguineous Israeli Muslim Arab family. *Mol Vis.* 2015;21:306-315.

405. Matsui R, McGuigan Iii DB, Gruzensky ML, et al. SPATA7: Evolving phenotype from cone-rod dystrophy to retinitis pigmentosa. *Ophthalmic Genet.* 2016;37(3):333-338.

406. Kannabiran C, Palavalli L, Jalali S. Mutation of SPATA7 in a family with autosomal recessive early-onset retinitis pigmentosa. *J Mol Genet Med.* 2012;6:301-303.

407. Chakarova CF, Papaioannou MG, Khanna H, et al. Mutations in TOPORS cause autosomal dominant retinitis pigmentosa with perivascular retinal pigment epithelium atrophy. *Am J Hum Genet.* 2007;81(5):1098-1103.

408. Bowne SJ, Sullivan LS, Gire AI, et al. Mutations in the TOPORS gene cause 1% of autosomal dominant retinitis pigmentosa. *Mol Vis.* 2008;14:922-927.

409. Latasiewicz M, Salvetti AP, MacLaren RE. A novel mutation in the dominantly inherited TOPORS gene supports haploinsufficiency as the mechanism of retinitis pigmentosa. *Ophthalmic Genet.* 2017:1-5.

410. Riazuddin SA, Iqbal M, Wang Y, et al. A splice-site mutation in a retina-specific exon of BBS8 causes nonsyndromic retinitis pigmentosa. *Am J Hum Genet.* 2010;86(5):805-812.

411. Goyal S, Jager M, Robinson PN, Vanita V. Confirmation of TTC8 as a disease gene for nonsyndromic autosomal recessive retinitis pigmentosa (RP51). *Clin Genet.* 2015.

412. Murphy D, Singh R, Kolandaivelu S, Ramamurthy V, Stoilov P. Alternative Splicing Shapes the Phenotype of a Mutation in BBS8 To Cause Nonsyndromic Retinitis Pigmentosa. *Mol Cell Biol.* 2015;35(10):1860-1870.

413. Downs LM, Wallin-Hakansson B, Bergstrom T, Mellersh CS. A novel mutation in TTC8 is associated with progressive retinal atrophy in the golden retriever. *Canine Genet Epidemiol.* 2014;1:4.

414. Ajmal M, Khan MI, Micheal S, et al. Identification of recurrent and novel mutations in TULP1 in Pakistani families with early-onset retinitis pigmentosa. *Mol Vis.* 2012;18:1226-1237.

415. den Hollander AI, van Lith-Verhoeven JJ, Arends ML, Strom TM, Cremers FP, Hoyng CB. Novel compound heterozygous TULP1 mutations in a family with severe early-onset retinitis pigmentosa. *Arch Ophthalmol.* 2007;125(7):932-935.

416. Paloma E, Hjelmqvist L, Bayes M, et al. Novel mutations in the TULP1 gene causing autosomal recessive retinitis pigmentosa. *Invest Ophthalmol Vis Sci.* 2000;41(3):656-659.

417. Khan AO, Bergmann C, Eisenberger T, Bolz HJ. A TULP1 founder mutation, p.Gln301*, underlies a recognisable congenital rod-cone dystrophy phenotype on the Arabian Peninsula. *Br J Ophthalmol.* 2015;99(4):488-492.

418. Ullah I, Kabir F, Iqbal M, et al. Pathogenic mutations in TULP1 responsible for retinitis pigmentosa identified in consanguineous familial cases. *Mol Vis.* 2016;22:797-815.

419. Noben-Trauth K, Naggert JK, North MA, Nishina PM. A candidate gene for the mouse mutation tubby. *Nature.* 1996;380(6574):534-538.

420. Xu W, Dai H, Lu T, Zhang X, Dong B, Li Y. Seven novel mutations in the long isoform of the USH2A gene in Chinese families with nonsyndromic retinitis pigmentosa and Usher syndrome Type II. *Mol Vis.* 2011;17:1537-1552.

421. Lenassi E, Vincent A, Li Z, et al. A detailed clinical and molecular survey of subjects with nonsyndromic USH2A retinopathy reveals an allelic hierarchy of disease-causing variants. *Eur J Hum Genet.* 2015.

422. Lenassi E, Robson AG, Luxon LM, Bitner-Glindzicz M, Webster AR. Clinical heterogeneity in a family with mutations in USH2A. *JAMA Ophthalmol.* 2015;133(3):352-355.

423. Pierrache LH, Hartel BP, van Wijk E, et al. Visual Prognosis in USH2A-Associated Retinitis Pigmentosa Is Worse for Patients

with Usher Syndrome Type IIa Than for Those with Nonsyndromic Retinitis Pigmentosa. *Ophthalmology.* 2016;123(5):1151-1160.

424. Trichonas G, Traboulsi EI, Ehlers JP. Correlation of ultra-widefield fundus autofluorescence patterns with the underlying genotype in retinal dystrophies and retinitis pigmentosa. *Ophthalmic Genet.* 2016:1-5.

425. Liu X, Bulgakov OV, Darrow KN, et al. Usherin is required for maintenance of retinal photoreceptors and normal development of cochlear hair cells. *Proc Natl Acad Sci U S A.* 2007;104(11):4413-4418.

426. Chen X, Sheng X, Liu X, et al. Targeted next-generation sequencing reveals novel USH2A mutations associated with diverse disease phenotypes: implications for clinical and molecular diagnosis. *PLoS One.* 2014;9(8):e105439.

427. Collin RW, Nikopoulos K, Dona M, et al. ZNF408 is mutated in familial exudative vitreoretinopathy and is crucial for the development of zebrafish retinal vasculature. *Proc Natl Acad Sci U S A.* 2013;110(24):9856-9861.

428. Li L, Nakaya N, Chavali VR, et al. A mutation in ZNF513, a putative regulator of photoreceptor development, causes autosomal-recessive retinitis pigmentosa. *Am J Hum Genet.* 2010;87(3):400-409.

429. Naz S, Riazuddin SA, Li L, et al. A novel locus for autosomal recessive retinitis pigmentosa in a consanguineous Pakistani family maps to chromosome 2p. *Am J Ophthalmol.* 2010;149(5):861-866.

430. Abu-Safieh L, Alrashed M, Anazi S, et al. Autozygome-guided exome sequencing in retinal dystrophy patients reveals pathogenetic mutations and novel candidate disease genes. *Genome Res.* 2013;23(2):236-247.

431. Strom SP, Clark MJ, Martinez A, et al. De Novo Occurrence of a Variant in ARL3 and Apparent Autosomal Dominant Transmission of Retinitis Pigmentosa. *PLoS One.* 2016;11(3):e0150944.

432. Sohocki MM, Sullivan LS, Mintz-Hittner HA, et al. A range of clinical phenotypes associated with mutations in CRX, a photoreceptor transcription-factor gene. *Am J Hum Genet.* 1998;63(5):1307-1315.

433. Swain PK, Chen S, Wang QL, et al. Mutations in the cone-rod homeobox gene are associated with the cone-rod dystrophy photoreceptor degeneration. *Neuron.* 1997;19(6):1329-1336.

434. Tran NM, Zhang A, Zhang X, Huecker JB, Hennig AK, Chen S. Mechanistically distinct mouse models for CRX-associated retinopathy. *PLoS genetics.* 2014;10(2):e1004111.

435. Ajmal M, Khan MI, Neveling K, et al. A missense mutation in the splicing factor gene DHX38 is associated with early-onset retinitis pigmentosa with macular coloboma. *J Med Genet.* 2014;51(7):444-448.

436. Harel T, Yesil G, Bayram Y, et al. Monoallelic and Biallelic Variants in EMC1 Identified in Individuals with Global Developmental Delay, Hypotonia, Scoliosis, and Cerebellar Atrophy. *Am J Hum Genet.* 2016;98(3):562-570.

437. Wang F, Li H, Xu M, et al. A homozygous missense mutation in NEUROD1 is associated with nonsyndromic autosomal recessive retinitis pigmentosa. *Invest Ophthalmol Vis Sci.* 2014;56(1):150-155.

438. Orosz O, Czegledi M, Kantor I, et al. Ophthalmological phenotype associated with homozygous null mutation in the NEUROD1 gene. *Mol Vis.* 2015;21:124-130.

439. Pennesi ME, Cho JH, Yang Z, et al. BETA2/NeuroD1 null mice: a new model for transcription factor-dependent photoreceptor degeneration. *J Neurosci.* 2003;23(2):453-461.

440. Musarella MA, Anson-Cartwright L, Leal SM, et al. Multipoint linkage analysis and heterogeneity testing in 20 X-linked retinitis pigmentosa families. *Genomics.* 1990;8(2):286-296.

441. Ott J, Bhattacharya S, Chen JD, et al. Localizing multiple X chromosome-linked retinitis pigmentosa loci using multilocus homogeneity tests. *Proc Natl Acad Sci U S A.* 1990;87(2):701-704.

442. Francke U, Ochs HD, de Martinville B, et al. Minor Xp21 chromosome deletion in a male associated with expression of Duchenne muscular dystrophy, chronic granulomatous disease, retinitis pigmentosa, and McLeod syndrome. *Am J Hum Genet.* 1985;37(2):250-267.

443. de Saint-Basile G, Bohler MC, Fischer A, et al. Xp21 DNA microdeletion in a patient with chronic granulomatous disease, retinitis pigmentosa, and McLeod phenotype. *Hum Genet.* 1988;80(1):85-89.

444. den Hollander AI, van der Velde-Visser SD, Pinckers AJ, Hoyng CB, Brunner HG, Cremers FP. Refined mapping of the gene for autosomal dominant retinitis pigmentosa (RP17) on chromosome 17q22. *Hum Genet.* 1999;104(1):73-76.

445. Finckh U, Xu S, Kumaramanickavel G, et al. Homozygosity mapping of autosomal recessive retinitis pigmentosa locus (RP22) on chromosome 16p12.1-p12.3. *Genomics.* 1998;48(3):341-345.

446. Gieser L, Fujita R, Goring HH, et al. A novel locus (RP24) for X-linked retinitis pigmentosa maps to Xq26-27. *Am J Hum Genet.* 1998;63(5):1439-1447.

447. Hameed A, Khaliq S, Ismail M, et al. A new locus for autosomal recessive RP (RP29) mapping to chromosome 4q32-q34 in a Pakistani family. *Invest Ophthalmol Vis Sci.* 2001;42(7):1436-1438.

448. Zhang Q, Zulfiqar F, Xiao X, et al. Severe autosomal recessive retinitis pigmentosa maps to chromosome 1p13.3-p21.2 between D1S2896 and D1S457 but outside ABCA4. *Hum Genet.* 2005;118(3-4):356-365.

449. Melamud A, Shen GQ, Chung D, et al. Mapping a new genetic locus for X linked retinitis pigmentosa to Xq28. *J Med Genet.* 2006;43(6):e27.

450. Kannabiran C, Singh HP, Jalali S. Mapping of locus for autosomal dominant retinitis pigmentosa on chromosome 6q23. *Hum Genet.* 2012;131(5):717-723.

451. Inglehearn C, Farrar J, Denton M, Gal A, Humphries P, Bhattacharya S. Evidence against a second autosomal dominant retinitis pigmentosa locus close to rhodopsin on chromosome 3q. *Am J Hum Genet.* 1993;53(2):536-537.

452. Kenna P, Mansergh F, Millington-Ward S, et al. Clinical and molecular genetic characterisation of a family segregating

autosomal dominant retinitis pigmentosa and sensorineural deafness. *Br J Ophthalmol.* 1997;81(3):207-213.

453. Kumar-Singh R, Farrar GJ, Mansergh F, et al. Exclusion of the involvement of all known retinitis pigmentosa loci in the disease present in a family of Irish origin provides evidence for a sixth autosomal dominant locus (RP8). *Hum Mol Genet.* 1993;2(7):875-878.

454. Mansergh FC, Millington-Ward S, Kennan A, et al. Retinitis pigmentosa and progressive sensorineural hearing loss caused by a C12258A mutation in the mitochondrial MTTS2 gene. *Am J Hum Genet.* 1999;64(4):971-985.

455. Mears AJ, Hiriyanna S, Vervoort R, et al. Remapping of the RP15 locus for X-linked cone-rod degeneration to Xp11.4-p21.1, and identification of a de novo insertion in the RPGR exon ORF15. *Am J Hum Genet.* 2000;67(4):1000-1003.

456. Pearlman JT, Flood TP, Seiff SR. Retinitis pigmentosa without pigment. *Am J Ophthalmol.* 1976;81(4):417-419.

457. Ma L, Sheng XL, Li HP, et al. Identification of a novel p.R1443W mutation in RP1 gene associated with retinitis pigmentosa sine pigmento. *Int J Ophthalmol.* 2013;6(4):430-435.

458. Priya S, Nampoothiri S, Sen P, Sripriya S. Bardet-Biedl syndrome: Genetics, molecular pathophysiology, and disease management. *Indian J Ophthalmol.* 2016;64(9):620-627.

459. Deveault C, Billingsley G, Duncan JL, et al. BBS genotype-phenotype assessment of a multiethnic patient cohort calls for a revision of the disease definition. *Hum Mutat.* 2011;32(6):610-619.

460. Flynn MF, Fishman GA, Anderson RJ, Roberts DK. Retrospective longitudinal study of visual acuity change in patients with retinitis pigmentosa. *Retina.* 2001;21(6):639-646.

461. Hajali M, Fishman GA, Anderson RJ. The prevalence of cystoid macular oedema in retinitis pigmentosa patients determined by optical coherence tomography. *Br J Ophthalmol.* 2008;92(8):1065-1068.

462. Sandberg MA, Brockhurst RJ, Gaudio AR, Berson EL. Visual acuity is related to parafoveal retinal thickness in patients with retinitis pigmentosa and macular cysts. *Invest Ophthalmol Vis Sci.* 2008;49(10):4568-4572.

463. Liew G, Moore AT, Webster AR, Michaelides M. Efficacy and prognostic factors of response to carbonic anhydrase inhibitors in management of cystoid macular edema in retinitis pigmentosa. *Invest Ophthalmol Vis Sci.* 2015;56(3):1531-1536.

464. Hettinga YM, van Genderen MM, Wieringa W, Ossewaarde-van Norel J, de Boer JH. Retinal Dystrophy in 6 Young Patients Who Presented with Intermediate Uveitis. *Ophthalmology.* 2016;123(9):2043-2046.

465. Murro V, Mucciolo DP, Sodi A, et al. Retinal capillaritis in a CRB1-associated retinal dystrophy. *Ophthalmic Genet.* 2017;38(6):555-558.

466. Yoshida N, Ikeda Y, Notomi S, et al. Clinical evidence of sustained chronic inflammatory reaction in retinitis pigmentosa. *Ophthalmology.* 2013;120(1):100-105.

467. Verhagen F, Kuiper J, Nierkens S, Imhof SM, Radstake T, de Boer J. Systemic inflammatory immune signatures in a patient with CRB1 linked retinal dystrophy. *Expert Rev Clin Immunol.* 2016;12(12):1359-1362.

468. Henderson RH, Mackay DS, Li Z, et al. Phenotypic variability in patients with retinal dystrophies due to mutations in CRB1. *Br J Ophthalmol.* 2011;95(6):811-817.

469. Khan JA, Ide CH, Strickland MP. Coats'-type retinitis pigmentosa. *Surv Ophthalmol.* 1988;32(5):317-332.

470. Bietti G. Su alcune forme atipiche o rare di degenerazione retinica (degenerazione tappetoretiniche e quadri morbosi similari). *Boll Oculist.* 1937;16:1159-1244.

471. Van Woerkom C, Ferrucci S. Sector retinitis pigmentosa. *Optometry.* 2005;76(5):309-317.

472. Abraham FA. Sector retinitis pigmentosa. Electrophysiological and psychophysical study of the visual system. *Doc Ophthalmol.* 1975;39(1):13-28.

473. Abraham FA, Ivry M, Tsvieli R. Sector retinitis pigmentosa: a fluorescein angiographic study. *Ophthalmologica.* 1976;172(4):287-297.

474. Ramon E, Cordomi A, Aguila M, et al. Differential light-induced responses in sectorial inherited retinal degeneration. *J Biol Chem.* 2014;289(52):35918-35928.

475. Hellner KA, Rickers J. Familiary Bilateral Segmental Retinopathia Pigmentosa. *Ophthalmologica.* 1973;166(5):327-341.

476. Heckenlively JR, Rodriguez JA, Daiger SP. Autosomal dominant sectoral retinitis pigmentosa: two families with transversion mutation in codon 23 of rhodopsin. *Arch Ophthalmol.* 1991;109(1):84-91.

477. Sullivan LJ, Makris GS, Dickinson P, et al. A new codon 15 rhodopsin gene mutation in autosomal dominant retinitis pigmentosa is associated with sectorial disease. *Arch Ophthalmol.* 1993;111(11):1512-1517.

478. Charng J, Cideciyan AV, Jacobson SG, et al. Variegated yet non-random rod and cone photoreceptor disease patterns in RPGR-ORF15-associated retinal degeneration. *Hum Mol Genet.* 2016;25(24):5444-5459.

479. Heckenlively JR. *Retinitis Pigmentosa.* Philedelphia: J.B. Lippincott Company; 1988.

480. de Crecchio G, Alfieri MC, Cennamo G, D'Esposito F, Forte R. Pericentral pigmentary retinopathy: long-term follow-up. *Eye (Lond).* 2006;20(12):1408-1410.

481. Sandberg MA, Brockhurst RJ, Gaudio AR, Berson EL. The association between visual acuity and central retinal thickness in retinitis pigmentosa. *Invest Ophthalmol Vis Sci.* 2005;46(9):3349-3354.

482. Kajiwara K, Sandberg MA, Berson EL, Dryja TP. A null mutation in the human peripherin/RDS gene in a family with autosomal dominant retinitis punctata albescens. *Nat Genet.* 1993;3(3):208-212.

483. Souied E, Soubrane G, Benlian P, et al. Retinitis punctata albescens associated with the Arg135Trp mutation in the rhodopsin gene. *Am J Ophthalmol.* 1996;121(1):19-25.

484. Morimura H, Berson EL, Dryja TP. Recessive mutations in the RLBP1 gene encoding cellular retinaldehyde-binding protein

in a form of retinitis punctata albescens. *Invest Ophthalmol Vis Sci.* 1999;40(5):1000-1004.

485. Burstedt MS, Sandgren O, Holmgren G, Forsman-Semb K. Bothnia dystrophy caused by mutations in the cellular retinaldehyde-binding protein gene (RLBP1) on chromosome 15q26. *Invest Ophthalmol Vis Sci.* 1999;40(5):995-1000.

486. Eichers ER, Green JS, Stockton DW, et al. Newfoundland rod-cone dystrophy, an early-onset retinal dystrophy, is caused by splice-junction mutations in RLBP1. *Am J Hum Genet.* 2002;70(4):955-964.

487. Burstedt MS, Forsman-Semb K, Golovleva I, Janunger T, Wachtmeister L, Sandgren O. Ocular phenotype of bothnia dystrophy, an autosomal recessive retinitis pigmentosa associated with an R234W mutation in the RLBP1 gene. *Arch Ophthalmol.* 2001;119(2):260-267.

488. Dessalces E, Bocquet B, Bourien J, et al. Early-onset foveal involvement in retinitis punctata albescens with mutations in RLBP1. *JAMA Ophthalmol.* 2013;131(10):1314-1323.

489. Acton JH, Greenberg JP, Greenstein VC, et al. Evaluation of multimodal imaging in carriers of X-linked retinitis pigmentosa. *Exp Eye Res.* 2013;113:41-48.

490. Lorenz B, Wabbels B, Wegscheider E, Hamel CP, Drexler W, Preising MN. Lack of fundus autofluorescence to 488 nanometers from childhood on in patients with early-onset severe retinal dystrophy associated with mutations in RPE65. *Ophthalmology.* 2004;111(8):1585-1594.

491. Wald G. The molecular basis of visual excitation. *Nature.* 1968;219(5156):800-807.

492. Stryer L. Cyclic GMP cascade of vision. *Annu Rev Neurosci.* 1986;9:87-119.

493. Gurevich VV, Gurevich EV, Cleghorn WM. Arrestins as multi-functional signaling adaptors. *Handb Exp Pharmacol.* 2008(186):15-37.

494. Palczewski K. Structure and functions of arrestins. *Protein Sci.* 1994;3(9):1355-1361.

495. Krispel CM, Chen D, Melling N, et al. RGS expression rate-limits recovery of rod photoresponses. *Neuron.* 2006;51(4):409-416.

496. Pugh EN, Jr. RGS expression level precisely regulates the duration of rod photoresponses. *Neuron.* 2006;51(4):391-393.

497. Koch KW, Stryer L. Highly cooperative feedback control of retinal rod guanylate cyclase by calcium ions. *Nature.* 1988;334(6177):64-66.

498. Haeseleer F, Sokal I, Li N, et al. Molecular characterization of a third member of the guanylyl cyclase-activating protein subfamily. *J Biol Chem.* 1999;274(10):6526-6535.

499. Tachibanaki S, Tsushima S, Kawamura S. Low amplification and fast visual pigment phosphorylation as mechanisms characterizing cone photoresponses. *Proc Natl Acad Sci U S A.* 2001;98(24):14044-14049.

500. Tachibanaki S, Arinobu D, Shimauchi-Matsukawa Y, Tsushima S, Kawamura S. Highly effective phosphorylation by G protein-coupled receptor kinase 7 of light-activated visual pigment in cones. *Proc Natl Acad Sci U S A.* 2005;102(26):9329-9334.

501. Liu J, Itagaki Y, Ben-Shabat S, Nakanishi K, Sparrow JR. The biosynthesis of A2E, a fluorophore of aging retina, involves the formation of the precursor, A2-PE, in the photoreceptor outer segment membrane. *J Biol Chem.* 2000;275(38):29354-29360.

502. Haeseleer F, Huang J, Lebioda L, Saari JC, Palczewski K. Molecular characterization of a novel short-chain dehydrogenase/reductase that reduces all-trans-retinal. *J Biol Chem.* 1998;273(34):21790-21799.

503. Rattner A, Smallwood PM, Nathans J. Identification and characterization of all-trans-retinol dehydrogenase from photoreceptor outer segments, the visual cycle enzyme that reduces all-trans-retinal to all-trans-retinol. *J Biol Chem.* 2000;275(15):11034-11043.

504. Gonzalez-Fernandez F. Evolution of the visual cycle: the role of retinoid-binding proteins. *J Endocrinol.* 2002;175(1):75-88.

505. Saari JC, Bredberg DL. Lecithin:retinol acyltransferase in retinal pigment epithelial microsomes. *J Biol Chem.* 1989;264(15):8636-8640.

506. Trehan A, Canada FJ, Rando RR. Inhibitors of retinyl ester formation also prevent the biosynthesis of 11-cis-retinol. *Biochemistry.* 1990;29(2):309-312.

507. Deigner PS, Law WC, Canada FJ, Rando RR. Membranes as the energy source in the endergonic transformation of vitamin A to 11-cis-retinol. *Science.* 1989;244(4907):968-971.

508. Moiseyev G, Chen Y, Takahashi Y, Wu BX, Ma JX. RPE65 is the isomerohydrolase in the retinoid visual cycle. *Proc Natl Acad Sci U S A.* 2005;102(35):12413-12418.

509. Mata NL, Radu RA, Clemmons RC, Travis GH. Isomerization and oxidation of vitamin a in cone-dominant retinas: a novel pathway for visual-pigment regeneration in daylight. *Neuron.* 2002;36(1):69-80.

510. Tang PH, Kono M, Koutalos Y, Ablonczy Z, Crouch RK. New insights into retinoid metabolism and cycling within the retina. *Prog Retin Eye Res.* 2013;32:48-63.

511. Sahu B, Maeda A. Retinol Dehydrogenases Regulate Vitamin A Metabolism for Visual Function. *Nutrients.* 2016;8(11).

512. Kaylor JJ, Yuan Q, Cook J, et al. Identification of DES1 as a vitamin A isomerase in Muller glial cells of the retina. *Nat Chem Biol.* 2013;9(1):30-36.

513. Kaylor JJ, Cook JD, Makshanoff J, Bischoff N, Yong J, Travis GH. Identification of the 11-cis-specific retinyl-ester synthase in retinal Muller cells as multifunctional O-acyltransferase (MFAT). *Proc Natl Acad Sci U S A.* 2014;111(20):7302-7307.

514. Stecher H, Gelb MH, Saari JC, Palczewski K. Preferential release of 11-cis-retinol from retinal pigment epithelial cells in the presence of cellular retinaldehyde-binding protein. *J Biol Chem.* 1999;274(13):8577-8585.

515. Saari JC, Nawrot M, Stenkamp RE, Teller DC, Garwin GG. Release of 11-cis-retinal from cellular retinaldehyde-binding protein by acidic lipids. *Mol Vis.* 2009;15:844-854.

516. Satir P, Christensen ST. Structure and function of mammalian cilia. *Histochem Cell Biol.* 2008;129(6):687-693.

517. Singla V, Reiter JF. The primary cilium as the cell's antenna: signaling at a sensory organelle. *Science.* 2006;313(5787):629-633.
518. Berbari NF, O'Connor AK, Haycraft CJ, Yoder BK. The primary cilium as a complex signaling center. *Curr Biol.* 2009;19(13):R526-535.
519. Hildebrandt F, Benzing T, Katsanis N. Ciliopathies. *N Engl J Med.* 2011;364(16):1533-1543.
520. Reiter JF, Leroux MR. Genes and molecular pathways underpinning ciliopathies. *Nat Rev Mol Cell Biol.* 2017;18(9):533-547.
521. Roepman R, Wolfrum U. Protein networks and complexes in photoreceptor cilia. *Subcell Biochem.* 2007;43:209-235.
522. Kozminski KG, Johnson KA, Forscher P, Rosenbaum JL. A motility in the eukaryotic flagellum unrelated to flagellar beating. *Proc Natl Acad Sci U S A.* 1993;90(12):5519-5523.
523. Bhogaraju S, Cajanek L, Fort C, et al. Molecular basis of tubulin transport within the cilium by IFT74 and IFT81. *Science.* 2013;341(6149):1009-1012.
524. Ye F, Breslow DK, Koslover EF, Spakowitz AJ, Nelson WJ, Nachury MV. Single molecule imaging reveals a major role for diffusion in the exploration of ciliary space by signaling receptors. *eLife.* 2013;2:e00654.
525. Hao L, Thein M, Brust-Mascher I, et al. Intraflagellar transport delivers tubulin isotypes to sensory cilium middle and distal segments. *Nat Cell Biol.* 2011;13(7):790-798.
526. Kubo T, Brown JM, Bellve K, et al. Together, the IFT81 and IFT74 N-termini form the main module for intraflagellar transport of tubulin. *J Cell Sci.* 2016;129(10):2106-2119.
527. Estrada-Cuzcano A, Roepman R, Cremers FP, den Hollander AI, Mans DA. Non-syndromic retinal ciliopathies: translating gene discovery into therapy. *Hum Mol Genet.* 2012;21(R1):R111-124.
528. Daiger SP, Rossiter BJF, Greenberg J, Christoffels A, Hide W. RetNet, the Retinal Information Network. 2017; http://www.sph.uth.tmc.edu/RetNet/. Accessed 13 april 2017, 2017.
529. Rosenbaum JL, Witman GB. Intraflagellar transport. *Nature reviews Molecular cell biology.* 2002;3(11):813-825.
530. Scholey JM. Intraflagellar transport. *Annu Rev Cell Dev Biol.* 2003;19:423-443.
531. Wren KN, Craft JM, Tritschler D, et al. A differential cargo-loading model of ciliary length regulation by IFT. *Curr Biol.* 2013;23(24):2463-2471.
532. Young RW. Passage of newly formed protein through the connecting cilium of retina rods in the frog. *J Ultrastruct Res.* 1968;23(5):462-473.
533. Besharse JC, Hollyfield JG, Rayborn ME. Turnover of rod photoreceptor outer segments. II. Membrane addition and loss in relationship to light. *J Cell Biol.* 1977;75(2 Pt 1):507-527.
534. Strissel KJ, Sokolov M, Trieu LH, Arshavsky VY. Arrestin translocation is induced at a critical threshold of visual signaling and is superstoichiometric to bleached rhodopsin. *J Neurosci.* 2006;26(4):1146-1153.
535. Sokolov M, Lyubarsky AL, Strissel KJ, et al. Massive light-driven translocation of transducin between the two major compartments of rod cells: a novel mechanism of light adaptation. *Neuron.* 2002;34(1):95-106.
536. Schwarz N, Lane A, Jovanovich K, et al. Arl3 and RP2 regulate the trafficking of ciliary tip kinesins. *Hum Mol Genet.* 2017;26(13):2480-2492.
537. Bhogaraju S, Engel BD, Lorentzen E. Intraflagellar transport complex structure and cargo interactions. *Cilia.* 2013;2(1):10.
538. Taschner M, Bhogaraju S, Lorentzen E. Architecture and function of IFT complex proteins in ciliogenesis. *Differentiation.* 2012;83(2):S12-22.
539. Nachury MV, Loktev AV, Zhang Q, et al. A core complex of BBS proteins cooperates with the GTPase Rab8 to promote ciliary membrane biogenesis. *Cell.* 2007;129(6):1201-1213.
540. Mourao A, Christensen ST, Lorentzen E. The intraflagellar transport machinery in ciliary signaling. *Curr Opin Struct Biol.* 2016;41:98-108.
541. Jin H, White SR, Shida T, et al. The conserved Bardet-Biedl syndrome proteins assemble a coat that traffics membrane proteins to cilia. *Cell.* 2010;141(7):1208-1219.
542. Mourao A, Nager AR, Nachury MV, Lorentzen E. Structural basis for membrane targeting of the BBSome by ARL6. *Nat Struct Mol Biol.* 2014;21(12):1035-1041.
543. Pretorius PR, Aldahmesh MA, Alkuraya FS, Sheffield VC, Slusarski DC. Functional analysis of BBS3 A89V that results in non-syndromic retinal degeneration. *Hum Mol Genet.* 2011;20(8):1625-1632.
544. Christensen ST, Pedersen LB, Schneider L, Satir P. Sensory cilia and integration of signal transduction in human health and disease. *Traffic.* 2007;8(2):97-109.
545. Emmer BT, Maric D, Engman DM. Molecular mechanisms of protein and lipid targeting to ciliary membranes. *J Cell Sci.* 2010;123(Pt 4):529-536.
546. Leroux MR. Taking vesicular transport to the cilium. *Cell.* 2007;129(6):1041-1043.
547. Nachury MV, Seeley ES, Jin H. Trafficking to the ciliary membrane: how to get across the periciliary diffusion barrier? *Annu Rev Cell Dev Biol.* 2010;26:59-87.
548. Goncalves J, Pelletier L. The Ciliary Transition Zone: Finding the Pieces and Assembling the Gate. *Mol Cells.* 2017;40(4):243-253.
549. Young RW. The renewal of photoreceptor cell outer segments. *J Cell Biol.* 1967;33(1):61-72.
550. Takao D, Verhey KJ. Gated entry into the ciliary compartment. *Cell Mol Life Sci.* 2016;73(1):119-127.
551. Chih B, Liu P, Chinn Y, et al. A ciliopathy complex at the transition zone protects the cilia as a privileged membrane domain.

Chapter 2.1

Nat Cell Biol. 2011;14(1):61-72.

552. Garcia-Gonzalo FR, Corbit KC, Sirerol-Piquer MS, et al. A transition zone complex regulates mammalian ciliogenesis and ciliary membrane composition. *Nat Genet.* 2011;43(8):776-784.

553. Sang L, Miller JJ, Corbit KC, et al. Mapping the NPHP-JBTS-MKS protein network reveals ciliopathy disease genes and pathways. *Cell.* 2011;145(4):513-528.

554. Megaw RD, Soares DC, Wright AF. RPGR: Its role in photoreceptor physiology, human disease, and future therapies. *Exp Eye Res.* 2015;138:32-41.

555. Eblimit A, Nguyen TM, Chen Y, et al. Spata7 is a retinal ciliopathy gene critical for correct RPGRIP1 localization and protein trafficking in the retina. *Hum Mol Genet.* 2015;24(6):1584-1601.

556. Sjostrand FS. The ultrastructure of the outer segments of rods and cones of the eye as revealed by the electron microscope. *J Cell Comp Physiol.* 1953;42(1):15-44.

557. Cohen AI. The fine structure of the extrafoveal receptors of the Rhesus monkey. *Exp Eye Res.* 1961;1:128-136.

558. Goldberg AF, Moritz OL, Williams DS. Molecular basis for photoreceptor outer segment architecture. *Prog Retin Eye Res.* 2016;55:52-81.

559. Ding JD, Salinas RY, Arshavsky VY. Discs of mammalian rod photoreceptors form through the membrane evagination mechanism. *J Cell Biol.* 2015;211(3):495-502.

560. Tubb BE, Bardien-Kruger S, Kashork CD, et al. Characterization of human retinal fascin gene (FSCN2) at 17q25: close physical linkage of fascin and cytoplasmic actin genes. *Genomics.* 2000;65(2):146-156.

561. Saishin Y, Ishikawa R, Ugawa S, et al. Retinal fascin: functional nature, subcellular distribution, and chromosomal localization. *Invest Ophthalmol Vis Sci.* 2000;41(8):2087-2095.

562. Cohen AI. Some cytological and initial biochemical observations on photoreceptors in retinas of rds mice. *Invest Ophthalmol Vis Sci.* 1983;24(7):832-843.

563. Edrington TCt, Lapointe R, Yeagle PL, Gretzula CL, Boesze-Battaglia K. Peripherin-2: an intracellular analogy to viral fusion proteins. *Biochemistry.* 2007;46(12):3605-3613.

564. Salinas RY, Pearring JN, Ding JD, Spencer WJ, Hao Y, Arshavsky VY. Photoreceptor discs form through peripherin-dependent suppression of ciliary ectosome release. *J Cell Biol.* 2017;216(5):1489-1499.

565. Nager AR, Goldstein JS, Herranz-Perez V, et al. An Actin Network Dispatches Ciliary GPCRs into Extracellular Vesicles to Modulate Signaling. *Cell.* 2017;168(1-2):252-263 e214.

566. Loewen CJ, Molday RS. Disulfide-mediated oligomerization of Peripherin/Rds and Rom-1 in photoreceptor disk membranes. Implications for photoreceptor outer segment morphogenesis and degeneration. *J Biol Chem.* 2000;275(8):5370-5378.

567. Fetter RD, Corless JM. Morphological components associated with frog cone outer segment disc margins. *Invest Ophthalmol Vis Sci.* 1987;28(4):646-657.

568. Yang Z, Chen Y, Lillo C, et al. Mutant prominin 1 found in patients with macular degeneration disrupts photoreceptor disk morphogenesis in mice. *J Clin Invest.* 2008;118(8):2908-2916.

569. Liu Q, Lyubarsky A, Skalet JH, Pugh EN, Jr., Pierce EA. RP1 is required for the correct stacking of outer segment discs. *Invest Ophthalmol Vis Sci.* 2003;44(10):4171-4183.

570. Yamashita T, Liu J, Gao J, et al. Essential and synergistic roles of RP1 and RP1L1 in rod photoreceptor axoneme and retinitis pigmentosa. *J Neurosci.* 2009;29(31):9748-9760.

571. Hollyfield JG. Hyaluronan and the functional organization of the interphotoreceptor matrix. *Invest Ophthalmol Vis Sci.* 1999;40(12):2767-2769.

572. Hageman GS, Marmor MF, Yao XY, Johnson LV. The interphotoreceptor matrix mediates primate retinal adhesion. *Arch Ophthalmol.* 1995;113(5):655-660.

573. Lazarus HS, Hageman GS. Xyloside-induced disruption of interphotoreceptor matrix proteoglycans results in retinal detachment. *Invest Ophthalmol Vis Sci.* 1992;33(2):364-376.

574. Yao XY, Hageman GS, Marmor MF. Retinal adhesiveness in the monkey. *Invest Ophthalmol Vis Sci.* 1994;35(2):744-748.

575. Marmor MF, Yao XY, Hageman GS. Retinal adhesiveness in surgically enucleated human eyes. *Retina.* 1994;14(2):181-186.

576. Hageman GS, Johnson LV. Structure, composition and function of the retinal interphotoreceptor matrix. In: Osborne N, Chader G, eds. *Retinal Research.* New York: Pergamon Press; 1991:207-249.

577. Rhodes JM, Simons M. The extracellular matrix and blood vessel formation: not just a scaffold. *J Cell Mol Med.* 2007;11(2):176-205.

578. Ishikawa M, Sawada Y, Yoshitomi T. Structure and function of the interphotoreceptor matrix surrounding retinal photoreceptor cells. *Exp Eye Res.* 2015;133:3-18.

579. Al-Ubaidi MR, Naash MI, Conley SM. A perspective on the role of the extracellular matrix in progressive retinal degenerative disorders. *Invest Ophthalmol Vis Sci.* 2013;54(13):8119-8124.

580. Kanan Y, Hoffhines A, Rauhauser A, Murray A, Al-Ubaidi MR. Protein tyrosine-O-sulfation in the retina. *Exp Eye Res.* 2009;89(4):559-567.

581. Inatani M, Tanihara H. Proteoglycans in retina. *Prog Retin Eye Res.* 2002;21(5):429-447.

582. Abd El-Aziz MM, Barragan I, O'Driscoll CA, et al. EYS, encoding an ortholog of Drosophila spacemaker, is mutated in autosomal recessive retinitis pigmentosa. *Nat Genet.* 2008;40(11):1285-1287.

583. Valverde D, Vazquez-Gundin F, del Rio E, Calaf M, Fernandez JL, Baiget M. Analysis of the IRBP gene as a cause of RP in 45

ARRP Spanish families. Autosomal recessive retinitis pigmentosa. Interstitial retinol binding protein. Spanish Multicentric and Multidisciplinary Group for Research into Retinitis Pigmentosa. *Ophthalmic Genet.* 1998;19(4):197-202.

584. Acharya S, Foletta VC, Lee JW, et al. SPACRCAN, a novel human interphotoreceptor matrix hyaluronan-binding proteoglycan synthesized by photoreceptors and pinealocytes. *J Biol Chem.* 2000;275(10):6945-6955.

585. Foletta VC, Nishiyama K, Rayborn ME, Shadrach KG, Young WS, 3rd, Hollyfield JG. SPACRCAN in the developing retina and pineal gland of the rat: spatial and temporal pattern of gene expression and protein synthesis. *J Comp Neurol.* 2001;435(3):354-363.

586. Husain N, Pellikka M, Hong H, et al. The agrin/perlecan-related protein eyes shut is essential for epithelial lumen formation in the Drosophila retina. *Dev Cell.* 2006;11(4):483-493.

587. Zelhof AC, Hardy RW, Becker A, Zuker CS. Transforming the architecture of compound eyes. *Nature.* 2006;443(7112):696-699.

588. Alfano G, Kruczek PM, Shah AZ, et al. EYS Is a Protein Associated with the Ciliary Axoneme in Rods and Cones. *PLoS One.* 2016;11(11):e0166397.

589. Lu Z, Hu X, Liu F, et al. Ablation of EYS in zebrafish causes mislocalisation of outer segment proteins, F-actin disruption and cone-rod dystrophy. *Sci Rep.* 2017;7:46098.

590. Branham K, Yashar BM. Providing comprehensive genetic-based ophthalmic care. *Clin Genet.* 2013;84(2):183-189.

591. Haer-Wigman L, van Zelst-Stams WA, Pfundt R, et al. Diagnostic exome sequencing in 266 Dutch patients with visual impairment. *Eur J Hum Genet.* 2017;25(5):591-599.

592. Huang XF, Wu J, Lv JN, Zhang X, Jin ZB. Identification of false-negative mutations missed by next-generation sequencing in retinitis pigmentosa patients: a complementary approach to clinical genetic diagnostic testing. *Genet Med.* 2015;17(4):307-311.

593. Carss KJ, Arno G, Erwood M, et al. Comprehensive Rare Variant Analysis via Whole-Genome Sequencing to Determine the Molecular Pathology of Inherited Retinal Disease. *Am J Hum Genet.* 2017;100(1):75-90.

594. Godino L, Turchetti D, Jackson L, Hennessy C, Skirton H. Impact of presymptomatic genetic testing on young adults: a systematic review. *Eur J Hum Genet.* 2016;24(4):496-503.

595. Herse P. Retinitis pigmentosa: visual function and multidisciplinary management. *Clin Exp Optom.* 2005;88(5):335-350.

596. Yoshida N, Ikeda Y, Murakami Y, et al. Factors affecting visual acuity after cataract surgery in patients with retinitis pigmentosa. *Ophthalmology.* 2015;122(5):903-908.

597. Nakamura Y, Mitamura Y, Hagiwara A, et al. Relationship between retinal microstructures and visual acuity after cataract surgery in patients with retinitis pigmentosa. *Br J Ophthalmol.* 2015;99(4):508-511.

598. Dikopf MS, Chow CC, Mieler WF, Tu EY. Cataract extraction outcomes and the prevalence of zonular insufficiency in retinitis pigmentosa. *Am J Ophthalmol.* 2013;156(1):82-88.e82.

599. De Rojas JO, Schuerch K, Mathews PM, et al. Evaluating structural progression of retinitis pigmentosa after cataract surgery. *Am J Ophthalmol.* 2017;180:117-123.

600. Bayyoud T, Bartz-Schmidt KU, Yoeruek E. Long-term clinical results after cataract surgery with and without capsular tension ring in patients with retinitis pigmentosa: a retrospective study. *BMJ Open.* 2013;3(4).

601. Hayashi K, Hayashi H, Matsuo K, Nakao F, Hayashi F. Anterior capsule contraction and intraocular lens dislocation after implant surgery in eyes with retinitis pigmentosa. *Ophthalmology.* 1998;105(7):1239-1243.

602. Jackson H, Garway-Heath D, Rosen P, Bird AC, Tuft SJ. Outcome of cataract surgery in patients with retinitis pigmentosa. *Br J Ophthalmol.* 2001;85(8):936-938.

603. Huang Q, Chen R, Lin X, Xiang Z. Efficacy of carbonic anhydrase inhibitors in management of cystoid macular edema in retinitis pigmentosa: A meta-analysis. *PLoS One.* 2017;12(10):e0186180.

604. Huckfeldt RM, Comander J. Management of Cystoid Macular Edema in Retinitis Pigmentosa. *Semin Ophthalmol.* 2017;32(1):43-51.

605. Thobani A, Fishman GA. The use of carbonic anhydrase inhibitors in the retreatment of cystic macular lesions in retinitis pigmentosa and X-linked retinoschisis. *Retina.* 2011;31(2):312-315.

606. Ikeda Y, Yoshida N, Murakami Y, et al. Long-term Surgical Outcomes of Epiretinal Membrane in Patients with Retinitis Pigmentosa. *Sci Rep.* 2015;5:13078.

607. Scholl HP, Strauss RW, Singh MS, et al. Emerging therapies for inherited retinal degeneration. *Sci Transl Med.* 2016;8(368):368rv366.

608. Bainbridge JW, Smith AJ, Barker SS, et al. Effect of gene therapy on visual function in Leber's congenital amaurosis. *N Engl J Med.* 2008;358(21):2231-2239.

609. Hauswirth WW, Aleman TS, Kaushal S, et al. Treatment of leber congenital amaurosis due to RPE65 mutations by ocular subretinal injection of adeno-associated virus gene vector: short-term results of a phase I trial. *Hum Gene Ther.* 2008;19(10):979-990.

610. Maguire AM, Simonelli F, Pierce EA, et al. Safety and efficacy of gene transfer for Leber's congenital amaurosis. *N Engl J Med.* 2008;358(21):2240-2248.

611. MacLaren RE, Groppe M, Barnard AR, et al. Retinal gene therapy in patients with choroideremia: initial findings from a phase 1/2 clinical trial. *Lancet.* 2014;383(9923):1129-1137.

612. Ghazi NG, Abboud EB, Nowilaty SR, et al. Treatment of retinitis pigmentosa due to MERTK mutations by ocular subretinal injection of adeno-associated virus gene vector: results of a phase I trial. *Hum Genet.* 2016;135(3):327-343.

613. Russell S, Bennett J, Wellman JA, et al. Efficacy and safety of voretigene neparvovec (AAV2-hRPE65v2) in patients with RPE65-mediated inherited retinal dystrophy: a randomised, controlled, open-label, phase 3 trial. Lancet. 2017;390(10097):849-860.

614. Collin RW, Garanto A. Applications of antisense oligonucleotides for the treatment of inherited retinal diseases. *Curr Opin Ophthalmol.* 2017;28(3):260-266.

615. Yanik M, Muller B, Song F, et al. In vivo genome editing as a potential treatment strategy for inherited retinal dystrophies. *Prog Retin Eye Res.* 2017;56:1-18.

616. Scholl HP, Moore AT, Koenekoop RK, et al. Safety and Proof-of-Concept Study of Oral QLT091001 in Retinitis Pigmentosa Due to Inherited Deficiencies of Retinal Pigment Epithelial 65 Protein (RPE65) or Lecithin:Retinol Acyltransferase (LRAT). *PLoS One.* 2015;10(12):e0143846.

617. Brito-Garcia N, Del Pino-Sedeno T, Trujillo-Martin MM, et al. Effectiveness and safety of nutritional supplements in the treatment of hereditary retinal dystrophies: a systematic review. *Eye (Lond).* 2017;31(2):273-285.

618. Rayapudi S, Schwartz SG, Wang X, Chavis P. Vitamin A and fish oils for retinitis pigmentosa. *Cochrane Database Syst Rev.* 2013;12:CD008428.

619. Tang Z, Zhang Y, Wang Y, et al. Progress of stem/progenitor cell-based therapy for retinal degeneration. *J Transl Med.* 2017;15(1):99.

620. Li Y, Chan L, Nguyen HV, Tsang SH. Personalized Medicine: Cell and Gene Therapy Based on Patient-Specific iPSC-Derived Retinal Pigment Epithelium Cells. *Adv Exp Med Biol.* 2016;854:549-555.

621. Chakradhar S. An eye to the future: Researchers debate best path for stem cell-derived therapies. *Nat Med.* 2016;22(2):116-119.

622. de Rham C, Villard J. Potential and limitation of HLA-based banking of human pluripotent stem cells for cell therapy. *J Immunol Res.* 2014;2014:518135.

623. Seiler MJ, Aramant RB. Cell replacement and visual restoration by retinal sheet transplants. *Prog Retin Eye Res.* 2012;31(6):661-687.

624. Mills JO, Jalil A, Stanga PE. Electronic retinal implants and artificial vision: journey and present. *Eye (Lond).* 2017;31(10):1383-1398.

625. da Cruz L, Dorn JD, Humayun MS, et al. Five-Year Safety and Performance Results from the Argus II Retinal Prosthesis System Clinical Trial. *Ophthalmology.* 2016;123(10):2248-2254.

626. Zrenner E, Bartz-Schmidt KU, Benav H, et al. Subretinal electronic chips allow blind patients to read letters and combine them to words. *Proc Biol Sci.* 2011;278(1711):1489-1497.

627. Stingl K, Schippert R, Bartz-Schmidt KU, et al. Interim Results of a Multicenter Trial with the New Electronic Subretinal Implant Alpha AMS in 15 Patients Blind from Inherited Retinal Degenerations. *Front Neurosci.* 2017;11:445.

628. Cheng DL, Greenberg PB, Borton DA. Advances in Retinal Prosthetic Research: A Systematic Review of Engineering and Clinical Characteristics of Current Prosthetic Initiatives. *Curr Eye Res.* 2017;42(3):334-347.

629. Zrenner E. Fighting blindness with microelectronics. *Sci Transl Med.* 2013;5(210):210ps216.

630. Busskamp V, Picaud S, Sahel JA, Roska B. Optogenetic therapy for retinitis pigmentosa. *Gene Ther.* 2012;19(2):169-175.

631. Okoye G, Zimmer J, Sung J, et al. Increased expression of brain-derived neurotrophic factor preserves retinal function and slows cell death from rhodopsin mutation or oxidative damage. *J Neurosci.* 2003;23(10):4164-4172.

632. Faktorovich EG, Steinberg RH, Yasumura D, Matthes MT, LaVail MM. Photoreceptor degeneration in inherited retinal dystrophy delayed by basic fibroblast growth factor. *Nature.* 1990;347(6288):83-86.

633. Liang FQ, Aleman TS, Dejneka NS, et al. Long-term protection of retinal structure but not function using RAAV.CNTF in animal models of retinitis pigmentosa. *Mol Ther.* 2001;4(5):461-472.

634. Dalkara D, Kolstad KD, Guerin KI, et al. AAV mediated GDNF secretion from retinal glia slows down retinal degeneration in a rat model of retinitis pigmentosa. *Mol Ther.* 2011;19(9):1602-1608.

635. Lenzi L, Coassin M, Lambiase A, Bonini S, Amendola T, Aloe L. Effect of exogenous administration of nerve growth factor in the retina of rats with inherited retinitis pigmentosa. *Vision Res.* 2005;45(12):1491-1500.

636. Byrne LC, Dalkara D, Luna G, et al. Viral-mediated RdCVF and RdCVFL expression protects cone and rod photoreceptors in retinal degeneration. *J Clin Invest.* 2015;125(1):105-116.

637. Birch DG, Bennett LD, Duncan JL, Weleber RG, Pennesi ME. Long-term Follow-up of Patients With Retinitis Pigmentosa Receiving Intraocular Ciliary Neurotrophic Factor Implants. *Am J Ophthalmol.* 2016;170:10-14.

638. Morimoto T, Fujikado T, Choi JS, et al. Transcorneal electrical stimulation promotes the survival of photoreceptors and preserves retinal function in royal college of surgeons rats. *Invest Ophthalmol Vis Sci.* 2007;48(10):4725-4732.

639. Schatz A, Rock T, Naycheva L, et al. Transcorneal electrical stimulation for patients with retinitis pigmentosa: a prospective, randomized, sham-controlled exploratory study. *Invest Ophthalmol Vis Sci.* 2011;52(7):4485-4496.

640. Schatz A, Pach J, Gosheva M, et al. Transcorneal Electrical Stimulation for Patients With Retinitis Pigmentosa: A Prospective, Randomized, Sham-Controlled Follow-up Study Over 1 Year. *Invest Ophthalmol Vis Sci.* 2017;58(1):257-269.

641. Wagner SK, Jolly JK, Pefkianaki M, et al. Transcorneal electrical stimulation for the treatment of retinitis pigmentosa: results from the TESOLAUK trial. *BMJ Open Ophthalmol.* 2017;2(1):e000096.

Appendix 1

See next page.

Differential diagnoses for non-syndromic RP

Disease	Clinical features	Refs
Inherited retinal diseases		
Progressive retinal disease		
Cone-rod dystrophy	Patients typically present with VA loss, dyschromatopsia and photoaversion. May experience nyctalopia. Primary loss of cone function on the ERG, followed by rod impairment. Syndromal associations.	[1,2]
Cone dystrophy	Progressive loss of VA and dyschromatopsia often accompanied by photoaversion and photophobia. Macula: ranging from normal to a bull's eye maculopathy or RPE atrophy. Reduced or nonrecordable photopic ERG.	[3]
Leber congenital amaurosis	Early-onset retinal dystrophy at birth or in first months of life, nystagmus, hyperopia, amaurotic pupils, oculo-digital sign, extinguished photopic and scotopic ERG. Syndromal associations.	[4]
Macular dystrophies (Stargardt disease, Sorsby fundus dystrophy)	Progressive loss of VA, advanced disease sometimes associated with night blindness and loss of peripheral vision.	[5]
Bietti crystalline corneoretinal dystrophy	Yellow-white crystalline retinal deposits throughout posterior pole and sometimes in corneal limbus. Sclerosis of the choroidal vessels. Often marked asymmetry in retinal findings.	[6]
Late-onset retinal degeneration	Perimacular yellow-white drusen-like lesions, long anterior zonules, and hyperpigmentation in the midperiphery. Gradual loss of dark adaptation in fifth-sixth decade. Reduced visual acuity in advanced stages caused by scalloped areas of RPE atrophy or neovascularization, accompanied by ERG changes (rod-cone pattern). Normal caliber of retinal vessels.	[7,8]
Stationary retinal disease		
Congenital stationary night blindness	Largely non-progressive. Nightblindness. Nystagmus and myopia with decreased VA if onset early in life. Most common ERG is 'negative' dark-adapted ERG. Oguchi disease and fundus albipunctatus are forms of CSNB.	[9]
Chorioretinal dystrophies		
Choroideremia	X-linked, pigment clumping at RPE level, followed by patchy loss of RPE and choriocapillaris with visible underlying large choroidal vessels and sclera. Normal appearing retinal vessels.	[10,11]
Gyrate atrophy	Well demarcated, circular areas of chorioretinal atrophy often starting in far periphery, early onset cataract formation, myopia, CME, elevated plasma ornithine, type II muscle fiber atrophy, hair thinning.	[12,13]
Helicoid peripapillary chorioretinal degeneration (Sveinsson chorioretinal atrophy)	Autosomal dominant, peripapillary chorioretinal atrophy with radially extending wing-shaped atrophy, no attenuation of retinal vessels.	[14,15]
Progressive bifocal chorioretinal atrophy	Slowly progressive, large atrophic lesions in macula and nasal to the optic disc. Nystagmus and myopia.	[16]
Vitreoretinal dystrophies		
X-linked juvenile retinoschisis	VA loss from the 1st/2nd decade of life. Cystoid macular lesions, typically in an spoke-wheel pattern, peripheral schisis in 50% of patients. ERG: selective reduction in b-wave amplitude.	[17]

Appendix 1. Continued

Disease	Clinical features	Refs
Enhanced S-cone syndrome/Goldmann-Favre Syndrome	ERG: enhanced S-cone sensitivity (pathognomic). Variable phenotype, hallmarks are nummular pigmentations at RPE level and cystoid or schisis-like maculopathy. Night blindness from birth and decreased VA.	[18,19]
Wagner syndrome/erosive vitreoretinopathy	Optically empty vitreous with avascular vitreous strands and veils, presenile cataract, moderate myopia, progressive chorioretinal atrophy sometimes with diffuse pigmentary changes, reduced VA, night blindness and visual field constriction. Retinal detachment in advanced stages of disease.	[20,21]
Snowflake vitreoretinopathy	Autosomal dominant, corneal guttae, cataract, fibrillar degeneration of the vitreous, retinal detachment, and peripheral retinal degeneration, including crystalline deposits referred to as snowflakes, vascular attenuation and chorioretinal pigmentation.	[22,23]
Female carriers of inherited retinal diseases		
Retinitis pigmentosa	Female carriers of XL-RP: highly variable presentation; from no abnormalities to RP phenotype. Tapetal-like reflex possible.	[24]
Choroideremia	Female carriers are generally asymptomatic, although chorioretinal atrophy and ERG changes similar to those in affected males can be observed.	[11]
Ocular albinism	Female carriers *GPR143* gene (OA1): patchy hypopigmentation of the RPE, iris transillumination.	[25]
Syndromic forms of retinitis pigmentosa		
Ciliopathies		
Usher syndrome	RP with partial or complete neurosensory hearing loss, sometimes vestibular dysfunction.	[26]
Bardet-Biedl syndrome	RP and obesity, postaxial polydactyly, hypogonadism, renal dysfunction, cognitive impairment.	[27]
Cohen syndrome	RP and myopia, mental retardation, hypotonia, fascial dysmorphism, short stature, neutropenia.	[28]
Joubert syndrome	RP/LCA with dysmorphic facial features, congenital hypotonia evolving in ataxia, developmental delay and unusual fast or slow breathing. Oculomotor apraxia and nystagmus may be present. The hallmark feature is the 'molar tooth sign' on MRI.	[29,30]
Senior-Løken syndrome	RP/LCA and nephronophthisis (NPHP).	[31]
Sensenbrenner syndrome (cranioectodermal dysplasia)	RP and craniosynostosis, ectodermal abnormalities.	[32,33]
Short-rib thoracic dysplasia with or without polydactyly (includes Jeune, Mainzer-Saldino, Ellis-van Creveld and short rib-polydactyly syndrome)	RP and thoracic hypoplasia, short stature, brachydactyly, polydactyly, chronic renal failure, (sometimes lethal) respiratory insufficiency.	[34,35]
Metabolic disorders		
Alfa-tocopherol transfer protein deficiency (familial isolated vitamin E deficiency)	RP with (Friedrich-like) ataxia, dysarthria, reduced proprioception and hyporeflexia.	[36,37]
Bassen-Kornzweig syndrome (abetalipoproteinemia)	Atypical RP with onset 1st-2nd decade. Wide spectrum of abnormalities including progressive cerebellar ataxia, gastrointestinal disorders, acanthocytosis and absence of apo-B containing lipoproteins.	[38,39]

Chapter 2.1

Appendix 1. Continued

Disease	Clinical features	Refs
Mucopolysaccharidoses	Group of disorders with RP, cloudy cornea and glaucoma and numerous symptoms in varying degree: cognitive impairment, developmental delay, hearing loss, hydrocephalus, facial abnormalities, dwarfism and hepato-splenomegaly.	40
Neuronal ceroid-lipofuscinoses, childhood onset (Batten disease)	RP with early vision loss, FAG: diffuse RPE atrophy with stippled hyperfluorescence, progressive neurodegeneration, seizures, may cause early death.	41
Refsum disease (phytanic acid oxidase deficiency)	RP and anosmia, miosis, attenuated effect of mydriatica, elevated phytanic acid levels, anosmia, hearing loss, ataxia, polyneuropathy, ichthyosis, cardiopathy.	42,43
Mevalonate kinase deficiency (mevalonic aciduria (MEVA) and hyper-immunoglobulin D and periodic fever syndrome (HIDS)	Spectrum of clinical phenotypes, sometimes with RP. HIDS: recurrent febrile attacks lymphadenopathy, arthralgia, gastrointestinal disturbances, skin rash and increased levels of serum immunoglobulin D. MEVA is the most severe form with psychomotore retardation, progressive cerebellar ataxia, dysmorphic features, recurrent febrile crises, and failure to thrive.	44,45
HARP syndrome (hypoprebetalipoproteinemia, acanthocytosis, RP and pallidal degeneration)	Part of the pantothenate kinase-associated neurodegeneration (PKAN) spectrum. RP with hypoprebetalipoproteinemia, acanthocytosis and pallidal degeneration (eye of the tiger sign on MRI).	46
PHARC syndrome (polyneuropathy, hearing loss, ataxia, RP, and cataract	RP with polyneuropathy, hearing loss, cerebellar ataxia and early-onset cataract.	47
Mitochondrial disorders		
Kearns-Sayre Syndrome	RP with progressive external ophthalmoplegia, heart conduction defect, cerebellar ataxia or elevated protein concentration in cerebrospinal fluid. Onset <20 years.	48
NARP syndrome (Neuropathy, Ataxia, RP)	RP and peripheral neuropathy, neurogenic muscle weakness, ataxia.	49
Pseudoretinitis pigmentosa		
Drug-induced		
Thioridazine and chlorpromazine	Nummular areas with loss of RPE and choriocapillaris perfusion. Chlorpromazine often leads to posterior subcapsular cataract.	50,51
Quinolines (e.g. (Hydroxy)chloroquine)	Bull's eye maculopathy, Asian patients: pericentral retinopathy. In case of poisoning: initially fixed dilated pupils, later miosis. Late fundus appearance.	52-54
Chorioretinal infections		
Syphilis, Lyme disease, acute retinal necrosis and other viral infections (rubella, chicken pox, measles, cytomegalovirus)	Often unilateral or sectorial retinal disease. History of infectious retinal disease.	55-61
Sequela of inflammatory disease		
Sarcoidosis	Ocular clinical criteria: mutton-fat or small granulomatous KPs and/or iris nodules; nodules in trabecular meshwork or tent-shaped PAS; vitreous snowballs; peripheral chorioretinal lesions; nodular/ segmental periphlebitis; optic disc nodule(s) and/or solitary choroidal nodule; bilaterality. Extraocular granulomas in: lymph nodes, lungs, skin, liver, spleen, salivary glands, heart, bones and nervous system.	62

Appendix 1. Continued

Disease	Clinical features	Refs
Acute posterior multifocal placoid pigment epitheliopathy	Sudden loss of VA, blurred vision and central scotomas. Often self-limiting, good prognosis with visual recovery.	[63]
Birdshot chorioretinopathy	Gradual decline in VA due to CME and retinal atrophy, nyctalopia, floaters, glare, dyschromatopsia and photopsia. Cream-colored, irregular or elongated choroidal lesions radiating from optic disc. Supportive: HLA-A29+ and retinal vasculitis.	[64]
Serpiginous choroidopathy	Symptoms: VA loss, metamorphopsia or central scotoma. Signs: recurrent gray-yellowish subretinal infiltrates, centrifugally spreading from peripapillar region in a serpiginous manner. They resolve in atrophy. Bilateral, but often asymmetric.	[65]
Diffuse unilateral subacute neuroretinitis (DUSN)	Early stage: vitritis, papillitis, clustered yellow-gray-white lesions. Later stage: optic atrophy, arteriolar narrowing, increased ILM reflex (Oréfice's sign), subretinal tunnels (Garcia's sign), diffuse RPE degeneration, and afferent pupillary defect. Nematode sometimes visible.	[66]
Systemic lupus erythematosus (SLE)	Extraocular SLE characteristics (fever, joint pain, rash, etc), cotton wool spots.	[67,68]
Miscellaneous		
Vitamin A deficiency	Xerophthalmia and nightblindness. Yellow and white retinal spots may be present in the periphery. Symptoms may be reversible with vitamin A treatment.	[69,70]
Paraneoplastic	Photopsias, history of primary tumor; most often breast - or lung carcinoma or melanoma.	[71,72]
Trauma	Patient history, unilateral.	[73]
Siderosis bulbi	Patient history, unilateral, inner retinal layers more severely affected than outer layers.	[74]
Old retinal detachment	Unilateral, history of retinal detachment.	
Pigmented paravenous retinochoroidal atrophy (PPRCA)	Pigment accumulation solely along retinal veins, no or very slow progression, often asymptomatic. Etiology unclear.	[75]
Acute zonal occult outer retinopathy	Acute onset, often initially unilateral; however, majority develops bilateral disease, scotoma, photopsias, fundus examination often apparently normal, later RPE disturbances. ERG: delayed implicit time of 30-Hz cone flicker response. EOG: reduction in the light rise.	[76]

Abbreviations: CME: cystoid macular edema, ERG: electroretinography, ILM: internal limiting membrane, FAG: fluorescein angiography, KPs: keratic precipitates, PAS: peripheral anterior synechiae, RP: retinitis pigmentosa, RPE: retinal pigment epithelium, VA: visual acuity

Chapter 2.1

References

1. Thiadens AA, Phan TM, Zekveld-Vroon RC, et al. Clinical course, genetic etiology, and visual outcome in cone and cone-rod dystrophy. *Ophthalmology.* 2012;119(4):819-826.
2. Hamel CP. Cone rod dystrophies. *Orphanet J Rare Dis.* 2007;2(1):7.
3. Michaelides M, Hardcastle AJ, Hunt DM, Moore AT. Progressive cone and cone-rod dystrophies: phenotypes and underlying molecular genetic basis. *Surv Ophthalmol.* 2006;51(3):232-258.
4. den Hollander AI, Roepman R, Koenekoop RK, Cremers FP. Leber congenital amaurosis: genes, proteins and disease mechanisms. *Prog Retin Eye Res.* 2008;27(4):391-419.
5. Querques G, Souied EH. *Macular Dystrophies.* 1 ed: Springer International Publishing 2016.
6. Okialda KA, Stover NB, Weleber RG, Kelly EJ. Bietti Crystalline Dystrophy. In: Pagon RA, Adam MP, Ardinger HH, et al., eds. *GeneReviews(R).* Seattle (WA): University of Washington, Seattle. GeneReviews is a registered trademark of the University of Washington, Seattle. All rights reserved.; 1993.
7. Borooah S, Collins C, Wright A, Dhillon B. Late-onset retinal macular degeneration: clinical insights into an inherited retinal degeneration. *Br J Ophthalmol.* 2009;93(3):284-289.
8. Soumplis V, Sergouniotis PI, Robson AG, et al. Phenotypic findings in C1QTNF5 retinopathy (late-onset retinal degeneration). *Acta Ophthalmol.* 2013;91(3):e191-195.
9. Zeitz C, Robson AG, Audo I. Congenital stationary night blindness: an analysis and update of genotype-phenotype correlations and pathogenic mechanisms. *Prog Retin Eye Res.* 2015;45:58-110.
10. Li S, Guan L, Fang S, et al. Exome sequencing reveals CHM mutations in six families with atypical choroideremia initially diagnosed as retinitis pigmentosa. *Int J Mol Med.* 2014;34(2):573-577.
11. MacDonald IM, Hume S, Chan S, Seabra MC. Choroideremia. In: Pagon RA, Adam MP, Ardinger HH, et al., eds. *GeneReviews(R).* Seattle (WA): University of Washington, Seattle. GeneReviews is a registered trademark of the University of Washington, Seattle. All rights reserved.; 1993.
12. Sergouniotis PI, Davidson AE, Lenassi E, Devery SR, Moore AT, Webster AR. Retinal structure, function, and molecular pathologic features in gyrate atrophy. *Ophthalmology.* 2012;119(3):596-605.
13. Valtonen M, Nanto-Salonen K, Heinanen K, Alanen A, Kalimo H, Simell O. Skeletal muscle of patients with gyrate atrophy of the choroid and retina and hyperornithinaemia in ultralow-field magnetic resonance imaging and computed tomography. *J Inherit Metab Dis.* 1996;19(6):729-734.
14. Fossdal R, Jonasson F, Kristjansdottir GT, et al. A novel TEAD1 mutation is the causative allele in Sveinsson's chorioretinal atrophy (helicoid peripapillary chorioretinal degeneration). *Hum Mol Genet.* 2004;13(9):975-981.
15. Sveinsson K. Helicoidal peripapillary chorioretinal degeneration. *Acta Ophthalmol (Copenh).* 1979;57(1):69-75.
16. Godley BF, Tiffin PA, Evans K, Kelsell RE, Hunt DM, Bird AC. Clinical features of progressive bifocal chorioretinal atrophy: a retinal dystrophy linked to chromosome 6q. *Ophthalmology.* 1996;103(6):893-898.
17. Sieving PA, MacDonald IM, Chan S. X-Linked Juvenile Retinoschisis. In: Pagon RA, Adam MP, Ardinger HH, et al., eds. *GeneReviews(R).* Seattle (WA): University of Washington, Seattle. GeneReviews is a registered trademark of the University of Washington, Seattle. All rights reserved.; 1993.
18. Yzer S, Barbazetto I, Allikmets R, et al. Expanded clinical spectrum of enhanced S-cone syndrome. *JAMA Ophthalmol.* 2013;131(10):1324-1330.
19. Marmor MF, Jacobson SG, Foerster MH, Kellner U, Weleber RG. Diagnostic clinical findings of a new syndrome with night blindness, maculopathy, and enhanced S cone sensitivity. *Am J Ophthalmol.* 1990;110(2):124-134.
20. Ronan SM, Tran-Viet KN, Burner EL, Metlapally R, Toth CA, Young TL. Mutational hot spot potential of a novel base pair mutation of the CSPG2 gene in a family with Wagner syndrome. *Arch Ophthalmol.* 2009;127(11):1511-1519.
21. Kloeckener-Gruissem B, Amstutz C. VCAN-Related Vitreoretinopathy. In: Adam MP, Ardinger HH, Pagon RA, et al., eds. *GeneReviews(R).* Seattle (WA): University of Washington, Seattle. GeneReviews is a registered trademark of the University of Washington, Seattle. All rights reserved.; 1993.
22. Lee MM, Ritter R, 3rd, Hirose T, Vu CD, Edwards AO. Snowflake vitreoretinal degeneration: follow-up of the original family. *Ophthalmology.* 2003;110(12):2418-2426.
23. Hejtmancik JF, Jiao X, Li A, et al. Mutations in KCNJ13 cause autosomal-dominant snowflake vitreoretinal degeneration. *Am J Hum Genet.* 2008;82(1):174-180.
24. Comander J, Weigel-DiFranco C, Sandberg MA, Berson EL. Visual Function in Carriers of X-Linked Retinitis Pigmentosa. *Ophthalmology.* 2015;122(9):1899-1906.
25. Lang GE, Rott HD, Pfeiffer RA. X-linked ocular albinism. Characteristic pattern of affection in female carriers. *Ophthalmic Paediatr Genet.* 1990;11(4):265-271.
26. Bonnet C, El-Amraoui A. Usher syndrome (sensorineural deafness and retinitis pigmentosa): pathogenesis, molecular diagnosis and therapeutic approaches. *Curr Opin Neurol.* 2012;25(1):42-49.
27. Mockel A, Perdomo Y, Stutzmann F, Letsch J, Marion V, Dollfus H. Retinal dystrophy in Bardet-Biedl syndrome and related syndromic ciliopathies. *Prog Retin Eye Res.* 2011;30(4):258-274.
28. Kivitie-Kallio S, Summanen P, Raitta C, Norio R. Ophthalmologic findings in Cohen syndrome. A long-term follow-up. *Ophthalmology.* 2000;107(9):1737-1745.

29. Maria BL, Boltshauser E, Palmer SC, Tran TX. Clinical features and revised diagnostic criteria in Joubert syndrome. *J Child Neurol.* 1999;14(9):583-590; discussion 590-581.

30. Parisi M, Glass I. Joubert Syndrome. In: Pagon RA, Adam MP, Ardinger HH, et al., eds. *GeneReviews(R).* Seattle (WA): University of Washington, Seattle. GeneReviews is a registered trademark of the University of Washington, Seattle. All rights reserved.; 1993.

31. Ronquillo CC, Bernstein PS, Baehr W. Senior-Loken syndrome: a syndromic form of retinal dystrophy associated with nephronophthisis. *Vision Res.* 2012;75:88-97.

32. Costet C, Betis F, Berard E, et al. [Pigmentosum retinis and tubulo-interstitial nephronophtisis in Sensenbrenner syndrome: a case report]. *J Fr Ophtalmol.* 2000;23(2):158-160.

33. Bredrup C, Saunier S, Oud MM, et al. Ciliopathies with skeletal anomalies and renal insufficiency due to mutations in the IFT-A gene WDR19. *Am J Hum Genet.* 2011;89(5):634-643.

34. Wang Z, Iida A, Miyake N, et al. Axial Spondylometaphyseal Dysplasia Is Caused by C21orf2 Mutations. *PLoS One.* 2016;11(3):e0150555.

35. Schmidts M. Clinical genetics and pathobiology of ciliary chondrodysplasias. *J Pediatr Genet.* 2014;3(2):46-94.

36. Yokota T, Shiojiri T, Gotoda T, Arai H. Retinitis pigmentosa and ataxia caused by a mutation in the gene for the alpha-tocopherol-transfer protein. *N Engl J Med.* 1996;335(23):1770-1771.

37. Yokota T, Shiojiri T, Gotoda T, et al. Friedreich-like ataxia with retinitis pigmentosa caused by the His101Gln mutation of the alpha-tocopherol transfer protein gene. *Ann Neurol.* 1997;41(6):826-832.

38. Bassen FA, Kornzweig AL. Malformation of the erytrocytes in a case of atypical retinitis pigmentosa. *Blood.* 1950;5:381-387.

39. Zamel R, Khan R, Pollex RL, Hegele RA. Abetalipoproteinemia: two case reports and literature review. *Orphanet J Rare Dis.* 2008;3:19.

40. Neufeld EF, Muenzer J. The Mucopolysaccharidoses. In: Beaudet AL, Vogelstein B, Kinzler KW, et al., eds. *The Online Metabolic and Molecular Bases of Inherited Disease.* New York, NY: The McGraw-Hill Companies, Inc.; 2014.

41. Hainsworth DP, Liu GT, Hamm CW, Katz ML. Funduscopic and angiographic appearance in the neuronal ceroid lipofuscinoses. *Retina.* 2009;29(5):657-668.

42. Refsum S, Salomonsen L, Skatvedt M. Heredopathia atactica polyneuritiformis in children. *J Pediatr.* 1949;35(3):335-343.

43. Ruether K, Baldwin E, Casteels M, et al. Adult Refsum disease: a form of tapetoretinal dystrophy accessible to therapy. *Surv Ophthalmol.* 2010;55(6):531-538.

44. Kellner U, Stohr H, Weinitz S, Farmand G, Weber BH. Mevalonate kinase deficiency associated with ataxia and retinitis pigmentosa in two brothers with MVK gene mutations. *Ophthalmic Genet.* 2017:1-5.

45. van der Burgh R, Ter Haar NM, Boes ML, Frenkel J. Mevalonate kinase deficiency, a metabolic autoinflammatory disease. *Clin Immunol.* 2013;147(3):197-206.

46. Orrell RW, Amrolia PJ, Heald A, et al. Acanthocytosis, retinitis pigmentosa, and pallidal degeneration: a report of three patients, including the second reported case with hypoprebetalipoproteinemia (HARP syndrome). *Neurology.* 1995;45(3 Pt 1):487-492.

47. Nishiguchi KM, Avila-Fernandez A, van Huet RA, et al. Exome sequencing extends the phenotypic spectrum for ABHD12 mutations: from syndromic to nonsyndromic retinal degeneration. *Ophthalmology.* 2014;121(8):1620-1627.

48. Kearns TP, Sayre GP. Retinitis pigmentosa, external ophthalmophegia, and complete heart block: unusual syndrome with histologic study in one of two cases. *AMA Arch Ophthalmol.* 1958;60(2):280-289.

49. Ortiz RG, Newman NJ, Shoffner JM, Kaufman AE, Koontz DA, Wallace DC. Variable retinal and neurologic manifestations in patients harboring the mitochondrial DNA 8993 mutation. *Arch Ophthalmol.* 1993;111(11):1525-1530.

50. Meredith TA, Aaberg TM, Willerson WD. Progressive chorioretinopathy after receiving thioridazine. *Arch Ophthalmol.* 1978;96(7):1172-1176.

51. Mathalone MB. Eye and skin changes in psychiatric patients treated with chlorpromazine. *Br J Ophthalmol.* 1967;51(2):86-93.

52. Melles RB, Marmor MF. Pericentral retinopathy and racial differences in hydroxychloroquine toxicity. *Ophthalmology.* 2015;122(1):110-116.

53. Francois J, De Rouck A, Cambie E. Retinal and optic evaluation in quinine poisoning. *Ann Ophthalmol.* 1972;4(3):177-185.

54. Fraunfelder FT, Fraunfelder FW, Chambers WA. *Clinical Ocular Toxicology E-Book: Drug-Induced Ocular Side Effects.* Elsevier Health Sciences; 2008.

55. Heckenlively JR. Secondary retinitis pigmentosa (syphilis). *Doc Ophthalmol Proc Ser.* 1977;13:245-255.

56. Karma A, Pirttila TA, Viljanen MK, Lahde YE, Raitta CM. Secondary retinitis pigmentosa and cerebral demyelination in Lyme borreliosis. *Br J Ophthalmol.* 1993;77(2):120-122.

57. Smith JR, Cunningham ET, Jr. Atypical presentations of ocular toxoplasmosis. *Curr Opin Ophthalmol.* 2002;13(6):387-392.

58. Cooper LZ, Krugman S. Clinical manifestations of postnatal and congenital rubella. *Arch Ophthalmol.* 1967;77(4):434-439.

59. Vijayalakshmi P, Kakkar G, Samprathi A, Banushree R. Ocular manifestations of congenital rubella syndrome in a developing country. *Indian J Ophthalmol.* 2002;50(4):307-311.

60. Weleber RG, Gregory-Evans K. Retinitis Pigmentosa and Allied Disorders. *Retina.* Vol 1: Elsevier Mosby; 2006:395-498.

61. Gass JD, Braunstein RA. Further observations concerning the diffuse unilateral subacute neuroretinitis syndrome. *Arch Ophthalmol.* 1983;101(11):1689-1697.

62.   Liu D, Birnbaum AD. Update on sarcoidosis. *Curr Opin Ophthalmol.* 2015;26(6):512-516.
63.   Fiore T, Iaccheri B, Androudi S, et al. Acute posterior multifocal placoid pigment epitheliopathy: outcome and visual prognosis. *Retina.* 2009;29(7):994-1001.
64.   Shah KH, Levinson RD, Yu F, et al. Birdshot chorioretinopathy. *Surv Ophthalmol.* 2005;50(6):519-541.
65.   Gupta V, Agarwal A, Gupta A, Bambery P, Narang S. Clinical characteristics of serpiginous choroidopathy in North India. *Am J Ophthalmol.* 2002;134(1):47-56.
66.   Relhan N, Pathengay A, Raval V, Nayak S, Choudhury H, Flynn HW, Jr. Clinical experience in treatment of diffuse unilateral subretinal neuroretinitis. *Clin Ophthalmol.* 2015;9:1799-1805.
67.   Peponis V, Kyttaris VC, Tyradellis C, Vergados I, Sitaras NM. Ocular manifestations of systemic lupus erythematosus: a clinical review. *Lupus.* 2006;15(1):3-12.
68.   Sekimoto M, Hayasaka S, Noda S, Setogawa T. Pseudoretinitis pigmentosa in patients with systemic lupus erythematosus. *Ann Ophthalmol.* 1993;25(7):264-266.
69.   Sommer A, Tjakrasudjatma S, Djunaedi E, Green WR. Vitamin A-responsive panocular xerophthalmia in a healthy adult. *Arch Ophthalmol.* 1978;96(9):1630-1634.
70.   Smith J, Steinemann TL. Vitamin A deficiency and the eye. *Int Ophthalmol Clin.* 2000;40(4):83-91.
71.   Sawyer RA, Selhorst JB, Zimmerman LE, Hoyt WF. Blindness caused by photoreceptor degeneration as a remote effect of cancer. *Am J Ophthalmol.* 1976;81(5):606-613.
72.   Thirkill CE, Roth AM, Keltner JL. Cancer-associated retinopathy. *Arch Ophthalmol.* 1987;105(3):372-375.
73.   Bastek JV, Foos RY, Heckenlively J. Traumatic pigmentary retinopathy. *Am J Ophthalmol.* 1981;92(5):621-624.
74.   Duke-Elder SM. System of ophthalmologyVolXIv: injuries part 1: Mechanical injuries. 1972.
75.   Huang HB, Zhang YX. Pigmented paravenous retinochoroidal atrophy (Review). *Exp Ther Med.* 2014;7(6):1439-1445.
76.   Monson DM, Smith JR. Acute zonal occult outer retinopathy. *Surv Ophthalmol.* 2011;56(1):23-35.

Appendix 2
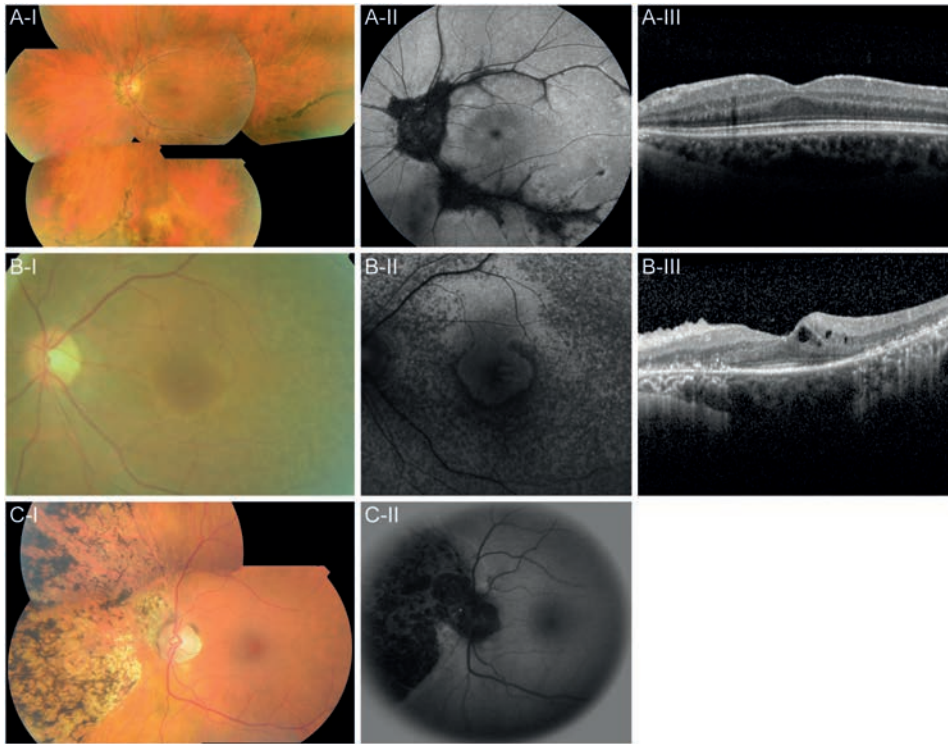
Multimodal images of three patients with pseudoretinitis pigmentosa

(A-I) Fundus photograph of a 41-year-old female with pigmented paravenous retinochoroidal atrophy, showing peripapillary atrophy, and both hyperpigmentation and RPE atrophy along the retinal vessels (A-II) visible as hypoautofluorescence on fundus autofluorescence (FAF). (A-III) Optical coherence tomography (OCT) image of the same patient showing intact central retinal layers.

(B-I) Fundus photograph of a 60-year-old female with a hydroxychloroquine retinopathy, showing a bull's eye maculopathy with mottled RPE atrophy in the posterior pole, a normal caliber of the retinal vessels, and temporal pallor of the optic disc. (B-II) FAF image of the same patient, showing a mottled pattern of hypo- and hyperautofluorescence, and annular hypoautofluorescence in the macula. (B-III) OCT scan revealing CME and the preservation of the ellipsoid zone at the fovea.

(C-I) Fundus photograph of a 51-year-old female with acute zonal occult outer retinopathy, showing severe hyperpigmentation and RPE atrophy confined to the nasal retina, (C-II) which corresponds to hypoautofluorescent regions on FAF. The contralateral eye of the patient showed no abnormalities.

Appendix 3

Atlas of color fundus photographs of non-syndromic retinitis pigmentosa

This atlas contains color fundus photographs of 75 of the 84 genetically defined RP subtypes. The photographs show the phenotypic characteristics of each subtype, and illustrate the heterogeneity of RP. Nevertheless, it is important to realize that even within a specific subtype, considerable phenotypic variation can occur.

In case photographs are reprinted from previous articles, permission to reprint has been obtained from the publisher, and a reference to the original article is provided.

Contents

Chapter 2.1

ABCA4

Fundus photograph of a 48-year old female, showing peripheral bone spicule pigmentations, mild attenuation of vessels, and mid-peripheral atrophy. Reprinted from Klevering et al., 2004 with permission from Nature Publishing Group.
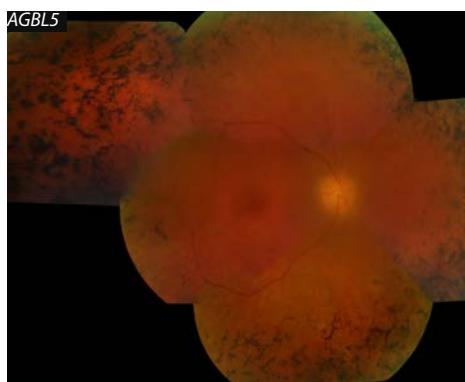
AGBL5

Composite fundus photograph of a 27-year old female, showing peripheral bone spicule pigmentation, vessel attenuation, and optic disc pallor. Reprinted from Astuti et al., 2016.[§]

AHI1
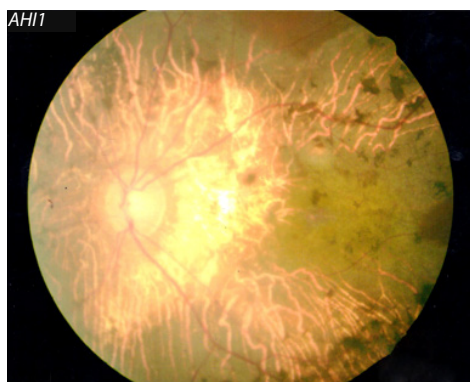
Fundus photograph of a female RP, showing severe RPE atrophy, and hyper-pigmentation in the macula. Reprinted from Huang et al., 2015.[*]

ARHGEF18
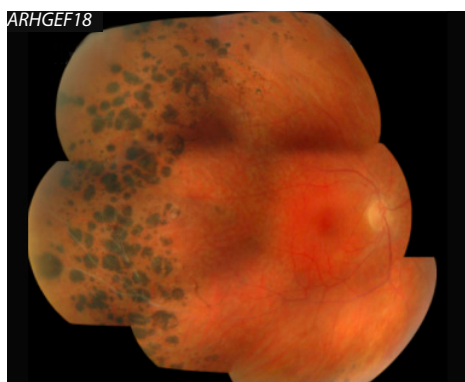
Composite fundus photograph of a 37-year old female, showing vascular attenuation and occlusion, peripheral RPE atrophy, white dots, and nummular pigmentation. Reprinted from Arno et al., 2017.[¥]

ARL2BP
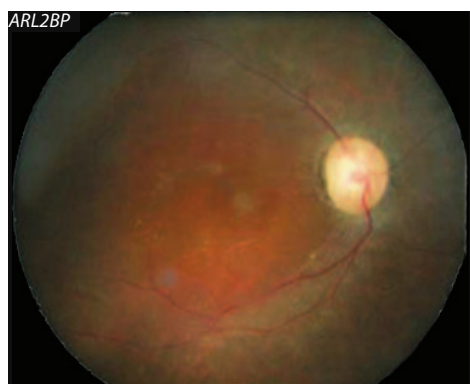
Relatively low quality fundus photograph image of a 36-year old female, showing vessel attenuation, macular atrophy and a pale optic disc. Reprinted from Audo et al., 2017 with permission from John Wiley and Sons.
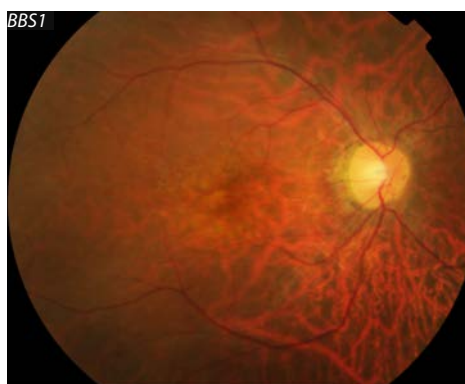
BBS1

Fundus photograph of a 33-year old male with BBS1-associated RP, showing attenuated vessels, RPE atrophy.

BEST1
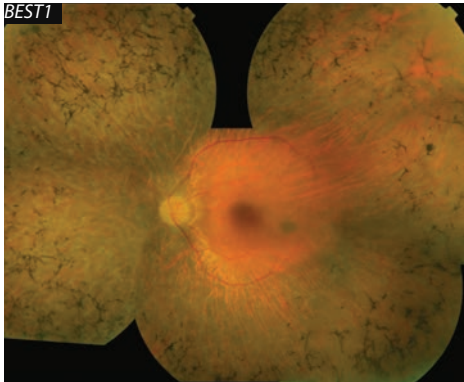
Composite fundus photograp of a 44-year old female, showing bone spicule pigmentation, vessel attenuation, and waxy pallor of the optic disc.

C2orf71
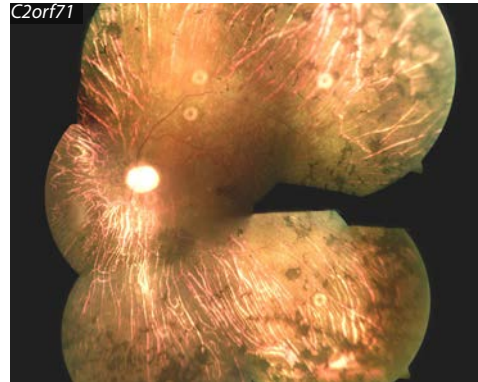
Composite fundus photograph of a 50-year old male, showing peripheral bone spicule pigmentation, attenuation of retinal vessels, severe retinal atrophy, and pallor of the optic disc. 4 round reflection artefacts. Reprinted from Collin et al., 2010.[¥]

C8orf37
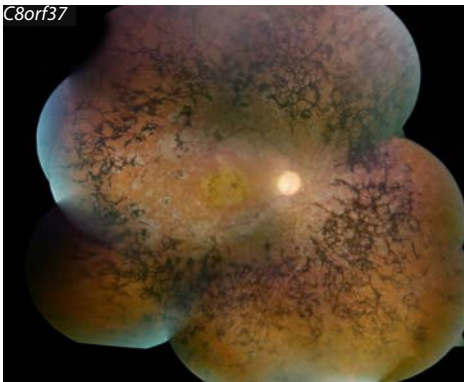
Fundus photograph of a 39-year old female, showing macular atrophy and pigmentation clumps, as well as pallor of the optic disc, attenuated vessels, paravascular atrophy of the RPE, and abundant bone spicules. Reprinted from Van Huet et al., 2013.

CA4
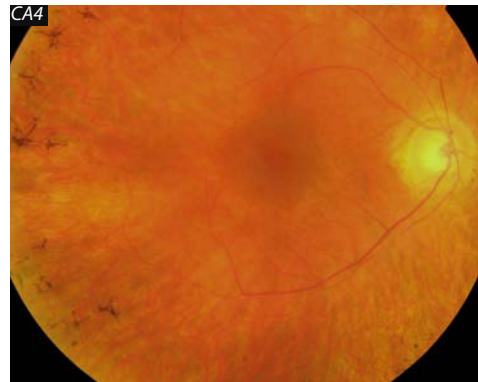
Fundus photograph of a 42-year old female RP, showing bone spicule pigmentation in the mid-periphery, and attenuated vessels.

CDHR1

Composite fundus photograph of a 46-year old male, showing vessel attenuation, bone spicule-like pigmentation, and (patchy) atrophy in the periphery and macula.

CERKL
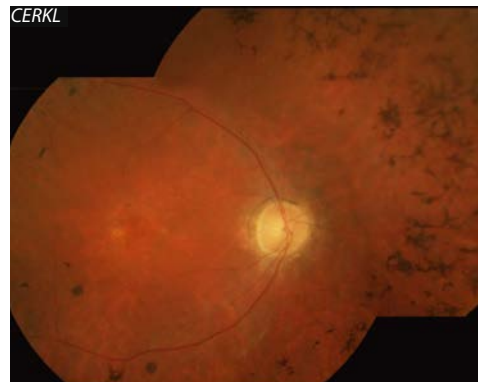
Composite fundus photograph of a 49-year old female, showing bone spicule pigmentation in the mid-periphery, attenuated vessels, and RPE alterations in the macula.

CLN3
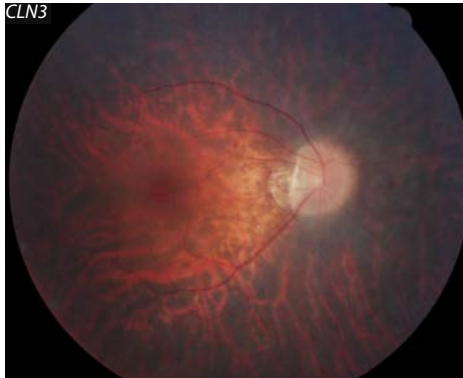
Fundus photograph of a female, showing profound retinal degeneration, attenuated vessels, pallor of the optic disc and parapapillary atrophy. Reprinted from Wang et al., 2014 with permission from Springer Nature.
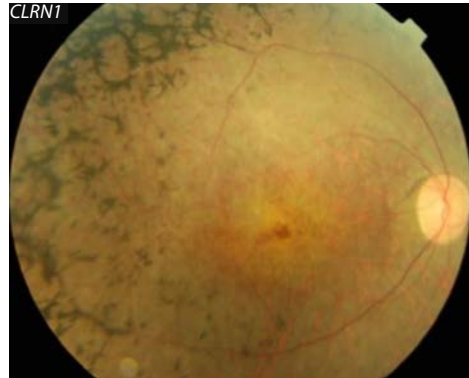
CLRN1

Fundus photograph of a 48-year old male, showing attenuated vessels, bone spicule pigmentation, and macular involvement. Reprinted from Khan et al., 2011 with permission from Elsevier.

CNGA1
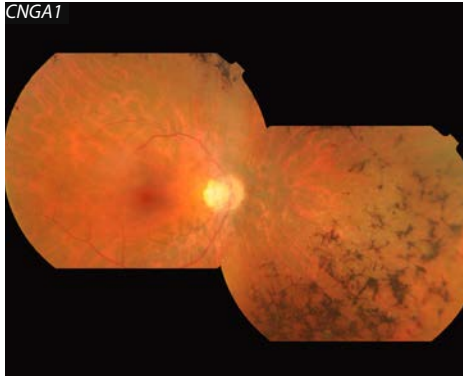
Composite fundus photographs of a 49-year old female, showing mid-peripheral bone spicule pigmentation, attenuated vessels and parapapillary atrophy.
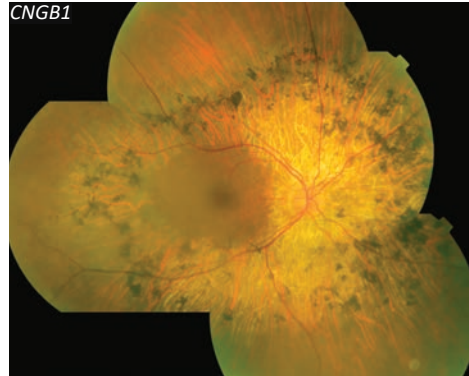
CNGB1

Composite fundus photograph of a 67-year old male, showing attenuated vessels, RPE atropy, and mid-peripheral pigment clumping.

CRB1
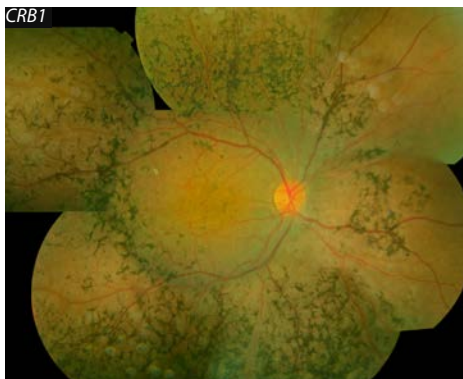
Composite fundus photograph of a 21-year old male RP, showing dense pigment migration with para-arteriolar absene of pigmentation.

CWC27

Composite fundus photograph of a 14-year old male, showing wide-spread grayish pigment flecks in the RPE. Reprinted from Xu et al., 2017 with permission from Elsevier.

DHDDS
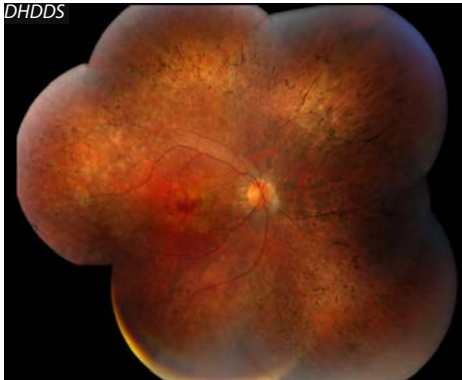
Composite fundus photograph of a male patient, showing diffuse pigmentary retinal degeneration with pigmentary clumping and vascular attenuation.
Reprinted from Züchner et al., 2011.[¥]

EYS
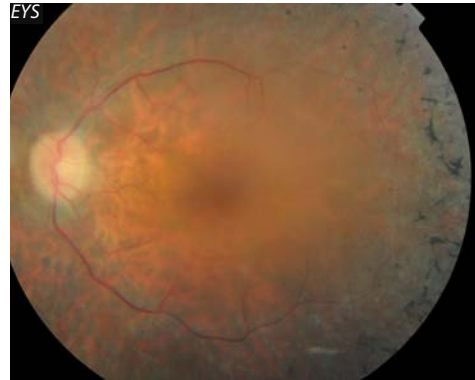
Fundus photograph of a 39-year old male, showing bone spicule pigmentation in the mid-periphery, attenuated vessels and RPE atrophy.

FAM161A

Fundus photograph of a 62-year old male, showing vessel attenuation, and extensive RPE atrophy that includes the macula.

FSCN2

Fundus photograph of a 28-year old male, showing mild vessel attenuation, and central involvement.

GNAT1
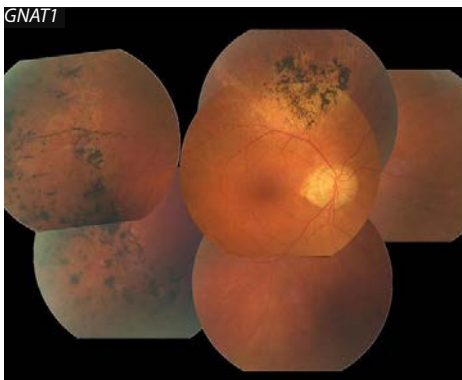
Composite fundus photograph of a 80-year old male, showing optic disc pallor, vessel attenuation, normal macula and scattered bone spicule pigment deposits. Reprinted from Carrigan et al., 2016.[§]

GUCA1B

Relatively low quality fundus photograph of a 23-year old female, showing mid-peripheral bone spicule pigmentation, mild attenuation of retinal vessels and perifoveal atrophy. Reprinted from Sato et al., 2005 with permission from Springer.

HGSNAT
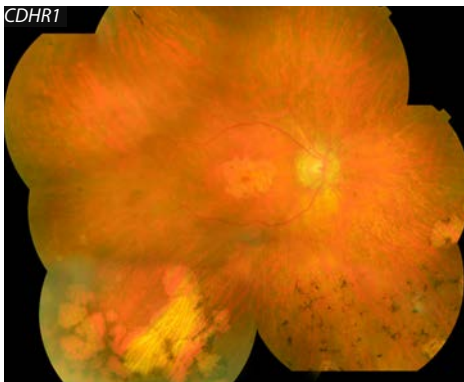
Composite fundus photograph of a 67-year old male, showing sparse bone spicule pigmentation, slight attenuation of retinal vessels, and RPE atrophy.

HK1

Composite fundus photograph of a 56-year old female, showing heavy pigmentary deposits and focal areas of hypopigmentation primarily in the mid-periphery. Retinal vessels are moderately attenuated. Reprinted from Sullivan et al., 2014.

IDH3A
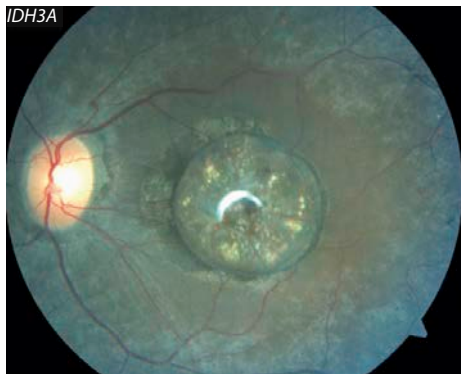
Fundus photograph of a 26-year old female, showing bone spicule pigmentary changes, and macular pigmentation with severe pseudocoloboma-like atrophy. Reprinted from Pierrache et al., 2017 with permission from Elsevier.

IFT140

Composite fundus photograph of a 44-year old male, showing central macular atrophy with mid-peripheral hypopigmentary dots. Reprinted from Hull et al., 2016.[§]

IFT172
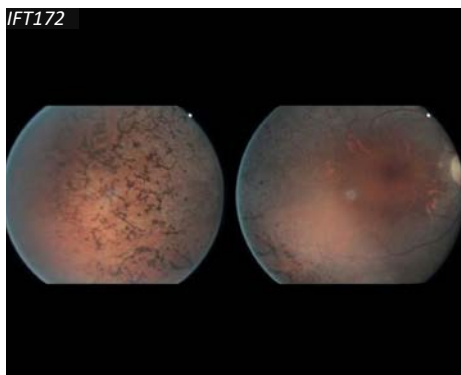
Fundus photographs of a 33-year old female, showing peripheral bone spicule pigmentation, attenuated vessels and optic disc pallor. Right photograph: round reflection artefact. Reprinted from Bujakowska et al., 2015 with permission from Oxford University Press.

IMPDH1
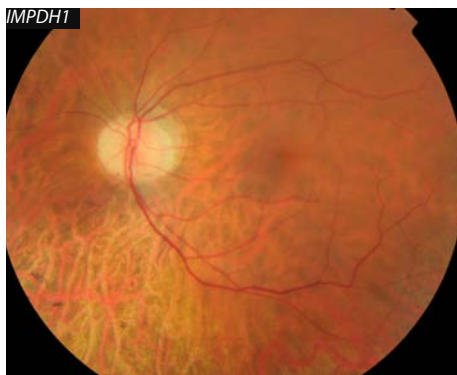
Fundus photograph of a 42-year old male, showing RPE atrophy, attenuated retinal vessels and optic disc pallor.

IMPG2
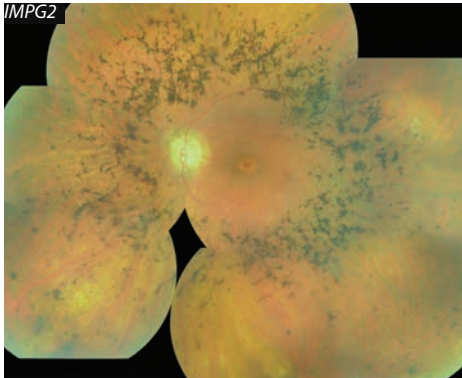
Composite fundus photograph of a 59-year old female, showing marked bone spicule pigmentation in the mid-periphery, waxy pallor of the optic disc, attenuated vessels, and macular atrophy.

KIZ

Fundus photograph of a 50-year old male, showing pigmentary changes in the peripheral retina, and atrophic changes in the macula. Reprinted from El Shamieh et al., 2014.¥

KLHL7

Fundus photograph of a 37-year old female, showing retinal degeneration and pigmentation.
Reprinted from Friedman et al., 2009.¥

LRAT
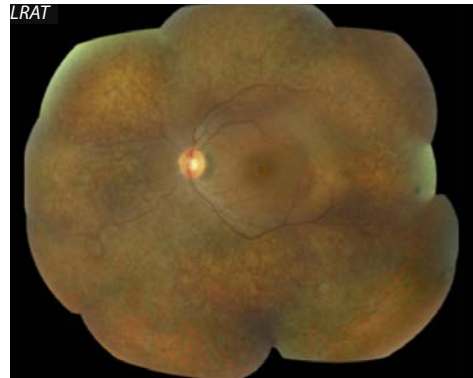
Composite fundus photograph of a 27-year old male, showing widespread RPE atrophy, arteriolar attenuation, and minimal retinal pigmentation. Reprinted from Dev Borman et al., 2012.

MAK

Fundus photograph of 41-year old male, showing attenuated vessels, pallor of the optic disc, and RPE atrophy.

MERTK

Fundus photograph of a 22-year old female, showing attenuated vessels, optic disc pallor, and an epiretinal membrane.

MVK

Fundus photograph of a 61-year old male, showing RPE atrophy in the mid-periphery with bone spicule pigmentation.
Reprinted from Siemiatkowska et al., 2013 with permission from Elsevier.

NR2E3
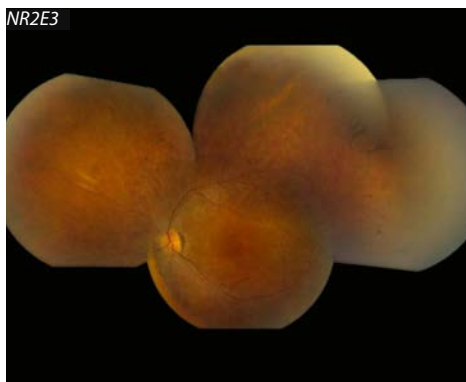
Low quality fundus photograph of a patient with autosomal dominant RP, showing attenuated vessels and bone spicule pigmentation.
Reprinted from Van Cauwenbergh et al., 2017.[†]

NRL
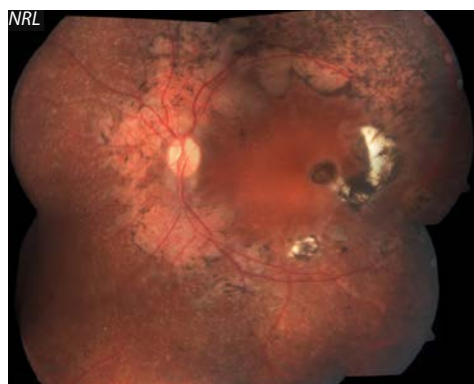
Composite fundus photograph of a female with autosomal recessive RP, showing subretinal scars in the temporal macula, and patches of retinal atropy along the arcades and around the optic disc with pigmentary cluming. Reprinted from Newman et al., 2016.[†]

OFD1

Composite fundus photograph of a 11-year old male, showing attenuated retinal arterioles and near-confluent changes in the pigment epithelium in the mid-periphery.
Reprinted from Hardcastle et al., 2000.

PDE6A

Fundus photograph of a 34-year old female, showing vessel attenuation, perifoveal hyperpigmentation and atrophy, and optic disc pallor.

PDE6B

Composite fundus photograph of a 27-year old female, showing bone spicule pigmentation in the mid-periphery, vessel attenuation, and cystoid macular edema (confirmed by OCT).

PDE6G

Fundus photograph of a 26-year old male, showing attenuated retinal blood vessels, a pale optic disc, and RPE atrophy.
Reprinted from Dvir et al., 2010.[¥]

POMGNT1

59-year old female with typical RP-associated characteristics; including attenuation of the retina blood vessels, bone spicule-like deposits, and waxy pallor of the optic disc.
Reprinted from Wang et al., 2016.[§]

PRCD

Fundus photograph of a 24-year old male, showing bone spicule-like pigmentation, attenuated vessels, maculopathy and optic disc pallor.
Reprinted from Pach et al., 2013.[*]

PROM1

Fundus photograph of a 67-year old female, showing some pigment deposits, slightly attenuated vessels and RPE atrophy.

PRPF3
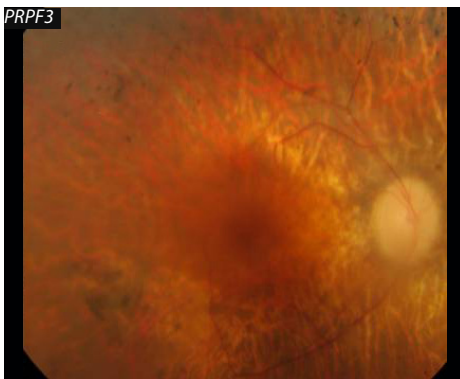
Fundus photograph of a 71-year old female, showing optic disc pallor, and bone spicule pigmentation in the mid-periphery.
Reprinted from Vaclavik et al., 2010.[*]

PRPF4

Relatively low quality fundus photograph of a 47-year old male, showing bone spicule pigmentation, attenuated vessels and pallor of the optic disc.
Reprinted from Chen et al., 2014 with permission from Oxford University Press.

121

PRPF6
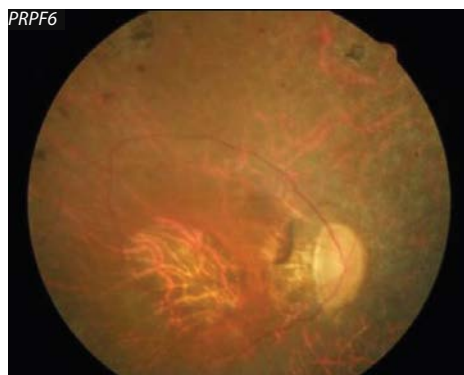
Fundus photograph of a 55-year old patient, showing attenuated retinal vessels, bone spicule pigmentation in the mid-periphery, macular atrophy, and waxy pallor of the optic disc.
Reprinted from Tanackovic et al., 2011.[¥]

PRPF8
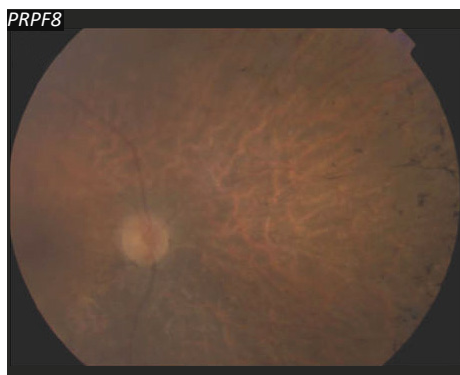
Relatively low quality fundus photograph of the nasal retina, showing optic disc pallor, vessel attenuation, and bone spicule pigmentation.
Reprinted from Ezquerra-Inchaust et al., 2017.[†]

PRPF31
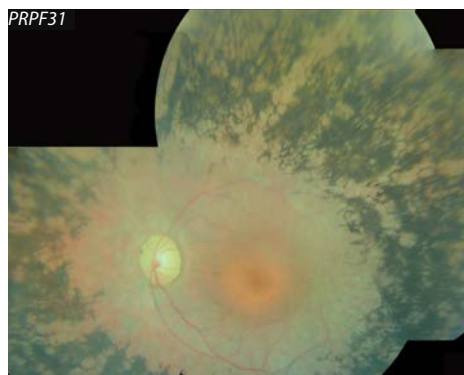
Composite fundus photograph of a 40-year old female, showing dense bone spicule pigmentation with **para-arteriolar sparing, attenuation of retinal vessels, and waxy pallor of the optic disc.**

PRPH2
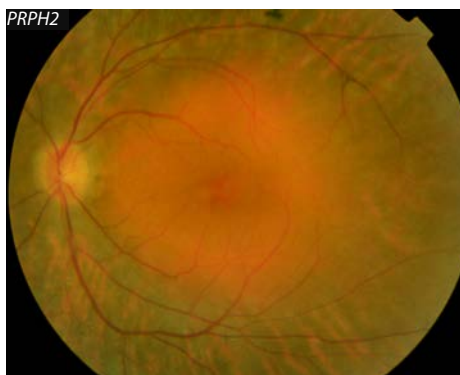
Fundus photograph of a 50-year old female, showing RPE atrophy, macular RPE alterations, and a couple of pigment deposits.

RBP3

Fundus photograph of a 56-year old male, showing attenuated vessels, bone spicule pigmentation, and macular involvement.

RDH12
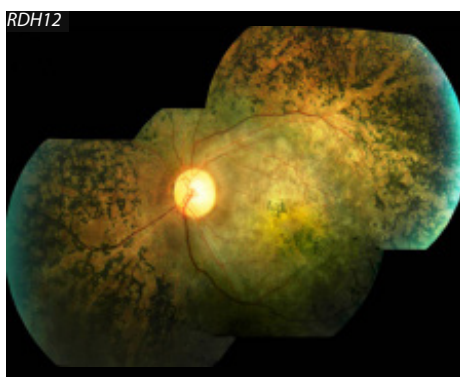
Composite fundus photograph of a 17-year old female, showing para-arteriolar sparing of the intraretinal pigmentation, macular hypopigmenation, and a pale optic disc.
Reprinted from Mackay et al., 2011.[*]

REEP6

Fundus photograph of a 40-year old male, showing macular deposits, attenuated vessels, and vascular sheathing.

RGR
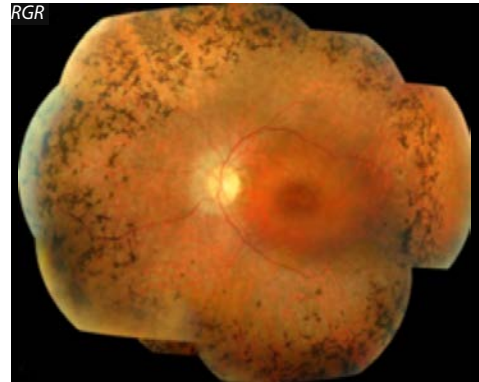
Composite fundus photograph of a 32-year old male, showing attenuated vessels, macular atrophy, mid-peripheral RPE atrophy and mid-peripheral bone spicule pigmentation.
Reprinted from Arno et al., 2015.[§]

RHO
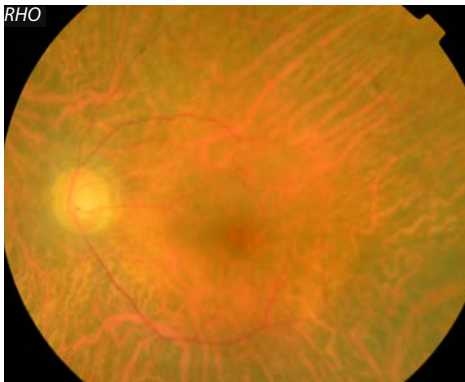
Fundus photograph of a 59-year old female with autosomal dominant RP, showing attenuated vessels and severe RPE atrophy.

RLBP1
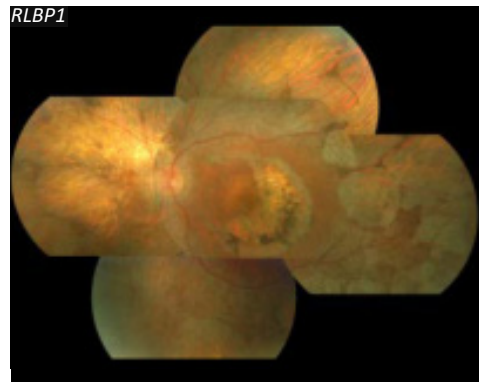
Relatively low quality composite fundus photograph of a 40-year old male, showing severe retinal atrophy.
Reprinted from Bocquet et al., 2013.[*]

RP1
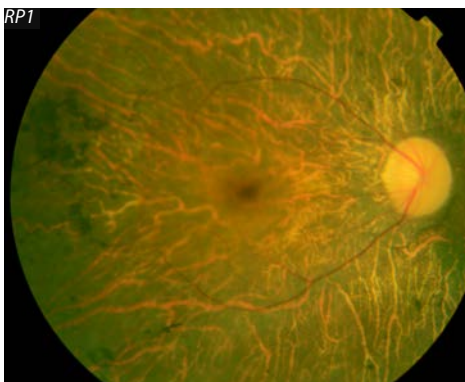
Fundus photograph of a 56-year old female, showing profound RPE atrophy, temporal pigment clumping, attenuated vessels, and a pale optic disc.

RP1L1
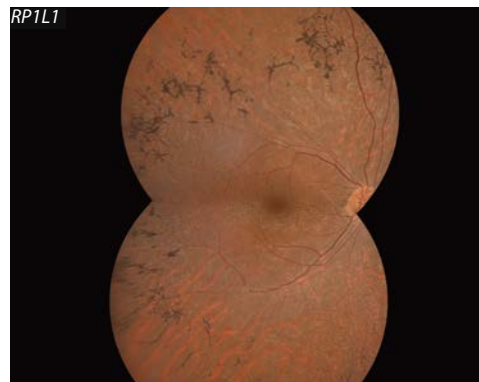
Fundus photograph of a 35-year old female, showing mid-peripheral bone spicule pigmentation, and attenuated vessels.

RP2
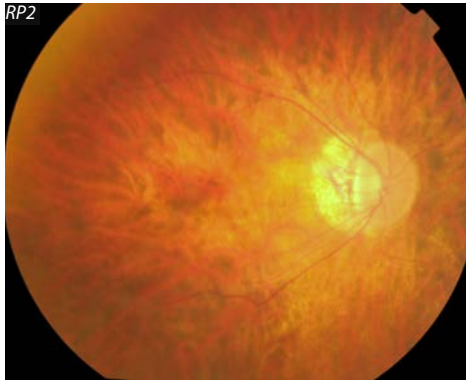
Fundus photograph of a 29-year old male, showing severely attenuated retinal vessels, and extensive RPE atrophy.

RPE65

Fundus photograph of a 13-year old female with autosomal recessive RP, showing attenuated retinal vessels, optic disc pallor, and relative absence of retinal hyperpigmentation.

RPGR
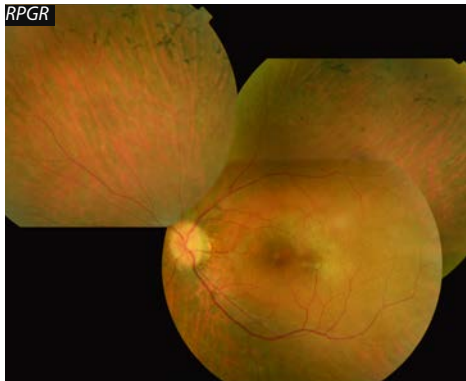
Composite fundus photograph of a 16-year old male, showing mid-peripheral bone spicule pigmentation, and mild attenuation of retinal vessels.

RPGRIP1
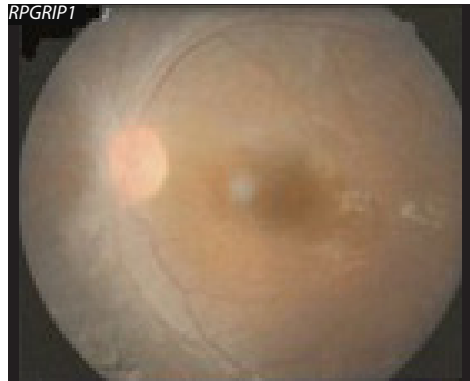
Low quality fundus photograph of a female patient, showing attenuated retinal vessels.
Reprinted from Huang et al., 2017.[‡]
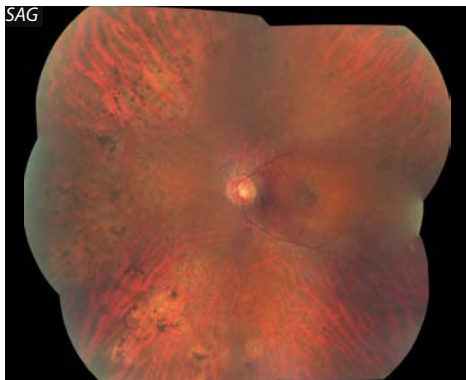
SAG

Composite fundus photograph of a 48-year old male, showing bone spicule pigmentation and patches of atrophy.
Reprinted from Sullivan et al., 2017.[§]

SAMD11
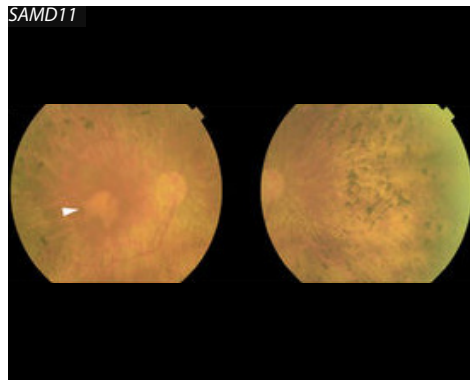
Relatively low quality fundus photographs of a 74-year old female, showing round- and bone spicule pigmentation, attenuated retinal vessels, and macular atrophy.
Reprinted from Corton et al., 2016.[†]

SLC7A14
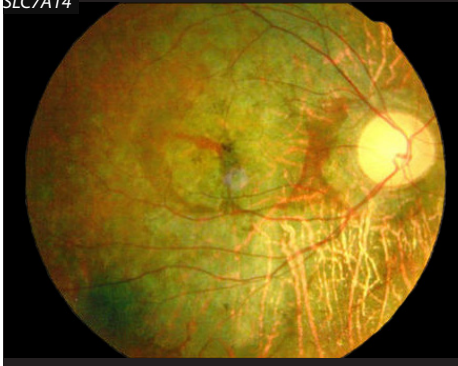
Fundus photograph of a male, showing extensive retinal atrophy, and waxy pallor of the optic disc.
Reprinted from Jin et al., 2014.[*]

SNRNP200

Fundus photograph of a 49-year old female, showing attenuated vessels, bone spicule pigmentation in the mid-periphery, atrophy of the RPE, waxy pallor of the optic disc, and a foveal reflection artefact.
Reprinted from Liu et al., 2012.[±]

SPATA7

Fundus photographs of a 55-year old male, showing pigmentary deposits, and attenuated retinal vessels.
Reprinted from Wang et al., 2009.[¥]

TOPORS

Fundus photograph of a 64-year old female, showing severe RPE atrophy, attenuated retinal vessels, pigment clumps and a waxy, pale optic disc.

TTC8
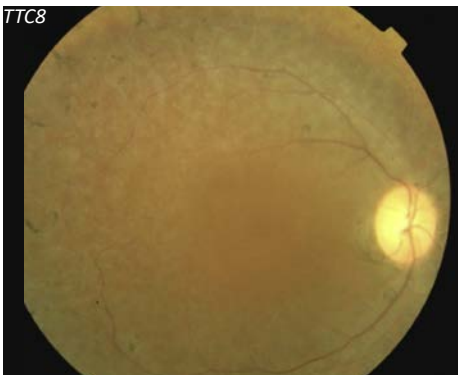
Fundus photograph of a male patient, showing waxy pallor of the optic disc, attenuated vessels, RPE atrophy and peripheral bone spicules.
Reprinted from Riazuddin et al., 2010. [¥]

TULP1
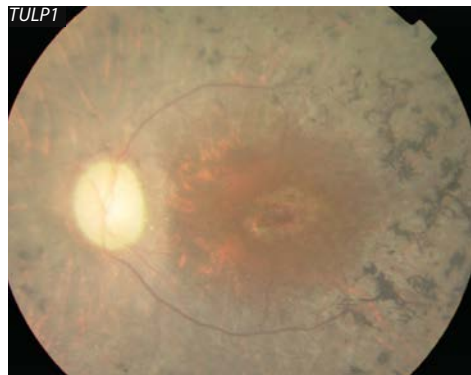
Fundus photograph of a 63-year old female, showing diffuse bone spicule pigmentation extending to the macular region, attenuated vessels, disc pallor, and RPE atrophy that includes the macula.
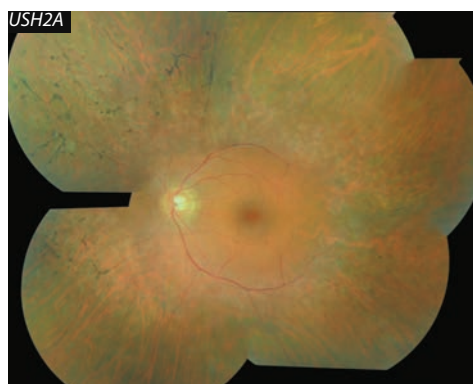
125

Composite fundus photograph of a 47-year old male, showing bone spicule pigmentation in the mid-periphery, and attenuated retinal vessels.
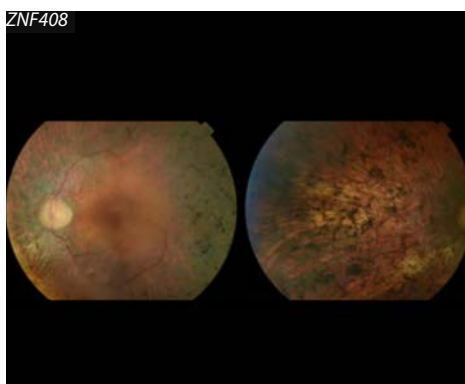
Fundus photographs of a 69-year old female, showing attenuated retinal vessels, extensive RPE atrophy, bone spicule pigmentation and a pale optic disc. Reprinted from Avila-Fernandez et al., 2015 with permission from Oxford University Press.
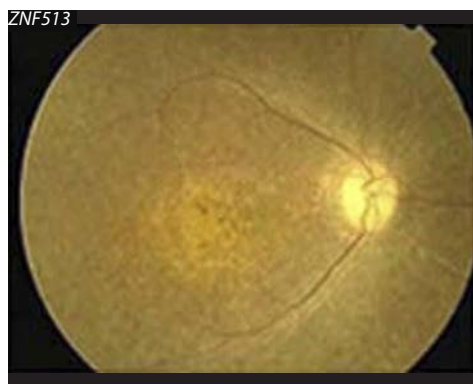
Low quality fundus photograph of a 32-year old male, showing waxy pallor of the optic disc, attenuated vessels, peripheral bone spicules, and atrophy of the RPE and macula.
Reprinted from Naz et al. 2010 with permission from Elsevier.

± Creative Commons Attribution (CC BY)
‡ Creative Commons Attribution 3.0 (CC BY 3.0)
† Creative Commons Attribution 4.0 (CC BY 4.0)
# Creative Commons Attribution-NonCommercial 4.0 (CC BY-NC 4.0)
* Creative Commons Attribution-NonCommercial-NoDerivs 3.0 (CC BY-NC-ND 3.0)
§ Creative Commons Attribution-NonCommercial-NoDerivs 4.0 (CC BY-NC-ND 4.0)
¥ Elsevier user license

References

1. Arno G, Agrawal SA, Eblimit A, et al. Mutations in REEP6 Cause Autosomal-Recessive Retinitis Pigmentosa. Am J Hum Genet 2016;99(6):1305-15.

2. Arno G, Carss KJ, Hull S, et al. Biallelic Mutation of ARHGEF18, Involved in the Determination of Epithelial Apicobasal Polarity, Causes Adult-Onset Retinal Degeneration. Am J Hum Genet 2017;100(2):334-42.

3. Arno G, Hull S, Carss K, et al. Reevaluation of the Retinal Dystrophy Due to Recessive Alleles of RGR With the Discovery of a Cis-Acting Mutation in CDHR1. Invest Ophthalmol Vis Sci 2016;57(11):4806-13.

4. Astuti GD, Arno G, Hull S, et al. Mutations in AGBL5, Encoding alpha-Tubulin Deglutamylase, Are ` 			Associated With Autosomal Recessive Retinitis Pigmentosa. Invest Ophthalmol Vis Sci 2016;57(14):6180-7.

5. Audo I, El Shamieh S, Mejecase C, et al. ARL2BP mutations account for 0.1% of autosomal recessive rod-cone dystrophies with the report of a novel splice variant. Clin Genet 2017;92(1):109-11.

6. Avila-Fernandez A, Perez-Carro R, Corton M, et al. Whole-exome sequencing reveals ZNF408 as a new gene associated with autosomal recessive retinitis pigmentosa with vitreal alterations. Hum Mol Genet 2015;24(14):4037-48.

7. Bocquet B, Marzouka NA, Hebrard M, et al. Homozygosity mapping in autosomal recessive retinitis pigmentosa families detects novel mutations. Mol Vis 2013;19:2487-500.

8. Bujakowska KM, Zhang Q, Siemiatkowska AM, et al. Mutations in IFT172 cause isolated retinal degeneration and Bardet-Biedl syndrome. Hum Mol Genet 2015;24(1):230-42.

9. Carrigan M, Duignan E, Humphries P, et al. A novel homozygous truncating GNAT1 mutation implicated in retinal degeneration. Br J Ophthalmol 2016;100(4):495-500.

10. Chen X, Liu Y, Sheng X, et al. PRPF4 mutations cause autosomal dominant retinitis pigmentosa. Hum Mol Genet 2014;23(11):2926-39.

11. Corton M, Avila-Fernandez A, Campello L, et al. Identification of the Photoreceptor Transcriptional Co-Repressor SAMD11 as Novel Cause of Autosomal Recessive Retinitis Pigmentosa. Sci Rep 2016;6:35370.

12. Dev Borman A, Ocaka LA, Mackay DS, et al. Early onset retinal dystrophy due to mutations in LRAT: molecular analysis and detailed phenotypic study. Invest Ophthalmol Vis Sci 2012;53(7):3927-38.

13. Dvir L, Srour G, Abu-Ras R, et al. Autosomal-recessive early-onset retinitis pigmentosa caused by a mutation in PDE6G, the gene encoding the gamma subunit of rod cGMP phosphodiesterase. Am J Hum Genet 2010;87(2):258-64.

14. El Shamieh S, Neuille M, Terray A, et al. Whole-exome sequencing identifies KIZ as a ciliary gene associated with autosomal-recessive rod-cone dystrophy. Am J Hum Genet 2014;94(4):625-33.

15. Ezquerra-Inchausti M, Barandika O, Anasagasti A, et al. High prevalence of mutations affecting the splicing process in a Spanish cohort with autosomal dominant retinitis pigmentosa. Sci Rep 2017;7:39652.

16. Friedman JS, Ray JW, Waseem N, et al. Mutations in a BTB-Kelch protein, KLHL7, cause autosomal-dominant retinitis pigmentosa. Am J Hum Genet 2009;84(6):792-800.

17. Hardcastle AJ, Thiselton DL, Zito I, et al. Evidence for a new locus for X-linked retinitis pigmentosa (RP23). Invest Ophthalmol Vis Sci 2000;41(8):2080-6.

18. Huang H, Wang Y, Chen H, et al. Targeted next generation sequencing identified novel mutations in RPGRIP1 associated with both retinitis pigmentosa and Leber's congenital amaurosis in unrelated Chinese patients. Oncotarget 2017;8(21):35176-83.

19. Huang XF, Huang F, Wu KC, et al. Genotype-phenotype correlation and mutation spectrum in a large cohort of patients with inherited retinal dystrophy revealed by next-generation sequencing. Genet Med 2015;17(4):271-8.

20. Hull S, Owen N, Islam F, et al. Nonsyndromic Retinal Dystrophy due to Bi-Allelic Mutations in the Ciliary Transport Gene IFT140. Invest Ophthalmol Vis Sci 2016;57(3):1053-62.

21. Jin ZB, Huang XF, Lv JN, et al. SLC7A14 linked to autosomal recessive retinitis pigmentosa. Nature Commun 2014;5:3517.

22. Khan MI, Kersten FF, Azam M, et al. CLRN1 mutations cause nonsyndromic retinitis pigmentosa. Ophthalmology 2011;118(7):1444-8.

23. Klevering BJ, Yzer S, Rohrschneider K, et al. Microarray-based mutation analysis of the ABCA4 (ABCR) gene in autosomal recessive cone-rod dystrophy and retinitis pigmentosa. Eur J Hum Genet 2004;12(12):1024-32.

24. Liu T, Jin X, Zhang X, et al. A novel missense SNRNP200 mutation associated with autosomal dominant retinitis pigmentosa in a Chinese family. PLoS One 2012;7(9):e45464.

25. Ku CA, Hull S, Arno G, et al. Detailed Clinical Phenotype and Molecular Genetic Findings in CLN3-Associated Isolated Retinal Degeneration. JAMA Ophthalmol 2017;135(7):749-60.

26. Mackay DS, Dev Borman A, Moradi P, et al. RDH12 retinopathy: novel mutations and phenotypic description. Mol Vis 2011;17:2706-16.

27. Naz S, Riazuddin SA, Li L, et al. A novel locus for autosomal recessive retinitis pigmentosa in a consanguineous Pakistani family maps to chromosome 2p. Am J Ophthalmol 2010;149(5):861-6.

28. Newman H, Blumen SC, Braverman I, et al. Homozygosity for a Recessive Loss-of-Function Mutation of the NRL Gene Is Associated With a Variant of Enhanced S-Cone Syndrome. Invest Ophthalmol Vis Sci 2016;57(13):5361-71.

29. Pach J, Kohl S, Gekeler F, Zobor D. Identification of a novel mutation in the PRCD gene causing autosomal recessive retinitis pigmentosa in a Turkish family. Mol Vis 2013;19:1350-5.

Chapter 2.1

127

30. Pierrache LHM, Kimchi A, Ratnapriya R, et al. Whole-Exome Sequencing Identifies Biallelic IDH3A Variants as a Cause of Retinitis Pigmentosa Accompanied by Pseudocoloboma. Ophthalmology 2017;124(7):992-1003.

31. Riazuddin SA, Iqbal M, Wang Y, et al. A splice-site mutation in a retina-specific exon of BBS8 causes nonsyndromic retinitis pigmentosa. Am J Hum Genet 2010;86(5):805-12.

32. Sato M, Nakazawa M, Usui T, et al. Mutations in the gene coding for guanylate cyclase-activating protein 2 (GUCA1B gene) in patients with autosomal dominant retinal dystrophies. Graefes Arch Clin Exp Ophthalmol 2005;243(3):235-42.

33. Siemiatkowska AM, van den Born LI, van Hagen PM, et al. Mutations in the mevalonate kinase (MVK) gene cause nonsyndromic retinitis pigmentosa. Ophthalmology 2013;120(12):2697-705.

34. Sullivan LS, Bowne SJ, Koboldt DC, et al. A Novel Dominant Mutation in SAG, the Arrestin-1 Gene, Is a Common Cause of Retinitis Pigmentosa in Hispanic Families in the Southwestern United States. Invest Ophthalmol Vis Sci 2017;58(5):2774-84.

35. Sullivan LS, Koboldt DC, Bowne SJ, et al. A dominant mutation in hexokinase 1 (HK1) causes retinitis pigmentosa. Invest Ophthalmol Vis Sci 2014;55(11):7147-58.

36. Tanackovic G, Ransijn A, Ayuso C, et al. A missense mutation in PRPF6 causes impairment of pre-mRNA splicing and autosomal-dominant retinitis pigmentosa. Am J Hum Genet 2011;88(5):643-9.

37. Vaclavik V, Gaillard MC, Tiab L, et al. Variable phenotypic expressivity in a Swiss family with autosomal dominant retinitis pigmentosa due to a T494M mutation in the PRPF3 gene. Mol Vis 2010;16:467-75.

38. Van Cauwenbergh C, Coppieters F, Roels D, et al. Mutations in Splicing Factor Genes Are a Major Cause of Autosomal Dominant Retinitis Pigmentosa in Belgian Families. PLoS One 2017;12(1):e0170038.

39. van Huet RA, Estrada-Cuzcano A, Banin E, et al. Clinical characteristics of rod and cone photoreceptor dystrophies in patients with mutations in the C8orf37 gene. Invest Ophthalmol Vis Sci 2013;54(7):4683-90.

40. Wang H, den Hollander AI, Moayedi Y, et al. Mutations in SPATA7 cause Leber congenital amaurosis and juvenile retinitis pigmentosa. Am J Hum Genet 2009;84(3):380-7.

41. Wang M, Gan D, Huang X, Xu G. Novel compound heterozygous mutations in CNGA1in a Chinese family affected with autosomal recessive retinitis pigmentosa by targeted sequencing. BMC Ophthalmol 2016;16:101.

42. Wang NH, Chen SJ, Yang CF, et al. Homozygosity Mapping and Whole-Genome Sequencing Links a Missense Mutation in POMGNT1 to Autosomal Recessive Retinitis Pigmentosa. Invest Ophthalmol Vis Sci 2016;57(8):3601-9.

43. Wang X, Wang H, Sun V, et al. Comprehensive molecular diagnosis of 179 Leber congenital amaurosis and juvenile retinitis pigmentosa patients by targeted next generation sequencing. J Med Genet 2013;50(10):674-88.

44. Xu M, Xie YA, Abouzeid H, et al. Mutations in the Spliceosome Component CWC27 Cause Retinal Degeneration with or without Additional Developmental Anomalies. Am J Hum Genet 2017;100(4):592-604.

45. Zuchner S, Dallman J, Wen R, et al. Whole-exome sequencing links a variant in DHDDS to retinitis pigmentosa. Am J Hum Genet 2011;88(2):201-6.

Appendix 4

See next page.

Overview of the genes associated with non-syndromic RP

Gene	Protein	Involved in
ABCA4	ATP-binding cassette protein A4	Visual (retinoid) cycle
ADGRA3	G protein-coupled receptor 125	Unknown
AGBL5	ATP/GTP binding protein-like 5	Ciliary structure and transport
AHI1	Abelson helper integration site 1 (Jouberin protein)	Ciliary structure and transport
ARHGEF18	Rho/Rac guanine nucleotide exchange factor 18	Cell-cell adhesion Retinal development
ARL2BP	ADP-ribosylation factor-like 2 binding protein	Ciliary transport
ARL3	ADP ribosylation factor-like GTPase 3	Ciliary structure and transport
ARL6	ADP-ribosylation factor-like 6	Ciliary transport
BBS1	BBS1 protein	Ciliary transport
BBS2	BBS2 protein	Ciliary transport
BBS9	Parathyroid hormone-responsive B1 protein	Ciliary transport
BEST1	Bestrophin 1	Retinal homeostasis
C2orf71	Chromosome 2 open reading frame 71	Ciliary structure and transport Retinal development
C8orf37	Chromosome 8 open reading frame 37	Ciliary structure, ciliary transport and/or ciliary gate
CA4	Carbonic anhydrase IV	Retinal homeostasis
CDHR1	Cadherin-related family member 1 (protocadherin 21)	Ciliary structure OS disc morphogenesis
CERKL	Ceramide kinase-like	Retinal homeostasis
CLN3	CLN3, battenin	Retinal homeostasis
CLRN1	Clarin 1	Ciliary structure
CNGA1	Rod cGMP-gated cation channel α-subunit	Phototransduction
CNGB1	Rod cGMP-gated cation channel β-subunit	Phototransduction
CRB1	Crumbs homologue 1	Cell-cell adhesion
CRX	Cone-rod otx-like photoreceptor homeobox transcription factor	Gene transcription
CWC27	CWC27 spliceosome associated protein homolog	RNA splicing
DHDDS	Dehydrodolichyl diphosphate synthetase	Phototransduction
DHX38	DEAH (Asp-Glu-Ala-His) box polypeptide 38	RNA splicing
EMC1	Endoplasmatic reticulum membrane protein complex subunit 1	Unknown
EYS	Eyes shut/spacemaker (*Drosophila*) homolog	Ciliary transport Interphotoreceptor matrix
FAM161A	Family with sequence similarity 161 member A	Ciliary structure and transport Retinal development
FSCN2	Retinal fascin homolog 2	Ciliary structure (OS disc morphology)

Function	Inheritance	Ref
Photoreceptor disc membrane flippase for all-trans-retinal.	Recessive	1-3
Unknown function	Recessive	4
Involved in posttranslational modifications of α- and β-tubulin (the main component of microtubules), cleaves branching point glutamates.	Recessive	5-8
Scaffold protein, for example in protein complex assembly or cell signaling processes, involved in ciliogenesis.	Recessive	9-11
Key component of tight junctions and adherence junctions.	Recessive	12
May play a role in trafficking of ciliary proteins and factors.	Recessive	13
Involved in ciliogenesis, interacts with RP2 and mediates localization of motor proteins for IFT.	Dominant	14-17
Binding site for BBSome, provides ciliary entrance to BBSome.	Recessive	18-20
BBSome component, involved in ciliary transport.	Recessive	18,20,21
BBSome component, involved in ciliary transport.	Recessive	20,22
BBSome component, involved in ciliary transport.	Recessive	20,23
Multifunctional protein in basolateral plasma membrane of RPE cells, transmembrane oligomeric chloride channels, probably involved in Ca2+ channels.	Recessive / Dominant	24,25
Protein localizes to primary cilia, exact function unknown.	Recessive	26,27
Protein localizes to basal body of connecting cilium in photoreceptor and RPE cells; exact function unclear.	Recessive	28,29
Membrane-anchored enzyme found in retinal choriocapillaris; Zn-containing enzyme that catalyze hydration of carbon dioxide; involved in pH regulation of retina and choriocapillaris.	Dominant	30
Involved in outer segment disc development, unlikely to be involved in cell-cell adhesion.	Recessive	31-33
Involved in neuronal cell survival and apoptosis in retinal ganglion cells.	Recessive	34
Involved in lysosomal function, likely located in the lysosomal/endosomal membrane.	Recessive	35,36
4-transmembrane protein with a possible role in hair cell and photoreceptor synapses, protein localizes to the plasma membrane of the connecting cilium.	Recessive	37-40
α-subunit of the cGMP-gated cation channel that enables sodium, calcium and magnesium influx in photoreceptor cells.	Recessive	41
β-subunit of the cGMP-gated cation channel that enables sodium, calcium and magnesium influx in photoreceptor cells.	Recessive	42-44
Localizes to the IS, transmembrane protein, adherent junctions between neighboring photoreceptors and photoreceptors and Müller cells.	Recessive / Dominant	45-48
Activator of retinal genes.	Dominant	49,50
May mediate protein-protein interactions during the assembly and rearrangement of spliceosome components.	Recessive	51
Enzyme in the dolichol synthesis pathway and dolichol is involved in biosynthesis of N-linked oligosaccharide chains on proteins such as rhodopsin.	Recessive	52
Putative RNA helicase involved in pre-RNA splicing.	Recessive	53
Subunit of the endoplasmic reticulum protein complex; possibly involved in protein folding and/or processing.	Recessive	4,54
Extracellular matrix protein; likely to have a role in the modeling of retinal architecture.	Recessive	55-57
Protein localizes to connecting cilium, basal body and daughter centriole; involved in development of retinal progenitors during embryogenesis; involved in microtubule stabilization.	Recessive	58-62
Photoreceptor-specific paralog of fascin which crosslinks and bundles f-actin; proposed to play a role in photoreceptor disc morphogenesis.	Dominant	63,64

Appendix 4. Continued

Gene	Protein	Involved in
GNAT1	G protein subunit alpha transducin 1	Phototransduction
GUCA1B	Guanylate cyclase activating protein 1B	Phototransduction
HK1	Hexokinase 1	Retinal metabolism
HGSNAT	Heparan-alpha-glucosaminide N-acetyltransferase	Retinal homeostasis
IDH3A	NAD(+)-specific isocitrate dehydrogenase 3 alpha	Retinal metabolism
IDH3B	NAD(+)-specific isocitrate dehydrogenase 3 beta	Retinal metabolism
IFT140	Intraflagellar transport 140 (*Chlamydomonas*) homolog	Ciliary transport Retinal development
IFT172	Intraflagellar transport 172	Ciliary transport Retinal development
IMPDH1	Inosine-5' monophosphate dehydrogenase type I	Nucleotide synthesis
IMPG2	Interphotoreceptor matrix proteoglycan 2	Interphotoreceptor matrix
KIAA1549	KIAA1549 protein	Unknown
KIZ	Kizuna centrosomal protein	Ciliary structure Cell division
KLHL7	Kelch-like 7 protein	Retinal homeostasis
LRAT	Lecithin retinol acetyltransferase	Visual (retinoid) cycle
MAK	Male germ-cell associated kinase	Ciliary structure
MERTK	Mer tyrosine kinase proto-oncogene	Retinal homeostasis
MVK	Mevalonate kinase	Retinal homeostasis
NEK2	NIMA (never in mitosis gene A)-related kinase 2	Retinal development
NEUROD1	Neuronal differentiation 1	Gene transcription
NR2E3	Nuclear receptor subfamily 2	Gene transcription
NRL	Neural retina leucine zipper	Gene transcription
OFD1	Oral-facial-digital syndrome 1 protein	Ciliary transport Retinal development
PANK2	Pantothenate kinase 2	Retinal metabolism
PDE6A	Rod cGMP-phosphodiesterase α-subunit	Phototransduction
PDE6B	Rod cGMP-phosphodiesterase β-subunit	Phototransduction
PDE6G	Rod cGMP-phosphodiesterase γ-subunit	Phototransduction
POMGNT1	O-linked mannose N-acetylglucosaminyltransferase 1 (beta 1,2-)	Ciliary structure and transport
PRCD	Progressive rod-cone degeneration protein	Unknown
PROM1	Prominin 1	Ciliary structure (OS disc morphology)
PRPF3	Precursor-mRNA processing factor 3	RNA splicing

Function	Inheritance	Ref
Rod-specific Gα transducin subunit, stimulates cyclic guanosine monophosphate (cGMP) phsphodiesterase (PDE).	Recessive	65,66
Calcium-binding protein that activates photoreceptor guanylate cyclases.	Dominant	67,68
Catalyzes the first step in glucose metabolism; the phosphorylation of glucose to glucose-6-phosphate.	Dominant	69,70
Acetylates heparin and heparan sulfate in lysosomes.	Recessive	71
Subunit of heterotetramer IDH3, catalyzes conversion of isocitrate to α-ketogluterate in the citric acid cycle in mitochondria.	Recessive	72
Subunit of heterotetramer IDH3, catalyzes conversion of isocitrate to α-ketogluterate in the citric acid cycle in mitochondria.	Recessive	73
Subunit of IFT-A complex, involved in photoreceptor development (ciliogenesis).	Recessive	74-77
Subunit of IFT-B complex, involved in transition of anterograde to retrograde transport, involved in ciliogenesis.	Recessive	78-80
Catalyzes the oxidation of inosine monophosphate to form xanthosine monophosphate during guanine synthesis.	Dominant / Recessive	81,82
Component of the retinal extracellular matrix; involved in the organization of the interphotoreceptor matrix, and photoreceptor OS growth and maintenance.	Recessive	83-85
May fuse with oncogene *BRAF*, which leads to activation of the mitogen-activated protein kinase pathway, function unknown.	Recessive	4
Protein localizes to basal body, stabilizes the ciliary centrosomes during cell division, may be involved in ciliary transport.	Recessive	86,87
Involved in the the ubiquitin-proteasome system mediated protein degradation.	Dominant	88-90
Isomerization of all-trans-retinol to all-trans-retinylester.	Recessive	91,92
Involved in regulation of ciliogenesis and regulation of cilium length.	Recessive	93-95
RPE receptor involved in outer segment phagocytosis.	Recessive	96
Peroxisomal enzyme; a key early enzyme in isoprenoid and sterol synthesis.	Recessive	97
Plays an important role in regulation of cell cycle progression through localization to the centrosomes and interaction with microtubules.	Recessive	98
Basic helix-loop-helix transcription factor.	Recessive	99
Ligand-dependent transcription factor.	Recessive / Dominant	100-102
Retinal transcription factor which interacts with CRX, promotes transcription of rhodopsin and other retinal genes, and is required for rod photoreceptor development.	Recessive / Dominant	103,104
Protein localizes to basal body of connecting cilium and centrosome, recruits IFT88, involved in ciliogenesis.	X-linked	105-110
Enzyme involved in the biosynthesis of CoA, metabolism of neurotransmitters and glutathione, fatty acid synthesis and degradation.	Recessive	111
Rod cGMP-phosphodiesterase hydrolyses cGMP to 5'-GMP.	Recessive	112,113
Rod cGMP-phosphodiesterase hydrolyses cGMP to 5'-GMP.	Recessive	112,113
Inhibitory subunit of cGMP phosphodiesterase.	Recessive	114
Localized at basal body and involved in membranogenesis and eye morphogenesis.	Recessive	115-117
Localizes to the photoreceptor OS, function unknown.	Recessive	118,119
5-transmembrane glycoprotein associated with plasma membrane evaginations in rod outer segments; exact function unknown.	Recessive	120,121
Member of the U4/U6-U5 tri-snRNP particle complex (spliceosome).	Dominant	122,123

Appendix 4. Continued

Gene	Protein	Involved in
PRPF31	Precursor-mRNA processing factor 31	RNA splicing
PRPF4	Precursor-mRNA processing factor 4	RNA splicing
PRPF6	Precursor-mRNA processing factor 6	RNA splicing
PRPF8	Precursor-mRNA processing factor 8	RNA splicing
PRPH2	Peripherin-2	Ciliary structure (OS [disc] morphology)
RBP3	Retinol binding protein 3	Visual (retinoid) cycle
RDH12	Retinol dehydrogenase 12	Visual (retinoid) cycle
REEP6	Receptor accessory protein	Retinal homeostasis
RGR	RPE-vitamin A G-protein coupled receptor	Visual (retinoid) cycle
RHO	Rhodopsin	Phototransduction
RLBP1	Retinaldehyde binding protein	Visual (retinoid) cycle
ROM1	Rod outer segment protein 1	Ciliary structure (OS disc morphology)
RP1	Retinitis pigmentosa 1, axonemal microtubule-associated protein	Ciliary structure
RP1L1	Retinitis pigmentosa 1-like protein 1	Ciliary structure and transport
RP2	Plasma membrane associated protein	Ciliary transport
RP9	PIM1-kinase associated protein 1	RNA splicing
RPE65	Vitamin A trans-cis isomerase	Visual (retinoid) cycle
RPGR	Retinitis pigmentosa GTPase regulator	Ciliary transport
RPGRIP1	RP GTPase regulator-interacting protein 1	Ciliary transport
SAG	Arrestin	Phototransduction
SAMD11	Sterile alpha motif domain containing 11	Gene transcription
SEMA4A	Semaphorin 4A (semaphorin B)	Retinal development
SLC7A14	Solute carrier family 7 member 14	Retinal development
SNRNP200	Small nuclear ribonucleoprotein 200kDa (U5)	RNA splicing
SPATA7	Spermatogenesis-associated protein 7	Ciliary transport
TOPORS	Topoisomerase I binding arginine/serine rich protein	Ciliary structure or transport Photoreceptor development
TTC8	Tetratricopeptide repeat domain 8	Ciliary transport
TULP1	Tubby-like protein 1	Ciliary transport
USH2A	Usherin	Ciliary structure and transport
ZNF408	Zinc finger protein 408	Retinal development
ZNF513	Zinc finger protein 513	Retinal development

Abbreviations: cGMP: cyclic guanosine monophosphate, IFT: intraflagellar transport, IS: inner segment, OS: outer segment, RNA: ribonucleic acid, RPE: retinal pigment epithelium.

Function	Inheritance	Ref
Member of the U4/U6-U5 tri-snRNP particle complex (spliceosome).	Dominant	124
Member of the U4/U6-U5 tri-snRNP particle complex (spliceosome).	Dominant	125
Member of the U4/U6-U5 tri-snRNP particle complex (spliceosome).	Dominant	126
Member of the U4/U6-U5 tri-snRNP particle complex (spliceosome).	Dominant	127
Transmembrane glycoprotein involved in OS development, localized at the peripheral rim of rod OS discs, and the 'closed' rim of cone OS lamellae.	Dominant / Digenic	128-131
Binds and transports retinoids in the interphotoreceptor matrix between the RPE and photoreceptors.	Recessive	132,133
Reduction of all-*trans*-retinal to all-*trans*-retinol.	Dominant	134,135
Involved in trafficking of cargo via a subset of Clathrin-coated vesicles to selected membrane sites in retinal rod photoreceptors.	Recessive	136-138
Binds all-*trans* retinal which light converts to 11-*cis* retinal in the RPE.	Recessive	139
G-protein coupled photon receptor; activation of transducin after photoactivation.	Dominant Recessive	140,141
11-cis-retinaldehyde carrier in visual cycle.	Recessive	142
Essential for disk morphogenesis; may also function as an adhesion molecule involved in stabilization and compaction of outer segment disks or in maintenance of rim curvature.	Dominant / Digenic	130,143
Localizes to the connecting cilium in rods and cones (OS axoneme), involved in regulation of ciliary length and stability, involved in localization of OS discs.	Recessive / Dominant	144-148
Same localization as RP1, synergist of RP1, involved in OS morphogenesis.	Recessive	149-151
Localizes to the plasma membrane of the connecting cilium of photoreceptors and RPE, interaction with ARL3, involved in ciliary transport.	X-linked	15,152-154
Has a role in pre-mRNA splicing and interacts with a U2-complex splice factor.	Dominant	155
Isomerization of all-trans-retinylester to 11-cis-retinol.	Recessive Dominant?	91
Localizes to the basal body and axoneme, involved in opsin transport, mediates ciliary transport.	X-linked	153, 156-158
Localizes to the axoneme, anchors RPGR to the axoneme.	Recessive	158-161
Arrestin binds to activated rhodopsin (metarhodopsin II) to stop the activation of transducin.	Recessive	140,162,163
Localizes to the nuclear layers of the retina, interacts with *CRX*.	Recessive	164
Involved in neuronal development and/or immune response; enhances T-cell activation.	Dominant	165,166
Potential cationic transporter protein with an unknown ligand.	Recessive	167
Member of the U4/U6-U5 tri-snRNP particle complex (spliceosome).	Dominant	168,169
Localizes to the connecting cilium, interacts with RPGRIP1.	Recessive	170,171
Localizes to the basal body of the connecting cilium, may play a key role in regulating primary cilia-dependent photoreceptor development and function.	Dominant	172,173
BBSome component, involved in ciliary transport.	Recessive	20,174,175
Localizes to the photoreceptor cytoplasm, possibly involved in transport of rhodopsin from IS to OS.	Recessive	176-179
Transmembrane adhesion protein; involved in Usher interactome, provides docking side for IFT cargo, extracellular strands between connecting cilium and calycal process.	Recessive	180-183
DNA binding protein that interacts with other proteins.	Recessive	184-186
Possible transcriptional regulator involved in retinal development.	Recessive	187

Chapter 2.1

References

1. Allikmets R, Singh N, Sun H, et al. A photoreceptor cell-specific ATP-binding transporter gene (ABCR) is mutated in recessive Stargardt macular dystrophy. *Nat Genet.* 1997;15(3):236-246.
2. Weng J, Mata NL, Azarian SM, Tzekov RT, Birch DG, Travis GH. Insights into the function of Rim protein in photoreceptors and etiology of Stargardt's disease from the phenotype in abcr knockout mice. *Cell.* 1999;98(1):13-23.
3. Sun H, Nathans J. Mechanistic studies of ABCR, the ABC transporter in photoreceptor outer segments responsible for autosomal recessive Stargardt disease. *J Bioenerg Biomembr.* 2001;33(6):523-530.
4. Abu-Safieh L, Alrashed M, Anazi S, et al. Autozygome-guided exome sequencing in retinal dystrophy patients reveals pathogenetic mutations and novel candidate disease genes. *Genome Res.* 2013;23(2):236-247.
5. Astuti GD, Arno G, Hull S, et al. Mutations in AGBL5, Encoding alpha-Tubulin Deglutamylase, Are Associated With Autosomal Recessive Retinitis Pigmentosa. *Invest Ophthalmol Vis Sci.* 2016;57(14):6180-6187.
6. Branham K, Matsui H, Biswas P, et al. Establishing the involvement of the novel gene AGBL5 in retinitis pigmentosa by whole genome sequencing. *Physiol Genomics.* 2016;48(12):922-927.
7. Kastner S, Thiemann IJ, Dekomien G, et al. Exome Sequencing Reveals AGBL5 as Novel Candidate Gene and Additional Variants for Retinitis Pigmentosa in Five Turkish Families. *Invest Ophthalmol Vis Sci.* 2015;56(13):8045-8053.
8. Patel N, Aldahmesh MA, Alkuraya H, et al. Expanding the clinical, allelic, and locus heterogeneity of retinal dystrophies. *Genet Med.* 2016;18(6):554-562.
9. Huang XF, Huang F, Wu KC, et al. Genotype-phenotype correlation and mutation spectrum in a large cohort of patients with inherited retinal dystrophy revealed by next-generation sequencing. *Genet Med.* 2015;17(4):271-278.
10. Nguyen TT, Hull S, Roepman R, et al. Missense mutations in the WD40 domain of AHI1 cause non-syndromic retinitis pigmentosa. *J Med Genet.* 2017.
11. Dixon-Salazar T, Silhavy JL, Marsh SE, et al. Mutations in the AHI1 gene, encoding jouberin, cause Joubert syndrome with cortical polymicrogyria. *Am J Hum Genet.* 2004;75(6):979-987.
12. Arno G, Carss KJ, Hull S, et al. Biallelic Mutation of ARHGEF18, Involved in the Determination of Epithelial Apicobasal Polarity, Causes Adult-Onset Retinal Degeneration. *Am J Hum Genet.* 2017;100(2):334-342.
13. Davidson AE, Schwarz N, Zelinger L, et al. Mutations in ARL2BP, Encoding ADP-Ribosylation-Factor-Like 2 Binding Protein, Cause Autosomal-Recessive Retinitis Pigmentosa. *Am J Hum Genet.* 2013.
14. Schwarz N, Lane A, Jovanovich K, et al. Arl3 and RP2 regulate the trafficking of ciliary tip kinesins. *Hum Mol Genet.* 2017;26(13):2480-2492.
15. Hanke-Gogokhia C, Wu Z, Gerstner CD, Frederick JM, Zhang H, Baehr W. Arf-like Protein 3 (ARL3) Regulates Protein Trafficking and Ciliogenesis in Mouse Photoreceptors. *The Journal of biological chemistry.* 2016;291(13):7142-7155.
16. Strom SP, Clark MJ, Martinez A, et al. De Novo Occurrence of a Variant in ARL3 and Apparent Autosomal Dominant Transmission of Retinitis Pigmentosa. *PLoS One.* 2016;11(3):e0150944.
17. Wright ZC, Singh RK, Alpino R, Goldberg AF, Sokolov M, Ramamurthy V. ARL3 regulates trafficking of prenylated phototransduction proteins to the rod outer segment. *Hum Mol Genet.* 2016;25(10):2031-2044.
18. Nachury MV, Loktev AV, Zhang Q, et al. A core complex of BBS proteins cooperates with the GTPase Rab8 to promote ciliary membrane biogenesis. *Cell.* 2007;129(6):1201-1213.
19. Mourao A, Nager AR, Nachury MV, Lorentzen E. Structural basis for membrane targeting of the BBSome by ARL6. *Nat Struct Mol Biol.* 2014;21(12):1035-1041.
20. Mourao A, Christensen ST, Lorentzen E. The intraflagellar transport machinery in ciliary signaling. *Curr Opin Struct Biol.* 2016;41:98-108.
21. Estrada-Cuzcano A, Koenekoop RK, Senechal A, et al. BBS1 mutations in a wide spectrum of phenotypes ranging from nonsyndromic retinitis pigmentosa to Bardet-Biedl syndrome. *Arch Ophthalmol.* 2012;130(11):1425-1432.
22. Shevach E, Ali M, Mizrahi-Meissonnier L, et al. Association between missense mutations in the BBS2 gene and nonsyndromic retinitis pigmentosa. *JAMA Ophthalmol.* 2015;133(3):312-318.
23. Abu-Safieh L, Al-Anazi S, Al-Abdi L, et al. In search of triallelism in Bardet-Biedl syndrome. *Eur J Hum Genet.* 2012;20(4):420-427.
24. Davidson AE, Millar ID, Urquhart JE, et al. Missense mutations in a retinal pigment epithelium protein, bestrophin-1, cause retinitis pigmentosa. *Am J Hum Genet.* 2009;85(5):581-592.
25. Marmorstein AD, Marmorstein LY, Rayborn M, Wang X, Hollyfield JG, Petrukhin K. Bestrophin, the product of the Best vitelliform macular dystrophy gene (VMD2), localizes to the basolateral plasma membrane of the retinal pigment epithelium. *Proc Natl Acad Sci U S A.* 2000;97(23):12758-12763.
26. Collin RW, Safieh C, Littink KW, et al. Mutations in C2ORF71 cause autosomal-recessive retinitis pigmentosa. *Am J Hum Genet.* 2010;86(5):783-788.
27. Nishimura DY, Baye LM, Perveen R, et al. Discovery and functional analysis of a retinitis pigmentosa gene, C2ORF71. *Am J Hum Genet.* 2010;86(5):686-695.
28. Estrada-Cuzcano A, Neveling K, Kohl S, et al. Mutations in C8orf37, encoding a ciliary protein, are associated with autosomal-recessive retinal dystrophies with early macular involvement. *Am J Hum Genet.* 2012;90(1):102-109.
29. van Huet RA, Estrada-Cuzcano A, Banin E, et al. Clinical characteristics of rod and cone photoreceptor dystrophies in patients with mutations in the C8orf37 gene. *Invest Ophthalmol Vis Sci.* 2013;54(7):4683-4690.

30. Yang Z, Alvarez BV, Chakarova C, et al. Mutant carbonic anhydrase 4 impairs pH regulation and causes retinal photoreceptor degeneration. *Hum Mol Genet.* 2005;14(2):255-265.

31. Duncan JL, Roorda A, Navani M, et al. Identification of a novel mutation in the CDHR1 gene in a family with recessive retinal degeneration. *Arch Ophthalmol.* 2012;130(10):1301-1308.

32. Riera M, Navarro R, Ruiz-Nogales S, et al. Whole exome sequencing using Ion Proton system enables reliable genetic diagnosis of inherited retinal dystrophies. *Sci Rep.* 2017;7:42078.

33. Goldberg AF, Moritz OL, Williams DS. Molecular basis for photoreceptor outer segment architecture. *Prog Retin Eye Res.* 2016;55:52-81.

34. Bornancin F, Mechtcheriakova D, Stora S, et al. Characterization of a ceramide kinase-like protein. *Biochim Biophys Acta.* 2005;1687(1-3):31-43.

35. Phillips SN, Benedict JW, Weimer JM, Pearce DA. CLN3, the protein associated with batten disease: structure, function and localization. *J Neurosci Res.* 2005;79(5):573-583.

36. Ratajczak E, Petcherski A, Ramos-Moreno J, Ruonala MO. FRET-assisted determination of CLN3 membrane topology. *PLoS One.* 2014;9(7):e102593.

37. Adato A, Vreugde S, Joensuu T, et al. USH3A transcripts encode clarin-1, a four-transmembrane-domain protein with a possible role in sensory synapses. *Eur J Hum Genet.* 2002;10(6):339-350.

38. Joensuu T, Hamalainen R, Yuan B, et al. Mutations in a novel gene with transmembrane domains underlie Usher syndrome type 3. *Am J Hum Genet.* 2001;69(4):673-684.

39. Khan MI, Kersten FF, Azam M, et al. CLRN1 mutations cause nonsyndromic retinitis pigmentosa. *Ophthalmology.* 2011;118(7):1444-1448.

40. Zallocchi M, Meehan DT, Delimont D, et al. Localization and expression of clarin-1, the Clrn1 gene product, in auditory hair cells and photoreceptors. *Hear Res.* 2009;255(1-2):109-120.

41. Dhallan RS, Macke JP, Eddy RL, et al. Human rod photoreceptor cGMP-gated channel: amino acid sequence, gene structure, and functional expression. *J Neurosci.* 1992;12(8):3248-3256.

42. Batra-Safferling R, Abarca-Heidemann K, Korschen HG, et al. Glutamic acid-rich proteins of rod photoreceptors are natively unfolded. *J Biol Chem.* 2006;281(3):1449-1460.

43. Korschen HG, Beyermann M, Muller F, et al. Interaction of glutamic-acid-rich proteins with the cGMP signalling pathway in rod photoreceptors. *Nature.* 1999;400(6746):761-766.

44. Poetsch A, Molday LL, Molday RS. The cGMP-gated channel and related glutamic acid-rich proteins interact with peripherin-2 at the rim region of rod photoreceptor disc membranes. *J Biol Chem.* 2001;276(51):48009-48016.

45. Pellikka M, Tanentzapf G, Pinto M, et al. Crumbs, the Drosophila homologue of human CRB1/RP12, is essential for photoreceptor morphogenesis. *Nature.* 2002;416(6877):143-149.

46. den Hollander AI, ten Brink JB, de Kok YJ, et al. Mutations in a human homologue of Drosophila crumbs cause retinitis pigmentosa (RP12). *Nat Genet.* 1999;23(2):217-221.

47. Quinn PM, Pellissier LP, Wijnholds J. The CRB1 Complex: Following the Trail of Crumbs to a Feasible Gene Therapy Strategy. *Front Neurosci.* 2017;11:175.

48. McKay GJ, Clarke S, Davis JA, Simpson DA, Silvestri G. Pigmented paravenous chorioretinal atrophy is associated with a mutation within the crumbs homolog 1 (CRB1) gene. *Invest Ophthalmol Vis Sci.* 2005;46(1):322-328.

49. Sohocki MM, Sullivan LS, Mintz-Hittner HA, et al. A range of clinical phenotypes associated with mutations in CRX, a photoreceptor transcription-factor gene. *Am J Hum Genet.* 1998;63(5):1307-1315.

50. Swaroop A, Wang QL, Wu W, et al. Leber congenital amaurosis caused by a homozygous mutation (R90W) in the homeodomain of the retinal transcription factor CRX: direct evidence for the involvement of CRX in the development of photoreceptor function. *Hum Mol Genet.* 1999;8(2):299-305.

51. Xu M, Xie YA, Abouzeid H, et al. Mutations in the Spliceosome Component CWC27 Cause Retinal Degeneration with or without Additional Developmental Anomalies. *Am J Hum Genet.* 2017;100(4):592-604.

52. Zelinger L, Banin E, Obolensky A, et al. A missense mutation in DHDDS, encoding dehydrodolichyl diphosphate synthase, is associated with autosomal-recessive retinitis pigmentosa in Ashkenazi Jews. *Am J Hum Genet.* 2011;88(2):207-215.

53. Ajmal M, Khan MI, Neveling K, et al. A missense mutation in the splicing factor gene DHX38 is associated with early-onset retinitis pigmentosa with macular coloboma. *J Med Genet.* 2014;51(7):444-448.

54. Harel T, Yesil G, Bayram Y, et al. Monoallelic and Biallelic Variants in EMC1 Identified in Individuals with Global Developmental Delay, Hypotonia, Scoliosis, and Cerebellar Atrophy. *Am J Hum Genet.* 2016;98(3):562-570.

55. Collin RW, Littink KW, Klevering BJ, et al. Identification of a 2 Mb human ortholog of Drosophila eyes shut/spacemaker that is mutated in patients with retinitis pigmentosa. *Am J Hum Genet.* 2008;83(5):594-603.

56. Lu Z, Hu X, Liu F, et al. Ablation of EYS in zebrafish causes mislocalisation of outer segment proteins, F-actin disruption and cone-rod dystrophy. *Sci Rep.* 2017;7:46098.

57. Alfano G, Kruczek PM, Shah AZ, et al. EYS Is a Protein Associated with the Ciliary Axoneme in Rods and Cones. *PLoS One.* 2016;11(11):e0166397.

58. Bandah-Rozenfeld D, Mizrahi-Meissonnier L, Farhy C, et al. Homozygosity mapping reveals null mutations in FAM161A as a cause of autosomal-recessive retinitis pigmentosa. *Am J Hum Genet.* 2010;87(3):382-391.

59. Langmann T, Di Gioia SA, Rau I, et al. Nonsense mutations in FAM161A cause RP28-associated recessive retinitis pigmentosa.

Am J Hum Genet. 2010;87(3):376-381.

60. Di Gioia SA, Letteboer SJ, Kostic C, et al. FAM161A, associated with retinitis pigmentosa, is a component of the cilia-basal body complex and interacts with proteins involved in ciliopathies. *Hum Mol Genet.* 2012;21(23):5174-5184.

61. Zach F, Stohr H. FAM161A, a novel centrosomal-ciliary protein implicated in autosomal recessive retinitis pigmentosa. *Adv Exp Med Biol.* 2014;801:185-190.

62. Zach F, Grassmann F, Langmann T, Sorusch N, Wolfrum U, Stohr H. The retinitis pigmentosa 28 protein FAM161A is a novel ciliary protein involved in intermolecular protein interaction and microtubule association. *Hum Mol Genet.* 2012;21(21):4573-4586.

63. Saishin Y, Ishikawa R, Ugawa S, et al. Retinal fascin: functional nature, subcellular distribution, and chromosomal localization. *Invest Ophthalmol Vis Sci.* 2000;41(8):2087-2095.

64. Tubb BE, Bardien-Kruger S, Kashork CD, et al. Characterization of human retinal fascin gene (FSCN2) at 17q25: close physical linkage of fascin and cytoplasmic actin genes. *Genomics.* 2000;65(2):146-156.

65. Mejecase C, Laurent-Coriat C, Mayer C, et al. Identification of a Novel Homozygous Nonsense Mutation Confirms the Implication of GNAT1 in Rod-Cone Dystrophy. *PLoS One.* 2016;11(12):e0168271.

66. Carrigan M, Duignan E, Humphries P, Palfi A, Kenna PF, Farrar GJ. A novel homozygous truncating GNAT1 mutation implicated in retinal degeneration. *Br J Ophthalmol.* 2016;100(4):495-500.

67. Payne AM, Downes SM, Bessant DA, et al. Genetic analysis of the guanylate cyclase activator 1B (GUCA1B) gene in patients with autosomal dominant retinal dystrophies. *J Med Genet.* 1999;36(9):691-693.

68. Sato M, Nakazawa M, Usui T, Tanimoto N, Abe H, Ohguro H. Mutations in the gene coding for guanylate cyclase-activating protein 2 (GUCA1B gene) in patients with autosomal dominant retinal dystrophies. *Graefe's Archive for Clinical and Experimental Ophthalmology = Albrecht Von Graefes Archiv fur Klinische und Experimentelle Ophthalmologie.* 2005;243(3):235-242.

69. Wang F, Wang Y, Zhang B, et al. A missense mutation in HK1 leads to autosomal dominant retinitis pigmentosa. *Invest Ophthalmol Vis Sci.* 2014;55(11):7159-7164.

70. Sullivan LS, Koboldt DC, Bowne SJ, et al. A dominant mutation in hexokinase 1 (HK1) causes retinitis pigmentosa. *Invest Ophthalmol Vis Sci.* 2014;55(11):7147-7158.

71. Haer-Wigman L, Newman H, Leibu R, et al. Non-syndromic retinitis pigmentosa due to mutations in the mucopolysaccharidosis type IIIC gene, heparan-alpha-glucosaminide N-acetyltransferase (HGSNAT). *Hum Mol Genet.* 2015;24(13):3742-3751.

72. Pierrache LHM, Kimchi A, Ratnapriya R, et al. Whole-Exome Sequencing Identifies Biallelic IDH3A Variants as a Cause of Retinitis Pigmentosa Accompanied by Pseudocoloboma. *Ophthalmology.* 2017;124(7):992-1003.

73. Hartong DT, Dange M, McGee TL, Berson EL, Dryja TP, Colman RF. Insights from retinitis pigmentosa into the roles of isocitrate dehydrogenases in the Krebs cycle. *Nat Genet.* 2008;40(10):1230-1234.

74. Absalon S, Blisnick T, Kohl L, et al. Intraflagellar transport and functional analysis of genes required for flagellum formation in trypanosomes. *Molecular biology of the cell.* 2008;19(3):929-944.

75. Miller KA, Ah-Cann CJ, Welfare MF, et al. Cauli: a mouse strain with an Ift140 mutation that results in a skeletal ciliopathy modelling Jeune syndrome. *PLoS genetics.* 2013;9(8):e1003746.

76. Hull S, Owen N, Islam F, et al. Nonsyndromic Retinal Dystrophy due to Bi-Allelic Mutations in the Ciliary Transport Gene IFT140. *Invest Ophthalmol Vis Sci.* 2016;57(3):1053-1062.

77. Xu M, Yang L, Wang F, et al. Mutations in human IFT140 cause non-syndromic retinal degeneration. *Hum Genet.* 2015;134(10):1069-1078.

78. Bujakowska KM, Zhang Q, Siemiatkowska AM, et al. Mutations in IFT172 cause isolated retinal degeneration and Bardet-Biedl syndrome. *Hum Mol Genet.* 2015;24(1):230-242.

79. Taschner M, Bhogaraju S, Lorentzen E. Architecture and function of IFT complex proteins in ciliogenesis. *Differentiation.* 2012;83(2):S12-22.

80. Taschner M, Weber K, Mourao A, et al. Intraflagellar transport proteins 172, 80, 57, 54, 38, and 20 form a stable tubulin-binding IFT-B2 complex. *EMBO J.* 2016;35(7):773-790.

81. Bowne SJ, Sullivan LS, Blanton SH, et al. Mutations in the inosine monophosphate dehydrogenase 1 gene (IMPDH1) cause the RP10 form of autosomal dominant retinitis pigmentosa. *Hum Mol Genet.* 2002;11(5):559-568.

82. Ali S, Khan SY, Naeem MA, et al. Phenotypic variability associated with the D226N allele of IMPDH1. *Ophthalmology.* 2015;122(2):429-431.

83. Acharya S, Foletta VC, Lee JW, et al. SPACRCAN, a novel human interphotoreceptor matrix hyaluronan-binding proteoglycan synthesized by photoreceptors and pinealocytes. *J Biol Chem.* 2000;275(10):6945-6955.

84. Foletta VC, Nishiyama K, Rayborn ME, Shadrach KG, Young WS, 3rd, Hollyfield JG. SPACRCAN in the developing retina and pineal gland of the rat: spatial and temporal pattern of gene expression and protein synthesis. *J Comp Neurol.* 2001;435(3):354-363.

85. Bandah-Rozenfeld D, Collin RW, Banin E, et al. Mutations in IMPG2, encoding interphotoreceptor matrix proteoglycan 2, cause autosomal-recessive retinitis pigmentosa. *Am J Hum Genet.* 2010;87(2):199-208.

86. El Shamieh S, Neuille M, Terray A, et al. Whole-exome sequencing identifies KIZ as a ciliary gene associated with autosomal-recessive rod-cone dystrophy. *Am J Hum Genet.* 2014;94(4):625-633.

87. Thomas Y, Peter M, Mechali F, Blanchard JM, Coux O, Baldin V. Kizuna is a novel mitotic substrate for CDC25B phosphatase. *Cell Cycle.* 2014;13(24):3867-3877.

88. Friedman JS, Ray JW, Waseem N, et al. Mutations in a BTB-Kelch protein, KLHL7, cause autosomal-dominant retinitis pigmentosa. *Am J Hum Genet.* 2009;84(6):792-800.

89. Kigoshi Y, Tsuruta F, Chiba T. Ubiquitin ligase activity of Cul3-KLHL7 protein is attenuated by autosomal dominant retinitis pigmentosa causative mutation. *The Journal of biological chemistry.* 2011;286(38):33613-33621.

90. Wen Y, Locke KG, Klein M, et al. Phenotypic characterization of 3 families with autosomal dominant retinitis pigmentosa due to mutations in KLHL7. *Arch Ophthalmol.* 2011;129(11):1475-1482.

91. Xue L, Gollapalli DR, Maiti P, Jahng WJ, Rando RR. A palmitoylation switch mechanism in the regulation of the visual cycle. *Cell.* 2004;117(6):761-771.

92. Saari JC, Bredberg DL. Lecithin:retinol acyltransferase in retinal pigment epithelial microsomes. *J Biol Chem.* 1989;264(15):8636-8640.

93. Omori Y, Chaya T, Katoh K, et al. Negative regulation of ciliary length by ciliary male germ cell-associated kinase (Mak) is required for retinal photoreceptor survival. *Proc Natl Acad Sci U S A.* 2010;107(52):22671-22676.

94. Ozgul RK, Siemiatkowska AM, Yucel D, et al. Exome sequencing and cis-regulatory mapping identify mutations in MAK, a gene encoding a regulator of ciliary length, as a cause of retinitis pigmentosa. *Am J Hum Genet.* 2011;89(2):253-264.

95. Stone EM, Luo X, Heon E, et al. Autosomal recessive retinitis pigmentosa caused by mutations in the MAK gene. *Invest Ophthalmol Vis Sci.* 2011;52(13):9665-9673.

96. Vollrath D, Feng W, Duncan JL, et al. Correction of the retinal dystrophy phenotype of the RCS rat by viral gene transfer of Mertk. *Proc Natl Acad Sci U S A.* 2001;98(22):12584-12589.

97. Siemiatkowska AM, van den Born LI, van Hagen PM, et al. Mutations in the mevalonate kinase (MVK) gene cause nonsyndromic retinitis pigmentosa. *Ophthalmology.* 2013;120(12):2697-2705.

98. Nishiguchi KM, Tearle RG, Liu YP, et al. Whole genome sequencing in patients with retinitis pigmentosa reveals pathogenic DNA structural changes and NEK2 as a new disease gene. *Proc Natl Acad Sci U S A.* 2013;110(40):16139-16144.

99. Wang F, Li H, Xu M, et al. A homozygous missense mutation in NEUROD1 is associated with nonsyndromic autosomal recessive retinitis pigmentosa. *Invest Ophthalmol Vis Sci.* 2014;56(1):150-155.

100. Coppieters F, Leroy BP, Beysen D, et al. Recurrent mutation in the first zinc finger of the orphan nuclear receptor NR2E3 causes autosomal dominant retinitis pigmentosa. *Am J Hum Genet.* 2007;81(1):147-157.

101. Escher P, Gouras P, Roduit R, et al. Mutations in NR2E3 can cause dominant or recessive retinal degenerations in the same family. *Hum Mutat.* 2009;30(3):342-351.

102. Gire AI, Sullivan LS, Bowne SJ, et al. The Gly56Arg mutation in NR2E3 accounts for 1-2% of autosomal dominant retinitis pigmentosa. *Mol Vis.* 2007;13:1970-1975.

103. Farjo Q, Jackson A, Pieke-Dahl S, et al. Human bZIP transcription factor gene NRL: structure, genomic sequence, and fine linkage mapping at 14q11.2 and negative mutation analysis in patients with retinal degeneration. *Genomics.* 1997;45(2):395-401.

104. Rehemtulla A, Warwar R, Kumar R, Ji X, Zack DJ, Swaroop A. The basic motif-leucine zipper transcription factor Nrl can positively regulate rhodopsin gene expression. *Proc Natl Acad Sci U S A.* 1996;93(1):191-195.

105. Ferrante MI, Zullo A, Barra A, et al. Oral-facial-digital type I protein is required for primary cilia formation and left-right axis specification. *Nat Genet.* 2006;38(1):112-117.

106. Ferrante MI, Giorgio G, Feather SA, et al. Identification of the gene for oral-facial-digital type I syndrome. *Am J Hum Genet.* 2001;68(3):569-576.

107. Romio L, Fry AM, Winyard PJ, Malcolm S, Woolf AS, Feather SA. OFD1 is a centrosomal/basal body protein expressed during mesenchymal-epithelial transition in human nephrogenesis. *Journal of the American Society of Nephrology : JASN.* 2004;15(10):2556-2568.

108. Giorgio G, Alfieri M, Prattichizzo C, Zullo A, Cairo S, Franco B. Functional characterization of the OFD1 protein reveals a nuclear localization and physical interaction with subunits of a chromatin remodeling complex. *Molecular biology of the cell.* 2007;18(11):4397-4404.

109. Lopes CA, Prosser SL, Romio L, et al. Centriolar satellites are assembly points for proteins implicated in human ciliopathies, including oral-facial-digital syndrome 1. *J Cell Sci.* 2011;124(Pt 4):600-612.

110. Singla V, Romaguera-Ros M, Garcia-Verdugo JM, Reiter JF. Ofd1, a human disease gene, regulates the length and distal structure of centrioles. *Dev Cell.* 2010;18(3):410-424.

111. Beheshtian M, Saee Rad S, Babanejad M, et al. Impact of whole exome sequencing among Iranian patients with autosomal recessive retinitis pigmentosa. *Arch Iran Med.* 2015;18(11):776-785.

112. Fung BK, Young JH, Yamane HK, Griswold-Prenner I. Subunit stoichiometry of retinal rod cGMP phosphodiesterase. *Biochemistry.* 1990;29(11):2657-2664.

113. Koutalos Y, Nakatani K, Yau KW. The cGMP-phosphodiesterase and its contribution to sensitivity regulation in retinal rods. *J Gen Physiol.* 1995;106(5):891-921.

114. Dvir L, Srour G, Abu-Ras R, Miller B, Shalev SA, Ben-Yosef T. Autosomal-recessive early-onset retinitis pigmentosa caused by a mutation in PDE6G, the gene encoding the gamma subunit of rod cGMP phosphodiesterase. *Am J Hum Genet.* 2010;87(2):258-264.

115. Xu M, Yamada T, Sun Z, et al. Mutations in POMGNT1 cause non-syndromic retinitis pigmentosa. *Hum Mol Genet.* 2016;25(8):1479-1488.

116. Wang NH, Chen SJ, Yang CF, et al. Homozygosity Mapping and Whole-Genome Sequencing Links a Missense Mutation in POMGNT1 to Autosomal Recessive Retinitis Pigmentosa. *Invest Ophthalmol Vis Sci.* 2016;57(8):3601-3609.

117. Lunardi A, Cremisi F, Dente L. Dystroglycan is required for proper retinal layering. *Dev Biol.* 2006;290(2):411-420.

118. Nevet MJ, Shalev SA, Zlotogora J, Mazzawi N, Ben-Yosef T. Identification of a prevalent founder mutation in an Israeli Muslim Arab village confirms the role of PRCD in the aetiology of retinitis pigmentosa in humans. *J Med Genet.* 2010;47(8):533-537.

119. Zangerl B, Goldstein O, Philp AR, et al. Identical mutation in a novel retinal gene causes progressive rod-cone degeneration in dogs and retinitis pigmentosa in humans. *Genomics.* 2006;88(5):551-563.

120. Maw MA, Corbeil D, Koch J, et al. A frameshift mutation in prominin (mouse)-like 1 causes human retinal degeneration. *Hum Mol Genet.* 2000;9(1):27-34.

121. Zhang Q, Zulfiqar F, Xiao X, et al. Severe retinitis pigmentosa mapped to 4p15 and associated with a novel mutation in the PROM1 gene. *Hum Genet.* 2007;122(3-4):293-299.

122. Lauber J, Plessel G, Prehn S, et al. The human U4/U6 snRNP contains 60 and 90kD proteins that are structurally homologous to the yeast splicing factors Prp4p and Prp3p. *Rna (New York, NY).* 1997;3(8):926-941.

123. Wang A, Forman-Kay J, Luo Y, et al. Identification and characterization of human genes encoding Hprp3p and Hprp4p, interacting components of the spliceosome. *Hum Mol Genet.* 1997;6(12):2117-2126.

124. Zhou Z, Licklider LJ, Gygi SP, Reed R. Comprehensive proteomic analysis of the human spliceosome. *Nature.* 2002;419(6903):182-185.

125. Chen X, Liu Y, Sheng X, et al. PRPF4 mutations cause autosomal dominant retinitis pigmentosa. *Hum Mol Genet.* 2014;23(11):2926-2939.

126. Tanackovic G, Ransijn A, Ayuso C, Harper S, Berson EL, Rivolta C. A missense mutation in PRPF6 causes impairment of pre-mRNA splicing and autosomal-dominant retinitis pigmentosa. *Am J Hum Genet.* 2011;88(5):643-649.

127. Umen JG, Guthrie C. Prp16p, Slu7p, and Prp8p interact with the 3' splice site in two distinct stages during the second catalytic step of pre-mRNA splicing. *Rna (New York, NY).* 1995;1(6):584-597.

128. Connell G, Bascom R, Molday L, Reid D, McInnes RR, Molday RS. Photoreceptor peripherin is the normal product of the gene responsible for retinal degeneration in the rds mouse. *Proc Natl Acad Sci U S A.* 1991;88(3):723-726.

129. Travis GH, Sutcliffe JG, Bok D. The retinal degeneration slow (rds) gene product is a photoreceptor disc membrane-associated glycoprotein. *Neuron.* 1991;6(1):61-70.

130. Dryja TP, Hahn LB, Kajiwara K, Berson EL. Dominant and digenic mutations in the peripherin/RDS and ROM1 genes in retinitis pigmentosa. *Invest Ophthalmol Vis Sci.* 1997;38(10):1972-1982.

131. Stuck MW, Conley SM, Naash MI. PRPH2/RDS and ROM-1: Historical context, current views and future considerations. *Prog Retin Eye Res.* 2016;52:47-63.

132. den Hollander AI, McGee TL, Ziviello C, et al. A homozygous missense mutation in the IRBP gene (RBP3) associated with autosomal recessive retinitis pigmentosa. *Invest Ophthalmol Vis Sci.* 2009;50(4):1864-1872.

133. Valverde D, Vazquez-Gundin F, del Rio E, Calaf M, Fernandez JL, Baiget M. Analysis of the IRBP gene as a cause of RP in 45 ARRP Spanish families. Autosomal recessive retinitis pigmentosa. Interstitial retinol binding protein. Spanish Multicentric and Multidisciplinary Group for Research into Retinitis Pigmentosa. *Ophthalmic Genet.* 1998;19(4):197-202.

134. Fingert JH, Oh K, Chung M, et al. Association of a novel mutation in the retinol dehydrogenase 12 (RDH12) gene with autosomal dominant retinitis pigmentosa. *Arch Ophthalmol.* 2008;126(9):1301-1307.

135. Parker RO, Crouch RK. Retinol dehydrogenases (RDHs) in the visual cycle. *Exp Eye Res.* 2010;91(6):788-792.

136. Arno G, Agrawal SA, Eblimit A, et al. Mutations in REEP6 Cause Autosomal-Recessive Retinitis Pigmentosa. *Am J Hum Genet.* 2016;99(6):1305-1315.

137. Hao H, Veleri S, Sun B, et al. Regulation of a novel isoform of Receptor Expression Enhancing Protein REEP6 in rod photoreceptors by bZIP transcription factor NRL. *Hum Mol Genet.* 2014;23(16):4260-4271.

138. Veleri S, Nellissery J, Mishra B, et al. REEP6 mediates trafficking of a subset of Clathrin-coated vesicles and is critical for rod photoreceptor function and survival. *Hum Mol Genet.* 2017.

139. Chen P, Hao W, Rife L, et al. A photic visual cycle of rhodopsin regeneration is dependent on Rgr. *Nat Genet.* 2001;28(3):256-260.

140. Hargrave PA. Rhodopsin structure, function, and topography the Friedenwald lecture. *Invest Ophthalmol Vis Sci.* 2001;42(1):3-9.

141. Azam M, Khan MI, Gal A, et al. A homozygous p.Glu150Lys mutation in the opsin gene of two Pakistani families with autosomal recessive retinitis pigmentosa. *Mol Vis.* 2009;15:2526-2534.

142. Saari JC, Nawrot M, Kennedy BN, et al. Visual cycle impairment in cellular retinaldehyde binding protein (CRALBP) knockout mice results in delayed dark adaptation. *Neuron.* 2001;29(3):739-748.

143. Clarke G, Goldberg AF, Vidgen D, et al. Rom-1 is required for rod photoreceptor viability and the regulation of disk morphogenesis. *Nat Genet.* 2000;25(1):67-73.

144. Pierce EA, Quinn T, Meehan T, McGee TL, Berson EL, Dryja TP. Mutations in a gene encoding a new oxygen-regulated photoreceptor protein cause dominant retinitis pigmentosa. *Nat Genet.* 1999;22(3):248-254.

145. Liu Q, Zhou J, Daiger SP, et al. Identification and subcellular localization of the RP1 protein in human and mouse photoreceptors. *Invest Ophthalmol Vis Sci.* 2002;43(1):22-32.

146. Liu Q, Zuo J, Pierce EA. The retinitis pigmentosa 1 protein is a photoreceptor microtubule-associated protein. *J Neurosci.* 2004;24(29):6427-6436.

147. Liu Q, Lyubarsky A, Skalet JH, Pugh EN, Jr., Pierce EA. RP1 is required for the correct stacking of outer segment discs. *Invest Ophthalmol Vis Sci.* 2003;44(10):4171-4183.

148. Gao J, Cheon K, Nusinowitz S, et al. Progressive photoreceptor degeneration, outer segment dysplasia, and rhodopsin mislocalization in mice with targeted disruption of the retinitis pigmentosa-1 (Rp1) gene. *Proc Natl Acad Sci U S A.* 2002;99(8):5698-5703.

149. Yamashita T, Liu J, Gao J, et al. Essential and synergistic roles of RP1 and RP1L1 in rod photoreceptor axoneme and retinitis pigmentosa. *J Neurosci.* 2009;29(31):9748-9760.

150. Bowne SJ, Daiger SP, Malone KA, et al. Characterization of RP1L1, a highly polymorphic paralog of the retinitis pigmentosa 1 (RP1) gene. *Mol Vis.* 2003;9:129-137.

151. Davidson AE, Sergouniotis PI, Mackay DS, et al. RP1L1 variants are associated with a spectrum of inherited retinal diseases including retinitis pigmentosa and occult macular dystrophy. *Hum Mutat.* 2013;34(3):506-514.

152. Veltel S, Gasper R, Eisenacher E, Wittinghofer A. The retinitis pigmentosa 2 gene product is a GTPase-activating protein for Arf-like 3. *Nature Structural & Molecular Biology.* 2008;15(4):373-380.

153. Lyraki R, Megaw R, Hurd T. Disease mechanisms of X-linked retinitis pigmentosa due to RP2 and RPGR mutations. *Biochem Soc Trans.* 2016;44(5):1235-1244.

154. Avidor-Reiss T, Maer AM, Koundakjian E, et al. Decoding cilia function: defining specialized genes required for compartmentalized cilia biogenesis. *Cell.* 2004;117(4):527-539.

155. Keen TJ, Hims MM, McKie AB, et al. Mutations in a protein target of the Pim-1 kinase associated with the RP9 form of autosomal dominant retinitis pigmentosa. *Eur J Hum Genet.* 2002;10(4):245-249.

156. Hong DH, Pawlyk B, Sokolov M, et al. RPGR isoforms in photoreceptor connecting cilia and the transitional zone of motile cilia. *Invest Ophthalmol Vis Sci.* 2003;44(6):2413-2421.

157. Khanna H, Hurd TW, Lillo C, et al. RPGR-ORF15, which is mutated in retinitis pigmentosa, associates with SMC1, SMC3, and microtubule transport proteins. *J Biol Chem.* 2005;280(39):33580-33587.

158. Roepman R, Wolfrum U. Protein networks and complexes in photoreceptor cilia. *Subcell Biochem.* 2007;43:209-235.

159. Hong DH, Yue G, Adamian M, Li T. Retinitis pigmentosa GTPase regulator (RPGRr)-interacting protein is stably associated with the photoreceptor ciliary axoneme and anchors RPGR to the connecting cilium. *The Journal of biological chemistry.* 2001;276(15):12091-12099.

160. Booij JC, Florijn RJ, ten Brink JB, et al. Identification of mutations in the AIPL1, CRB1, GUCY2D, RPE65, and RPGRIP1 genes in patients with juvenile retinitis pigmentosa. *J Med Genet.* 2005;42(11):e67.

161. Huang H, Wang Y, Chen H, et al. Targeted next generation sequencing identified novel mutations in RPGRIP1 associated with both retinitis pigmentosa and Leber's congenital amaurosis in unrelated Chinese patients. *Oncotarget.* 2017;8(21):35176-35183.

162. Gurevich VV, Gurevich EV, Cleghorn WM. Arrestins as multi-functional signaling adaptors. *Handb Exp Pharmacol.* 2008(186):15-37.

163. Nakazawa M, Wada Y, Tamai M. Arrestin gene mutations in autosomal recessive retinitis pigmentosa. *Arch Ophthalmol.* 1998;116(4):498-501.

164. Corton M, Avila-Fernandez A, Campello L, et al. Identification of the Photoreceptor Transcriptional Co-Repressor SAMD11 as Novel Cause of Autosomal Recessive Retinitis Pigmentosa. *Sci Rep.* 2016;6:35370.

165. Rice DS, Huang W, Jones HA, et al. Severe retinal degeneration associated with disruption of semaphorin 4A. *Invest Ophthalmol Vis Sci.* 2004;45(8):2767-2777.

166. Abid A, Ismail M, Mehdi SQ, Khaliq S. Identification of novel mutations in the SEMA4A gene associated with retinal degenerative diseases. *J Med Genet.* 2006;43(4):378-381.

167. Jin ZB, Huang XF, Lv JN, et al. SLC7A14 linked to autosomal recessive retinitis pigmentosa. *Nature Communications.* 2014;5:3517.

168. Benaglio P, McGee TL, Capelli LP, Harper S, Berson EL, Rivolta C. Next generation sequencing of pooled samples reveals new SNRNP200 mutations associated with retinitis pigmentosa. *Hum Mutat.* 2011;32(6):E2246-2258.

169. Zhao C, Bellur DL, Lu S, et al. Autosomal-dominant retinitis pigmentosa caused by a mutation in SNRNP200, a gene required for unwinding of U4/U6 snRNAs. *Am J Hum Genet.* 2009;85(5):617-627.

170. Wang H, den Hollander AI, Moayedi Y, et al. Mutations in SPATA7 cause Leber congenital amaurosis and juvenile retinitis pigmentosa. *Am J Hum Genet.* 2009;84(3):380-387.

171. Eblimit A, Nguyen TM, Chen Y, et al. Spata7 is a retinal ciliopathy gene critical for correct RPGRIP1 localization and protein trafficking in the retina. *Hum Mol Genet.* 2015;24(6):1584-1601.

172. Chakarova CF, Khanna H, Shah AZ, et al. TOPORS, implicated in retinal degeneration, is a cilia-centrosomal protein. *Hum Mol Genet.* 2011;20(5):975-987.

173. Chakarova CF, Papaioannou MG, Khanna H, et al. Mutations in TOPORS cause autosomal dominant retinitis pigmentosa with perivascular retinal pigment epithelium atrophy. *Am J Hum Genet.* 2007;81(5):1098-1103.

174. Ansley SJ, Badano JL, Blacque OE, et al. Basal body dysfunction is a likely cause of pleiotropic Bardet-Biedl syndrome. *Nature.* 2003;425(6958):628-633.

Chapter 2.1

175. Blacque OE, Reardon MJ, Li C, et al. Loss of C. elegans BBS-7 and BBS-8 protein function results in cilia defects and compromised intraflagellar transport. *Genes Dev.* 2004;18(13):1630-1642.
176. den Hollander AI, van Lith-Verhoeven JJ, Arends ML, Strom TM, Cremers FP, Hoyng CB. Novel compound heterozygous TULP1 mutations in a family with severe early-onset retinitis pigmentosa. *Arch Ophthalmol.* 2007;125(7):932-935.
177. Xi Q, Pauer GJ, Marmorstein AD, Crabb JW, Hagstrom SA. Tubby-like protein 1 (TULP1) interacts with F-actin in photoreceptor cells. *Invest Ophthalmol Vis Sci.* 2005;46(12):4754-4761.
178. Hagstrom SA, Adamian M, Scimeca M, Pawlyk BS, Yue G, Li T. A role for the Tubby-like protein 1 in rhodopsin transport. *Invest Ophthalmol Vis Sci.* 2001;42(9):1955-1962.
179. Hagstrom SA, Watson RF, Pauer GJ, Grossman GH. Tulp1 is involved in specific photoreceptor protein transport pathways. *Adv Exp Med Biol.* 2012;723:783-789.
180. Rivolta C, Sweklo EA, Berson EL, Dryja TP. Missense mutation in the USH2A gene: association with recessive retinitis pigmentosa without hearing loss. *Am J Hum Genet.* 2000;66(6):1975-1978.
181. Dreyer B, Tranebjaerg L, Rosenberg T, Weston MD, Kimberling WJ, Nilssen O. Identification of novel USH2A mutations: implications for the structure of USH2A protein. *Eur J Hum Genet.* 2000;8(7):500-506.
182. Bernal S, Meda C, Solans T, et al. Clinical and genetic studies in Spanish patients with Usher syndrome type II: description of new mutations and evidence for a lack of genotype--phenotype correlation. *Clin Genet.* 2005;68(3):204-214.
183. Baux D, Larrieu L, Blanchet C, et al. Molecular and in silico analyses of the full-length isoform of usherin identify new pathogenic alleles in Usher type II patients. *Hum Mutat.* 2007;28(8):781-789.
184. Avila-Fernandez A, Perez-Carro R, Corton M, et al. Whole-exome sequencing reveals ZNF408 as a new gene associated with autosomal recessive retinitis pigmentosa with vitreal alterations. *Hum Mol Genet.* 2015;24(14):4037-4048.
185. Collin RW, Nikopoulos K, Dona M, et al. ZNF408 is mutated in familial exudative vitreoretinopathy and is crucial for the development of zebrafish retinal vasculature. *Proc Natl Acad Sci U S A.* 2013;110(24):9856-9861.
186. Habibi I, Chebil A, Kort F, Schorderet DF, El Matri L. Exome sequencing confirms ZNF408 mutations as a cause of familial retinitis pigmentosa. *Ophthalmic Genet.* 2017:1-4.
187. Li L, Nakaya N, Chavali VR, et al. A mutation in ZNF513, a putative regulator of photoreceptor development, causes autosomal-recessive retinitis pigmentosa. *Am J Hum Genet.* 2010;87(3):400-409.

Genotype

Homozygous variants in KIAA1549, encoding a ciliary protein, are associated with autosomal recessive retinitis pigmentosa

Suzanne E. de Bruijn, Sanne K. Verbakel, Erik de Vrieze, Hannie Kremer, Frans P.M. Cremers, Carel B. Hoyng, L. Ingeborgh van den Born, Susanne Roosing

Abstract

Background

Retinitis pigmentosa (RP) shows substantial genetic heterogeneity. It has been estimated that in approximately 60-80% of RP cases the genetic diagnosis can be found using whole exome sequencing (WES). In this study, the purpose was to identify causative variants in individuals with genetically unexplained retinal disease, which included one consanguineous family with two affected siblings and one case with RP.

Methods

To identify the genetic defect, WES was performed in both probands and clinical analysis was performed. To obtain insight into the function of KIAA1549 in photoreceptors, mRNA expression, knockdown and protein localization studies were performed.

Results

Through analysis of WES data, based on population allele frequencies, and *in silico* prediction tools we identified a homozygous missense variant and a homozygous frameshift variant in *KIAA1549* that segregate in two unrelated families. Kiaa1549 was found to localize at the connecting cilium of the photoreceptor cells and the synapses of the mouse retina. Both variants affect the long transcript of *KIAA1549* which encodes a 1950-amino acid protein and shows prominent brain expression. The shorter transcript encodes a 734-amino acid protein with a high retinal expression and is affected by the identified missense variant. Strikingly, knockdown of the long transcript also leads to decreased expression of the short transcript likely explaining the nonsyndromic retinal phenotype caused by the two variants targeting different transcripts.

Conclusion

In conclusion, our results underscore the causality of segregating variants in *KIAA1549* for autosomal recessive RP. Moreover, our data indicates that KIAA1549 plays a role in photoreceptor function.

Introduction

Retinitis pigmentosa (RP; MIM: #268000) encompasses a clinical and genetic heterogeneous group of progressive inherited retinal dystrophies (IRD). RP is characterized by the primary degeneration of rod photoreceptor cells, followed by the loss of cone photoreceptor cells and retinal pigment epithelium (RPE). With a prevalence of approximately 1 in 4,000 persons, it is considered the most common form of inherited retinal dystrophy.[1] RP typically displays night blindness in early adulthood or adolescence, followed by the progressive loss of the peripheral visual field. The visual acuity can be relatively preserved until the advanced disease stages, but RP leads to severe visual impairment or blindness in a large number of patients.[2]

Besides clinical heterogeneity, RP is also characterized by its broad range of genetic heterogeneity. A large number of genes has been implicated in the pathogenesis of RP, and pathogenic variants can be inherited in a recessive, dominant or X-linked manner (RetNet; available at https://sph.uth.edu/retnet/). Recently, it has been estimated that in only 60-80% of RP cases the genetic explanation can be found using whole exome sequencing (WES), which is currently the most widely applied method for disease gene identification.[3,4] A better understanding of the underlying disease mechanisms, the role of variants in the pathogenesis of disease in currently known RP genes, and genotype-phenotype correlations are required to provide further insights towards developing therapeutic approaches.

Recently, *KIAA1549* (GenBank: NM_001164665; MIM: *613344) has been proposed as a candidate RP gene; however, supporting evidence is limited. In an autosomal recessive RP (arRP) family a homozygous frameshift variant in *KIAA1549* was described to be the only variant remaining after applying filtering criteria on WES data.[4]

In this study, we report on homozygous variants in KIAA1549 in two families with arRP. In addition, protein localization studies have been performed to provide insight in the involvement of KIAA1549 in photoreceptor function, supporting its role as an RP gene.

Methods

Subjects and clinical examinations

Two families with individuals with genetically unexplained RP were included in this study; one consanguineous Iranian family with two affected siblings, and one case from the Netherlands (Figure 1A). This study was approved by the Institutional Review Boards of the participating centers, and adhered to the tenets of the declaration of Helsinki. All subjects provided informed consent prior to inclusion in the study.

Clinical data were collected from the medical records of two patients from Family A (A-II:1, A-II:2) and one patient from Family B (B-II:1), including information regarding best-corrected Snellen visual acuity, and results of slit-lamp biomicroscopy and ophthalmoscopy. In patient A-II:2 and B-II:1, fundus photography, spectral-domain optical tomography (SD-OCT; Spectralis, Heidelberg
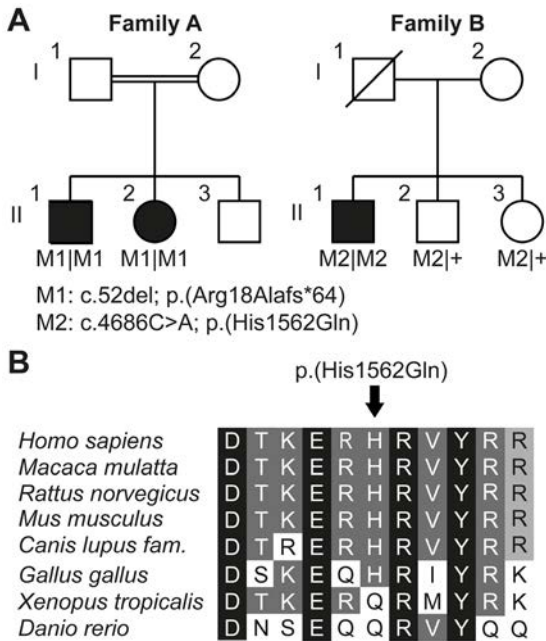
Figure 1. *KIAA1549* variants detected in patients in two families with retinitis pigmentosa. (A) Pedigrees of two families with RP associated to homozygous variants in *KIAA1549* (NM_001164665). (B) Evolutionary conservation of the mutated amino acid (M2) identified in Family B. Black boxes indicate fully conserved amino acid residues, whereas dark grey boxes indicate highly conserved and light grey boxes moderately conserved amino acid residues. M, mutation.

Engineering) and Goldmann kinetic perimetry were performed, and full-field electroretinography was recorded according to the International Society for Clinical Electrophysiology of Vision guidelines and assessed by applying local standard values.[5] In addition, fundus autofluorescence (Spectralis, Heidelberg Engineering) images, were available for patient B-II:1.

Whole exome sequencing and variant interpretation

Genomic DNA was isolated from peripheral blood using standard isolation methods and WES was performed in both probands. For proband A-II:2, exome enrichment was performed using the Agilent SureSelect Human All Exome V6 kit. Read mapping along the hg19 reference genome (GrCH37/hg19) and variant calling were performed using BWA version 0.78 and the haplotype caller module of GATK (Broad Institute). CNV detection was performed using CoNIFER version 0.2.2. Exome enrichment for proband B-II:1 was carried out with the Agilent SureSelect XT Human All Exon V5 enrichment kit. Mapping of sequencing reads along the hg19 reference genome and variant calling were performed using Lifescope version 1.3 (Life Technologies). CNV detection was performed using ExomeDepth version 1.1.1.

For both datasets, the obtained variants were filtered based on population allele frequencies ≤ 0.5% in gnomAD, ExAC, dbSNP, and an in-house exome database (containing 15,576 alleles). Only nonsense, indels, splice site (-14/+14 nucleotides), missense and synonymous variants were assessed. Missense variants were only assessed when predicted to be possibly pathogenic by at least one *in silico* predictor; a Grantham score ≥80, PhyloP ≥2.7 or CADD-Phred score ≥15. Synonymous variants were only assessed when predicted to have an effect on splicing by one

of the splice prediction tools that are embedded in the AlamutVisual software (version 2.10). Candidate genes in which remaining variants were found were compared to currently known IRD-associated genes listed on RetNet (accessed on 1st June 2018). Validation of found variants and segregation analysis were performed by Sanger sequencing. Primer sequences and PCR conditions are available upon request.

KIAA1549 expression in human tissues

KIAA1549 expression was determined in human adult tissues using commercially available cDNA panels. Total RNA derived from heart, lung, brain, kidney and bone marrow (Bio-Chain) and total RNA derived from skeletal muscle, liver, duodenum, stomach, spleen, thymus and testis (Stratagene) were utilized. Total RNA from retina was obtained from a healthy anonymous donor. Subsequently, cDNA was prepared using the iScript cDNA Synthesis kit (Bio-RaD) and purified with NucleoSpin Gel and PCR Clean-up Columns (Machery-Nagel). Quantitative PCR was performed using GoTaq qPCR Master Mix (Promega) according to manufacturer's protocol. Transcript-specific intron-spanning primers have been designed and validated for the long (NM_001164665) and short transcript (XM_935390) of *KIAA1549,* and for the reference gene *GUSB* (MIM: #611499). Primer locations and sequences can be found in Table S1. Amplifications were performed with the Applied Biosystem Fast 7900 System (Applied Biosystems). All PCR reactions were executed in duplicate and relative gene expression levels compared to the reference gene *GUSB* were determined with the delta-delta Ct method.

Immunofluoresence of Kiaa1549 in mouse retinal sections

An eye obtained from a healthy 2-month-old mouse was dissected and cryoprotected for 30 minutes with 10% sucrose in PBS before embedding Tissue-Tek OCT (Sakura). Subsequently, sections were frozen in isopentane cooled by liquid nitrogen. For immunofluorescence, unfixed cryosections (7μm) were permeabilized in 0.01% Tween20 in PBS for 20 minutes. After washing with PBS, blocking was performed for 1 hour using a blocking solution containing 0.1% ovalbumin and 0.5% fish gelatin in PBS. Primary antibodies against Kiaa1549 (1:500; cat.# HPA019560, Sigma-Aldrich) and Centrin (1:500; cat.# 04-1624, Millipore) were diluted in blocking solution and incubated on the sections overnight at 4°C. Subsequently, sections were rinsed with PBS and incubated with secondary antibodies goat-anti-rabbit Alexa 568 and goat-anti-mouse Alexa 488 (1:500; Molecular Probes) and DAPI (1:8000; Molecular Probes) in blocking solution for 45 minutes. Finally, sections were post-fixed with 4% PFA for 10 minutes before mounting with Prolong Gold (Molecular Probes). Sections were analyzed using a Zeiss Axio Imager Z2 fluorescence microscope equipped with an Apotome using several magnifications.

Knockdown of KIAA1549 in vitro using siRNAs

Silencer® Select siRNAs targeting *KIAA1549* (s33562 and s33563) and non-targeting Negative Control No. 1 were obtained from Thermo Fisher Scientific (Table S2). For transfection, hTERT-

RPE1 or HEK293 cells (ATCC) were transfected with a single siRNA in duplicate (15 nM final concentration), using Lipofectamine RNAiMax transfection reagent (Thermo Fisher Scientific) according to manufacturer's protocol. After 24 hours of transfection, cells were serum starved (0.2% FCS) for 48 hours to induce ciliogenesis. To assess the effect of the siRNAs on *KIAA1549* expression, RNA was isolated using the NucleoSpin RNA kit (Macherey-Nagel), and expression was quantified by qPCR. To evaluate the effect of knockdown of the long transcript on expression of the short transcript, HEK293 cells were used. HEK293 cells express both the long and short transcript abundantly, unlike hTERT-RPE1 cells which only express the long transcript.

For immunofluorescence, transfected hTERT-RPE1 cells were fixed with 2% PFA for 20 minutes, and permeabilized using 1% Triton X-100 in PBS for 5 minutes. Subsequently, cells were blocked with 2% BSA in PBS for 45 minutes. Primary antibodies against the primary cilium (anti-ARL13B; 1:500; cat.# 17711-1AP; ProteinTech) and the ciliary transition zone (anti-RPGRIP1L; 1:500; cat.# SNC039; [6]) diluted in blocking solution were incubated for 1 hour. After incubation with secondary antibodies in blocking solution for 45 minutes, samples were mounted by VECTASHIELD containing DAPI (Vector Laboratories). Cells were imaged using a Zeiss Axio Imager Z2 fluorescence microscope and a 63x magnification. Percentage of ciliated cells and cilium length were calculated using Fiji Is Just ImageJ (FIJI).[7] Each experiment was performed three independent times.

Results

Identification of KIAA1549 variants

To identify the genetic defect underlying the arRP in two affected siblings of an Iranian consanguineous family (Family A; Figure 1A), exome sequencing was performed in individual A-II:2. After analysis of the WES data, the frameshift variant c.52del (Hg19:g.138,665,964del; p.(Arg18Alafs*64)) was detected in the candidate RP gene *KIAA1549* (Family A). This variant is located in the second largest homozygous region of 13.2 Mb. Presence of the homozygous variant was confirmed and segregation analysis was performed using Sanger sequencing. The variant is absent from population frequency databases gnomAD, ExAC, dbSNP and the in-house database. Moreover, the variant is absent from the Iranome database, which contains whole exome sequencing data of 800 healthy individuals from eight major ethnic groups in Iran. The variant causes a frameshift in exon 1, and is predicted to result in degradation of *KIAA1549* mRNA due to nonsense-mediated decay. Previously, a heterozygous variant in *CRB1* was reported for Family A in both affected siblings.[8] Analysis of the WES data of patient A-II:2 did not yield additional variants or copy number variants in this gene. Moreover, the c.2816A>G (p.(Asn894Ser)) variant was predicted to be benign by *in silico* predictions suggesting that *CRB1*–variants are unlikely to cause disease in this family. No CNVs or other compound heterozygous or homozygous variants were detected in currently known IRD-associated genes. Also, no heterozygous candidate variants were found in causative genes related to the patient's phenotype. WES was performed in patient B-II:1

affected with RP (Family B, Figure 1A), and revealed a homozygous missense variant in *KIAA1549*; c.4686C>A (Hg19:g.138,554,373G>T; p.(His1562Gln)). After analysis, this was the only homozygous variant remaining in an IRD-associated gene and no compound heterozygous variants were observed. The homozygous variant was validated in the proband and segregation analysis was performed by Sanger sequencing in two unaffected siblings. The moderately conserved mutated histidine residue is located in a highly conserved region (Figure 1B), has a CADD-Phred score of 24.2, a PhyloP score of 0.53 and a Grantham score of 24. Additionally, the prediction tools MutationTaster[9], PolyPhen-2[10] and SIFT[11] predicted the variant to be disease causing (p-value: 0.835), possibly damaging (HumDiv: 0.889; HumVar: 0.651) and tolerated (0.17), respectively. Moreover, putative changes are predicted by Human Splicing Finder. The binding sites of the splicing factors SRp40 and SF2/ASF are no longer present, and a potential creation of an exonic splicing silencer site is predicted.[12] Heterozygous variants in currently known IRD-associated genes were found in *ABCA4* (c.2588G>C(;)5603A>T; p.[Gly863Ala, Gly863del](;)(Asn1868Ile)) and *CDHR1* (c.512C>G; p.(Thr171Ser)), but no second pathogenic alleles could be detected for these genes. No CNVs were detected in regions overlapping with known IRD-associated genes.

Clinical evaluation

Clinical data were collected from the medical records of two patients from Family A (A-II:1, A-II:2) and one patient from Family B (B-II:1). An overview of the clinical characteristics of the three affected individuals with damaging *KIAA1549* variants at the most recent examination is provided in Table 1 and clinical images of patient A-II:2 and B-II:1 are shown in Figure 2. All affected individuals were diagnosed with RP. They all initially experienced night blindness, followed by a gradual decline of their visual fields and visual acuity. The age of onset varied from the first decade (patient A-II:1) to the fifth decade (patient B-II:1) and all patients were myopic. Cortical cataract was observed in patient A-II:1 (age 38), whereas patient A-II:2 underwent a cataract extraction at the age of 38 (right eye) and 52 years (left eye). Ophthalmoscopy revealed characteristic RP features in all three patients, including attenuated retinal vessels, waxy pallor of the optic disc, and bone spicule pigmentation (Figure 2A, 2D). In addition, nummular deep pigmentations were visible in the mid-periphery. SD-OCT imaging in patient A-II:2 showed profound atrophy of the outer retinal layers with preservation of the photoreceptors in the fovea. This patient was treated for Coats-like exudative vasculopathy related to her RP in the past. Fundus autofluorescense imaging in patient B-II:1 showed the characteristic hyperautofluorescent ring that represents the transition zone between intact and degenerated photoreceptor outer segments, corresponding with a preserved ellipsoid zone within the ring on SD-OCT, and loss of the ellipsoid zone external to the ring (Figure 2E-F). In addition, the SD-OCT image of patient B-II:1 showed evident cystoid macular edema, that was refractory to topical treatment with nonsteroidal anti-Inflammatory drugs, steroids, as well as both topical and oral carbonic anhydrase inhibitor treatment (Figure 2F). Electrophysiology examination demonstrated a generalized retinal dystrophy with non-recordable rod and cone-driven responses in patient A-II:2 at the age of 32 years, and severely reduced rod and cone-driven responses in patient B-II:1 at 54 years of age. Finally, perimetric analysis revealed a severely

constricted visual field up to 5 degrees in patient A-II:2, and a complete and partial ring scotoma in the right and left eye of patient B-II:1, respectively. No visual field testing was performed in patient A-II:1, yet he reported severe visual field constriction. All patients were in good general health, and no non-ocular conditions were reported.

Expression of KIAA1549 transcripts in human tissues

To gain knowledge on the specific role of *KIAA1549*, its relative expression was determined in a set of human adult tissues. Two major KIAA1549 isoforms have been identified (Uniprot: Q9HCM3), a long primary isoform (NM_001164665) of 1950 amino acids (aa) and a short isoform (XM_935390) of 734 aa (Figure 3A) which is produced from an alternative transcript transcribed from an alternative promoter sequence located in intron 8. The nomenclature of all genetic or protein elements is based on the long isoform. The expression of both *KIAA1549* transcripts and of the reference gene *GUSB* was evaluated in cDNA of human tissues by qPCR (Figure 3B). The long transcript showed a low to moderate expression in retina and other tissues, such as heart and kidney, and is predominantly expressed in brain as has been previously described.[13] On the contrary, the less characterized short transcript showed an abundant expression in the retina
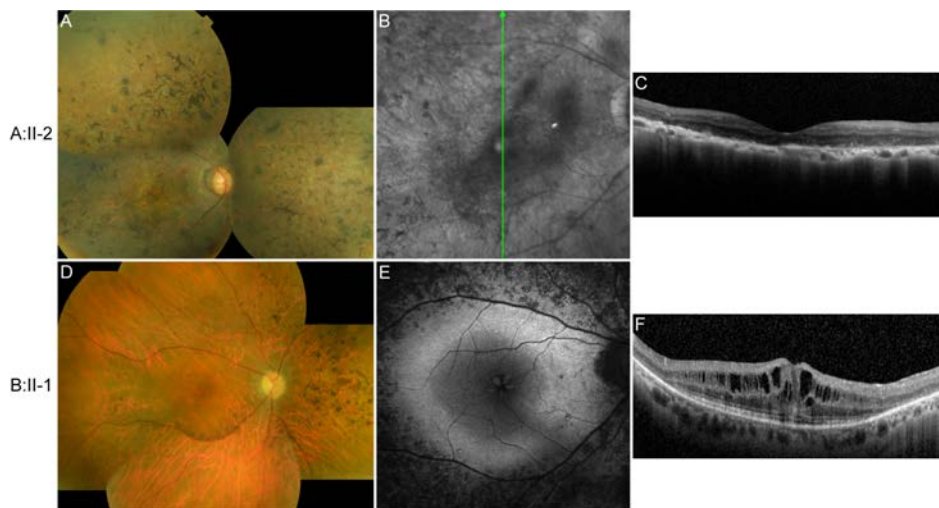
Figure 2. Multimodel retinal imaging of patients with segregating *KIAA1549* variants.
A–C, Clinical characteristics of patient II:2 of Family A. (A) Composite fundus photograph of the right eye of patient A-II:2 showing attenuated retinal vessels, bone spicule and nummular pigmentation, moderate optic disc pallor, and a remnant of RPE between optic disc and macula, and at the fovea. (B) Infrared image of the posterior pole of the right eye of patient A-II:2, indicating the position of the corresponding optical coherence tomography (OCT) examination. (C) Spectral-domain OCT showing atrophy of the outer retina with intact photoreceptors in the fovea. D–F, Clinical characteristics of patient II:1 of Family B. (D) Composite fundus photograph of the right eye of patient B-II:1, showing attenuated retinal vessels, waxy pallor of the optic disc, and mid-peripheral bone spicule and nummular pigmentation. (E) Fundus autofluorescence of the right eye of patient B-II:1, showing a central hyperautofluorescent ring surrounding the normal appearing retina, hypoautofluorescence spots along and external to the vascular arcade, and a spoke wheel pattern in the fovea corresponding to the cystoid macular edema visible on OCT. (F) SD-OCT scan taken along the horizontal meridian of the central retina, revealing peripheral loss of the outer retina with central preservation of the ellipsoid band, and macular cysts.

(~200 times; normalized for *GUSB*), compared to only minimal expression in brain and other tissues. This suggests that the short KIAA1549 isoform may harbor a retina-specific function.

Localization of Kiaa1549 in mouse retina sections

To confirm the presence of KIAA1549 in the retina, as well as to define its specific localization in this tissue, immunofluorescence was performed in retina sections obtained from a healthy, 2-month-old mouse. Costaining was performed with anti-Centrin, a well-defined marker for the connecting cilium within the photoreceptor cell.[14] Results showed that Kiaa1549 colocalized with Centrin, and thus is located at the connecting cilium of the photoreceptor cells (Figure 4). Moreover, positive staining of Kiaa1549 was also observed at the outer plexiform layer of the mouse retina. This layer contains neural synapses between the photoreceptors and the bipolar and horizontal cells in the retina.
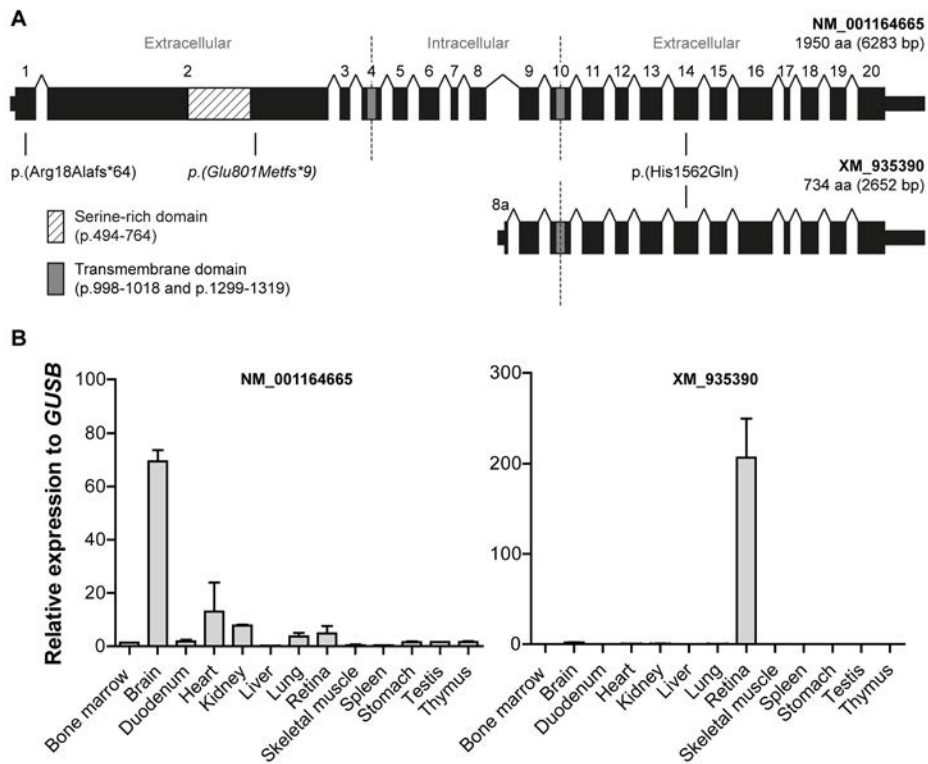
Figure 3. Expression of *KIAA1549* transcripts in human tissues. (A) Schematic representation of the major long and short *KIAA1549* transcripts and identified segregating variants. A previously reported *KIAA1549* variant by Abu-Safieh et al. is depicted in italics.[4] The short transcript is transcribed from an alternative promoter sequence present in intron 8, and includes a transcript-specific exon referred to as exon 8a. (B) Relative *KIAA1549* expression in human tissues determined by qPCR. Expression of the transcript encoding the long isoform (NM_001164555) is depicted in the left panel, and expression of the transcript encoding the short isoform (XM_935390) is depicted in the right panel. The long transcript is predominantly expressed in the brain, whereas expression of the short transcript is significantly increased in the retina compared to other tissues.

Table 1. Clinical features at most recent examination in patients with segregating KIAA1549 variants

Patient	Sex/Age	Initial symptom, age (y)	Visual acuity		Spherical equivalent		Lens status	Ophthalmoscopy results	ERG		Goldmann perimetry
			RE	LE	RE	LE			scot	phot	
A-II:1	M/38	Night blindness (8)	20/40	20/50	-4.38	-5.25	Cortical cataracts	Severely attenuated retinal vessels, RPE atrophy with bone spicule and nummular pigmentation in the periphery, preserved posterior pole, and absence of optic disc pallor.	NP	NP	NP
A-II:2	F/53	Night blindness (28)	20/400	20/400	-6.50*	-7.25	Pseudo-phakia	Attenuated retinal vessels, severe RPE atrophy BE, with recognizable foveal island, moderate optic disc pallor, bone spicule and nummular pigmentations, white epiretinal changes, and old Coats-like exudative vasculopathy inferior quadrants BE.	NR‡	NR‡	Constricted VF, central residue <5° (age 48)
B-II:1	M/54	Night blindness (~45)	20/60	20/20	-2.00	-2.13	Clear	Attenuated vessels, mid-peripheral bone spicule and nummular pigmentation, waxy pallor of the optic discs, and CME (RE>LE).	SR	MR	RE: mid-peripheral ring scotoma LE: partial mid-peripheral ring scotoma. VF affected temporal>nasal BE

BE, both eyes; CME, cystoid macular edema; ERG, electroretinography; F, female; LE, left eye; M, male; MR, moderately reduced; NP, not performed; NR, non-recordable; phot, photopic; RE, right eye; scot, scotopic; SR, severely reduced; VF, visual field; y, years. * Prior to cataract surgery. ‡ ERG performed at the age of 32.
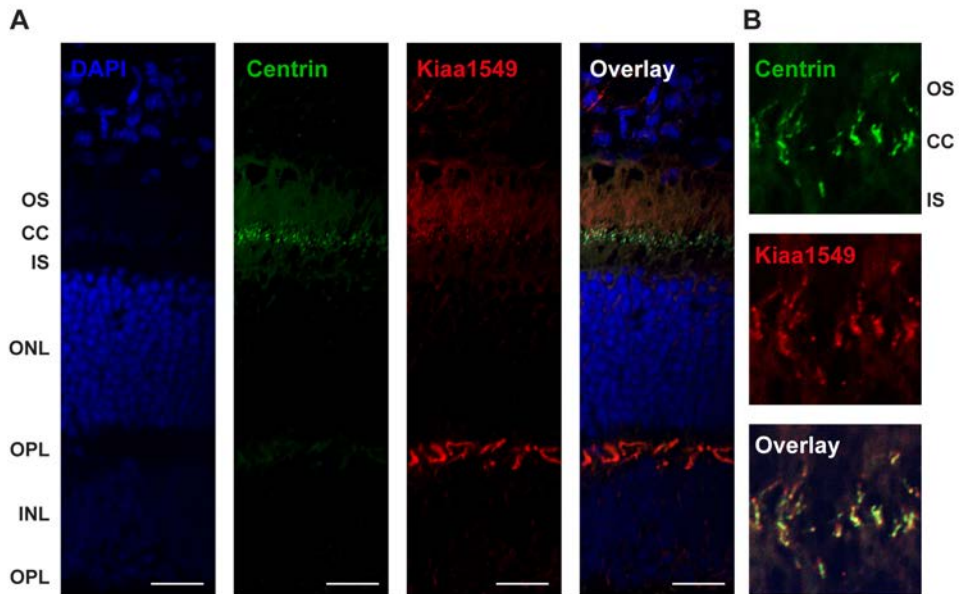
Figure 4. Localization of Kiaa1549 in the retina of an adult mouse. Immunofluorescence analysis of Kiaa1549 (red) stained on an unfixed retina section obtained from a healthy 2-month-old mouse. Costaining was performed with an antibody for Centrin (green), a connecting cilium marker of the photoreceptor. (A) Provides an overview of the retina section and was imaged using a 40x magnification. The scale bar represents 20 μm. Kiaa1549 is detected at the connecting cilium photoreceptor cells and the outer plexiform layer of the mouse retina. (B) Focused image of the photoreceptor region taken using a 63x magnification. The signal of Kiaa1549 at the connecting cilium shows overlap with that of Centrin. CC, connecting cilium; INL, inner nuclear layer; IPL, inner plexiform layer; IS, inner photoreceptor segment; ONL, outer nuclear layer; OPL, outer plexiform layer; OS, outer photoreceptor segment.

Assessing the function of KIAA1549

To investigate whether KIAA1549 plays a role in ciliogenesis, an *in vitro* study was performed in which *KIAA1549* was knocked down in hTERT-RPE1 cells with two different siRNAs targeting the long transcript. The efficiency of *KIAA1549* knockdown was validated by qPCR analysis, and induced ciliogenesis was studied using immunocytochemistry. The percentage of ciliated cells and average cilium length showed no significant difference when comparing cells treated with *KIAA1549*-targeting siRNAs or the non-targeting siRNA (Figure S1), suggesting that KIAA1549 does not have a function in the formation of cilia however KIAA1549 may be involved in other processes that are performed at the primary cilium.

Discussion

In this study, we report on two families in which autosomal recessive RP is associated with homozygous variants in *KIAA1549*. The retinal phenotype in both families is typical for RP, and patients' complaints started with night blindness with subsequent constriction of the visual

field. Fundus examination revealed the hallmark RP features. However, patients in Family A are more severely affected compared to the patient in Family B, which is displayed in a lower age at onset, severely constricted visual fields, and more severely reduced ERG responses.

In Family A, a homozygous frameshift variant was found in exon 1 (c.52del; p.(Arg18Alafs*64)) by WES. Although putative alternative start codons are present in exon 2, exon 1 encodes the signal peptide of the protein (aa 1-60). Therefore, a shorter protein is potentially mislocalized, impairing protein function. In Family B, a homozygous missense variant was found in exon 14 (c.4686C>A; p.(His1562Gln)), that affects a highly conserved region of the protein. The damaging nature of these variants is supported by a probability of loss of function intolerance (pLi) score of 1.00 (Scale 0-1) in gnomAD (accessed on 1st June 2018) and that no homozygous variants have been reported in the entire *KIAA1549* gene. Combined, this suggests that the identified *KIAA1549* variants in both families can be associated to the RP-phenotype of the patients. Regardless, the presence of pathogenic variants present in non-coding regions uncovered by WES cannot be ruled out.

KIAA1549 encodes a transmembrane protein and is described to be predominantly expressed in the brain and is involved in oncogenesis when fused to *BRAF* (MIM: *164757).[4,15] *BRAF-KIAA1549* in-frame fusion genes are caused by a 2 Mb tandem duplication at 7q34, and are found to induce BRAF kinase activity and consequently, activation of the MAPK pathway which is involved in the development of cancer. For this reason, these fusion genes are the major cause (66%) for pilocytic astrocytomas, the most frequently occurring central nervous system tumor in children and young adolescents.

Besides this role in oncogenesis, knowledge about the function of KIAA1549 is limited. Recently, a homozygous truncating variant in *KIAA1549* was found in an arRP family with two affected siblings in a study performed by Abu-Safieh et al.[4] Involvement of KIAA1549 in photoreceptor function was suggested, however no functional data was provided.[4] Nevertheless, *KIAA1549* is reported to be among the top 4% of genes being enriched for binding sites for the photoreceptor specific transcription factor CRX.[16] *Kiaa1549* expression was evaluated in a *Nrl*^{-/-} knockout mouse that is characterized by degenerated rod photoreceptors. In this mouse, *Kiaa1549* expression was found to be reduced ~88% (WT: 106 reads, KO: 13 reads) when compared to the wild type mouse, based on number of sequencing reads.[16]

In this study, expression levels of the major short and long transcripts of *KIAA1549* have been evaluated in a set of human tissues, which demonstrated that both isoforms are present in the retina, of which the expression of the transcript encoding the short isoform is significantly higher in retina compared to other tissues. We hypothesize that both isoforms are required for the correct function of the protein in the retina, as the homozygous frameshift variant affecting the long isoform has detrimental consequences as observed in Family A and the family previously described in the study of Abu-Safieh et al. By performing an *in vitro* experiment in which HEK293 cells were transfected with *KIAA1549*-targeting siRNAs that specifically recognize the long transcript of *KIAA1549* (Table S1), also a significant decrease in expression of the short transcript was observed (Figure S2) which suggests a functional dependency between the two transcripts.

Hence, observed variants in the long transcript likely cause a decrease in the abundant retinal expression of the short transcript and thereby could lead to retinal degeneration. The fact that the identified variants have different consequences on the two *KIAA1549* transcripts could explain the phenotypic differences observed among the affected individuals. The phenotype of the family described by Abu-Safieh et al. (a non-recordable ERG at age 35) (personal communication Prof. F.S. Alkuraya and N. Patel, PhD) is more comparable with Family A (Non-recordable ERG at age 32 in patient A-II:2) than Family B (severely reduced photopic and moderately reduced scotopic ERG at age 54), which may be in line with the genotype having a damaging variant in the long transcript. Identification of additional families with *KIAA1549*-associated RP are required to provide deeper insight into a possible phenotype-genotype correlation. [17]

In addition, we showed localization of KIAA1549 at the connecting cilium of mouse photoreceptor cells, providing the first information on KIAA1549 function in photoreceptors. Moreover, KIAA1549 localization was also noted at the outer plexiform layer of the mouse retina. Proteins localized at the ribbon synapses of the outer plexiform layer are often structural or synaptic vesicle proteins or are involved synaptic vesicle trafficking.[18,19] The KIAA1549 antibody will recognize both isoforms and thus does not provide additional knowledge on alternative localization of the isoforms. Hypothetically, the long and short isoforms may harbor a unique function at either one of the identified locations. Additional research is required to unravel the functional differences between the short isoform and the ubiquitously expressed long isoform of KIAA1549. Besides localization in the photoreceptor, there is additional evidence for ciliary function is at the molecular level. A recent study based on proximity-dependent biotinylation revealed an interaction between KIAA1549 and TMEM17 (MIM: *614950).[20] TMEM17 is a part of the Meckel syndrome (MKS) protein complex located in the ciliary transition zone, in which it facilitates cilium formation. Also, pathogenic variants in genes encoding proteins in this complex are known to cause (severe) ciliopathies.[21] *TMEM17* pathogenic variants have been reported to cause oral-facial-digital syndrome type 6 (MIM: #277170).[21] The MKS complex contains both cytoplasmic and transmembrane proteins, and functions as a barrier preventing rapid diffusion of transmembrane proteins between cilia and plasma membranes.[22] The interaction between KIAA1549 and TMEM17 was only observed in cells in non-ciliated conditions, which suggests that the interaction is involved in a cilium-related process.[13]

We have studied the role of KIAA1549 in ciliogenesis, by knocking down the expression of the gene in hTERT-RPE1 cells using siRNAs. siRNA-transfected cells did not show a difference in percentage of ciliated cells or ciliumlength, suggesting that KIAA1549 does not have a direct role in the cilium formation explaining the nonsyndromic phenotype observed in the patients of Family A and B, as well as the family of Abu-Safieh et al., which is restricted to the retina. Pathogenic variants that do affect genes essential for ciliogenesis, such as *TMEM17*, would give rise to a phenotype likely affecting multiple organs as in ciliopathies. Transmembrane proteins present at the transition zone are often involved in the sensing and transducing of extracellular signals. Like TMEM17, KIAA1549 is a transmembrane protein, therefore it is plausible that

Chapter 3.1

KIAA1549 may be involved in these processes at the primary cilium of the photoreceptors specifically.[22]

In conclusion, by employing WES we have identified that homozygous frameshift or missense variants in *KIAA1549* are associated with RP in two families. We demonstrated retina-specific expression of the short isoform of *KIAA1549* and provide evidence that damaging variants targeting the long transcript may cause RP by reducing the expression of the short transcript. Moreover, we showed that KIAA1549 resided in the connecting cilium of the mouse retina, thereby providing supporting evidence that KIAA1549 might act as an essential photoreceptor protein.

Web Resources

AlamutVisual version 2.10, http://www.interactive-biosoftware.com/alamut- visual/
BWA version 0.78, https://bio-bwa.sourceforge.net/
CADD, https://cadd.gs.washington.edu/
CoNIFER version 0.2.2, https://conifer.sourceforge.net
dbSNP, https://www.ncbi.nlm.nih.gov/projects/SNP/
ExAC, https://exac.broadinstitute.org/
ExomeDepth version 1.1.10, https://cran.r-project.org/web/packages
Fiji, https://imagej.net/Fiji
GnomAD, https://gnomad.broadinstitute.org/
HaplotypeCaller GATK, https://www.broadinstitute.org/gatk/
Human Splicing Finder V3, https://umd.be/HSF3/
Iranome, https://www.iranome.ir
MutationTaster, https://www.mutationtaster.org
OMIM, https://www.omim.org/
PolyPhen-2, https://genetics.bwh.harvard.edu/pph2/
RetNet, https://sph.uth.edu/retnet/
SIFT, https://sift.jcvi.org/
Uniprot, https://www.uniprot.org/

Chapter 3.1

References

1.   Hamel C. Retinitis pigmentosa. *Orphanet Journal of Rare Diseases.* 2006;1:40-40.
2.   Hartong DT, Berson EL, Dryja TP. Retinitis pigmentosa. *The Lancet.* 2006;368(9549):1795-1809.
3.   Haer-Wigman L, van Zelst-Stams WAG, Pfundt R, et al. Diagnostic exome sequencing in 266 Dutch patients with visual impairment. *European Journal of Human Genetics.* 2017;25(5):591-599.
4.   Abu-Safieh L, Alrashed M, Anazi S, et al. Autozygome-guided exome sequencing in retinal dystrophy patients reveals pathogenetic mutations and novel candidate disease genes. *Genome Research.* 2013;23(2):236-247.
5.   McCulloch DL, Marmor, M.F., Brigell, M.G., Hamilton, R., Holder, G.E., Tzekov, R., and Bach, M. ISCEV Standard for full-field clinical electroretinography (2015 update). *Doc Ophthalmologica.* 2015;130(1):1-12.
6.   Arts HH, Doherty D, van Beersum SEC, et al. Mutations in the gene encoding the basal body protein RPGRIP1L, a nephrocystin-4 interactor, cause Joubert syndrome. *Nature Genetics.* 2007;39:882.
7.   Schindelin J, Arganda-Carreras I, Frise E, et al. Fiji - an Open Source platform for biological image analysis. *Nature methods.* 2012;9(7):10.1038/nmeth.2019.
8.   Hollander AId, Heckenlively JR, van den Born LI, et al. Leber Congenital Amaurosis and Retinitis Pigmentosa with Coats-like Exudative Vasculopathy Are Associated with Mutations in the Crumbs Homologue 1 (CRB1) Gene. *American Journal of Human Genetics.* 2001;69(1):198-203.
9.   Schwarz JM, Cooper DN, Schuelke M, Seelow D. MutationTaster2: mutation prediction for the deep-sequencing age. *Nature Methods.* 2014;11:361.
10.   Adzhubei IA, Schmidt S, Peshkin L, et al. A method and server for predicting damaging missense mutations. *Nature methods.* 2010;7(4):248-249.
11.   Kircher M, Witten DM, Jain P, O'Roak BJ, Cooper GM, Shendure J. A general framework for estimating the relative pathogenicity of human genetic variants. *Nature genetics.* 2014;46(3):310-315.
12.   Desmet F-O, Hamroun D, Lalande M, Collod-Béroud G, Claustres M, Béroud C. Human Splicing Finder: an online bioinformatics tool to predict splicing signals. *Nucleic Acids Research.* 2009;37(9):e67-e67.
13.   Sadighi Z, Slopis J. Pilocytic astrocytoma. *Journal of Child Neurology.* 2013;28(5):625-632.
14.   Gießl A, Trojan P, Rausch S, Pulvermüller A, Wolfrum U. Centrins, gatekeepers for the light-dependent translocation of transducin through the photoreceptor cell connecting cilium. *Vision Research.* 2006;46(27):4502-4509.
15.   Jones DTW, Kocialkowski S, Liu L, et al. Tandem duplication producing a novel oncogenic BRAF fusion gene defines the majority of pilocytic astrocytomas. *Cancer research.* 2008;68(21):8673-8677.
16.   Özgül Rıza K, Siemiatkowska Anna M, Yücel D, et al. Exome sequencing and cis-regulatory mapping identify mutations in MAK, a gene encoding a regulator of ciliary length, as a cause of retinitis pigmentosa. *American Journal of Human Genetics.* 2011;89(2):253-264.
17.   Kevany BM, Palczewski K. Phagocytosis of retinal rod and cone photoreceptors. *Physiology (Bethesda, Md).* 2010;25(1):8-15.
18.   Ullrich B, Südhof TC. Distribution of synaptic markers in the retina: Implications for synaptic vesicle traffic in ribbon synapses. *Journal of Physiology-Paris.* 1994;88(4):249-257.
19.   Mercer AJ, Thoreson WB. The dynamic architecture of photoreceptor ribbon synapses: Cytoskeletal, extracellular matrix, and intramembrane proteins. *Visual neuroscience.* 2011;28(6):453-471.
20.   Gupta Gagan D, Coyaud É, Gonçalves J, et al. A dynamic protein interaction landscape of the human centrosome-cilium interface. *Cell.* 2015;163(6):1484-1499.
21.   Li C, Jensen VL, Park K, et al. MKS5 and CEP290 dependent assembly pathway of the ciliary transition zone. *PLoS Biology.* 2016;14(3):e1002416.
22.   Chih B, Liu P, Chinn Y, et al. A ciliopathy complex at the transition zone protects the cilia as a privileged membrane domain. *Nature Cell Biology.* 2011;14:61.

Appendix 1

Supplementary tables

Table S1. Sequences of primers used for qPCR to determine tissue-specific expression levels

Primer name	Location (NM_001164665)	Sequence (5'-3')
KIAA1549_long_Fw	Exon 2	ACACCAACACTGGCTACTGC
KIAA1549_long_Rev	Exon 3	TGATGTACTCCTGCACAGCTC
KIAA1549_short_Fw	Exon 8a	AGCTTCTGCAATGTGAATGG
KIAA1549_short_Rev	Exon 9	TGTACCGGATTGTCATCTCC

Table S2. siRNAs used for KIAA1549 knockdown in vitro experiments

siRNA ID	Location (NM_001164665)	Sequence (5'-3')
s33562 (siRNA 1)	Exon 3	GGAGUACAUCAUUACAGCAtt
s33563 (siRNA 2)	Exon 5	CAGGGAACGUAUAACCUCAtt

Chapter 3.1

Appendix 2

Supplementary figures
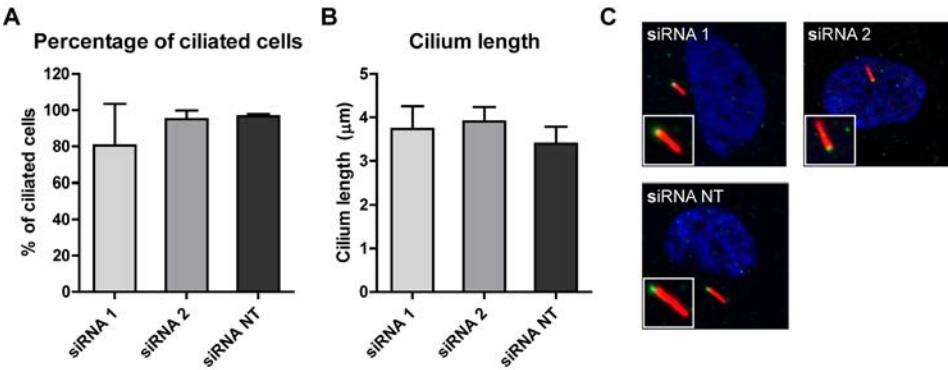
Figure S1. Effect of KIAA1549 knockdown on ciliogenesis.
hTERT-RPE1 cells were transfected with two different siRNAs targeting KIAA1549 (siRNA 1 and 2) and one non-targeting siRNA (siRNA NT). After transfection of the cells, ciliogenesis was induced and immunofluorescence was used for analysis. Primary cilia were stained using an anti-ARL13B antibody (red), and the transition zone was stained using an anti-RPGRIP1L antibody (green). (A) Percentage of ciliated cells calculated and (B) measured cilium lengths for hTERT-RPE1 cells transfected with the different siRNAs. (C) Images of ciliated cells transfected with one of the siRNAs. A close-up picture of the primary cilium is shown to visualize the transition zone.
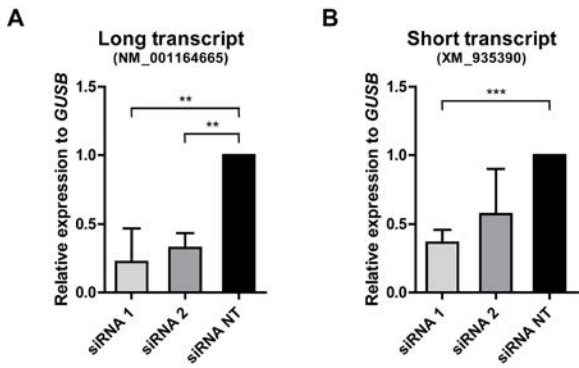
Figure S2. Expression levels of *KIAA1549* transcripts in HEK293 after knockdown using siRNAs.
HEK293 cells were transfected with two different siRNAs targeting the long *KIAA1549* transcript specifically (siRNA 1 and 2) and one non-targeting siRNA (siRNA NT) in two independent experiments. After transfection of the cells, expression levels of both the short and the long transcript were quantified using qPCR. (A) Using siRNA 1 and 2, a significant knockdown of the long *KIAA1549* transcript was established. (B) Also, decreased expression levels of the short transcript were observed, which was found significant for siRNA 1. Significance was calculated using an unpaired t-test, ** p-value < 0.01, *** p-value < 0.001.

Chapter 3.1

The identification of a RNA splice variant in *TULP1* in two siblings with early-onset photoreceptor dystrophy

Sanne K. Verbakel, Zeinab Fadaie, B. Jeroen Klevering, Maria M. van Genderen, Ilse Feenstra, Frans P.M. Cremers, Carel B. Hoyng, Susanne Roosing

Abstract

Background

Early-onset photoreceptor dystrophies are a major cause of irreversible visual impairment in children and young adults. This clinically heterogeneous group of disorders can be caused by mutations in many genes. Nevertheless, to date, 30%-40% of cases remain genetically unexplained. In view of expanding therapeutic options, it is essential to obtain a molecular diagnosis in these patients as well. In this study, we aimed to identify the genetic cause in two siblings with genetically unexplained retinal disease.

Methods

Whole exome sequencing was performed to identify the causative variants in two siblings in whom a single pathogenic variant in *TULP1* was found previously. Patients were clinically evaluated, including assessment of the medical history, slit-lamp biomicroscopy, and ophthalmoscopy. In addition, a functional analysis of the putative splice variant in *TULP1* was performed using a midigene assay.

Results

Clinical assessment showed a typical early-onset photoreceptor dystrophy in both the patients. Whole exome sequencing identified two pathogenic variants in *TULP1*, a c.1445G>A (p. (Arg482Gln)) missense mutation and an intronic c.718+23G>A variant. Segregation analysis confirmed that both siblings were compound heterozygous for the *TULP1* c.718+23G>A and c.1445G>A variants, while the unaffected parents were heterozygous. The midigene assay for the c.718+23G>A variant confirmed an elongation of exon 7 leading to a frameshift.

Conclusion

Here, we report the first near exon RNA splice variant that is not present in a consensus splice site sequence in *TULP1*, which was found in a compound heterozygous manner with a previously described pathogenic variant in two patients with an early-onset photoreceptor dystrophy. We provide proof of pathogenicity for this splice variant by performing an in vitro midigene splice assay, and highlight the importance of analysis of noncoding regions beyond the noncanonical splice sites in patients with inherited retinal diseases.

Introduction

Inherited retinal diseases are characterized by the progressive degeneration of photoreceptor and/or retinal pigment epithelium cells, and are a major cause of irrecoverable visual impairment. Retinitis pigmentosa (RP) encompasses the most common group of inherited retinal diseases, with a worldwide prevalence of approximately 1 in 4,000 individuals.[1] RP is characterized by the rod photoreceptor degeneration that precedes cone photoreceptor degeneration. Patients generally present with night blindness, followed by a gradual constriction of the visual field. The visual acuity typically remains relatively preserved until the final stages of disease. Characteristic fundus features include bone spicule pigmentation, attenuation of retinal vessels, and a waxy pallor of the optic disc. RP can follow all Mendelian patterns of inheritance: autosomal dominant, autosomal recessive and X-linked. In contrast, Leber congenital amaurosis (LCA) is considered the most severe form of inherited retinal disease. It is characterized by severe loss of visual function, nystagmus, photophobia, amaurotic pupils (i.e., sluggish or near-absent pupillary responses), high hyperopia, oculo-digital signs such as poking, pressing, and rubbing the eyes, and severely reduced or absence of electroretinogram responses. LCA is generally inherited in an autosomal recessive manner.[2,3]

Early onset RP and LCA represent a continuum of retinal dystrophies, and are generally differentiated based on the age of onset; patients with an onset after infancy (variably defined as age one or two) are diagnosed as having RP, while LCA generally presents in the first months of life.[4] This arbitrary cut-off point gives rise to large clinical and genetic overlap between both phenotypes. In addition, both RP and LCA display large clinical and genetic heterogeneity. The genetic heterogeneity is illustrated by the 87 genes that have been associated with nonsyndromic RP, and the 25 genes that are associated with LCA (Retnet; available at https://sph.uth.edu/retnet/).[4,5] Ten genes have been associated with both RP and LCA, among which *TULP1* (OMIM: 602280).[5]

The *TULP1* gene has been associated with LCA, early-onset RP and cone(-rod) dystrophy.[6-10] *TULP1* encodes a 542-aa (61kDa) photoreceptor-specific tubby-like protein (i.e., tubby-like protein-1, TULP1) that is likely involved in the transport of several phototransduction proteins from the photoreceptor inner segment to the outer segments, particularly from the opsin (e.g., rhodopsin and cone opsin) and guanylate cyclase carrier pathways (e.g., guanylate cyclase 1 and guanylate cyclase-activating proteins 1 and 2).[11-13]

To date, a molecular diagnosis can be identified by whole exome sequencing (WES) in approximately 60%–70% of RP and LCA patients.[4,14-16] In the remaining cases, the causative variants could be located in a gene that has not yet been associated with early-onset retinal dystrophies. Alternatively, the genetic defect could reside in a gene that has previously been associated with RP, but the mutation may not have been detected using WES because the variant resides in a GC-rich region, concerns a structural variant, or was not covered for another reason. Finally, the pathogenic variant could have been missed because of too stringent variant filtering procedures or because it resides outside of the coding regions and splice sites.

With the advent of therapeutic options for inherited retinal disorders it becomes essential to also obtain a molecular diagnosis in patients without a conclusive genetic diagnosis.

In recent years, various studies have shown the importance of searching for variants beyond the coding and splice site regions. Up to 15% of LCA patients carry a deep-intronic mutation (c.2991+1655A>G) in *CEP290*[17-19] and these patients may benefit from an upcoming treatment with antisense oligonucleotides (AONs)[20](ClinicalTrials.gov NCT03140969). Additionally, studies in Stargardt disease have identified numerous variants leading to an alternative splicing or pseudoexon inclusion in *ABCA4*.[21] In this study, we provide evidence for pathogenicity of the first intronic variant outside of the splice site consensus sequence in *TULP1*, which we coin a near-exon aberrant RNA (NEAR) splice variant, segregating with a previously described pathogenic missense variant in two siblings with early-onset retinal dystrophy.

Methods

Ethical compliance

The study adhered to the tenets of the Declaration of Helsinki and was approved by the local ethics committee. Written informed consent was obtained from both patients and their parents prior to inclusion in this study.

Clinical evaluation

A family with two siblings with an autosomal recessive early-onset retinal dystrophy was clinically examined at the Radboud university medical center in Nijmegen, the Netherlands. Clinical data were obtained from the medical records of the patients. Patients' medical history was registered with special attention for the age at onset, initial symptoms and the course of the disease. In addition, both patients were re-evaluated after the identification of the genetic cause of disease. We performed a detailed ophthalmic examination, which included best-corrected visual acuity, slit-lamp biomicroscopy, and ophthalmoscopy. Fundus photography, spectral-domain optical coherence tomography (SD-OCT; Spectralis HRA+OCT, Heidelberg Engineering, Heidelberg, Germany) and fundus autofluorescence (FAF; HRA+OCT, Heidelberg Engineering, Heidelberg, Germany) imaging were performed. The visual field was assessed using a Goldmann perimeter. Full-field electroretinography (ffERG) recordings were performed according to the International Society for Clinical Electrophysiology of Vision (ISCEV) guidelines and assessed applying local standard values.[22]

Genetic analysis

Genomic DNA was extracted from peripheral lymphocytes according to standard procedures. WES was performed in a certified DNA diagnostic laboratory in both siblings.[14] The exome was enriched using Agilent's SureSelectXT Human all Exon V5 (Agilent Technologies, Santa Clara, CA). Subsequently, next-generation sequencing using an Illumina HiSeq 4000 sequencer

(Illumina, Inc. San Diego, CA), read alignment to the human reference genome (Genome Reference Consortium Human Reference 37/hg19) using Burrows-Wheeler Aligner, and variant calling with the Genome Analysis Toolkit were performed at BGI-Europe (Copenhagen, Denmark). Copy number variants were detected using CoNIFER 0.2.0, and variants were annotated using a custom designed in-house annotation strategy.

Variant prioritizing

Prioritizing candidate variants for causality was based on their presence in both affected siblings, a minor allele frequency of < 0.5% in ExAC, dbSNP and the Nijmegen in-house database consisting of 15,576 individuals, their effect (i.e., nonsense, frameshift, canonical (donor +1 and +2, acceptor -1 and -2) and noncanonical (donor +3 to +6, acceptor -3 to -14) splice site variants), and the occurrence in a homozygous or compound heterozygous state. Moreover, for the remaining heterozygous variants in currently known retinal dystrophy-associated genes we manually assessed the BAM-files to verify if all exons (potentially harboring pathogenic variants) were covered.

The pathogenicity of missense variants was evaluated by combining *in silico* prediction tools, such as SIFT (http://sift-dna.org/), PolyPhen-2 (http://genetics.bwh.harvard.edu/pph2/), and Mutation Taster (http://www.mutationtaster.org/), and by using the PhyloP score (range -14.1–6.4; predicted pathogenic ≥2.7)[23], CADD-PHRED (range 1–99; predicted pathogenic ≥15) (https://cadd.gs.washington.edu/) and Grantham scores (range 0–215; predicted pathogenic ≥80)[24]. The *in silico* prediction of non-canonical splice variants was assessed using algorithms (i.e., SpliceSiteFinder-like,[25] MaxEntScan (http://genes.mit.edu/burgelab/maxent/Xmaxentscan_scoreseq.html), GeneSplicer (https://www.cbcb.umd.edu/software/GeneSplicer/gene_spl.shtml), and Human Splicing Finder (http://www.umd.be/HSF/)) embedded in the Alamut Visual software version 2.10 (Interactive Biosoftware, Rouen, France; http://www.interactive-biosoftware.com).

In vitro midigene splice assay

TULP1 (GenBank: NM_003322.5) is a photoreceptor-specific protein and not expressed in available somatic cells. Therefore, a functional analysis of the putative splice variant c.718+23G>A in *TULP1* was performed using a midigene assay. We designed two midigene constructs with an insert of 6.3 kb, a wild-type and mutant multi-exon splice vector, using a modified protocol of the previously described method (Figure 4).[26] In short, exon 4–11 of *TULP1* of the genomic DNA from a control individual was amplified using forward primer 5'-GGAGATCCCTAGGGTGAGGA-3' and reverse primer: 5'-ATCAAAGCGAGAGGCCCTA-3'. Both primers have an attB1 and attB2 tag at 5' end to enable Gateway cloning. The wild-type construct served as a template to generate the mutant construct of c.718+23G>A by mutagenesis PCR. Subsequently, wild-type and mutant constructs were incorporated into the pCI-NEO-*RHO* Gateway-adapted vector as previously described.[26] This resulted in a wild-type midigene c.718+23G and a mutant midigene c.718+23A. Finally, we transfected HEK293T cells with the wild-type or mutant midigene and studied the

transcripts with reverse transcription–polymerase chain reaction with primers in exons 4 and 11 (RT-PCR) (Forward primer: 5'-GTCTACGCCAGGTTCCTCAG-3' and Reverse primer: 5'-TCCTCGGGACAGATTGGTAG-3').

Results

Clinical findings

Figure 1 shows the pedigree of the two siblings we studied, both were from Dutch ancestry and presented with a retinal dystrophy that we classified as very early-onset forms of RP. An overview of the clinical characteristics at the most recent examination is provided in Table 1. The eldest patient, individual II:1, presented with a fine horizontal nystagmus at the age of three. Subsequently, he developed night blindness that became apparent at the age of five. His visual acuity gradually deteriorated from 20/50 at age five to 20/100 when he was 15 years of age. His younger sister (patient II:2) presented with a subtle horizontal nystagmus at the age of one. Her visual acuity deteriorated from 20/50 at the age of three to 20/60 at age 13, and she also experienced impaired night vision in early childhood. At the most recent examination, both siblings complained of photophobia. In addition, patient II:1 reported photopsias, particularly after a sudden increase in light intensity. Perimetry showed constriction of the visual field from age 11 in patient II:1, with a central island measuring up to 10 degrees at the age of 15 years. In patient II:2, the constriction of the visual field started at age 10 and progressed to a constriction up to 20–30 degrees at the age of 13 years. High hyperopia was present in both siblings, with spherical equivalent refractions ranging from 6.13 to 7.25. Both siblings were in good general health, and no extra-ocular conditions were reported.

Ophthalmoscopy showed peripheral bone spicule pigmentation, attenuated retinal vessels, and small hyperemic optic discs (often found in high hyperopia) in both siblings (Figure 2). Fundus autofluorescence imaging revealed the characteristic hyperautofluorescent ring that represents the transition zone between intact and degenerated photoreceptor outer segments.

M1: c.1445G>A p.(Arg482Gln)
M2: c.718+23G>A p.(Thr241Glyfs*23)
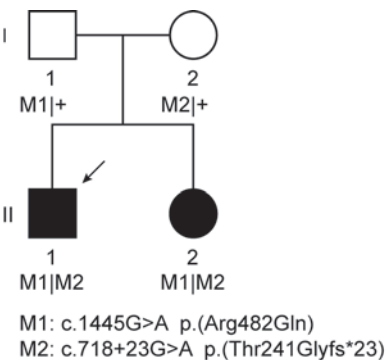
Figure 1. Pedigree of the family included in this study. The variants in *TULP1* segregate with the disease.
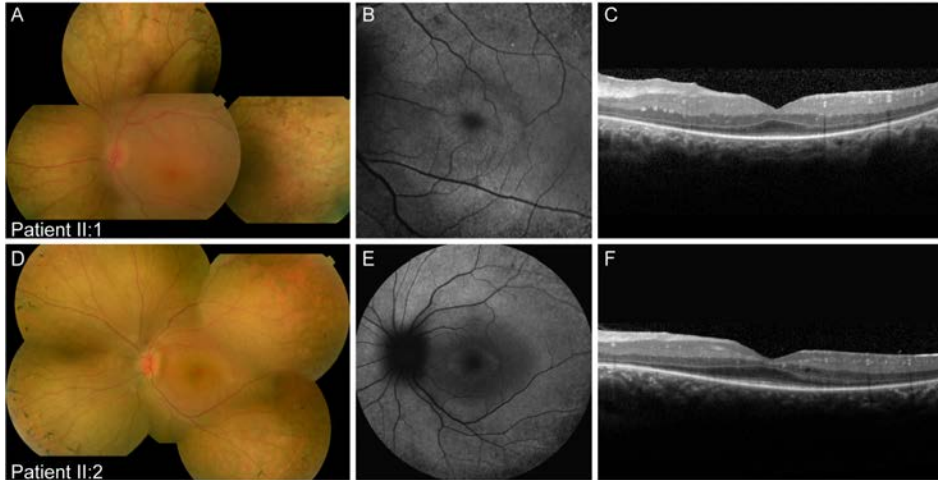
Figure 2. Multimodal images of both siblings. (A-C) Multimodal imaging of the left eye of patient II:1 at the age of 15 years. (A) Composite fundus photograph showing a hyperemic optic disc, sparse bone spicule pigmentation in the periphery, and slightly attenuated vessels. (B) 30° fundus autofluorescence image revealing a characteristic hyperautofluorescent ring, (C) which corresponds to preservation of the ellipsoid zone within the ring, as visible on spectral-domain optical coherence tomography (SD-OCT). In addition, SD-OCT imaging also showed a thickened retina. (D-F) Multimodal imaging of the left eye of patient II:2 at the age of 13 years. (D) Composite fundus photograph showing a small and hyperemic optic disc, attenuation of the retinal vessels, and bone spicule pigmentation in the periphery. (E) 55° fundus autofluorescence image showing a central hyperautofluorescent ring. (F) The SD-OCT scan reveals preserved photoreceptor layers at the fovea, and multiple small intraretinal cysts.

This was confirmed by SD-OCT images that showed an intact ellipsoid zone layer inside the ring, and loss of the outer retinal layers outside of the hyperautofluorescent ring area. In addition, the SD-OCT image revealed diffuse thickening of the retina in patient II:1, which proved refractory to treatment with 125 mg oral carbonic anhydrase inhibitors three times a day. Cystoid macular edema was identified in patient II:2 at age 11. However, in her case, the cystoid macular edema revolved after treatment with carbonic anhydrase inhibitors, and did not recur—or at least in a severely reduced fashion—after sustained treatment with 125 mg oral carbonic anhydrase inhibitors two times a day. Electrophysiological examination at the age of five (patient II:1) and six (patient II:2) demonstrated a generalized photoreceptor dystrophy with severely affected photoreceptor responses in a rod-cone pattern.

Genetic findings

Initial analysis of WES data in patient II:1 detected two heterozygous variants, a c.1445G>A (p.(Arg482Gln)) missense variant in *TULP1* and a c.1567C>T (p.(Arg523*)) nonsense variant in *FAM161A*. Subsequently, WES was performed in patient II:2; she also carried the heterozygous missense variant in *TULP1*, as well as a heterozygous c.3683A>G (p.(Tyr1228Cys)) missense variant in *RPGRIP1*. All coding regions of *TULP1* were covered in the WES data of both siblings, and uncovered exons from *RPGRIP1* and *FAM161A* were Sanger sequenced but did not reveal additional putative pathogenic variants in either sibling. Moreover, no copy number variants were identified in *FAM161A*, *RPGRIP1* or *TULP1* in both individuals. As the *FAM161A* and *RPGRIP1*

Chapter 3.2

173
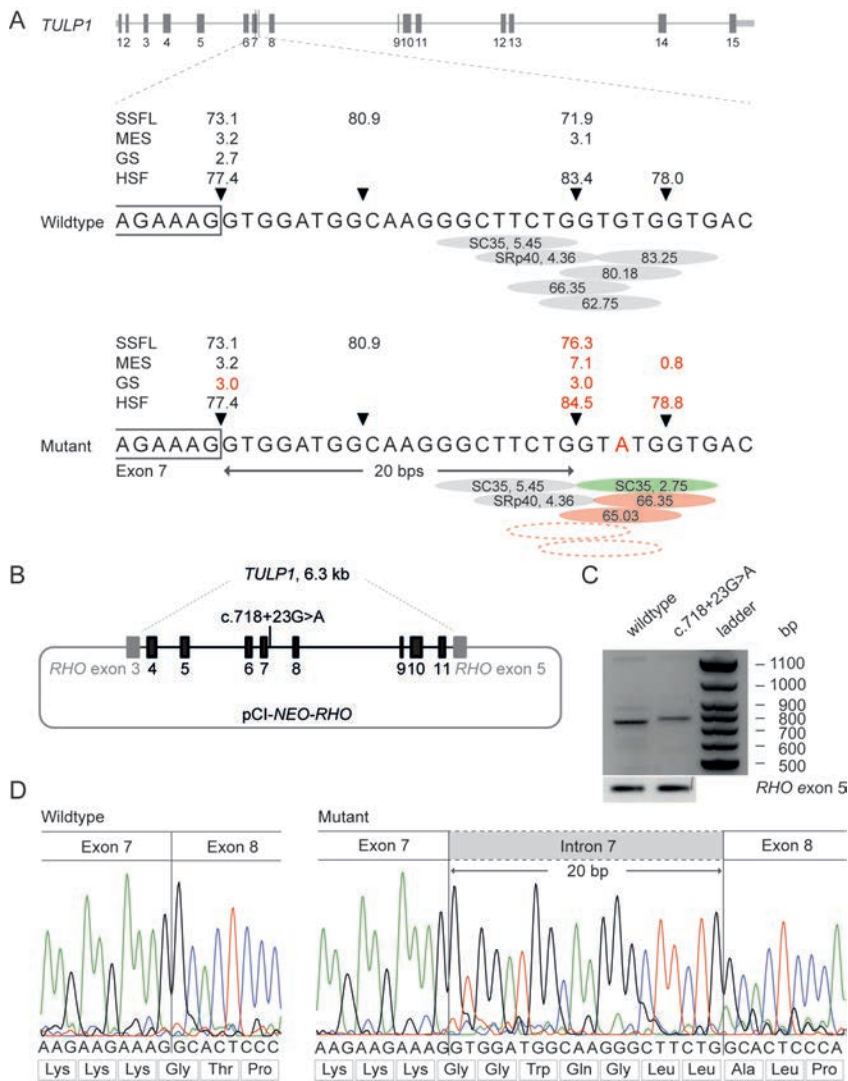
Figure 3. Molecular genetic characterization of the splice effect of the c.718+23G>A variant in *TULP1*. (A) Schematic representation of the *TULP1* gene and enlargement of the wild-type and mutant DNA sequences at the exon-intron boundary of exon 7 of *TULP1*. The SpliceSiteFinder-like (SSFL, range 0–100), MaxEntScan (MES, range 0-12), GeneSplicer (GS, range 0–24) and Human Splicing Finder (HSF, range 0–100) scores for the splice donor site are indicated above the gene. The red "A" highlights the variant c.718+23G>A identified in both siblings. The red numbers represent altered scores compared to the wild-type. The green circle implies a newly recognized SC35 motif. Dotted circles indicate exonic splice silencers no longer present by prediction tools (B) Schematic representation of the mutant pCI-NEO-*RHO* vector, containing exon 4–11 of the *TULP1* gene used to transfect HEK293T cells with a wild-type or mutant midigene. (C) RT-PCR products of the wild-type and mutant midigene showing the expected 832-bp wild-type fragment and a 852-bp fragment of the mutant midigene corresponding to a 20-nucleotide elongation of the mRNA encoded by exon 7. The wild-type fragment was absent in the cells transfected with the mutant midigene. RT-PCR analysis of RHO exon 5 was performed as a control for efficient transfection. (D) Sanger sequence analysis of the RT-PCR fragments confirmed the wild-type and the 20-bp elongation of exon 7 in the mutant.

pathogenic variant were not shared between the siblings, we pursued to study *TULP1* in more detail. The previously described variant c.1445G>A (p.(Arg482Gln) has a CADD-Phred score of 23.2, a PhyloP score of 6.1 and a Grantham score of 43. [7] An expanded analysis beyond the coding regions and putative splice site regions resulted in the identification of a heterozygous intronic variant, c.718+23G>A (Figure 3), found in both siblings. Segregation analysis confirmed that both siblings were compound heterozygous for the c.718+23G>A and c.1445G>A variants, while the unaffected parents were heterozygous (Figure 1). Although the c.718+23G>A variant, based on splice score prediction algorithms, does not alter the nearby splice donor site, this deep-intronic variant increased the splice prediction scores at position c.718+20 when using programs SpliceSiteFinder-like (+4.4%), MaxEntScan (+33.33%), GeneSplice (+12.5%) and Human Splicing Finder (+1.1%) (Figure 3). Additionally, c.718+23G>A introduced a new exonic splice enhancer (ESE) motif recognized by the SC35 exonic splice enhancer at the c.718+21 to c.718+29 positions where a putative splice donor site is already located in the wild-type mRNA, and reduces the number and strength of exonic splice silencer (ESS) motifs present in the reference sequence.

In vitro midigene splice assay
Reverse transcription polymerase chain reaction showed the expected 832-bp wild-type fragment (Figure 3). In contrast, the mutant midigene showed a product that corresponds to a larger fragment, and absence of the wild-type fragment. Sanger sequencing verified that the mutant mRNA product contained a 20-nucleotide elongation of exon 7, which can be explained by the use of a cryptic splice donor site 20 nucleotides downstream of exon 7 (Figure 3). This elongation causes a frameshift and results in early protein truncation (p.(Thr241Glyfs*23)).

Discussion

In the present study, we identified a near-exon aberrant RNA splice variant that we termed a "NEAR" splice variant in *TULP1* in *trans* with a previously described exonic variant in two siblings with early-onset RP. Both siblings showed a nystagmus, night blindness and a reduced visual acuity early in life. Fundus examination at the age of 15 (patient II:1) and 13 years (patients II:2) showed bone spicule pigmentation, attenuation of the retinal vessels and a small, hyperemic optic disc. High hyperopia (i.e., refractive error of more than +5.00 D) was present in both siblings. *TULP1*-associated disease has previously been associated with myopia [6,27-29] and hyperopia.[29,30] However, high hyperopia has only been described in patients with LCA, and is thought to result from impaired emmetropization caused by early-onset visual impairment.[2,30]
Both siblings were diagnosed with early-onset RP based on an onset after the age of one. However, they also show characteristic aspects of LCA such as a nystagmus and hyperopia. The difficulty in classifying such patients arises from the strict and rather arbitrary separation of both entities, when in fact they represent a continuum of retinal dystrophies.

Thus far, three noncanonical splice site variants in the *TULP1* gene (i.e., c.999+5G>C, c.1224+4A>G, and c.1496-6C>A) have been reported in patients with *TULP1*-associated disease.[29,31,32] We identified two pathogenic variants in *TULP1*, a c.1445G>A (p.(Arg482Gln)) missense mutation and an intronic c.718+23G>A variant. The *TULP1* p.(Arg482Gln) mutation, previously described in patients with early-onset RP, alters the structure and function of the Tubby domain, and is expected to affect TULP1 function [7]. To our knowledge, pathogenicity of mutations in *TULP1* such as the c.718+23G>A variant, which we coin as a NEAR splice variant, has not been described before. Our definition of a NEAR splice variant is a variant located outside of the splice site consensus sequence leading to an alteration of the splicing of a nearby exon, whereas a deep-intronic variant often leads to the inclusion or alteration of a cryptic exon.

The consequence of a NEAR splice variant depends on the context of the variant, such as the strength of nearby splice acceptor and splice donor sites, the presence and size of flanking exons, and the effect on the appearance or removal of ESE, ESS, intronic splice enhancer, and intronic splice silencer motifs. To assess the effect of this variant on splicing, we generated a midigene assay which contained exon 4 to 11 of *TULP1*. This analysis showed the use of a cryptic splice donor site 20 bp downstream, which causes a shift of the reading frame resulting in early termination of protein synthesis. The severe nature of the c.718+23G>A NEAR splice variant is supported by the absence of a wild-type fragment in cells transfected with the mutant midigene and corresponds with the severe phenotype observed in the patients.

The donor splice site of exon 7 of the *TULP1* gene contains a fairly weak splice site as indicated by the score of 77.4 for Human Slicing Finder. A natural stronger cryptic splice donor site is present at the c.718+20 position in the wild-type mRNA with a score of 83.4 for the Human Splicing Finder prediction.[33] The presence of ESSs located in and near the c.718+20 position likely explain why the cryptic donor site is not utilized by the splice machinery in wild-type cells. The c.718+23G>A variant, however, shows a decreased number of ESSs in this region, and consequently enables recognition of the putative splice donor site by the spliceosome (http://www.umd.be/HSF3/). In addition, according to ESE predictions, this variant also creates a new binding site for exonic splice enhancer SC35 at the c.718+21 to c.718+29 positions that strengthens this putative splice donor site and generates preference for the c.718+20 donor instead of the canonical splice donor site. This supports the role of ESEs and ESSs in the splicing process, and highlights the importance of these factors when analyzing the pathogenicity of variants within or outside of the coding and splice site regions.

While this is the first intronic variant outside of the splice site consensus sequences deemed pathogenic in *TULP1*, the causality of deep-intronic variants has also been described in nine other retinal dystrophy genes: *ABCA4, CEP290, CHM, OA1, OAT, OFD1, PROM1, PRPF31,* and *USH2A* [17,34-43](www.dbass.soton.ac.uk). Intronic variants are likely to explain a substantial portion of the current genetically unexplained or monoallelic retinal dystrophy cases, and underscore the importance of genetic tests uncovering those regions, such as whole genome sequencing. Future studies with whole genome sequencing will likely increase the number of genetically solved patients. However, the increase in the use of whole genome sequencing will be

accompanied by the detection of a large number of variants of unknown significance, and determining the functional role of these variants will remain a challenge.

The identification of biallelic variants in patients with a retinal dystrophy is essential for eligibility for upcoming genetic therapies. Besides gene augmentation therapy, patients with a *TULP1* NEAR splice variant may benefit from AONs treatment, which can suppress the aberrant splicing effect by binding to the mutated region in the pre-mRNA. To date, proof-of-concept of AONs has been shown in both cell-based models and animal models for four retinal dystrophy genes: *CEP290*,[20, 44-46] *CHM*,[47] RHO,[48] and *USH2A*,[49] and represents a promising therapy for retinal dystrophies.[50]

In conclusion, we identified a pathogenic NEAR splice variant in *TULP1* in trans with a known pathogenic missense variant in two siblings with an early-onset photoreceptor dystrophy in whom analysis of the exonic and consensus splice site regions did not identify the cause of disease. This highlights the importance of investigating noncoding regions in order to obtain a conclusive molecular diagnosis in patients with a hereditary retinal dystrophy.

Chapter 3.2

References

1. Pagon RA. Retinitis pigmentosa. Surv Ophthalmol 1988;33(3):137-77.
2. Weleber RG, Francis PJ, Trzupek KM, Beattie C. Leber Congenital Amaurosis. In: Adam MP, Ardinger HH, Pagon RA, ` et al., eds. GeneReviews (R). Seattle, WA: University of Washington, 1993.
3. den Hollander AI, Roepman R, Koenekoop RK, Cremers FP. Leber congenital amaurosis: genes, proteins and disease mechanisms. Prog Retin Eye Res 2008;27(4):391-419.
4. Kumaran N, Moore AT, Weleber RG, Michaelides M. Leber congenital amaurosis/early-onset severe retinal dystrophy: clinical features, molecular genetics and therapeutic interventions. Br J Ophthalmol 2017;101(9):1147-54.
5. Verbakel SK, van Huet RAC, Boon CJF, et al. Non-syndromic retinitis pigmentosa. Prog Retin Eye Res 2018;66:157-86.
6. den Hollander AI, van Lith-Verhoeven JJ, Arends ML, et al. Novel compound heterozygous TULP1 mutations in a family with severe early-onset retinitis pigmentosa. Arch Ophthalmol 2007;125(7):932-5.
7. Ajmal M, Khan MI, Micheal S, et al. Identification of recurrent and novel mutations in TULP1 in Pakistani families with early-onset retinitis pigmentosa. Mol Vis 2012;18:1226-37.
8. Roosing S, van den Born LI, Hoyng CB, et al. Maternal uniparental isodisomy of chromosome 6 reveals a TULP1 mutation as a novel cause of cone dysfunction. Ophthalmology 2013;120(6):1239-46.
9. Hanein S, Perrault I, Gerber S, et al. Leber congenital amaurosis: comprehensive survey of the genetic heterogeneity, refinement of the clinical definition, and genotype-phenotype correlations as a strategy for molecular diagnosis. Hum Mutat 2004;23(4):306-17.
10. Ullah I, Kabir F, Iqbal M, et al. Pathogenic mutations in TULP1 responsible for retinitis pigmentosa identified in consanguineous familial cases. Mol Vis 2016;22:797-815.
11. Xi Q, Pauer GJ, Marmorstein AD, et al. Tubby-like protein 1 (TULP1) interacts with F-actin in photoreceptor cells. Invest Ophthalmol Vis Sci 2005;46(12):4754-61.
12. Grossman GH, Watson RF, Pauer GJ, et al. Immunocytochemical evidence of Tulp1-dependent outer segment protein transport pathways in photoreceptor cells. Exp Eye Res 2011;93(5):658-68.
13. Hagstrom SA, Watson RF, Pauer GJ, Grossman GH. Tulp1 is involved in specific photoreceptor protein transport pathways. Adv Exp Med Biol 2012;723:783-9.
14. Haer-Wigman L, van Zelst-Stams WA, Pfundt R, et al. Diagnostic exome sequencing in 266 Dutch patients with visual impairment. Eur J Hum Genet 2017;25(5):591-9.
15. Tiwari A, Bahr A, Bahr L, et al. Next generation sequencing based identification of disease-associated mutations in Swiss patients with retinal dystrophies. Sci Rep 2016;6:28755.
16. Zhao L, Wang F, Wang H, et al. Next-generation sequencing-based molecular diagnosis of 82 retinitis pigmentosa probands from Northern Ireland. Hum Genet 2015;134(2):217-30.
17. den Hollander AI, Koenekoop RK, Yzer S, et al. Mutations in the CEP290 (NPHP6) gene are a frequent cause of Leber congenital amaurosis. Am J Hum Genet 2006;79(3):556-61.
18. Coppieters F, Casteels I, Meire F, et al. Genetic screening of LCA in Belgium: predominance of CEP290 and identification of potential modifier alleles in AHI1 of CEP290-related phenotypes. Hum Mutat 2010;31(10):E1709-66.
19. Perrault I, Delphin N, Hanein S, et al. Spectrum of NPHP6/CEP290 mutations in Leber congenital amaurosis and delineation of the associated phenotype. Hum Mutat 2007;28(4):416.
20. Dulla K, Aguila M, Lane A, et al. Splice-Modulating Oligonucleotide QR-110 Restores CEP290 mRNA and Function in Human c.2991+1655A>G LCA10 Models. Mol Ther Nucleic Acids 2018;12:730-40.
21. Albert S, Garanto A, Sangermano R, et al. Identification and Rescue of Splice Defects Caused by Two Neighboring Deep-Intronic ABCA4 Mutations Underlying Stargardt Disease. Am J Hum Genet 2018;102(4):517-27.
22. McCulloch DL, Marmor MF, Brigell MG, et al. ISCEV Standard for full-field clinical electroretinography (2015 update). Doc Ophthalmol 2015;130(1):1-12.
23. Pollard KS, Hubisz MJ, Rosenbloom KR, Siepel A. Detection of nonneutral substitution rates on mammalian phylogenies. Genome Res 2010;20(1):110-21.
24. Grantham R. Amino acid difference formula to help explain protein evolution. Science 1974;185(4154):862-4.
25. Zhang MQ. Statistical features of human exons and their flanking regions. Hum Mol Genet 1998;7(5):919-32.
26. Sangermano R, Bax NM, Bauwens M, et al. Photoreceptor Progenitor mRNA Analysis Reveals Exon Skipping Resulting from the ABCA4 c.5461-10T-->C Mutation in Stargardt Disease. Ophthalmology 2016;123(6):1375-85.
27. Hendriks M, Verhoeven VJM, Buitendijk GHS, et al. Development of Refractive Errors-What Can We Learn From Inherited Retinal Dystrophies? Am J Ophthalmol 2017;182:81-9.
28. Souzeau E, Thompson JA, McLaren TL, et al. Maternal uniparental isodisomy of chromosome 6 unmasks a novel variant in TULP1 in a patient with early onset retinal dystrophy. Mol Vis 2018;24:478-84.
29. den Hollander AI, Lopez I, Yzer S, et al. Identification of novel mutations in patients with Leber congenital amaurosis and juvenile RP by genome-wide homozygosity mapping with SNP microarrays. Invest Ophthalmol Vis Sci 2007;48(12):5690-8.
30. Khan AO, Bergmann C, Eisenberger T, Bolz HJ. A TULP1 founder mutation, p.Gln301*, underlies a recognisable congenital rod-cone dystrophy phenotype on the Arabian Peninsula. Br J Ophthalmol 2015;99(4):488-92.

31. Gu S, Lennon A, Li Y, et al. Tubby-like protein-1 mutations in autosomal recessive retinitis pigmentosa. Lancet 1998;351(9109):1103-4.
32. Hagstrom SA, North MA, Nishina PL, et al. Recessive mutations in the gene encoding the tubby-like protein TULP1 in patients with retinitis pigmentosa. Nat Genet 1998;18(2):174-6.
33. Tang R, Prosser DO, Love DR. Evaluation of Bioinformatic Programmes for the Analysis of Variants within Splice Site Consensus Regions. Adv Bioinformatics 2016;2016:5614058.
34. Bax NM, Sangermano R, Roosing S, et al. Heterozygous deep-intronic variants and deletions in ABCA4 in persons with retinal dystrophies and one exonic ABCA4 variant. Hum Mutat 2015;36(1):43-7.
35. Braun TA, Mullins RF, Wagner AH, et al. Non-exomic and synonymous variants in ABCA4 are an important cause of Stargardt disease. Hum Mol Genet 2013;22(25):5136-45.
36. Naruto T, Okamoto N, Masuda K, et al. Deep intronic GPR143 mutation in a Japanese family with ocular albinism. Sci Rep 2015;5:11334.
37. Carss KJ, Arno G, Erwood M, et al. Comprehensive Rare Variant Analysis via Whole-Genome Sequencing to Determine the Molecular Pathology of Inherited Retinal Disease. Am J Hum Genet 2017;100(1):75-90.
38. Rio Frio T, McGee TL, Wade NM, et al. A single-base substitution within an intronic repetitive element causes dominant retinitis pigmentosa with reduced penetrance. Hum Mutat 2009;30(9):1340-7.
39. Mayer AK, Rohrschneider K, Strom TM, et al. Homozygosity mapping and whole-genome sequencing reveals a deep intronic PROM1 mutation causing cone-rod dystrophy by pseudoexon activation. Eur J Hum Genet 2016;24(3):459-62.
40. Liquori A, Vache C, Baux D, et al. Whole USH2A Gene Sequencing Identifies Several New Deep Intronic Mutations. Hum Mutat 2016;37(2):184-93.
41. Vache C, Besnard T, le Berre P, et al. Usher syndrome type 2 caused by activation of an USH2A pseudoexon: implications for diagnosis and therapy. Hum Mutat 2012;33(1):104-8.
42. Webb TR, Parfitt DA, Gardner JC, et al. Deep intronic mutation in OFD1, identified by targeted genomic next-generation sequencing, causes a severe form of X-linked retinitis pigmentosa (RP23). Hum Mol Genet 2012;21(16):3647-54.
43. van den Hurk JA, van de Pol DJ, Wissinger B, et al. Novel types of mutation in the choroideremia (CHM) gene: a full-length L1 insertion and an intronic mutation activating a cryptic exon. Hum Genet 2003;113(3):268-75.
44. Garanto A, Chung DC, Duijkers L, et al. In vitro and in vivo rescue of aberrant splicing in CEP290-associated LCA by antisense oligonucleotide delivery. Hum Mol Genet 2016;25(12):2552-63.
45. Collin RW, den Hollander AI, van der Velde-Visser SD, et al. Antisense Oligonucleotide (AON)-based Therapy for Leber Congenital Amaurosis Caused by a Frequent Mutation in CEP290. Mol Ther Nucleic Acids 2012;1:e14.
46. Parfitt DA, Lane A, Ramsden CM, et al. Identification and Correction of Mechanisms Underlying Inherited Blindness in Human iPSC-Derived Optic Cups. Cell Stem Cell 2016;18(6):769-81.
47. Garanto A, van der Velde-Visser SD, Cremers FPM, Collin RWJ. Antisense Oligonucleotide-Based Splice Correction of a Deep-Intronic Mutation in CHM Underlying Choroideremia. Adv Exp Med Biol 2018;1074:83-9.
48. Murray SF, Jazayeri A, Matthes MT, et al. Allele-Specific Inhibition of Rhodopsin With an Antisense Oligonucleotide Slows Photoreceptor Cell Degeneration. Invest Ophthalmol Vis Sci 2015;56(11):6362-75.
49. Slijkerman RW, Vache C, Dona M, et al. Antisense Oligonucleotide-based Splice Correction for USH2A-associated Retinal Degeneration Caused by a Frequent Deep-intronic Mutation. Mol Ther Nucleic Acids 2016;5(10):e381.
50. Collin RW, Garanto A. Applications of antisense oligonucleotides for the treatment of inherited retinal diseases. Curr Opin Ophthalmol 2017;28(3):260-6.

Chapter 3.2

Phenotype

Macular dystrophy and cone-rod dystrophy caused by mutations in the RP1 gene: extending the RP1 disease spectrum

Sanne K. Verbakel, Ramon A.C. van Huet, Anneke I. den Hollander, Maartje J. Geerlings, Eveline Kersten, B. Jeroen Klevering, Caroline C.W. Klaver, Astrid S. Plomp, Nieneke L. Wesseling, Arthur A.B. Bergen, Konstantinos Nikopoulos, Carlo Rivolta, Yasuhiro Ikeda, Koh-Hei Sonoda, Yuko Wada, Camiel J.F. Boon, Toru Nakazawa, Carel B. Hoyng, Koji M. Nishiguchi

Abstract

Purpose

To describe the clinical and genetic spectrum of *RP1*-associated retinal dystrophies.

Methods

In this multicenter case series, we included 22 patients with *RP1*-associated retinal dystrophies from 19 families from the Netherlands and Japan. Data on clinical characteristics, visual acuity, visual field, electroretinography (ERG), and retinal imaging were extracted from medical records over a mean follow-up of 8.1 years.

Results

Eleven patients were diagnosed with autosomal recessive macular dystrophy (arMD) or autosomal recessive cone-rod dystrophy (arCRD), five with autosomal recessive retinitis pigmentosa (arRP), and six with autosomal dominant RP (adRP). The mean age of onset was 40.3 years (range 14–56) in the patients with arMD/arCRD, 26.2 years (range 18–40) in adRP, and 8.8 years (range 5–12) in arRP patients. All patients with arMD/arCRD carried either the hypomorphic p.Arg1933* variant positioned close to the C-terminus (8 of 11 patients) or a missense variant in exon 2 (3 of 11 patients), compound heterozygous with a likely deleterious frameshift or nonsense mutation, or the p.Gln1916* variant. In contrast, all mutations identified in adRP and arRP patients were frameshift and/or nonsense variants located far from the C-terminus.

Conclusions

Mutations in the *RP1* gene are associated with a broad spectrum of progressive retinal dystrophies. In addition to adRP and arRP, our study provides further evidence that arCRD and arMD are *RP1*-associated phenotypes as well. The macular involvement in patients with the hypomorphic *RP1* variant suggests that macular function may remain compromised if expression levels of RP1 do not reach adequate levels after gene augmentation therapy.

Retinitis pigmentosa (RP) encompasses a heterogeneous group of inherited retinal dystrophies characterized by rod photoreceptor degeneration that precedes cone photoreceptor degeneration. The *RP1* gene is one of the more than 80 genes associated with RP. Besides *RP1*, seven other RP-genes—*BEST1*, *NR2E3*, *NRL*, *RHD12*, *RHO*, *RPE65*, and *SAG*—have been associated with both autosomal dominant and autosomal recessive modes of inheritance.[1] In general, RP patients with an autosomal recessive inheritance pattern have a more severe disease course compared with patients with autosomal dominant RP (adRP). This also applies to patients with *RP1*-associated RP: autosomal recessive *RP1* patients generally have a lower age of onset compared to autosomal dominant *RP1* patients, as well as a worse long-term prognosis with respect to retaining central vision due to the occurrence of early macular atrophy or cystoid macular edema.[1,2]

The *RP1* gene, mapped to chromosome 8q12.1, contains four exons, three of which are coding, and encodes a photoreceptor-specific microtubule-associated protein that plays a vital role in the architecture of both rod and cone photoreceptor outer segments.[3,4] RP1 is located at the photoreceptor axoneme, where it links outer segment discs to the axonemal microtubules, and thereby regulates the length and stability of the axoneme.[5] The interaction with the microtubules is mediated primarily by two doublecortin (DCX) domains encoded by exons 2 and 3.[5] In addition, RP1 contains a third putative domain, between amino acid residues 486 and 635, that shares homology with the *Drosophilia melangomaster* bifocal (BIF) protein, which is required for normal photoreceptor morphogenesis.[6] *RP1* mutations that are known to cause adRP are clustered in a relatively small region in exon 4 between amino acid residues 500 and 1053,[7] and result in the production of a truncated protein with a presumed dominant-negative activity.[8] In contrast, most mutations located more toward the N- or C-terminus of RP1 result in autosomal recessive RP (arRP).[7]

In 2016, Ellingford et al.[9] identified compound heterozygous mutations in *RP1* (i.e., p.Tyr41His and p.Leu172Arg) in a patient diagnosed with macular dystrophy (MD)/presumed Stargardt disease. However, because this new genotype-phenotype correlation was identified in only a single family, they concluded that reevaluation of the clinical phenotype was warranted.[9] Knowledge about the entire disease spectrum associated with certain genes is important, particularly in view of novel therapeutic options, as the prognosis and disease course between phenotypes may differ markedly. In this study, we report patients diagnosed with MD and cone-rod dystrophy (CRD) in addition to patients with RP, and expand the clinical spectrum associated with mutations in the *RP1* gene.

Chapter 4.1

Methods

Patients

Twenty-two patients (19 families) with a retinal dystrophy and mutations in the *RP1* gene were clinically examined at the Radboud university medical center in Nijmegen, The Netherlands (families A, B, M, N , P, and Q); the Tohoku University Graduate School of Medicine in Sendai, Japan (families C–E, J and L); the Kyushu University Hospital, Fukuoka, Japan (families F and K); the Yuko Wada Eye Clinic, Sendai, Japan (family G); and the Amsterdam UMC, The Netherlands (families H, I, O, R and S). The genetic evaluation was performed between June 2013 and May 2018. Informed consent was obtained from all patients before data collection and additional ophthalmic examinations. The study adhered to the tenets of the Declaration of Helsinki, and was approved by the local ethics committees.

Genetic analysis

In all families, genomic DNA was extracted from peripheral lymphocytes according to standard procedures. The genetic data of the Japanese patients was obtained in context of another study.[10] In short, whole exome sequencing was performed in patients A-II:2, A-II:4, A-II:5, B-II:8, H-II:2, I-II:2, M-II:2, P-II:13 and Q-III:4. The exome data were analyzed using a vision gene panel consisting of 220 (patients H-II:2 and I-II:2), 342 (patient P-II:13), 366 (patient B-II:7), and 395 genes (patients M-II:2 and Q-III:4) or without the use of a gene filter (family A). See Supplementary Table S1 for an overview of the genes included in these panels. Targeted panel sequencing covering 256 (patient R-IV:2) or 266 vision genes (patients O-II:1 and S-III:4) was performed in a certified DNA diagnostic laboratory, with additional Sanger sequencing for all areas with a coverage below 30 reads (Supplementary Table 1). Mutational screening in patient N-III:9 was performed using an arrayed primer extension microarray for autosomal dominant RP (containing 414 variants in 16 genes), according to a previously described protocol.[11] All variants detected by microarray analysis were verified by direct sequencing. Patients C to G and J to L had their *RP1* open reading frame screened by means of Sanger sequencing as previously reported.[10] In addition, molecular inversion probes were used to exclude variants in 109 other inherited retinal dystrophy genes in patient C to F, J and K,[10] and targeted resequencing containing 83 nonsyndromic RP genes was performed in patient L-II:2 (Supplementary Table 1). The pathogenicity of novel missense variants was assessed combining cosegregation analysis and *in silico* prediction tools, including SIFT and Polyphen-2, and by using the PhyloP, CADD-PHRED and Grantham scores. For an extensive description of the genetic analysis, see Appendix 1.

Clinical evaluation

Clinical data were obtained from the medical records of the patients. In addition, three patients (family A) were reevaluated after the identification of the causative *RP1* mutations. We performed a detailed ophthalmic examination, which included visual acuity testing, slit-lamp biomicroscopy, and detailed ophthalmoscopy. Most patients also underwent conventional

fundus photography and/or ultra-widefield fundus imaging (Optos P200Tx; Optos, Dunfermline, UK), Goldmann perimetry, as well as spectral-domain optical coherence tomography (SD-OCT) using a confocal scanning laser ophthalmoscope (Spectralis HRA+OCT; Heidelberg Engineering, Heidelberg, Germany, Cirrus; Carl Zeiss Meditec, Inc., Dublin, CA, or Topcon 3D OCT-2000; Topcon, Inc, Tokyo, Japan). Fundus autofluorescence (FAF) imaging was performed using the Spectralis HRA+OCT 30° x 30° field of view centered on the macula,[12] or the 200° field of view from the ultra-widefield imaging device. All patients underwent full-field ERG, and multifocal electroretinography (mfERG) was performed in patients B-II:8, C-II:2, D-II:1 and E-II:2. Electrophysiological recordings were performed according to the International Society for Clinical Electrophysiology of Vision guidelines and assessed by applying local standard values.[13,14]

Patients were diagnosed based on their (initial) symptoms, fundus abnormalities, ERG findings, and overall course of the disease. They received the diagnosis MD if they experienced central vision loss without symptoms of night blindness, ophthalmoscopy and multimodal imaging revealed no signs of peripheral involvement, in the presence of an intact peripheral visual field, normal to marginally abnormal scotopic ERG responses, and normal to moderately reduced photopic ERG responses. Patients with a panretinal phenotype received the diagnosis CRD or RP, depending on which photoreceptor function was affected first. CRD was diagnosed when the onset of loss of central vision preceded that of night blindness, presence of a central scotoma, no or mild constriction of the visual field, and reduced ERG responses in a cone-rod pattern. Patients were diagnosed with RP when they presented with night blindness, constriction of the visual field, and reduced ERG responses in a rod-cone pattern. The clinical distinction between MD and CRD, however, can be difficult and is sometimes arbitrary in view of the significant clinical overlap. In addition, in individual MD patients the MD may progress in a more generalized disorder that fits the criteria of CRD. In the present study, we therefore grouped the MD and CRD spectrum into a single category for further analysis.

Results

Genetic findings

Genetic analysis detected 16 unique variants in the *RP1* gene, including six newly identified variants, in the 19 families (Figure 1).[10] The novel variants included five nonsense and frameshift mutations, as well as the p.Val190Gly missense variant that is likely pathogenic according to the guideline proposed by the American College of Medical Genetics and Genomics.[15] The variant segregates with the disease (M8, family H), affects a highly conserved amino acid that is located in the DCX domain, is extremely rare in the gnomAD database (1/249046), and is predicted to be pathogenic with a high Grantham score (109/215) and CADD-PRHED score (22.2) including a high SIFT (pathogenic) and PolyPhen-2 score (probably damaging). Heterozygous variants in other inherited retinal dystrophy genes are listed in Supplementary Table S2.

Chapter 4.1
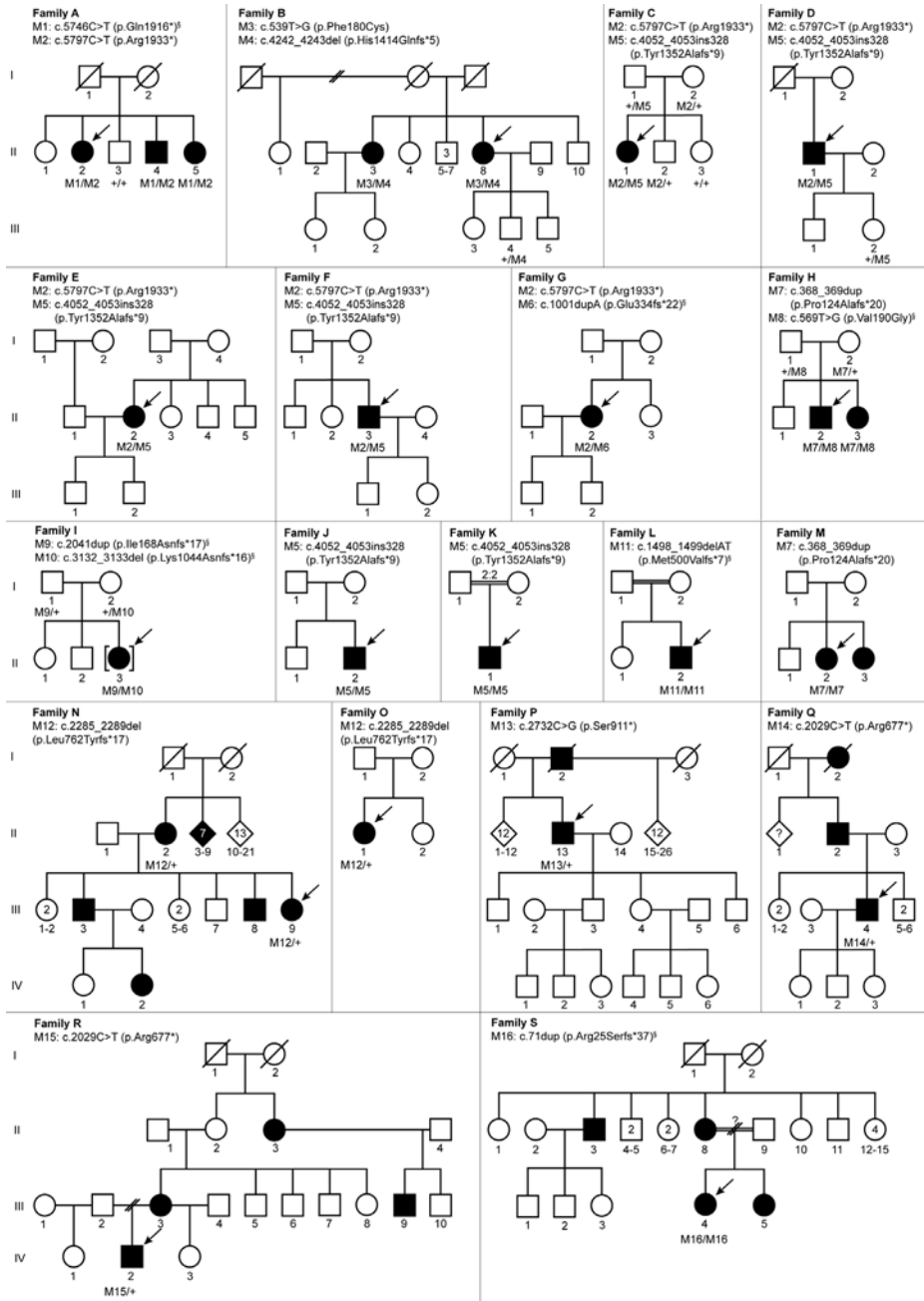
Figure 1. Pedigrees of the families included in this study. Squared boxes indicate men, circles indicate women, filled symbols represent affected persons, and unfilled symbols represent unaffected persons. The plus sign denotes the wild-type allele, and the arrow indicates the proband of the family. Double lines point out consanguineous marriages, the number above the lines indicates the degree of consanguinity. Where relatives were available (family A, B, C, D, H, I, and N), the mutations segregate with the disease. Families C to F, J and K have previously been described by Nikopoulos et al.10 § Novel variants.

Notably, compound heterozygous mutations were identified in all patients with autosomal recessive MD (arMD)/autosomal recessive CRD (arCRD). In particular, the p.Arg1933* mutation, which was identified in a compound heterozygous state with another nonsense or frameshift mutation in six of eight families with arMD/arCRD, from both East Asian and Caucasian origins (Figure 1). The remaining two families with arMD/arCRD (families B and H) carried a heterozygous missense mutation (p.Phe180Cys or p.Val190Gly) located in exon 2, in the region that encodes the DCX domain, together with a frameshift mutation on the second allele. Families with an identical combination of mutations were identified; p.Arg1933* in combination with p. Tyr1352Alafs*9 was previously identified in four families of East Asian origin (families C to F).[10] In contrast, in five out of six families with arRP, homozygous nonsense or frameshift variants were identified. Remarkably, the p.Tyr1352Alafs*9 mutation that was found in patients with arMD/arCRD in combination with p.Arg1933* in families C–F, was identified in a homozygous state in two families with arRP (families J and K), as described.[10] In addition, the p.Pro124Alafs*20 mutation that causes arMD/arCRD in combination with the p.Val190Gly missense mutation in patient H, was also identified in a homozygous state in arRP family N.

Clinical findings

An overview of the individual clinical characteristics of the patients with an *RP1* mutation is provided in the Table. The clinical characteristics stratified by phenotype are provided in Supplementary Table S3. Of the 22 patients, 11 patients (seven arMD and four arCRD patients from eight families) were diagnosed with arMD/arCRD, five patients (five families) with arRP, and six patients (six families) with adRP. Patient B-II:8 was initially diagnosed with a hydroxychloroquine-associated maculopathy as she received treatment with hydroxychloroquine for rheumatoid arthritis. The correct diagnosis of *RP1*-associated MD was made based on her clinical presentation that was atypical for hydroxychloroquine maculopathy, the low cumulative dose of 280 g of hydroxychloroquine, and an affected sister free of the medication. Subsequent molecular genetic testing revealed compound heterozygous mutations in the *RP1* gene in both of them.

Patients with arMD/arCRD

The patients with arMD/arCRD presented the latest of the three phenotypes (mean age of onset 40.3 years; standard deviation (SD) 13.1 years, range 14–56 years), although they showed overlap in age at onset with the adRP patients (mean 26.2 years, SD 8.2 years, range 18–40 years, p=0.025) (Supplementary Table 3). Their initial symptom was a decrease in visual acuity or metamorphopsia, sometimes accompanied by photophobia (patient C-II:2) or night blindness (patient F-II:3 and G-II:2). With progression of the disease, 8 of 11 patients developed photophobia. All patients were myopic (range of spherical equivalents: -9.50 diopters [D] to -0.25D). Biomicroscopy revealed several types of lens opacities in 6 of 11 patients of which patient F-II:3 underwent cataract extraction at the age of 61 years (Table 1, Supplementary Table S3). The course of the visual acuity for each patient is represented in Figure 2. Ten patients

Chapter 4.1
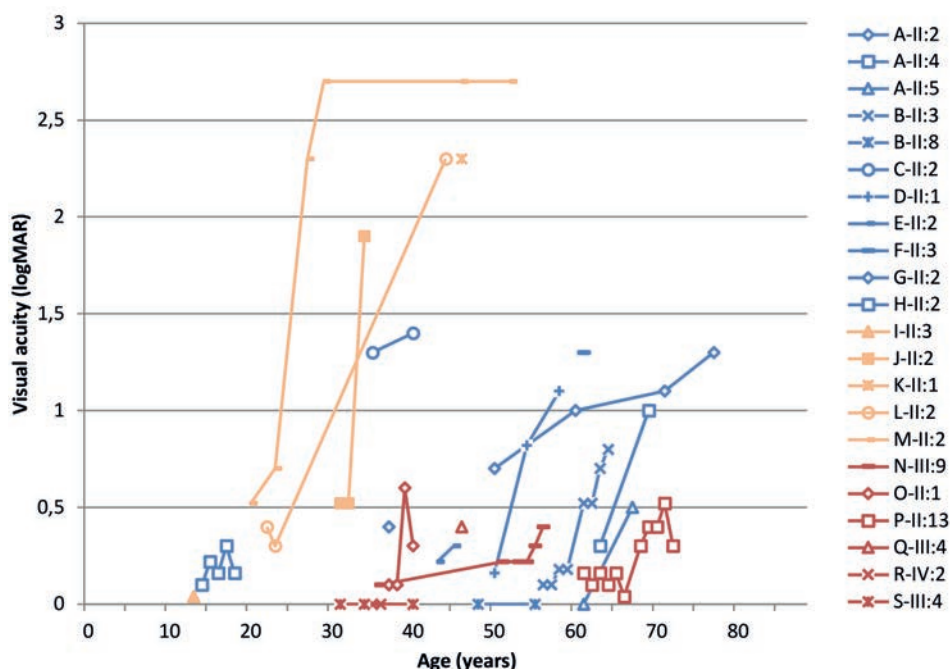
Figure 2. Graph showing the course of visual acuity over time in patients with mutations in the RP1 gene. The three phenotypes are indicated with different colors: arMD/arCRD in blue, arRP in orange, and adRP in red. The visual acuity of the best eye is displayed. Snellen visual acuity was converted into logMAR. A logMAR value of 1.9 was assigned to counting fingers (CF), 2.3 to hand movements (HM), and 2.7 to light perception (LP).

revealed mild to moderate visual acuity impairment during working life, which eventually led to acuity levels of 20/400 in the eighth decade (patient A-II:2). However, patient C-II:2 already had a visual acuity of 20/400 at the age of 41 years. Visual field testing revealed an absolute central scotoma, except for a paracentral scotoma in the left eye of patient B-II:8 (age 55 years), and a central, relative scotoma in patient B-II:3 (age 64 years). In addition, the visual field was mildly constricted in patients B-II:3, F-II:3 and G-II:2.

Ophthalmoscopy showed RPE alterations or atrophy in the macula (Table and Figure 3). Attenuation of the retinal vessels was present in patients A-II:4, B-II:3, F-II:3 and G-II:2, focal bone spicule pigmentations were observed in patient F-II:3, and a single nummular pigmentation in patient G-II:2. A bull's eye maculopathy was noticed in the left eye of patient B-II:8 (age 55) and both eyes of patient E-II:2 at the most recent examination. In patient A-II:5, the bull's eye maculopathy had progressed to macular atrophy with foveal involvement (Figure 4). A posterior staphyloma was visible in patient A-II:2 with spherical equivalents of -8.38/-8.00D. SD-OCT images revealed loss of the outer retinal layers in the macula, with sparing of the foveal photoreceptors in the patients with a bull's eye maculopathy and the left eye of patient B-II:3 (age 64), in which the photoreceptors and RPE at the fovea were preserved in a foveal sparing-like pattern (Figure 3F). The right eye of patient B-II:3 initially showed foveal sparing at the age

of 56 years, although shortly afterward the foveal cells degenerated as well, with a corresponding loss in visual acuity. FAF imaging showed a round to oval zone of reduced FAF or a speckled pattern of alternating normal and decreased FAF, bordered by a band of increased FAF (Figure 3); except for patient E:II-2, in whom an oval zone of increased FAF was visible without a reduced autofluorescence signal. FAF images of patients F-II:3 and G-II:2 were not acquired. Full-field ERG ranged from normal rod and cone responses to patients in whom both cone and rod responses were moderately or severely reduced (Table). The mfERG, performed in patients B-II:8, C-II:2, D-II:1 and E-II:2, was severely reduced in all patients except for patient B-II:8 in whom a decreased response in the parafoveal ring was visible in the right eye and moderately reduced responses in the left eye.

Autosomal recessive RP

The arRP patients were affected at the earliest age, with a mean age of onset of 8.8 years and an onset at the age of only 5 years in the youngest patient (SD 2.8; range 5–12 years; Supplementary Table S3). The initial symptom in the arRP patients was night blindness in all cases and all patients were myopic (range of spherical equivalents: -9.00D to -1.63D; Table, Supplementary Table S3). Despite their young age, all four patients for whom data were available already showed lens opacities at a mean age of 33 years. The visual acuity deteriorated from adolescence or early adulthood to levels of light perception in the sixth decade of life and constriction of the visual field with a residue of less than 10 degrees at the most recent examination was present in three of four patients (Table 1, Figure 2).

Ophthalmoscopy showed the three hallmark RP signs—bone spicule pigmentations, attenuation of the retinal vessels, and pallor of the optic disc—often accompanied by profound peripheral RPE atrophy. In addition, macular atrophic lesions were present in four of five patients, with sparing of the fovea in two of them (Table 1). This was confirmed by an intact ellipsoid zone layer in the fovea on SD-OCT (Figure 3R, Supplementary Table S3). Finally, ERG responses were severely reduced or nonrecordable under scotopic and photopic conditions in all RP patients.

Autosomal dominant RP

Patients with adRP presented with night blindness, at a mean age of 26.2 years (SD 8.2; range 18–40 years). Five of six patients were myopic (range of spherical equivalents: -10.00 to +4.00), except for patient O-II:13 who was hyperopic with spherical equivalents of +1.50D and +4.00D (Table). Biomicroscopy revealed several types of lens opacities in four of six patients of whom three patients underwent cataract extraction (Table, Supplementary Table S3). The visual acuity was relatively preserved, as all patients retained a visual acuity of 20/80 or better, even at the age of 72 (patient O-II:13) (Figure 2, Supplementary Table S3). However, the visual field showed severe constriction with a central residue of less than 10 degrees in two of six patients at a mean age of 48 years (Table, Supplementary Table S3).

Table. Clinical features of patients carrying pathogenic mutations in *RP1*.

ID/Sex/Age of onset(y)/Age Race	Initial symptom	Visual acuity		SER†		Lens status
		RE	LE	RE	LE	
Macular dystrophy/cone-rod dystrophy						
A-II:2/F/31/77 Caucasian	Decrease in VA/ metamorphopsia	20/400	20/400	-8.38	-8.00	Mild PSC, severe cortical and nuclear cataract
A-II:4/M/50/69 Caucasian	Decrease in VA	20/200	20/200	-2.00	-2.00	Cortical and nuclear cataract
A-II:5/F/45/67 Caucasian	Metamorphopsia	20/500	20/63	-5.50	-4.88	Cortical and nuclear cataract, mild PSC
B-II:3/F/56/64 Caucasian	Decrease in VA	20/110	20/125	-2.00	-1.00	Mild cortical and nuclear cataract
B-II:8/F/55/55 Caucasian	Decrease in VA	20/400	20/17	-1.00	-0.50	Clear
C-II:2/F/25/41 East Asian	Decrease in VA/ photophobia	20/500	20/400	-9.00	-9.50	Clear
D-II:1/M/44/54 East Asian	Decrease in VA	20/222	20/133	-2.50	-2.50	Clear
E-II:2/F/36/43 East Asian	Decrease in VA	20/33	20/50	-0.25	-0.25	Clear
F-II:3/M/50/61 East Asian	Decrease in VA/ night blindness	20/630	20/400	-0.50	-2.50	Moderate cortical and mild nuclear cataract; extracted at 60y
G-II:2/F/37/37 East Asian	Decrease in VA/ night blindness	20/50	20/200	-1.25	-1.00	Clear
H-II:2/M/14/18 Caucasian	Decrease in VA	20/28	20/50	-3.00	-2.00	Clear
Autosomal recessive retinitis pigmentosa						
I-II:3/F/11/13 Caucasian	Night blindness	20/25	20/22	-2.13	-1.63	Unknown
J-II:2/M/6/32 Caucasian	Night blindness	20/67	LP	-4.00	-4.50	Mild nuclear cataract

Ophthalmoscopy results	ERG results		Goldmann perimetry	Dx	Mutation(s)
	Scot	Phot			
Well-demarcated area of central and peripapillary chorioretinal atrophy. Normal aspect of retinal vessels and optic disc. Posterior staphyloma LE>RE.	SN	MR	Central scotoma	arMD	p.Gln1916* p.Arg1933*
Well-demarcated area of central and peripapillary chorioretinal atrophy. Normal optic disc, mild attenuation of retinal veins. No intraretinal hyperpigmentation.	N	N	Central scotoma	arMD	p.Gln1916* p.Arg1933*
Macular and peripapillary atrophy. Normal aspect of vasculature and optic disc. No intraretinal hyperpigmentation.	N	N	Central scotoma	arMD	p.Gln1916* p.Arg1933*
Severe atrophy and gliosis in the macula BE, with foveal sparing in the LE. Peripapillary atrophy, attenuated vessels, and no intraretinal hyperpigmentation.	SR	SR	Slightly constricted VF (RE>LE), moderate central sensitivity loss	arCRD	p.Phe180Cys p.His1414Glnfs*5
Well-demarcated area of macular atrophy in the RE, and RPE alterations with a bull's eye configuration in the LE. Normal aspect of the retinal vessels and optic disc. No intraretinal hyperpigmentation.	N	SN	Central scotoma RE, paracentral scotoma LE	arMD	p.Phe180Cys p.His1414Glnfs*5
RPE alterations in the macula with small, parafoveal areas of atrophy. Normal aspect of the optic disc and retinal vessels. No intraretinal hyperpigmentation.	SN	MR	Central scotoma	arMD	p.Arg1933* p.Tyr1352Alafs*9
RPE alterations in the macula with small, parafoveal areas of RPE atrophy. Peripapillary atrophy. Normal aspect of the optic disc and retinal vessels. No intraretinal hyperpigmentation.	SN	MR	Central scotoma	arMD	p.Arg1933* p.Tyr1352Alafs*9
Granular pigment alterations in the macula in a bull's eye pattern. Normal aspect of the optic disc and retinal vessels. No intraretinal hyperpigmentation.	SN	MR	Central scotoma	arMD	p.Arg1933* p.Tyr1352Alafs*9
Macular atrophy, mild attenuation of retinal vessels, nummular hyperpigmentation LE.	MR	MR	Central scotoma and mild VF constriction	arCRD	p.Arg1933* p.Tyr1352Alafs*9
Macular atrophy, mild attenuation of retinal vessels. Sporadic nummular pigmentation in LE.	SR	SR	Central scotoma and VF constriction (nasal>temporal)	arCRD	p.Arg1933* p.Glu334fs*22
Mild RPE alterations in the macula. Periphery normal.	MR	MR	Intact peripheral VF	arCRD	p.Pro124Alafs*20 p.Val190Gly
Bone spicule pigmentation, attenuated vessels, pallor op the optic disc, and peripheral atrophy.	NR	SR	Constricted VF to 10-15°	arRP	p.Ile168Asnfs*17 p.Lys1044Asnfs*16
Macular atrophy, attenuation of retinal vessels, bone spicule pigmentation, and pallor of the optic disc.	NR	NR	Constricted VF <10°	arRP	p.Tyr1352Alafs*9 p.Tyr1352Alafs*9

Chapter 4.1

ID/Sex/Age of onset(y)/Age Race	Initial symptom	Visual acuity		SER†		Lens status
		RE	LE	RE	LE	
K-II:1/M/12/46 East Asian	Night blindness	HM	HM	-1.25	-2.00	PSC and ASC; extracted at 45y
L-II:2/M/10/22 East Asian	Night blindness	20/67	20/50	-5.50	-5.25	Congenital coronary cataract BE
M-II:2/F/5/52 Caucasian	Night blindness	LP	LP	-9.00	-8.25	Mild PSC, mild cortical and nuclear cataract
Autosomal dominant retinitis pigmentosa						
N-III:9/F/18/56 East Asian	Night blindness	20/50	20/50	-9.38	-10.00	Moderate nuclear cataract; extracted at 55y
O-II:1/F/childhood/40 Caucasian	Night blindness	20/66	20/40	-5.75	-5.50	Mild cataract
P-II:13/M/40/72 Caucasian	Night blindness	20/40	20/63	+1.50	+4.00	Moderate nuclear cataract; extracted at 70y
Q-III:4/M/25/46 African	Night blindness	20/55	20/46	-4.00	-4.00	Extracted at 34y
R-IV:2/M/25/35 Caucasian	Night blindness	20/20	20/20	-1.25	-2.25	Clear
S-III:4/F/23/40 Caucasian	Night blindness	20/20	20/34	-3.38	-3.38	Clear

All features are present symmetrically, unless mentioned otherwise. ad = autosomal dominant; ar = autosomal recessive; ASC = anterior subcapsular cataract; BE = both eyes; CRD = cone-rod dystrophy; Dx = final diagnosis; ERM = epiretinal membrane; F = female; HFA = Humphrey field analyzer; HM = hand movements; LE = left eye; LP = light perception; phot = photopic; PSC = posterior subcapsular cataract; RE = right eye; M = male; MD = macular dystrophy; MR = moderately reduced; N = normal; NP = not performed; NR = non-recordable; RP = retinitis pigmentosa; scot = scotopic; SER = spherical equivalent refraction; SN = subnormal; SR = severely reduced; VA = visual acuity; VF = visual field. † If cataract surgery has been performed, the preoperative spherical equivalent was reported.

	Ophthalmoscopy results	ERG results		Goldmann perimetry	Dx	Mutation(s)
		Scot	Phot			
	Profound panretinal degeneration, abundant bone spicule pigmentation, and severely attenuated vessels. Vascular sheathing LE.	NP	NP	Constricted VF <10°	arRP	p.Tyr1352Alafs*9 p.Tyr1352Alafs*9
	Bone spicule pigmentation, attenuated retinal vessels, pallor of the optic disc, and central RPE alterations with small islands of macular atrophy.	SR	SR	Constricted VF <10°	arRP	p.Met500fs*33 p.Met500fs*33
	Generalized retinal dystrophy with macular atrophy, bone spicule pigmentation, attenuated retinal vessels, and waxy pallor of the optic disc.	NR (46y)	NR (46y)	No VF measurable	arRP	p.Pro124Alafs*20 p.Pro124Alafs*20
	Tessellated fundus with RPE atrophy in the periphery, dense nummular and bone spicule pigmentation, severely attenuated retinal vessels, and waxy pallor of the optic disc.	NR (51y)	NR (51y)	Constricted VF to 10° with a small temporal residue	adRP	p.Leu762Tyrfs*17
	Profound atrophy with some sparing of the center, bone spicule pigmentation, attenuated retinal vessels, and pallor of the optic disc.	NR (36y)	SR (36y)	Constricted VF to 10°, with a inferonasal residue (RE) and temporal residue (LE)	adRP	p.Leu762Tyrfs*17
	Profound (mid-)peripheral atrophy, extensive bone spicule and nummular pigmentation, severe attenuation of retinal vessels, and waxy pallor of the optic disc.	NR (71y)	NR (71y)	Constricted VF to 15° (RE) and 20° (LE)	adRP	p.Ser911*
	Profound bone spicule pigmentations, severe attenuation of retinal vessels, peripapillary atrophy and some (waxy) pallor of the optic disc.	NR	NR	Constricted VF to 5° (RE) and 3° (LE)	adRP	p.Arg677*
	Bone spicule pigmentation in the midperiphery (particularly nasal retina), mild attenuation of the retinal vessels, normal aspect of the optic disc. Mild ERM right eye.	NP	NP	Constricted VF <10°	adRP	p.Arg677*
	Bone spicule pigmentation, attenuated retinal vessels, generalized retinal atrophy with foveal sparing.	NR	SR	HFA 30-2: central residue	adRP	p.Arg25Serfs*37

Chapter 4.1

195
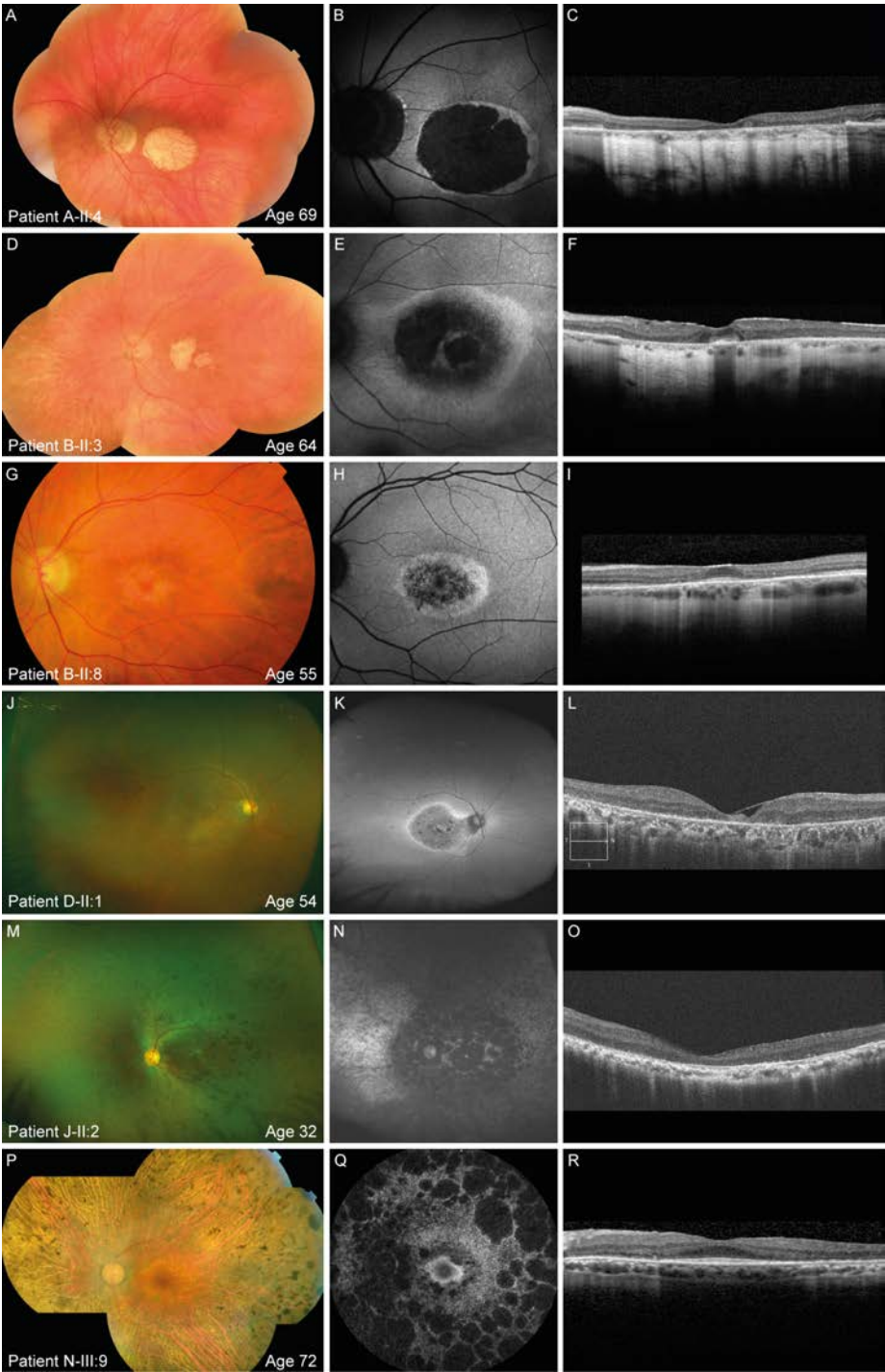
The patients with adRP also showed bone spicule pigmentation and attenuation of the retinal vessel, often accompanied by profound peripheral RPE atrophy and macular atrophy in four of six patients (Table). However, the fovea was spared from the atrophic lesions in all patients (except for the left eye of patient O-II:1). Patient O-II:1 previously underwent a pars plana vitrectomy with peeling of the internal limiting membrane in both eyes for macular holes. Cystoid macular edema was present in patient Q-III:4, with a moderate response to oral carbonic anhydrase inhibitors. Finally, ERG responses were nonrecordable under scotopic conditions and severely reduced or nonrecordable under photopic conditions.

◀ **Figure 3.** Multimodal images of patients with mutations in RP1. (A–C) Multimodal images of the left eye of patient A-II:4. (A) Composite fundus photograph showing a well-demarcated area of chorioretinal atrophy involving the fovea. (B) This area corresponds with an oval zone of absent FAF, bordered by a small residual band of increased FAF. (C) SD-OCT scan revealing loss of the outer retinal layers in the macula. (D–F) Multimodal imaging of the left eye of patient B-II:3. (D) Composite fundus photograph showing macular atrophy, attenuated retinal vessels, and no hyperpigmentation. (E) FAF image revealing decreased autofluorescence surrounded by a hyperautofluorescent ring. (F) SD-OCT scan showing preservation of the RPE, ellipsoid zone and external limiting membrane layer in the fovea, and an epiretinal membrane. (G–I) Multimodal imaging of the left eye of patient B-II:8, at the age of 55 years. (G) Fundus photograph showing a bull's eye maculopathy, a normal aspect of the optic disc and vasculature, and no intraretinal hyperpigmentation. (H) FAF shows a corresponding oval area of speckled hyper- and hypoautofluorescence, surrounded by a ring of hyperautofluorescence. (I) SD-OCT image revealing the parafoveal loss of outer retinal layers with preservation of the ellipsoid zone and external limiting membrane layer in the fovea. (J–L) Multimodal imaging of the right eye of patient D-II:1. (J) Ultra-widefield fundus photograph showing RPE alterations in the macula, peripapillary atrophy, no hyperpigmentations, and a normal aspect of the optic disc and retinal vessels. (K) Ultra-widefield FAF image showing a speckled pattern of hyper- and hypoautofluorescence, surrounded by a band of increased FAF. (L) OCT scan showing generalized loss of photoreceptor inner and outer segments, and an epiretinal membrane. (M–O) Multimodal imaging of the left eye of patient J-II:2. (M) Ultra-widefield fundus photograph showing RPE atrophy, bone spicule pigmentation, and attenuation of the retinal vessels. (N) Autofluorescence image revealing decreased autofluorescence in the macula and along and surrounding to the vascular arcades. (O) SD-OCT scan showing generalized loss of the outer retinal layers in the macula. (P–R) Multimodal imaging of the left eye of patient N-III:9. (P) Composite fundus photograph showing profound peripheral atrophy, severe attenuation of retinal vessels, extensive bone spicule and nummular pigmentation, and waxy pallor of the optic disc. (Q) FAF image showing a hyperautofluorescent ring in the macula, surrounded by a speckled pattern of hyper- and hypoautofluorescence, and nummular areas of decreased macular and peripheral autofluorescence. (R) SD-OCT scan revealing the preservation of the photoreceptor layer at the fovea.
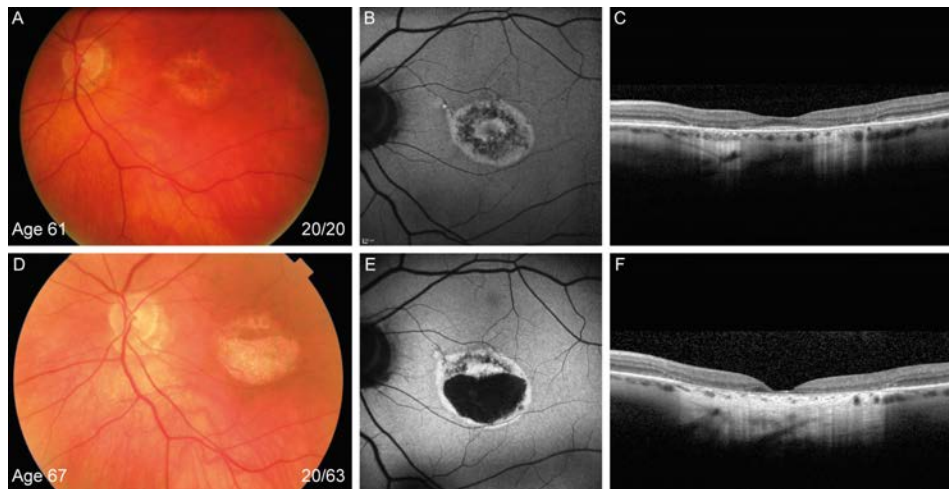
Figure 4. Multimodal images of the left eye of patient A-II:5 over an interval of 6 years. (A) Fundus photograph showing a bull's eye maculopathy, some peripapillary atrophy, and a normal aspect of the optic disc and retinal vessels. (B) The FAF image reveals an oval area of hyperautofluorescence containing a ring of hyper-and hypoautofluorescence. (C) Horizontal SD-OCT showing perifoveal loss of the outer retinal layers. (D) Fundus photograph 6 years later showing macular atrophy, and (E) FAF showing the corresponding area of hypoautofluorescence surrounded by a zone of increased autofluorescence. (F) The OCT scan shows the loss of the outer retinal layers that now also involves the fovea.

Discussion

Mutations in the *RP1* gene have previously been described in patients with adRP and arRP. In the present study, we provide a detailed clinical description of these phenotypes and report two additional *RP1*-associated diagnoses: arMD and arCRD, which may represent a single spectrum of retinal degeneration.

The patients with *RP1*-associated arMD/arCRD presented with a decrease in visual acuity or metamorphopsia, generally first noticed in the fourth decade, which eventually progressed to legal blindness. Considerable macular abnormalities were observed at the most recent examination including a bull's eye maculopathy in two patients. This bull's eye maculopathy may eventually progress to macular atrophy with foveal involvement, as was observed in patient A-II:5. Unfortunately, longitudinal data of the other patients to confirm this hypothesis were not available.

MD and CRD may show large overlap in clinical and genetic findings. This overlap also occurs in time: an MD phenotype can eventually progress to a more generalized disorder and converge into a CRD phenotype. This may explain the intrafamilial differences in family B, as patient B-II:8 shows abnormalities limited to the macular region, whereas her older sister displays generalized disease, which may represent a later disease stage. It might also explain the more severe phenotype in patient F-II:3, who carries the same mutations as the younger patients C to E with less severe disease. In addition, the mean age of onset of both phenotypes was the same

(p=0.817). Therefore, arMD and arCRD might represent the longitudinal progression of macular/ cone predominant *RP1*-associated disease. Nevertheless, some patients may never show progression to a CRD phenotype and other (genetic) modifiers may also exert their effect on the final phenotype. Because the focus of our manuscript lies on the description of patients with a phenotype that does not match the existing phenotypes with predominant rod involvement, we have combined them into the all-embracing term "arMD/arCRD".

The arMD/arCRD shows similarities with other MDs (e.g., central areolar choroidal dystrophy and Stargardt disease), multifocal pattern dystrophy simulating Stargardt disease, and cone dystrophies and, because of its later age of onset, can mimic AMD.[16-18] It is, however, important to distinguish these disorders to provide the patient with valuable and correct prognostic information and accurate treatment. An adequate family history, the absence of drusen, and the symmetrical presentation of the macular atrophy can help the clinician in distinguishing hereditary forms of MDs from AMD.[17] The absence of irregular yellowish (pisciform) and/or hyperautofluorescent flecks can help to differentiate *RP1*-associated disease from Stargardt disease, pseudo-Stargardt and certain cases of central areolar choroidal dystrophy, and ERG responses can help to differentiate from cone dystrophies.

The phenotype of the RP patients was in accordance with earlier reports on RP caused by *RP1* mutations in literature. The five patients with arRP experienced night blindness in the first or second decade of life and showed early involvement of the macular region, whereas the age of onset in the six patients with adRP was between the second and fourth decades, and the fovea remained relatively intact during the course of the disease.[1,2] Myopia, in varying degrees, is a common feature, and was found in 96% of patients. This association of myopia and *RP1*-related disease has previously been described, particularly in arRP patients.[19,20]

Together, these four retinal dystrophies now form the spectrum of *RP1*-associated disease. It is however important to realize that the RP phenotypes are not simply a more extensive form of the more centrally located form of *RP1*-associated disease. This is illustrated by the visual acuity in the adRP patients that can remain relatively preserved even in advanced RP cases as well as the different predominantly affected photoreceptors

The phenotype is, to a large extent, determined by the location and severity of the mutations in the *RP1* gene. Several classifications of mutations have been proposed.[7,21,22] In Supplementary Figure S1, we provide the latest overview of mutations and their location. The mutations responsible for adRP reside in a hotspot region in exon 4 between amino acid residues 500 and 1053, and are expected to result in a truncated protein with dominant-negative activity.[8] In contrast, arRP is caused by the presence of two nonsense or frameshift mutations in *RP1*. Patients with arMD/arCRD carry a heterozygous variant that is expected to have a mild effect on protein function (p.Phe180Cys, p.Val190Gly, or p.Arg1933*) in combination with a more severe nonsense or frameshift mutation, or a combination of two predicted mild variants such as p. Gln1916* and p.Arg1933* in family 1 and the compound heterozygous missense variants (p. Tyr41His and p.Leu172Arg) reported by Ellingford et al. in a single MD patient (Figure 1).[9] The p.Arg1933* variant—a recurrent variant in the Japanese population (allele frequency: 0.6%)—

does not cause a retinal dystrophy in homozygous carriers, at least not before the age of 80 years.[10] Although, in combination with a pathogenic variant such as p.Glu334fs*22, p. Tyr1352Alafs*9 or another likely hypomorphic variant p.Gln1916*, the effect of this hypomorphic allele seems to be sufficient to cause retinal disease (Figure 1).

Although these findings are consistent within our study, there are reports, albeit with limited clinical information, that conflict with our findings. For example, p.Arg1933* was found in trans with the p.Tyr834* nonsense variant in a patient with arRP.[23] In addition, other previously reported variants, such as p.D202E, p.I1988Nfs*3, and p.I2061Sfs*12, could also be predicted to be mild or hypomorphic variants considering their location; however, they have been associated with arRP, although the clinical phenotype has not been described in detail.[23-25] The explanation for this clinical heterogeneity remains to be elucidated, but might be explained by additional (genetic-) modifying factors, the presence of a structural variant or a variant in the non-coding regions of *RP1*, pathogenic variants in another RP gene, or inaccurate phenotyping, the latter of which should be considered particularly in advanced RP and CRD, in which the distinction can be difficult and depends on patients' self-reported disease course. A potential genetic modifier for *RP1*-associated disease may be RP1L1, because these proteins have synergistic roles in the photoreceptor axoneme.[26] However, we did not find any rare variants in the *RP1L1*, although intronic or structural variants cannot be excluded (Supplementary Table S2).

RP1 is an interesting candidate for gene therapy, because of its relatively high prevalence in RP.[1] However, important challenges must be overcome before gene therapy for *RP1* can reach the clinic. For example, knowledge about the natural course of the disease is required to be able to evaluate treatment efficacy, particularly in view of the different phenotypes. In addition, in case of gene augmentation therapy, the maximum cargo capacity of the AAVs (~4.7 kb) is too limited to fit the *RP1* gene (6.5 kb),[27,28] and the optimal expression levels of the RP1 protein need to be determined.[8] This could be more important than previously anticipated if our hypothesis that a hypomorphic variant in combination with a deleterious variant causes arMD/arCRD is correct. Insufficient dosage of the *RP1* gene by gene transfer may mimic this condition and could in that case result in the development of an iatrogenic MD. Obviously, this would be a serious concern when treating arRP patients with preserved macular function with the goal to halt the progression of central visual field loss. Although patients with adRP might also benefit from an elevation of wild-type RP1 levels,[8] the mutant protein that possesses dominant negative activity remains present in the cell and competes with the wild-type. Therefore, other genetic therapies such as treatment with antisense oligonucleotides, of which proof-of-concept has been shown in an animal model with *RHO*-associated RP,[29] or genome editing may be alternative approaches.

In conclusion, mutations in the *RP1* gene can lead to different clinical phenotypes, varying from RP to arMD/arCRD, depending on the residual *RP1* function. Together, these dystrophies form a spectrum of *RP1*-associated phenotypes that can be clinically distinguished from each other based on the clinical findings, inheritance pattern, age of onset and disease course. However, additional longitudinal studies are essential to improve the diagnostic process and to study

the role of potential modifiers. With the advent of novel therapeutic options such as gene therapy, recognition of the entire clinical spectrum associated with *RP1* mutations is essential to aid the selection of patients eligible for treatment, and to evaluate the effect of the treatment provided.

References

1. Verbakel SK, van Huet RAC, Boon CJF, et al. Non-syndromic retinitis pigmentosa. Prog Retin Eye Res 2018;66:157-86.
2. Lafont E, Manes G, Senechal A, et al. Patients with retinitis pigmentosa due to RP1 mutations show greater severity in recessive than in dominant cases. Journal of Clinical & Experimental Ophthalmology 2011;2:194.
3. Liu Q, Lyubarsky A, Skalet JH, et al. RP1 is required for the correct stacking of outer segment discs. Invest Ophthalmol Vis Sci 2003;44(10):4171-83.
4. Gao J, Cheon K, Nusinowitz S, et al. Progressive photoreceptor degeneration, outer segment dysplasia, and rhodopsin mislocalization in mice with targeted disruption of the retinitis pigmentosa-1 (Rp1) gene. Proc Natl Acad Sci U S A 2002;99(8):5698-703.
5. Liu Q, Zuo J, Pierce EA. The retinitis pigmentosa 1 protein is a photoreceptor microtubule-associated protein. J Neurosci 2004;24(29):6427-36.
6. Pierce EA, Quinn T, Meehan T, et al. Mutations in a gene encoding a new oxygen-regulated photoreceptor protein cause dominant retinitis pigmentosa. Nat Genet 1999;22(3):248-54.
7. Siemiatkowska AM, Astuti GD, Arimadyo K, et al. Identification of a novel nonsense mutation in RP1 that causes autosomal recessive retinitis pigmentosa in an Indonesian family. Mol Vis 2012;18:2411-9.
8. Liu Q, Collin RW, Cremers FP, et al. Expression of wild-type Rp1 protein in Rp1 knock-in mice rescues the retinal degeneration phenotype. Plos One 2012;7(8):e43251.
9. Ellingford JM, Barton S, Bhaskar S, et al. Molecular findings from 537 individuals with inherited retinal disease. J Med Genet 2016;53(11):761-7.
10. Nikopoulos K, Cisarova K, Quinodoz M, et al. A frequent variant in the Japanese population determines quasi-Mendelian inheritance of rare retinal ciliopathy. bioRxiv 2018. https://doi.org/10.1101/257634.
11. Zernant J, Kulm M, Dharmaraj S, et al. Genotyping microarray (disease chip) for Leber congenital amaurosis: detection of modifier alleles. Invest Ophthalmol Vis Sci 2005;46(9):3052-9.
12. Pichi F, Abboud EB, Ghazi NG, Khan AO. Fundus autofluorescence imaging in hereditary retinal diseases. Acta Ophthalmol 2018;96(5):e549-e61.
13. Hood DC, Bach M, Brigell M, et al. ISCEV standard for clinical multifocal electroretinography (mfERG) (2011 edition). Doc Ophthalmol 2012;124(1):1-13.
14. McCulloch DL, Marmor MF, Brigell MG, et al. ISCEV Standard for full-field clinical electroretinography (2015 update). Doc Ophthalmol 2015;130(1):1-12.
15. Richards S, Aziz N, Bale S, et al. Standards and guidelines for the interpretation of sequence variants: a joint consensus recommendation of the American College of Medical Genetics and Genomics and the Association for Molecular Pathology. Genet Med 2015;17(5):405-24.
16. Boon CJ, van Schooneveld MJ, den Hollander AI, et al. Mutations in the peripherin/RDS gene are an important cause of multifocal pattern dystrophy simulating STGD1/fundus flavimaculatus. Br J Ophthalmol 2007;91(11):1504-11.
17. Saksens NT, Fleckenstein M, Schmitz-Valckenberg S, et al. Macular dystrophies mimicking age-related macular degeneration. Prog Retin Eye Res 2014;39:23-57.
18. Roosing S, Thiadens AA, Hoyng CB, et al. Causes and consequences of inherited cone disorders. Prog Retin Eye Res 2014;42:1-26.
19. Chassine T, Bocquet B, Daien V, et al. Autosomal recessive retinitis pigmentosa with RP1 mutations is associated with myopia. Br J Ophthalmol 2015;99(10):1360-5.
20. Berson EL, Grimsby JL, Adams SM, et al. Clinical features and mutations in patients with dominant retinitis pigmentosa-1 (RP1). Invest Ophthalmol Vis Sci 2001;42(10):2217-24.
21. Chen LJ, Lai TY, Tam PO, et al. Compound heterozygosity of two novel truncation mutations in RP1 causing autosomal recessive retinitis pigmentosa. Invest Ophthalmol Vis Sci 2010;51(4):2236-42.
22. Avila-Fernandez A, Corton M, Nishiguchi KM, et al. Identification of an RP1 prevalent founder mutation and related phenotype in Spanish patients with early-onset autosomal recessive retinitis. Ophthalmology 2012;119(12):2616-21.
23. Li S, Yang M, Liu W, et al. Targeted Next-Generation Sequencing Reveals Novel RP1 Mutations in Autosomal Recessive Retinitis Pigmentosa. Genet Test Mol Biomarkers 2018;22(2):109-14.
24. Mendez-Vidal C, Bravo-Gil N, Gonzalez-Del Pozo M, et al. Novel RP1 mutations and a recurrent BBS1 variant explain the co-existence of two distinct retinal phenotypes in the same pedigree. BMC Genet 2014;15:143.
25. Aldahmesh MA, Safieh LA, Alkuraya H, et al. Molecular characterization of retinitis pigmentosa in Saudi Arabia. Mol Vis 2009;15:2464-9.
26. Yamashita T, Liu J, Gao J, et al. Essential and synergistic roles of RP1 and RP1L1 in rod photoreceptor axoneme and retinitis pigmentosa. J Neurosci 2009;29(31):9748-60.
27. Carvalho LS, Vandenberghe LH. Promising and delivering gene therapies for vision loss. Vision Res 2015;111(Pt B):124-33.
28. Wu Z, Yang H, Colosi P. Effect of genome size on AAV vector packaging. Mol Ther 2010;18(1):80-6.
29. Murray SF, Jazayeri A, Matthes MT, et al. Allele-Specific Inhibition of Rhodopsin With an Antisense Oligonucleotide Slows Photoreceptor Cell Degeneration. Invest Ophthalmol Vis Sci 2015;56(11):6362-75.

Appendix 1

Method section – genetic analysis

In all families, genomic DNA was extracted from peripheral lymphocytes according to standard procedures. The proband of family A was initially screened for variants in the *ABCA4*, *CNGB3 (*exon 10), *MFSD8* (p.E336Q/p.D368H/p.E381*), and *PRPH2* genes. Sanger sequencing of these genes revealed no disease-associated variants. Subsequently, whole exome sequencing (WES) was performed in the 3 affected siblings and their unaffected brother. WES capture was obtained using Nimblegen SegCap EZ Exome v2 kit (Roche Nimblegen, Inc., Madison WI) on Illumina HiSeq sequencer using TruSeq V3 chemistry (Illumina, Inc. San Diego, CA), followed by downstream quality control and genotyping of the samples, as previously described.[1] We selected candidate variants based on their segregation with the disease phenotype, their presence in all three affected siblings, their function (nonsynonymous, presumed loss of function or splicing variants located in coding or near-splice site regions), and minor allele frequency less than 1% in the public databases dbSNP, 1000 Genomes Project, Exome Variant Server, and GoNL. Sanger sequencing was performed to confirm all single-nucleotide variants of interest. Finally, we used restriction enzymes to confirm that variants were located on different alleles.

Exome sequencing in patients B-II:8, H-II:2, I-II:2, M-II:2, P-II:13 and Q-III:4 was performed in a certified diagnostic laboratory.[2] In patients B-II:8, M-II:2, P-II:13 and Q-III:4, the exome was enriched using Agilent's SureSelectXT Human All Exon 50Mb Kit (Agilent Technologies, Santa Clara, CA, USA). Subsequently, next-generation sequencing using an Illumina HiSeq sequencer (Illumina, Inc. San Diego, CA), read alignment to the human reference genome (Genome Reference Consortium Human Reference 37/hg19) using Burrows-Wheeler Aligner (BWA), and variant calling with the Genome Analysis Toolkit (GATK) were performed at BGI-Europe (Copenhagen, Denmark). After the copy number variants were detected using CoNIFER 0.2.0, variants were annotated with a custom designed in-house annotation strategy. The exome data was analyzed using a vision gene filter consisting of 342 (version DG-2.4.1), 366 (version DG-2.8), or 395 genes (version DG-2.11), in patients P-II:13, B-II:8 and M-II:2/Q-III:4, respectively (https://www.radboudumc.nl/en/patientenzorg/onderzoeken/exome-sequencing-diagnostics/exomepanelspreviousversions/vision-disorders; Supplemental Table 1). Segregation analysis of the candidate variants of patient B-II:8 was performed in the son and affected sister. In patients H-II:2 and I-II:2 the DNA was enriched using Roche/NimbleGen's SeqCap EZ Human Exome Library v.3.0 (Roche NimbleGen, Basel, Switzerland). Subsequently, next-generation sequencing was performed on a Illumina HiSeq2500TM sequencer, read sequences were mapped to the human reference genome (GRCh37/hg19) using BWA version 0.7.5, and variants called with GATK. Detected variants were analysed in Cartagenia 3.0 applying a vision-related gene filter consisting of 220 genes (https://sph.uth.edu/RetNet/sum-dis.htm#B-diseases; June 2014).

In patients O-II:1, R-II:2 and S-III:4, targeted panel sequencing covering 256 vision-related genes (patient R-II:2) or 266 genes (patients O-II:1 and S-III:4) was performed in a certified DNA diagnostic laboratory (Supplemental Table 1). The DNA was enriched using the Nimblegen SeqCap easy choice (OID 42193, version BHv2 or OID 43443, version BHv3), after which next-generation sequencing was performed on a MiSeq sequencer using MiSeq Reagent Kit v2 (Illumina, Inc. San Diego, CA), reads were aligned to the human reference genome (GRCh37.hg19) using BWA, and variants were called using the GATK. Sanger sequencing was performed for all areas with a coverage below 30 reads.

Mutational screening in patient N-III:9 was performed using an arrayed primer extension (APEX) microarray chip (Asper, Biotech, Tartu, Estonia) for autosomal dominant RP (version 3.0: containing 414 variants in 16 genes), according to a previously described protocol.[3] All variants detected by microarray analysis were verified by direct sequencing. Patients C–G and J–L had their *RP1* open reading frame screened by means of Sanger sequencing as previously reported.[4] In addition, except for patient G-II:2, molecular inversion probes (MIPs) were used to exclude variants in 109 other known inherited retinal dystrophy genes in patient C–F, J and K,[4] and targeted re-sequencing containing 83 non-syndromic RP genes was performed in patient L-II:2 (Supplemental Table 1). The pathogenicity of novel missense variants was assessed combining co-segregation analysis and *in silico* prediction tools, including SIFT and Polyphen-2, and by using the PhyloP, CADD-PHRED and Grantham scores.

In addition, we performed an extensive review of the literature (PubMed: accessed April 12, 2018) to identify all known mutations in the *RP1* gene (including those reported herein) that have been associated with hereditary retinal dystrophies.

References

1. Geerlings MJ, Kremlitzka M, Bakker B, et al. The Functional Effect of Rare Variants in Complement Genes on C3b Degradation in Patients With Age-Related Macular Degeneration. JAMA Ophthalmol 2017;135(1):39-46.
2. Haer-Wigman L, van Zelst-Stams WA, Pfundt R, et al. Diagnostic exome sequencing in 266 Dutch patients with visual impairment. Eur J Hum Genet 2017;25(5):591-9.
3. Zernant J, Kulm M, Dharmaraj S, et al. Genotyping microarray (disease chip) for Leber congenital amaurosis: detection of modifier alleles. Invest Ophthalmol Vis Sci 2005;46(9):3052-9.
4. Nikopoulos K, Cisarova K, Koskiniemi-Kuendig H, et al. Frequent variants in the Japanese population determine quasi-Mendelian inheritance of rare retinal ciliopathy. bioRxiv 2018:257634.

Appendix 2

autosomal dominant
RP

autosomal recessive
RP/MD/CRD

p.S2Rfs*16
p.A25Sfs*37
p.H31Qfs*47
p.Y41H†
p.V51Dfs*27
p.P124Afs*20
p.H36Rfs*8
p.V157Wfs*15
p.I168Nfs*17
p.L172R
p.F180C
p.Q185Yfs*4
p.V190C
p.D202E
p.A221Gfs*43
p.P229Qfs*35
p.G230*
p.Q248*
p.I263Nfs*8
p.E334fs*22
p.R338*
p.T373I
p.R396*
p.G402Afs*7
p.K443Nfs*12
p.E488*
p.M500Vfs*7
p.S542*
p.S574Cfs*7
p.S676Ifs*22
p.R793Efs*55
p.D799*
p.Y834*
p.N949Kfs*32
p.S953Qfs*12
p.K1044Nfs*16
p.W1131*
p.G1140Kfs*4
p.N1143Ifs*25
p.E1227Mfs*29
p.S1233Pfs*22
p.Y1352Afs*9
p.R1364Vfs*8
p.K1370E†
p.H1390Lfs*6
p.C1399Lfs*5
p.H1414Qfs*5
p.K1518*
p.R1519Efs*2
p.I1528Vfs*10
p.S1529Rfs*9
p.Q1602*
p.P1648fs*13
p.R1652L†
p.Q1725*
p.N1751Ifs*4
p.Q1916*
p.R1933*
p.I1988Nfs*3
p.I2061Sfs*12

p.M500Sfs*33
p.R533Kfs*12
p.P658Hfs*4
p.A669T†
p.K675Nfs*7
p.S676Ifs*6
p.R677*
p.R677Dfs*5
p.Q678*
p.Q679* (in cis with
p.P1793S)
p.Q686*
p.Q689*
p.E700*
p.G706Vfs*7
p.K722Efs*16
p.G723*
p.G724Efs*9
p.I725Rfs*6
p.I725Tfs*13
p.I725Dfs*4
p.C727*
p.E729Kfs*9
p.Q732*
p.S734Vfs*4
p.T736Ifs*4
p.C744*
p.S747Vfs*16
p.L749*
p.R759*
p.L762-N763del
p.L762Yfs*17
p.N763Lfs*11
p.K769Rfs*6
p.K769Ffs*2
p.K778*
p.S781*
p.S862*
p.I864Kfs*11
p.T865_L866delinsI
p.L866*
p.R872Tfs*2
p.S911*
p.D984G†
p.Y1053Tfs*4

1
2
3
exon 4

Group 1
Group 2
Group 3
Group 4
Group 5
Group 6
DCX domain
region homologous to BIF domain

Supplementary Figure 1

We performed an extensive review of the literature (PubMed: accessed April 12, 2018) to identify all known mutations in the RP1 gene (including those reported herein) that have been associated with hereditary retinal dystrophies.

Schematic representation of the mutations in the RP1 gene and their location. Mutations that have been associated with autosomal dominant RP are indicated left from the gene, whereas mutations that have been associated with autosomal recessive RP, MD or CRD are indicated on the right side. The portion of the gene that encodes the doublecortin (DCX) and a region homologous to the Drosophila melanogaster bifocal (BIF) domain, are indicated with the striped and checkered pattern, respectively. Mutations indicated with an arrowhead represent novel mutations that are identified in this study.
† Missense mutation with uncertain pathogenicity.
The mutations can be divided into 6 groups: group 1 mutations (in grey) reside in a hotspot region in exon 4 and are expected to result in a truncated protein with dominant-negative activity; group 2 (orange) includes protein-truncating mutations located in exon 2 and 3, whose transcripts are thought to be subject to nonsense mediated decay (NMD); group 3 (red) encompasses protein-truncating mutations in the proximal part of exon 4; group 4 (green) includes mutations in exon 4 which, considering their location, could lead to autosomal dominant RP, yet they are not pathogenic in a heterozygous state; group 5 (purple) includes protein-truncation mutations in the distal part of exon 4 with residual function; group 6 (black) containse missense variants.

Appendix 3 Supplementary Tables

Table S1. Gene lists of the genetic tests performed in this study.

Test	MIPs screening	Targeted re-sequencing	Targeted panel		Exome sequencing, vision gene filter			
Version			BHv2	BHv3		Version DG-2.4.1	Version DG-2.8	Version DG-2.11
Performed in patient:	C–F, J and K	L	R	O and S	H and I	P	B	M and Q
Total number of genes	109	83	256	266	220	342	366	395
	ABCA4	ABCA4	ABCA4	ABCA4	ABCA4	https://www.radboudumc.nl/ en/patientenzorg/ onderzoeken/exome- sequencing-diagnostics/ exomepanelspreviousversions/ vision-disorders		
	ABDH12	ADIPOR1	ABCB6	ABCB6	ABCC6			
	ADAM9	AGBL5	ABCC6	ABCC6	ABHD12			
	ADAMTS18	ARL2BP	ABHD12	ABHD12	ACBD5			
	AIPL1	ARL3	ACO2	ACO2	ADAM9			
	ARL2BP	ARL6	ADAM9	ADAM9	ADAMTS18			
	ARL6	BBS1	ADAMTS18	ADAMTS18	ADGRA3			
	BBS1	BBS2	AHI1	AHI1	ADGRV1			
	BBS2	BEST1	AIPL1	AIPL1	AHI1			
	BEST1	C2orf71	ALMS1	ALMS1	AIPL1			
	C21orf2	C8orf37	AP3B1	AP3B1	ALMS1			
	C2orf71	CA4	ARL2BP	ARL2BP	ARL2BP			
	C8orf37	CERKL	ARL6	ARL6	ARL6			
	CA4	CLRN1	ATF6	ATF6	ARMS2			
	CABP4	CNGA1	ATXN7	ATXN7	ATXN7			
	CACNA1F	CNGB1	BBIP1	BBIP1	ATXN7			
	CACNA2D4	CRB1	BBS1	BBS1	BBIP1			
	CDHR1	CRX	BBS10	BBS10	BBS1			
	CEP290	CYP4V2	BBS12	BBS12	BBS10			
	CERKL	DHDDS	BBS2	BBS2	BBS12			
	CHM	DHX38	BBS4	BBS4	BBS2			
	CLN3	EMC1	BBS5	BBS5	BBS4			
	CLRN1	EYS	BBS7	BBS7	BBS5			
	CNGA1	FAM161A	BBS9	BBS9	BBS7			
	CNGA3	FSCN2	BCOR	BCOR	BBS9			
	CNGB1	GPR125	BEST1	BEST1	BEST1			
	CNGB3	GUCA1B	BLOC1S3	BLOC1S3	C12orf65			
	CNNM4	HGSNAT	BLOC1S6	BLOC1S6	C1QTNF5			
	CRB1	HK1	BMP4	BMP4	C21orf2			
	CRX	IDH3B	C10orf11	C10orf11	C2orf71			
	CYP4V2	IFT140	C12orf65	C12orf65	C8orf37			
	DHDDS	IFT172	C1QTNF5	C1QTNF5	CA4			

Test	MIPs screening	Targeted re-sequencing	Targeted panel		Exome sequencing, vision gene filter		
Version			BHv2	BHv3	Version DG-2.4.1	Version DG-2.8	Version DG-2.11
	DTHD1	IMPDH1	C21orf2	C21orf2	CABP4		
	EMC1	IMPG2	C2orf71	C2orf71	CACNA1F		
	EYS	KIAA1549	C5ORF42	C5ORF42	CACNA2D4		
	FAM161A	KIZ	C8orf37	C8orf37	CAPN5		
	FSCN2	KLHL7	CA4	CA4	CC2DA		
	GPR125	LRAT	CABP4	CABP4	CDH23		
	GUCA1A	MAK	CACNA1F	CACNA1F	CDH3		
	GUCA1B	MERTK	CACNA2D4	CACNA2D4	CDHR1		
	GUCY2D	MVK	CAPN5	CAPN5	CEP164		
	IDH3B	NEK2	CC2DA	CC2DA	CEP290		
	IMPDH1	NEUROD1	CDH23	CDH23	CERKL		
	IMPG1	NR2E3	CDH3	CDH3	CFB		
	IMPG2	NRL	CDHR1	CDHR1	CFH		
	IQCB1	OFD1	CEP164	CEP164	CHM		
	ITM2B	PDE6A	CEP250	CEP250	CIB2		
	KCNJ13	PDE6B	CEP290	CEP290	CLN3		
	KCNV2	PDE6G	CEP41	CEP41	CLRN1		
	KIAA1549	POMGNT1	CERKL	CERKL	CNGA1		
	KLHL7	PRCD	CFH	CFH	CNGA3		
	LCA5	PROM1	CHM	CHM	CNGB1		
	LRAT	PRPF3	CIB2	CIB2	CNGB3		
	MAK	PRPF31	CLN3	CLN3	CNNM4		
	MERTK	PRPF4	CLRN1	CLRN1	COL11A1		
	MFRP	PRPF6	CNGA1	CNGA1	COL2A1		
	MIP	PRPF8	CNGA3	CNGA3	COL9A1		
	NEK2	PRPH2	CNGB1	CNGB1	CRB1		
	NMNAT1	RBP3	CNGB3	CNGB3	CRX		
	NR2E3	RDH12	CNNM4	CNNM4	CSPP1		
	NRL	RGR	COL11A1	COL11A1	CYP4V2		
	OFD1	RHO	COL2A1	COL2A1	DFNB31		
	OTX2	RLBP1	COL9A1	COL9A1	DHDDS		
	PDE6A	ROM1	COL9A2	COL9A2	DHX38		
	PDE6B	RP1	CRB1	CRB1	DTHD1		
	PDE6C	RP1L1	CRX	CRX	EFEMP1		
	PDE6G	RP2	CSPP1	CSPP1	ELOVL4		
	PDE6H	RP9	CYP4V2	CYP4V2	EMC1		

Chapter 4.1

Table S1. Continued

Test	MIPs screening	Targeted re-sequencing	Targeted panel		Exome sequencing, vision gene filter			
Version			BHv2	BHv3		Version DG-2.4.1	Version DG-2.8	Version DG-2.11
	PDZD7	RPE65	DFNB31	DFNB31	ERCC6			
	PITPNM3	RPGR	DHDDS	DHDDS	EYS			
	PRCD	SAG	DHX38	DHX38	FAM161A			
	PROM1	SEMA4A	DRAM2	DRAM2	FBLN5			
	PRPF3	SLC7A14	DTHD1	DTHD1	FLVCR1			
	PRPF31	SNRNP200	DTNBP1	DTNBP1	FZD4			
	PRPF6	SPATA7	EFEMP1	EFEMP1	GDF6			
	PRPF8	SPP2	ELOVL4	ELOVL4	GNAT1			
	PRPH2	TOPORS	EMC1	EMC1	GNAT2			
	RAB28	TRNT1	EYS	EYS	GNPTG			
	RAX2	TTC8	FAM161A	FAM161A	GPR179			
	RBP3	TULP1	FLVCR1	FLVCR1	GRK1			
	RD3	USH2A	FOXE3	FOXE3	GRM6			
	RDH12	ZNF408	FSCN2	FSCN2	GUCA1A			
	RDH5	ZNF513	FZD4	FZD4	GUCA1B			
	RGR		GDF6	GDF6	GUCY2D			
	RHO		GNAT1	GNAT1	HARS			
	RIMS1		GNAT2	GNAT2	HMCN1			
	RLBP1		GNPTG	GNPTG	HTRA1			
	ROM1		GPR125	GPR125	IDH3B			
	RP1		GPR143	GPR143	IFT140			
	RP1L1		GPR179	GPR179	IFT27			
	RP2		GPR98	GPR98	IMPDH1			
	RP9		GRK1	GRK1	IMPG1			
	RPE65		GRM6	GRM6	IMPG2			
	RPGR		GUCA1A	GUCA1A	INPP5E			
	RPGRIP1		GUCA1B	GUCA1B	INVS			
	SAG		GUCY2D	GUCY2D	IQCB1			
	SEMA4A		HARS	HARS	ITM2B			
	SNRNP200		HCCS	HCCS	JAG1			
	SPATA7		HGSNAT	HGSNAT	JAG1			
	TOPORS		HK1	HK1	KCNJ13			
	TTC8		HMX1	HMX1	KCNV2			
	TULP1		HPS1	HPS1	KIF11			
	UNC119		HPS3	HPS3	KIZ			
	USH1C		HPS4	HPS4	KLHL7			
	USH2A		HPS5	HPS5	LCA5			
	VCAN		HPS6	HPS6	LRAT			

Table S1. Continued

Test	MIPs screening	Targeted re-sequencing	Targeted panel		Exome sequencing, vision gene filter			
Version			BHv2	BHv3		Version DG-2.4.1	Version DG-2.8	Version DG-2.11
	WDR19		IDH3B	IDH3B	LRIT3			
	ZNF408		IFT140	IFT140	LRP5			
	ZNF513		IFT172	IFT172	LZTFL1			
			IFT27	IFT27	MAK			
			IMPDH1	IMPDH1	MERTK			
			IMPG1	IMPG1	MFN2			
			IMPG2	IMPG2	MFRP			
			INPP5E	INPP5E	MKKS			
			INVS	INVS	MKS1			
			IQCB1	IQCB1	MTTP			
			ITM2B	ITM2B	MVK			
			JAG1	JAG1	MYO7A			
			KCNJ13	KCNJ13	NDP			
			KCNV2	KCNV2	NEK2			
			KIAA1549	KIAA1549	NMNAT1			
			KIF11	KIF11	NPHP1			
			KIZ	KIZ	NPHP3			
			KLHL7	KLHL7	NPHP4			
			LCA5	LCA5	NR2E3			
			LRAT	LRAT	NR2F1			
			LRIT3	LRIT3	NRL			
			LRP5	LRP5	NYX			
			LYST	LYST	OAT			
			LZTFL1	LZTFL1	OFD1			
			MAK	MAK	OPA1			
			MC1R	MC1R	OPA3			
			MERTK	MERTK	OPN1LW			
			MFN2	MFN2	OPN1MW			
			MFRP	MFRP	OPN1SW			
			MIR204	MIR204	OTX2			
			MITF	MITF	PANK2			
			MKKS	MKKS	PAX2			
			MKS1	MKS1	PCDH15			
			MLPH	MLPH	PCYT1A			
			MMACHC	MMACHC	PDE6A			
			MTTP	MTTP	PDE6B			
			MVK	MVK	PDE6C			
			MYO5A	MYO5A	PDE6G			

Table S1. Continued

Test	MIPs screening	Targeted re-sequencing	Targeted panel		Exome sequencing, vision gene filter		
Version			BHv2	BHv3	Version DG-2.4.1	Version DG-2.8	Version DG-2.11
			MYO7A	MYO7A	PDE6H		
			NDP	NDP	PDZD7		
			NEK2	NEK2	PEX1		
			NEUROD1	NEUROD1	PEX2		
			NMNAT1	NMNAT1	PEX7		
			NPHP1	NPHP1	PGK1		
			NPHP3	NPHP3	PHYH		
			NPHP4	NPHP4	PITPNM3		
			NR2E3	NR2E3	PLA2G5		
			NR2F1	NR2F1	PRCD		
			NRL	NRL	PROM1		
			NYX	NYX	PRPF3		
			OAT	OAT	PRPF31		
			OCA2	OCA2	PRPF4		
			OFD1	OFD1	PRPF6		
			OPA1	OPA1	PRPF8		
			OPA3	OPA3	PRPH2		
			OPN1LW	OPN1LW	RAB28		
			OPN1MW	OPN1MW	RAX2		
			OPN1SW	OPN1SW	RB1		
			OR2W3	OR2W3	RBP3		
			OTX2	OTX2	RBP4		
			PANK2	PANK2	RD3		
			PAX2	PAX2	RDH11		
			PCDH15	PCDH15	RDH12		
			PCYT1A	PCYT1A	RDH5		
			PDE6A	PDE6A	RGR		
			PDE6B	PDE6B	RGS9		
			PDE6C	PDE6C	RGS9BP		
			PDE6G	PDE6G	RHO		
			PDE6H	PDE6H	RIMS1		
			PDZD7	PDZD7	RLBP1		
			PEX1	PEX1	ROM1		
			PEX2	PEX2	RP1		
			PEX7	PEX7	RP1L1		
			PGK1	PGK1	RP2		
			PHYH	PHYH	RP9		
			PITPNM3	PITPNM3	RPE65		

Table S1. Continued

Test	MIPs screening	Targeted re-sequencing	Targeted panel		Exome sequencing, vision gene filter			
Version			BHv2	BHv3		Version DG-2.4.1	Version DG-2.8	Version DG-2.11
			PLA2G5	PLA2G5	RPGR			
			POC1B	POC1B	RPGRIP1			
			PRCD	PRCD	RPGRIP1L			
			PROM1	PROM1	RS1			
			PRPF3	PRPF3	SAG			
			PRPF31	PRPF31	SDCCAG8			
			PRPF4	PRPF4	SEMA4A			
			PRPF6	PRPF6	SLC24A1			
			PRPF8	PRPF8	SLC7A14			
			PRPH2	PRPH2	SNRNP200			
			PXDN	PXDN	SPATA7			
			RAB27A	RAB27A	TEAD1			
			RAB28	RAB28	TIMM8A			
			RBP3	RBP3	TIMP3			
			RBP4	RBP4	TLR3			
			RD3	RD3	TLR4			
			RDH11	RDH11	TMEM126A			
			RDH12	RDH12	TMEM237			
			RDH5	RDH5	TOPORS			
			RGR	RGR	TREX1			
			RGS9	RGS9	TRIM32			
			RGS9BP	RGS9BP	TRPM1			
			RHO	RHO	TSPAN12			
			RIMS1	RIMS1	TTC8			
			RLBP1	RLBP1	TTLL5			
			ROM1	ROM1	TTPA			
			RP1	RP1	TUB			
			RP1L1	RP1L1	TULP1			
			RP2	RP2	UNC119			
			RP9	RP9	USH1C			
			RPE65	RPE65	USH1G			
			RPGR	RPGR	USH2A			
			RPGRIP1	RPGRIP1	VCAN			
			RPGRIP1L	RPGRIP1L	WDPCP			
			RS1	RS1	WDR19			
			SAG	SAG	WFS1			
			SDCCAG8	SDCCAG8	ZNF423			
			SEMA4A	SEMA4A	ZNF513			

Chapter 4.1

Table S1. Continued

Test	MIPs screening	Targeted re-sequencing	Targeted panel		Exome sequencing, vision gene filter		
Version			BHv2	BHv3	Version DG-2.4.1	Version DG-2.8	Version DG-2.11
			SIX6	SIX6			
			SLC24A1	SLC24A1			
			SLC24A5	SLC24A5			
			SLC38A8	SLC38A8			
			SLC45A2	SLC45A2			
			SLC7A14	SLC7A14			
			SNRNP200	SNRNP200			
			SPATA7	SPATA7			
			TEAD1	TEAD1			
			TIMM8A	TIMM8A			
			TIMP3	TIMP3			
			TMEM126A	TMEM126A			
			TMEM237	TMEM237			
			TMEM67	TMEM67			
			TOPORS	TOPORS			
			TREX1	TREX1			
			TRIM32	TRIM32			
			TRPM1	TRPM1			
			TSPAN12	TSPAN12			
			TTC8	TTC8			
			TTLL5	TTLL5			
			TUB	TUB			
			TULP1	TULP1			
			TYR	TYR			
			TYRP1	TYRP1			
			UNC119	UNC119			
			USH1C	USH1C			
			USH1G	USH1G			
			USH2A	USH2A			
			VCAN	VCAN			
			WDPCP	WDPCP			
			WDR19	WDR19			
			WFS1	WFS1			
			ZNF408	ZNF408			
			ZNF423	ZNF423			
			ZNF513	ZNF513			

Table S2. Rare genetic variants in other inherited retinal dystrophy genes in patients with arMD/arCRD.

Patient	Gene	Genomic start position	Nucleotide change	Protein change	SNP ID
A-II:2	SLC24A1	65944011	c.2797T>G	p.Ser933Ala	-
	ADGRV1	90106175	c.15098T>C	p.Phe5033Ser	-
	MYO7A	76919484	c.5866G>A	p.Val1956Ile	rs142293185
A-II:4	SLC24A1	65944011	c.2797T>G	p.Ser933Ala	-
	ADGRV1	90106175	c.15098T>C	p.Phe5033Ser	-
	MYO7A	76919484	c.5866G>A	p.Val1956Ile	rs142293185
A-II:5	SLC24A1	65944011	c.2797T>G	p.Ser933Ala	-
	ADGRV1	90106175	c.15098T>C	p.Phe5033Ser	-
	MYO7A	76919484	c.5866G>A	p.Val1956Ile	rs142293185
B-II:3	Unknown				
B-II:8	POMGNT1	46655585	c.1726G>A	p.Val576Met	rs142895576
	USH2A	215972392	c.9815C>T	p.Pro3272Leu	rs764182950
	ADGRV1	89948189	c.3443G>A	p.Gly1148Asp	rs200945405
C-II:2	SEMA4A	156144730	c.1433A>G	p.Gln478Arg	-
	IMPG1	76751697	c.214G>A	p.Ala72Thr	rs769499134
D-II:1	ADGRA3	22390250	c.3044T>C	p.Leu1015Ser	rs201588033
	TULP1	35467892	c.1361C>T	p.Thr454Met	rs138200747
E-II:2	NEK2	211846971	c.409G>A	p.Val137Ile	rs151049149
	GUCA1A	42147086	c.551A>G	p.Gln184Arg	rs149998844
	KIAA1549	138546067	c.5065T>A	p.Ser1689Thr	-
	RBP3	48381942	c.3707G>A	p.Arg1236Lys	-
	SPATA7	88894018	c.890A>T	p.Asp297Val	rs769211713
	SPATA7	88897520	c.1033A>G	p.Met345Val	rs375371982
F-II:3	No other rare variants				
G-II:2	EYS	65300863	c.7919G>A	p.Trp2640X	rs527236066
H-II:2	No other rare variants				

ExAC: Exome Aggregation Consortium. [a] Frequency is based on a non-Finnish European population. [b] Frequency is based on a East-Asian population. SIFT: Sorting Intolerant from Tolerant. D: Deleterious (score ≤0.05); T: tolerated (score >0.05). PolyPhen2 HDIV: Polymorphism Phenotyping version 2. D: Probably damaging (score ≥0.957), P: possibly damaging (0.453≤ score ≤0.956); B: benign (score ≤ 0.452). PhyloP score: predicted pathogenic ≥2.7 (range -14.1–6.4).[1] CADD: Combined Annotation Dependent Depletion (PHRED = scaled CADD-score; CADD-PHRED score of 10 means 10% most deleterious variants, 20 = 1% most deleterious, 30 = 0.1% most deleterious, etc.) (https://cadd.gs.washington.edu/). Grantham score: predicted pathogenic ≥80 (range 0–215).[2]

gnomAD	Prediction algorithms					Remarks
	SIFT	Polyphen2 HDIV	PhyloP	CADD-PHRED	Grantham score	
-	T (0.19)	B (0.076)	0.948	15.35	99	Also present in unaffected sibling A-II:3
0.00001562[a]	T (0.21)	B (0.223)	1.858	23	155	
0.005451[a]	T (0.2)	B (0.007)	3.52	17.42	29	Also present in unaffected sibling A-II:3
-	T (0.19)	B (0.076)	0.948	15.35	99	Also present in unaffected sibling A-II:3
0.00001562[a]	T (0.21)	B (0.223)	1.858	23	155	
0.005451[a]	T (0.2)	B (0.007)	3.52	17.42	29	Also present in unaffected sibling A-II:3
-	T (0.19)	B (0.076)	0.948	15.35	99	Also present in unaffected sibling A-II:3
0.00001562[a]	T (0.21)	B (0.223)	1.858	23	155	
0.005451[a]	T (0.2)	B (0.007)	3.52	17.42	29	Also present in unaffected sibling A-II:3
0.00002644[a]	T (0.07)	D (0.979)	5.868	25.7	21	
0.00004406[a]	D (0.02)	D (0.999)	5.59	32	98	
0.002529[a]	D (0)	D (0.992)	6.374	27	94	
-	T (0.23)	B (0.042)	2.902	23.3	43	
0.000[b]	T (0.4)	B (0.009)	-0.556	12.23	58	
0.0003822[b]	D (0)	B (0.287)	4.867	24.9	145	
0.00005012[b]	D 0.01)	B (0.375)	1.688	23.5	81	
0.0001503[b]	T (0.46)	B (0.242)	6.033	22.2	29	
0.001308[b]	T (0.4)	B (0.027)	3.762	21.5	43	
-	D (0)	D (0.998)	4.577	27.3	58	
0.002812[b]	T (1)	B (0.039)	0.798	8.087	26	
0.0003519[b]	D (0.01)	P (0.448)	2.282	22.5	152	
0.0007517[b]	T (1)	B (0)	-2.847	0.001	21	Predicted to be benign
-						

Table S3. Characteristics of the patients included in this study, stratified by disease.

Characteristics	arMD/arCRD (n=11)	arRP (n=5)	adRP (n=6)	Total (n=22)
Mean age of onset, years ± SD (range)	40.3 ± 13.1 (14-56)	8.8 ± 3.1 (5-12)	26.2 ± 8.2 (18-40)	29.4 ± 16.6 (5-56)
Mean age at latest examination, years ± SD (range)	53.3 ± 17.2 (18-77)	33.0 ± 16.2 (13-52)	48.0 ± 13.8 (35-72)	47.3 ± 17.4 (13-77)
Origin, n (%)				
• Caucasian	6/11 (55)	2/5 (40)	4/6 (67)	12/22 (55)
• East Asian	5/11 (45)	3/5 (60)	1/6 (17)	9/22 (41)
• African	0/11 (0)	0/5 (0)	1/6 (17)	1/22 (5)
Reported first symptom, n (%)				
• Decrease of VA	10/11 (91)	0/5 (0)	0/6 (0)	10/22 (45)
• Metamorphopsia	2/11 (18)	0/5 (0)	0/6 (0)	1/22 (5)
• Photophobia	1/11 (9)	0/5 (0)	0/6 (0)	1/22 (5)
• Night blindness	2/11 (18)	5/5 (100)	6/6 (100)	14/22 (64)
Photophobia, n (%)	7/11 (64)	0/5 (0)	0/6 (0)	7/22 (32)
Mean refractive error, diopters (range), SER, D (n=22)	-3.2 ± 3.0 (-9.50 to -0.25)	-4.1 ± 3.1 (-9.00 to -0.63)	-3.6 ± 4.1 (-10.00 to +4.00)	-3.5 ± 3.2 (-10.00 to +4.00)
• High myopia (<-6D), n (%)	2/11 (18)	1/5 (20)	1/6 (17)	4/22 (18)
• Moderate myopia (-3D > SER ≥ -6D), n (%)	1/11 (9)	2/5 (40)	3/6 (60)	6/22 (27)
• Mild myopia (-0.75D > SER ≥ -3D), n (%)	7/11 (64)	2/5 (40)	1/6 (17)	10/22 (45)
• ≥-0.75D, n (%)	1/11 (9)	0/5 (0)	2/6 (33)	2/22 (9)
At the most recent examination:				
Lens status, n (%) (n=21)				
• Cataract	5/11 (45)	3/4 (75)	1/6 (17)	9/21 (43)
• Pseudophakic	0/11 (0)	1/4 (25)	3/6 (50)	4/21 (19)
• No cataract	6/11 (55)	0/4 (0)	2/6 (33)	8/21 (38)
Fundoscopic examination, n (%)				
• Macular atrophy	8/11 (73)	4/5 (80)	4/6 (67)	16/22 (73)
• Bull's eye maculopathy	2/11 (18) [‡]	0/5 (0)	0/6 (0)	2/22 (9)
• Peripheral RPE atrophy	0/11 (0)	5/5 (100)	6/6 (100)	11/22 (50)
• Bone spicule pigmentation	2/11 (18) [§]	5/5 (100)	6/6 (100)	13/22 (59)
• Optic disc pallor	0/11 (0)	5/5 (100)	4/6 (67)	9/22 (41)
• Vascular attenuation	4/11 (36)	5/5 (100)	6/6 (100)	15/22 (68)
OCT: intact foveal photoreceptors	3/11 (27) [†]	3/5 (60) [†]	6/6 (100) [†]	12/22 (55)
Scotopic ERG, n (%) (n=20)				
• (Sub)normal	7/11 (64)	0/4 (0)	0/5 (0)	7/20 (35)
• Moderately reduced	2/11 (18)	0/4 (0)	0/5 (0)	2/20 (10)
• Severely reduced	2/11 (18)	1/4 (25)	0/5 (0)	3/20 (15)
• Nonrecordable	0/11 (0)	3/4 (75)	5/5 (100)	9/20 (45)
Photopic ERG, n (%) (n=20)				

Table S3. Continued

Characteristics	arMD/arCRD (n=11)	arRP (n=5)	adRP (n=6)	Total (n=22)
• (Sub)normal	3/11 (27)	0/4 (0)	0/5 (0)	3/20 (15)
• Moderately reduced	6/11 (55)	0/4 (0)	0/5 (0)	6/20 (30)
• Severely reduced	2/11 (18)	2/4 (50)	2/5 (40)	5/20 (25)
• Nonrecordable	0/11 (0)	2/4 (50)	3/5 (60)	6/20 (30)
Visual field characteristics (n=21)				
• Central scotoma	9/11 (82)	0/4 (0)	0/6 (0)	9/21 (43)
• Constricted VF ≥10°	3/11 (27)	1/4 (25)	4/6 (67)	8/21 (38)
• Constricted VF <10°	0/11 (0)	3/4 (75)	2/6 (33)	5/21 (24)

adRP = autosomal dominant retinitis pigmentosa; arRP = autosomal recessive retinitis pigmentosa; arCRD = autosomal recessive cone-rod dystrophy; arMD = autosomal recessive macular dystrophy; ND = non-recordable; SER = spherical equivalent refraction; VA = visual acuity; VF = visual field.
§ Nummular hyperpigmentation in the left eye of patient F-II:3 and G-II:2.
‡ Bull's eye maculopathy in the left eye of patient B-II:8 and chorioretinal atrophy in the right eye.
† Intact foveal photoreceptors in one eye; the right eye of patient J-II:2, and the left eye of patient B-II:3, B-II:8 and O-III:9.

References

1. Pollard KS, Hubisz MJ, Rosenbloom KR, Siepel A. Detection of nonneutral substitution rates on mammalian phylogenies. Genome Res 2010;20(1):110-21.
2. Grantham R. Amino acid difference formula to help explain protein evolution. Science 1974;185(4154):862-4.

Chapter 4.1

IMPG1 variant causes autosomal dominant retinitis pigmentosa; revision of the benign concentric annular macular dystrophy phenotype

Sanne K. Verbakel, Carel B. Hoyng, Hanka Venselaar, B. Jeroen Klevering, Susanne Roosing

Submitted

Abstract

Purpose
To revisit theclinical diagnosis of a large Dutch family with autosomal dominant benign concentric annular macular dystrophy (BCAMD) .

Methods
Ten affected family members were clinically evaluated, including extensive medical history taking, slit-lamp biomicroscopy, ophthalmoscopy, kinetic perimetry, color fundus photography, fundus autofluorescence imaging, spectral-domain optical coherence tomography and electroretinography. Whole exome sequencing was performed in two patients.

Results
The first symptom was night blindness (9/10 patients) or metamorphopsia (1/10 patients) at a mean age of 29.3 years (standard deviation 8.66, range 17–45 years). The visual acuity was initially preserved, but gradually deteriorated after the fourth decade of life. Despite the fundus alterations which initially seemed limited to the macular area, ERG recordings indicated panretinal disease in a rod-cone pattern. Over time, fundus abnormalities typically for retinitis pigmentosa emerged. Whole exome sequencing analyses revealed the p.Leu579Pro missense variant in *IMPG1* as the single segregating variant within the disease locus at 6p12.3-q16, which is predicted to be pathogenic by *in silico* prediction tools, and is located in the SEA domain putatively resulting in a structural change in the protein.

Conclusions
This study supports the causal role of the autosomal dominant p.Leu579Pro missense change in *IMPG1*. Since the peripheral photoreceptors are already involved in early disease stages, we propose to revise the diagnosis of BCAMD to *IMPG1*-associated retinitis pigmentosa with relative early macular involvement. Consequently, *IMPG1* should be added to the list of genes associated with autosomal dominant retinitis pigmentosa.

Introduction

Retinitis pigmentosa (RP) is considered a group of retinal disorders that shares a common phenotype, although the underlying genetic cause varies greatly. With an estimated prevalence of 1:4,000, RP is a major cause of visual impairment.[1, 2] Patients generally present with complaints of night blindness, followed by a gradual constriction of the visual field. The visual acuity is typically preserved until late stages. The clinical findings may vary, but hallmark fundus signs of RP include bone spicule pigmentation, attenuation of retinal vessels, and a waxy pallor of the optic disc. There is a large genetic heterogeneity: more than 80 genes have been implicated in non-syndromic RP.[1] Several genetic subtypes have been associated with relative early macular involvement and associated vision loss.[1] Molecular genetic analysis to identify the correct genetic subtype is therefore important, as this may help to better predict the clinical disease course and identify patients eligible for emerging therapeutics at an early stage.

The interphotoreceptor matrix proteoglycan-1 (*IMPG1*) gene encodes the sialoprotein associated with cones and rods (SPACR) protein, a glycoprotein located in the photoreceptor outer segments and the interphotoreceptor matrix (IPM), the extracellular matrix that fills the subretinal space.[3-5] The IPM has an important function in many processes, including retinal adhesion to the retinal pigment epithelium, growth factor presentation, photoreceptor alignment, intercellular communication, and transport of nutrients and metabolites (e.g. retinoids). It is not surprising that dysfunction of the IPM can underlie certain types of RP as well as other forms of progressive retinal disease.[6-12] SPACR is involved in the stabilization of the IPM by binding to glycosaminoglycans such as hyaluronan, which form the basis of the insoluble IPM scaffold, via its receptor for HA-mediated motility (RHAMM) HA-binding motif.[3, 4] Moreover, a recent study has shown that SPACR plays an important role in the development of photoreceptors and the formation of the IPM.[5]

Pathogenic variants in the *IMPG1* gene have been described in patients with autosomal dominant and autosomal recessive vitelliform macular dystrophy,[13-15] and has been suggested to cause a generalized photoreceptor dystrophy.[16] In 2004, Van Lith-Verhoeven et al. described a large Dutch family with autosomal dominant benign concentric annular macular dystrophy (BCAMD),[17] a term coined by Deutman et al. in 1974.[18] Although there was no definite molecular diagnosis, the p.Leu579Pro missense change in *IMPG1* was identified. The retinal dystrophy in this family was described as a bull's eye maculopathy, which eventually progressed to a RP-like phenotype.[17] The present study supports the causal role of the *IMPG1* p.Leu579Pro missense variant in this family, and we revise the original phenotype of BCAMD to RP with early macular involvement.

Materials and methods

Patients and clinical evaluation

Ten affected family members from the previously described Dutch 'BCAMD' family were included in this study (Figure 1). Written informed consent was obtained from all participants. The study

adhered to the tenets of the Declaration of Helsinki, and was approved by the local ethics committee. In addition to the available clinical data from the previous study, we performed additional detailed ophthalmic examination in four patients from three different generations (patient II:11, III:2, IV:1, and IV:3), which included best-correlated visual acuity, slit-lamp biomicroscopy, ophthalmoscopy, and color fundus photography. We assessed the visual field using a Goldmann perimeter and performed full-field electroretinography (ERG) recordings according to the International Society for Clinical Electrophysiology of Vision (ISCEV) guidelines using local standard values in our analysis.[19] Additionally, spectral-domain optical coherence tomography (SD-OCT; Spectralis HRA+OCT, Heidelberg Engineering, Heidelberg, Germany) and fundus autofluorescence (FAF; HRA+OCT, Heidelberg, Germany) imaging was performed in patient II:11, III:2 and IV:1.

Genetic analysis

DNA isolation and linkage analysis have been performed previously.[17] Additionally, whole exome sequencing was performed in patient IV:1 and IV:3 in a certified DNA diagnostic laboratory.[20] After the exome was enriched using Aligent's SureSelectXT Human All Exon 50Mb Kit (Agilent Technologies, Santa Clara, CA, USA), next-generation sequencing using an Illumina HiSeq sequencer (Illumina, Inc. San Diego, CA) was performed at BGI-Europe (Copenhagen, Denmark). Subsequently, sequence reads were alignment to the human reference genome (GrCH37/reference 37/hg19) using Burrows-Wheeler Aligner, and variants were called with the Genome Analysis Toolkit software. Finally, copy number variants were detected using CoNIFER 0.2.0, and annotation was performed using a custom designed in-house annotation strategy.

The previously described 45.5 Mb linkage region 6p12.3-q16,[17] was assessed in both patients and candidate variants were prioritized based on their presence in both patients, minor allele frequency of <0.5% in ExAC, dbSNP, gnomAD and the Nijmegen in-house database consisting of 15,576 individuals. Remaining variants were assessed for their predicted effect on evolutionary conservation (PhyloP and Grantham score), deleteriousness (CADD-PHRED) location in a functional domain, and prediction of *in silico* prediction tools. Moreover, we used MetaDome, a web server that maps population variation and makes use of protein domain homology within the human genome, to explore the prevalence of the variant within human homologues.[21]

Variant modeling

No experimentally solved structure of IMPG1 was available, therefore we created a homology model based on a Plasmodium Falciparum surface protein Pfs25 obtained from PDB file 6B0G.[22] We used a standard modeling script in the WHAT IF & YASARA Twinset with default parameters for modeling and subsequent analysis.[23, 24] The model and template sequences show only 22% identity over residues 554-597, which is just below the modeling threshold as has been defined by Sander and Schnieder .[25] The model should therefore be interpreted with caution.
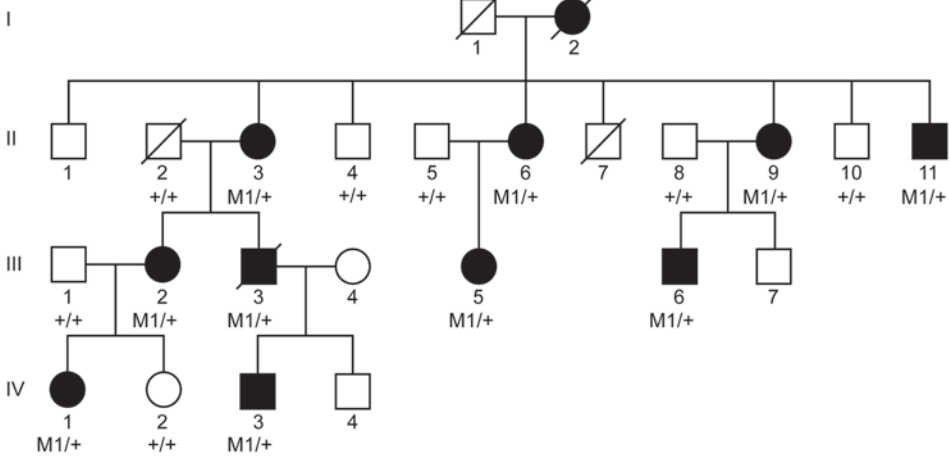
Figure 1. Pedigree of the family included in this study. The p.Leu579Pro pathogenic variant in *IMPG1* segregates with the disease. This pedigree is slightly updated compared to the pedigree in the previous article.[16]

Results

Clinical findings

An overview of the individual clinical characteristics of the patients is provided in Table 1. The mean age at which patients noticed their first symptom was 29.3 years (standard deviation 8.66; range: 17–45 years). The first symptom they experienced was night blindness (9/10 patients) or metamorphopsia (1/10 patients). Despite early macular abnormalities, the visual acuity only deteriorated from the fourth to fifth decade. In two patients (patient II:3 and patient II:6, at the age of 83 and 84, respectively) visual function was reduced to light perception. Patient III:2 was an exception in that she had an amblyopic right eye with 20/60 vision and had retinal detachment surgery in both left and right eye, at respectively age 14 and 17. Patient III:3 and IV:3 were diagnosed with RP during screening, respectively 9 and 3 years before the disease became symptomatic. In the first four decades of life, ophthalmoscopy showed fundus alterations ranging from macular pigment alterations to a bull's eye maculopathy, in few occasions accompanied by sparse bone spicule pigmentation, pallor of the optic disc and attenuation of the retinal arterioles (Figure 2). Over the years, disease progressed showing from the seventh decade onwards, profound macular atrophy, attenuated retinal vessels, pallor of the optic disc and bone spicule pigmentation was visible (Figure 2). Bone spicule pigmentation was generally sparse, except for patient III:2, who showed profound bone spicule pigmentation at age 61 (Figure 2G). When available, SD-OCT and FAF images revealed the loss of the outer retinal layers with sparing of the foveal photoreceptors (patients II:11, III:2 (OS), IV:1 and IV:3) (Figure 2). Goldmann perimetry showed visual fields ranging from normal to a (relative) ring scotoma, to severe constriction of the visual field. For example, in

patient II:11, visual field testing showed a relative, partial ring scotoma at the age of 47 years, which progressed to constriction of the visual field up to 20-30 degrees at the age of 67. In patient III:2, the visual field was constricted with a central island measuring up to 10 degrees at age 61. ERG responses were reduced in a rod-cone pattern (i.e., there was a slight predominance of rod dysfunction above cone dysfunction) in all patients. In patient IV:1, at the age of 17, the responses were only slightly abnormal as the scotopic responses were subnormal but the photopic responses were still normal. However, an ERG 18 years later showed nonrecordable scotopic and reduced photopic responses. An extensive overview of the clinical characteristics from 1974 to 2002 is provided in Van Lith-Verhoeven et al.[17]
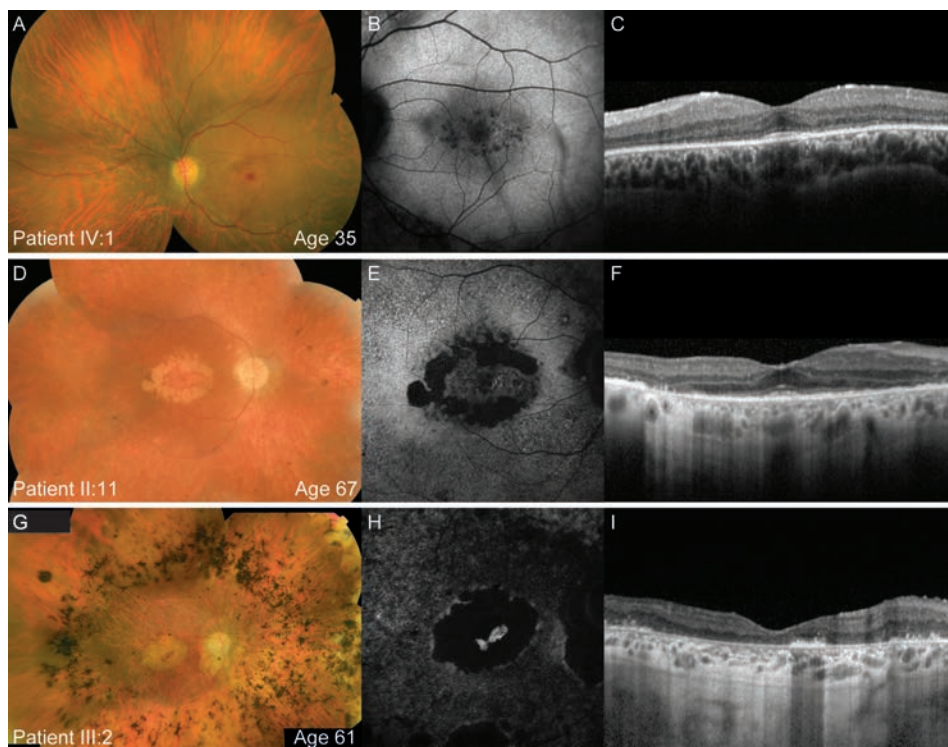

Figure 2. Multimodal images of three patients with *IMPG1*-associated RP. (A–C) Multimodal imaging of the left eye of patient IV:1 at the age of 35 years. (A) Composite fundus photograph showing a bull's eye maculopathy, attenuated retinal arterioles and no bone spicule pigmentation. (B) The fundus autofluorescence (FAF) image reveals an annular pattern of hypoautofluorescence in the macula and two eyelash artefacts. (C) Spectral-domain optical coherence tomography (SD-OCT) image showing preserved photoreceptor layers at the fovea. (D–F) Multimodal imaging of the right eye of patient II:11 at the age of 67. (D) Composite fundus photograph showing profound macular atrophy, attenuated retinal vessels, pallor of the optic disc and bone spicule pigmentation in the mid-periphery. (E) FAF image showing a speckled pattern of hyper- and hypoautofluorescence with a perifoveal ring of absent autofluorescence. (F) SD-OCT imaging reveals an intact ellipsoid zone layer at the fovea, with surrounding atrophy of the outer retinal layers. (G–I) Multimodal images of the right eye of patient III:2, at the age of 61 years. (G) Composite fundus photograph showing profound bone spicule pigmentation in the mid-periphery, macular and peripapillary atrophy, attenuated retinal vessels, waxy pallor of the optic disc, and atrophy in the nasal periphery. (H) FAF image reveals a central area of absent autofluorescence, with a small zone of increased autofluorescence. (I) SD-OCT image showing a small, parafoveal zone with preservation of the RPE layer that corresponds to the area with increased autofluorescence.
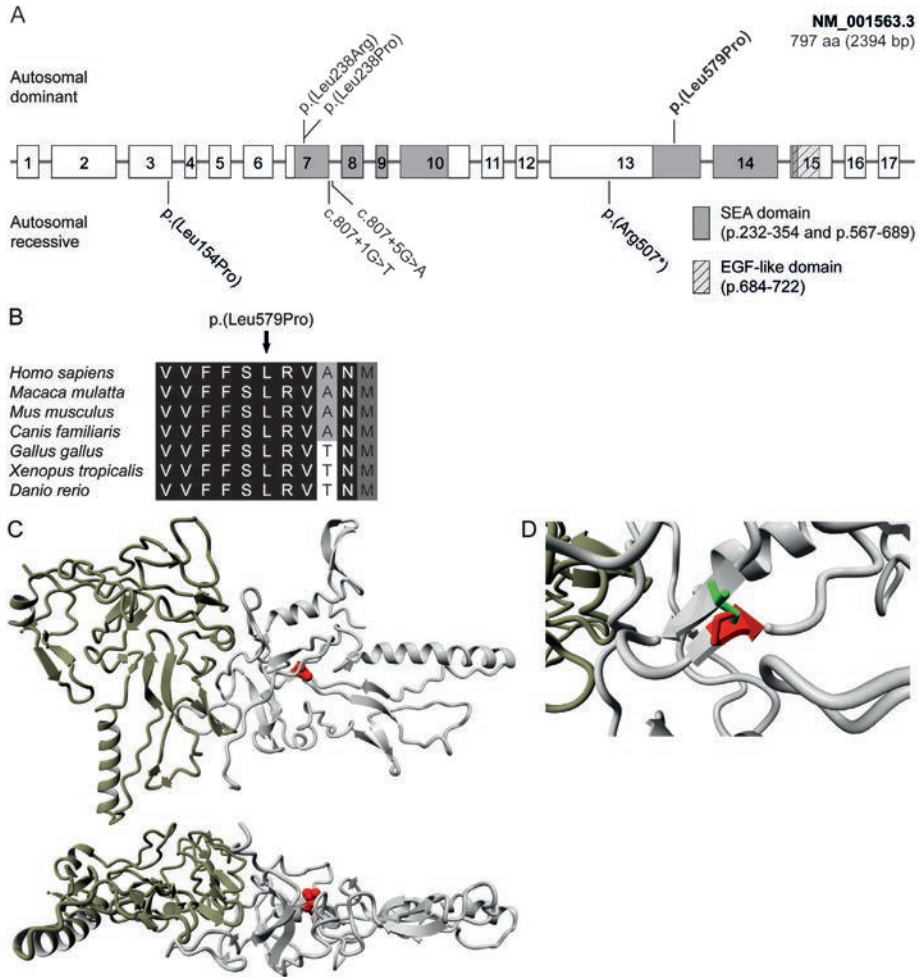
Figure 3. Overview of *IMPG1* gene, evolutionary conservation and effect on the IMPG1 structure of the *IMPG1* pathogenic variant p.Leu579Pro. (A) Schematic representation of the pathogenic variants in *IMPG1* and their location. Pathogenic variants that have been associated with autosomal dominant disease are indicated above the gene, whereas pathogenic variants that have been associated with autosomal recessive disease are indicated below the gene. The missense variant described in this study causing adRP is indicated in bold. The two variants depicted in normal font have been associated with vitelliform macular dystrophy. The portion of the gene that encodes the SEA and EGF-like domain is indicated in grey or with a striped pattern, respectively. (B) Evolutionary conservation of the mutated amino acid. Black boxes represent fully conserved amino acid residues, dark grey boxes represent highly conserved amino acid residues, and light grey boxes indicate moderately conserved amino acid residues. The p.Leu579Pro missense variant is located in a fully conserved region. (C) Visualization of the relatively flat IMPG1 structure (residues 556–798) from the front and the side. The leucine residue at position 579 is indicated in red, and the two monomers that form the dimer are indicated with different shades of grey. (D) Visualization of the p.Leu579Pro change in the IMPG1 structure. The wild-type amino acid is shown in green, whereas the mutation amino acid is depicted in red. Destabilization of the structure may occur by the change of the hydrophobic leucine to the smaller and more rigid proline.

Table 1. Clinical features of the patients described in this study at their most recent visit.

ID/Sex/Age of onset(y)/Age	Initial symptom	Visual acuity	SER[†]	ERG results			
		RE LE	RE LE	Scot 0.01	Scot 3.0	Phot 3.0	Phot 30Hz Flicker
II:3/F/34/83	Night blindness	LP LP	6.00 6.00	NR (54)	NR (54)	SR (54)	SR (54)
II:6/F/unknown/84	Night blindness	LP LP	0.38 plano	NR (65)	NR (65)	NR (65)	NR (65)
II:9/F/45/60	Night blindness	20/25 20/25	2.50 3.13	NR	SR	SR	MR
II:11/M/32/67	Night blindness	20/40 20/32	Plano -0.25	NR	NR	NR	NR
III:2/F/17/61	Night blindness	20/400 20/100	1.00 1.38	NR	NR	NR	NR
III:3/M/35/41	Metamorphopsia	20/15 20/40	unknown unknown	NR	NR	N	N
III:5/F/24/39	Night blindness	20/20 20/15	2.00 2.00	NR	NR	NR	NR
III:6/F/20/33	Night blindness	20/20 20/20	unknown unknown	NR	SR	SR	SR
IV:1/F/32/34	Night blindness	20/20 20/20	plano plano	NR	NR	SR	SR
IV:3/M/25/33	Night blindness	20/20 20/20	-0.88 plano	SR (22)	SR (22)	N (22)	N (22)

All features are present symmetrically, unless mentioned otherwise. BEM = bull's eye maculopathy; F = female; LE = left eye; LP = light perception; phot = photopic; M = male; N = normal; NR = non-recordable; RE = right eye; scot = scotopic; SER = spherical equivalent refraction; SR = severely reduced; VF = visual field. † If cataract surgery has been performed, the preoperative spherical equivalent was reported.

Ophthalmoscopy results[§]	Goldmann perimetry[§]
54y: BEM, attenuated retinal vessels, and pallor of the optic disc	54y: generalized reduced sensitivity, superior constricted VF (BE) with a centrocoecal scotoma RE
65y: macular atrophy with foveal sparing, abundant bone spicule pigmentation, attenuated retinal vessels, and waxy pallor of the optic disc	65y: constricted VF to10-20° with inferotemporal residue
45y: BEM, slightly attenuated retinal vessels, and normal aspect of the optic disc	Constricted VF, particularly superior to 20-30°
Macular atrophy with foveal sparing, bone spicule pigmentation in the mid-periphery, attenuated retinal vessels, and pallor of the optic disc	Constricted VF to to10-20° (RE) and 20-30° (LE)
Macular and peripapillary atrophy, abundant bone spicule pigmentation, attenuated retinal vessels, and waxy pallor of the optic disc	Constricted VF <10° (RE) and <5° (LE)
Central atrophy in a bull's eye pattern, pallor of the optic disc, peripapillary atrophy, and attenuated retinal vessels	No evident constriction of the VF
24y: macular pigment alterations, sparse bone spicule pigmentations, and mild peripapillary atrophy. Lattice degeneration in the LE.	Partial ringscotoma
BEM, some peripheral bone spicules, attenuated retinal vessels, and pallor of the optic disc	No VF loss
Red foveal zone surrounded by a ring of hypopigmentation, bone spicule pigmentation, attenuated retinal vessels, and pallor of the optic disc.	Reduced sensitivity with a relative midperipheral ringscotoma
Macular pigment alterations, sparse bone spicule pigmentation (LE>RE), and slightly attenuated retinal vessels	Central and mid-peripheral reduced sensitivity

Chapter 4.2

Genetic findings

When analyzing the overlapping variants residing in the mapped locus on chromosome 6 merely one variant predicted to be pathogenic was identified in patient IV:1 and IV:3. The c.1736T>C (p.Leu579Pro) heterozygous missense variant, which is absent in the ExAC, dbSNP, gnomAD and the Nijmegen in-house database, has a PhyloP score of 8.96 (range -14.1–6.4; predicted pathogenic ≥2.7), a Grantham score of 98 (range 0–215; predicted pathogenic ≥80), a CADD-PHRED score of 24.4 (range 1–99; predicted pathogenic ≥15), affects one of the two SEA-domains of *IMPG1* (Figure 3A–B), and is predicted deleterious and disease causing by the SIFT and MutationTaster prediction tools. The single remaining variant excluded the option of an alternative causative gene locating in the disease locus. The c.1736T>C variant was confirmed by Sanger sequence analysis, and segregates with the disease in all tested family members, which results in a LOD score of 4.2, which is genome wide significant. According to the American College of Medical Genetics criteria, this variant is considered likely pathogenic (PM1, PM2, and PP1–PP4).[26] Using the MetaDome web server we have analyzed within-human homologous variation at the position p.579 in IMPG1. The position p.579 corresponds to 34 codons within the human genome that is never found to be a proline, nor are these found in either ClinVar or gnomAD to change to a proline. This indicated that a proline is extremely rare at this position. Other residues that are regularly found at this position are Phe, Val, Iso, Leu, or Met.

Variant modeling

The predicted 3-dimensional structure of IMPG1 residues 556–798 is presented in Figure 3C–D. This part of IMPG1 consist of two connected monomers that form a fairly flat protein structure. Molecular modeling predicts that substitution of the leucine amino acid for proline in the second SEA-domain of IMPG1 causes a change in the structure of the protein by altering the backbone confirmation. Additionally, the hydrophobic leucine residue is lost, which may result in loss of potential hydrophobic interaction and small local alterations in the structure.

Discussion

The members of this family have been diagnosed with BCAMD based on typical early annular hypopigmentation in the macula and a relatively preserved visual acuity.[17, 18, 27] In the present study, we re-analyzed this family, using long-term clinical data, complemented with whole exome sequencing.

The follow-up data show that, although the visual acuity is preserved in the initial stage of disease, progression certainly occurs from the fourth to fifth decade. In addition, consecutive ERG recordings clearly show a generalized, progressive retinal disorder with photoreceptor dysfunction in a rod-cone pattern. Van Lith-Verhoeven et al. previously touched upon this and described that the initial parafoveal hypopigmentation progresses to an RP-like phenotype with typical RP findings such as night blindness, constriction of the visual field, bone spicule

pigmentation, attenuation of the retinal vessels and pallor of the optic disc.[17] In view of the natural history, which is far from benign, and the generalized character of the disorder, we propose to reject the term BCAMD and revise the diagnosis to RP with relative early macular involvement. Although early RP typically manifests in the midperiphery, early macular abnormalities have been described in other genetic subtypes of RP, including *CERKL-*, *IMPG2-* and *RP2* associated RP.[1, 28, 29]

The causative genetic defect in this family was previously mapped at 6p12.3-q16. Using whole exome sequencing, we identified one likely causative variant: the previously identified p. Leu579Pro missense change in the *IMPG1* gene.[17] This variant segregates with the disease (Figure 1) and affects a highly conserved amino acid located in the second SEA domain of *IMPG1* (Figure 3A–B). Modeling of the variant, although resolution was low, predicted a structural change due to the loss of hydrophobic interactions and the very specific structure of the proline residue. Although the exact function of the SEA domain (named after the first three proteins in which it was discovered; sea urchin sperm protein, enterokinase, and agrin) remains to be elucidated,[30] it may play a role in cleavage and might contribute to the adaptive ability of the extracellular matrixes.[13, 31] Pathogenic variants in *IMPG1* have previously been associated with vitelliform macular dystrophy with both autosomal dominant and recessive inheritance patterns,[13-15] and have been suggested to cause autosomal dominant RP.[16] Figure 3A shows the previously reported variants in *IMPG1*, and illustrates that the p.Leu579Pro and the previously reported p.Leu608Pro variant are the only variants located in the second SEA domain. Homologues domain analysis showed the absence of proline at position 579 in all 34 corresponding codon, indicating the rareness of this presence. We hypothesize that these variants cause RP instead of vitelliform macular dystrophy likely due to a dominant negative effect. This is supported by the heterozygous p.Arg507* nonsense variant which only causes a vitelliform retinal dystrophy with another pathogenic variant in trans,[13] which makes a haploinsufficiency mechanism less likely. The *IMPG1* gene encodes the SPACR protein, a glycoprotein located in the photoreceptor outer segments and the interphotoreceptor matrix (IPM). The exact function of SPACR and the interaction with other proteins remains to be elucidated to fully explain the occurrence of two different phenotypes.

IMPG1 is highly similar to *IMPG2*, which encodes the proteoglycan SPACRCAN (i.e., sialoproteoglycan associated with cones and rods) that is also located in the interphotoreceptor matrix. They both contain two SEA-domains, an EGF-like domain and a RHAMM HA-binding motif. Similar to *IMPG1*, pathogenic variants in *IMPG2* have been associated with vitelliform macular dystrophy and RP with relative early macular involvement.[14, 15, 28, 32] However, despite the large similarities, there are also differences. First, *IMPG2*-associated RP is inherited in an autosomal recessive fashion and has an earlier age of onset, with a mean age of 10.5 years (range 4–20 years).[28] Early macular involvement is also present in *IMPG2*-associated RP although loss of visual acuity generally occurs much earlier in these patients. Secondly, SPACRCAN contains a chondroitin sulfate glycosaminoglycan side chain.[4] Since these side chains may also interact with hyaluronan, SPACRCAN can potentially link two hyaluronan molecules and stabilize

the IPM scaffold.[33] However, in contrast to foveate retinas, SPACR also contains these chondroitin sulfate chains in non-foveate retinas.[4] Third, *IMPG1* is expressed earlier in the developing human retina and may have a role in the photoreceptor development, whereas *IMPG2* is involved in photoreceptor maturation.[5] These differences in function between SPACR and SPACRCAN may explain the phenotypic differences when the function is compromised.

In conclusion, the clinical diagnosis of the phenotype in this family should be revised to RP and the inaccurate, descriptive term BCAMD should be rejected. This study provides supporting evidence on the causal role of the p.Leu579Pro missense change in *IMPG1* in this family. This enlarges the clinical spectrum of disorders caused by pathogenic variants in *IMPG1* that previously consisted of dominant and recessive forms of vitelliform macular dystrophy. The *IMPG1* gene should be added to the list of genes that, when mutated, can cause autosomal dominant forms of RP.

References

1. Verbakel SK, van Huet RAC, Boon CJF, et al. Non-syndromic retinitis pigmentosa. Prog Retin Eye Res 2018;66:157-86.
2. Pagon RA. Retinitis pigmentosa. Surv Ophthalmol 1988;33(3):137-77.
3. Acharya S, Rodriguez IR, Moreira EF, et al. SPACR, a novel interphotoreceptor matrix glycoprotein in human retina that interacts with hyaluronan. J Biol Chem 1998;273(47):31599-606.
4. Hollyfield JG. Hyaluronan and the functional organization of the interphotoreceptor matrix. Invest Ophthalmol Vis Sci 1999;40(12):2767-9.
5. Felemban M, Dorgau B, Hunt NC, et al. Extracellular matrix component expression in human pluripotent stem cell-derived retinal organoids recapitulates retinogenesis in vivo and reveals an important role for IMPG1 and CD44 in the development of photoreceptors and interphotoreceptor matrix. Acta Biomater 2018;74:207-21.
6. Al-Ubaidi MR, Naash MI, Conley SM. A perspective on the role of the extracellular matrix in progressive retinal degenerative disorders. Invest Ophthalmol Vis Sci 2013;54(13):8119-24.
7. Lazarus HS, Hageman GS. Xyloside-induced disruption of interphotoreceptor matrix proteoglycans results in retinal detachment. Invest Ophthalmol Vis Sci 1992;33(2):364-76.
8. Hageman GS, Marmor MF, Yao XY, Johnson LV. The interphotoreceptor matrix mediates primate retinal adhesion. Arch Ophthalmol 1995;113(5):655-60.
9. Gonzalez-Fernandez F. Interphotoreceptor retinoid-binding protein--an old gene for new eyes. Vision Res 2003;43(28):3021-36.
10. Hageman GS, Kirchoff-Rempe MA, Lewis GP, et al. Sequestration of basic fibroblast growth factor in the primate retinal interphotoreceptor matrix. Proc Natl Acad Sci U S A 1991;88(15):6706-10.
11. Ishikawa M, Sawada Y, Yoshitomi T. Structure and function of the interphotoreceptor matrix surrounding retinal photoreceptor cells. Exp Eye Res 2015;133:3-18.
12. Rhodes JM, Simons M. The extracellular matrix and blood vessel formation: not just a scaffold. J Cell Mol Med 2007;11(2):176-205.
13. Manes G, Meunier I, Avila-Fernandez A, et al. Mutations in IMPG1 cause vitelliform macular dystrophies. Am J Hum Genet 2013;93(3):571-8.
14. Meunier I, Manes G, Bocquet B, et al. Frequency and clinical pattern of vitelliform macular dystrophy caused by mutations of interphotoreceptor matrix IMPG1 and IMPG2 genes. Ophthalmology 2014;121(12):2406-14.
15. Brandl C, Schulz HL, Charbel Issa P, et al. Mutations in the Genes for Interphotoreceptor Matrix Proteoglycans, IMPG1 and IMPG2, in Patients with Vitelliform Macular Lesions. Genes (Basel) 2017;8(7).
16. Zhang Q, Xu M, Verriotto JD, et al. Next-generation sequencing-based molecular diagnosis of 35 Hispanic retinitis pigmentosa probands. Sci Rep 2016;6:32792.
17. van Lith-Verhoeven JJ, Hoyng CB, van den Helm B, et al. The benign concentric annular macular dystrophy locus maps to 6p12.3-q16. Invest Ophthalmol Vis Sci 2004;45(1):30-5.
18. Deutman AF. Benign concentric annular macular dystrophy. Am J Ophthalmol 1974;78(3):384-96.
19. McCulloch DL, Marmor MF, Brigell MG, et al. ISCEV Standard for full-field clinical electroretinography (2015 update). Doc Ophthalmol 2015;130(1):1-12.
20. Haer-Wigman L, van Zelst-Stams WA, Pfundt R, et al. Diagnostic exome sequencing in 266 Dutch patients with visual impairment. Eur J Hum Genet 2017;25(5):591-9.
21. Wiel L, Baakman C, Gilissen D, et al. MetaDome: Pathogenicity analysis of genetic variants through aggregation of homologous human protein domains. Hum Mutat 2019.
22. Scally SW, McLeod B, Bosch A, et al. Molecular definition of multiple sites of antibody inhibition of malaria transmission-blocking vaccine antigen Pfs25. Nat Commun 2017;8(1):1568.
23. Krieger E, Koraimann G, Vriend G. Increasing the precision of comparative models with YASARA NOVA--a self-parameterizing force field. Proteins 2002;47(3):393-402.
24. Vriend G. WHAT IF: a molecular modeling and drug design program. J Mol Graph 1990;8(1):52-6, 29.
25. Sander C, Schneider R. Database of homology-derived protein structures and the structural meaning of sequence alignment. Proteins 1991;9(1):56-68.
26. Richards S, Aziz N, Bale S, et al. Standards and guidelines for the interpretation of sequence variants: a joint consensus recommendation of the American College of Medical Genetics and Genomics and the Association for Molecular Pathology. Genet Med 2015;17(5):405-24.
27. van den Biesen PR, Deutman AF, Pinckers AJ. Evolution of benign concentric annular macular dystrophy. Am J Ophthalmol 1985;100(1):73-8.
28. van Huet RA, Collin RW, Siemiatkowska AM, et al. IMPG2-associated retinitis pigmentosa displays relatively early macular involvement. Invest Ophthalmol Vis Sci 2014;55(6):3939-53.
29. Avila-Fernandez A, Riveiro-Alvarez R, Vallespin E, et al. CERKL mutations and associated phenotypes in seven Spanish families with autosomal recessive retinitis pigmentosa. Invest Ophthalmol Vis Sci 2008;49(6):2709-13.
30. Bork P, Patthy L. The SEA module: a new extracellular domain associated with O-glycosylation. Protein Sci 1995;4(7):1421-5.
31. Palmai-Pallag T, Khodabukus N, Kinarsky L, et al. The role of the SEA (sea urchin sperm protein, enterokinase and agrin) module in cleavage of membrane-tethered mucins. FEBS J 2005;272(11):2901-11.
32. Bandah-Rozenfeld D, Collin RW, Banin E, et al. Mutations in IMPG2, encoding interphotoreceptor matrix proteoglycan 2, cause autosomal-recessive retinitis pigmentosa. Am J Hum Genet 2010;87(2):199-208.
33. Chen Q, Cai S, Shadrach KG, et al. Spacrcan binding to hyaluronan and other glycosaminoglycans. Molecular and biochemical studies. J Biol Chem 2004;279(22):23142-50.

Chapter 4.2

Treatment

Carbonic anhydrase inhibitors for the treatment of cystic macular lesions in children with X-linked juvenile retinoschisis

Sanne K. Verbakel, Johannes P.H. van de Ven, Linda M.P. Le Blanc , Joannes M.M. Groenewoud, Eiko K. de Jong, B. Jeroen Klevering, Carel B. Hoyng

Abstract

Purpose
Little is known regarding the therapeutic effect of carbonic anhydrase inhibitors (CAIs) in the management of cystic macular lesions in children with X-linked juvenile retinoschisis (XLRS) despite the fact that this disease often manifests during childhood. Therefore, our goal was to determine the efficacy of CAIs in the treatment of cystic macular lesions in children with XLRS.

Methods
We used CAIs to treat cystic macular lesions in 18 eyes of nine children with XLRS. We evaluated the therapeutic effect of CAI treatment with the best-corrected visual acuity and foveal zone thickness (FZT) with spectral-domain optical coherence tomography. A reduction of at least 22,4% in FZT was defined as objective evidence of response.

Results
Five of nine (55.6%) XLRS patients showed a significant reduction of FZT in both eyes over a median treatment interval of 6,8 months (range, 1-23). In four of five (80.0%) patients, this reduction was already apparent after 1 month of treatment. An improvement of visual acuity was observed in five eyes (27.8%) of three patients (33.3%). Six patients (66.6%) reported minor side effects.

Conclusions
Treatment with CAIs decreased FZT in more than half of the children with XLRS. This effect was observed within 1 month in the majority of patients. Carbonic anhydrase inhibitor treatment restores retinal anatomy and may contribute to creating optimal circumstances for gene therapy.

Introduction

X-linked juvenile retinoschisis (XLRS) is the leading cause of hereditary juvenile macular degeneration in males with an estimated prevalence ranging from 1 in 5,000 to 1 in 25,000.[1] The onset of XLRS has been attributed to pathogenic mutations in the retinoschisin gene (*RS1*) on the X chromosome, which encodes a cell adhesion protein responsible for the architectural integrity of the retina.[2] Cystic macular lesions are the hallmark features in the early stage of XLRS.[3] The pathogenesis of these cystic macular lesions is not entirely understood, but they should not be confused with cystoid macular edema as the normal appearance of the macula on fluorescein angiography in patients with XLRS suggests that vascular leakage plays a minor role, if any, in the pathogenesis of these cystic lesions.

Both oral and topical carbonic anhydrase inhibitors (CAIs) have been used successfully in the management of cystic lesions in macular dystrophies, including XLRS.[4] The clinical effect of CAIs is thought to be through their action on the membrane-bound carbonic anhydrase receptors present in the retinal pigment epithelium (RPE).[5] Moreover, other carbonic anhydrase receptors in different cells of the neural retina may also play a role.[6] Carbonic anhydrase inhibitors act both on retinal and RPE cell function by acidifying the subretinal space, decreasing the standing potential as well as raising retinal adhesiveness, probably by increasing RPE fluid transport.[5,7]

The vast majority of previous studies investigated the effects of CAI treatment in managing XLRS associated cystic macular lesions in adults.[4, 8-13] Few studies reported the effect of topical CAIs in the management of cystic macular lesions in children.[13-16] To the best of our knowledge, only eight cases on the effect of oral acetazolamide on cystic macular lesions in children with XLRS have been reported in the literature.[16-18] This is surprising since restoration of retinal function, albeit temporarily, is more likely to occur in younger patients as compared to adults, where structural alterations may prevent visual improvement despite anatomical recovery.[12] The aim of this study was therefore to determine the efficacy of CAI treatment in children with XLRS-associated cystic macular lesions.

Methods

Patients

This retrospective cohort study adhered to the tenets of the Declaration of Helsinki, and informed consent was obtained from all participants. We included nine XLRS patients (18 eyes) with a mean age of 12.3 years (range, 6.4–16.6), who were treated with oral CAIs for cystic macular lesions between March 2014 and March 2016 at the Institute of Ophthalmology of the Radboud University Medical Center Nijmegen (the Netherlands). A 10th patient was excluded from the study because he choose to discontinue treatment because of paresthesias in the second week of treatment, as were patients over 18 years of age and patients who did not take CAIs for at least 4 weeks.

The diagnosis of XLRS was molecularly confirmed in four out of nine patients. In the remaining five patients, no molecular analysis was performed and the diagnosis of XLRS was based on the combination of information regarding family history, a decrease in visual acuity, a spoke-wheel pattern in the macula on high magnification ophthalmoscopy, and bilateral foveoschisis on spectral-domain optical coherence tomography (SD-OCT).

All nine patients were treated with oral acetazolamide with a dose ranging from 125 mg two times a day to 250 mg three times a day. In addition, six patients also used topical CAIs such as brinzolamide (four patients) or dorzolamide (two patients)(Table 1). CAI doses were mainly dependent on the patients' age, although adjustments were made based on side effects and the effect on cystic macular lesions seen on SD-OCT. The minimum effective CAI dose was pursued.

Ophthalmic data collection

Information regarding best-corrected Snellen visual acuity and retinal thickness measured on SD-OCT was collected from baseline to the most recent visit during CAI treatment. For statistical analysis, the best-corrected Snellen visual acuity was converted into logarithm of the minimal angle of resolution (logMAR) values. A change of 0.14 logMAR, corresponding with a change of seven or more letters on the Early Treatment Diabetic Retinopathy Study (ETDRS) chart, was considered significant.[11,12] Cross-sectional images were obtained using SD-OCT (trSpectralis HRA+OCT; Heidelberg Engineering, Heidelberg, Germany). The foveal zone thickness (FZT) was calculated using Heidelberg Eye Explorer software version 1.8.6.0) in the central 1000-μm diameter circle (C1) of the ETDRS grid. The intervisit variability of SD-OCT measurements was calculated using a previously described method based on the FZT change in both eyes of four XLRS patients (no. 1, no. 6, no. 7 and no. 10, who was excluded from the rest of the study). Baseline FZT was compared with the first preceding FZT up to 6 months prior to starting treatment, with a mean interval of 3.3 months (range, 2–6).[12,19]

The average difference was 10.1% and the "average + 2SD" was 22.4%. Hence, in this study, a reduction of more than 22.4% in FZT was considered a significant response due to CAI treatment. During treatment, patients were advised to regularly eat potassium-rich food to prevent possible hypokalemia caused by the CAIs. Potassium levels were checked by the attending ophthalmologist or general practitioner.

Statistical analysis

Prognostic factors for the response to CAIs were analyzed with a multivariable logistic regression analysis. Two-sided *P* values of less than 0.05 were considered statistically significant. Data were analyzed using SPSS Software (version 22.0; SPSS Inc., Chicago, IL).

Results

Five of nine (55.6%) XLRS patients showed a significant reduction of FZT in both eyes over a median treatment interval of 6.8 months (range, 1–23) (Table 1; Figures 1, 2,3). In four of five (80.0%) patients, this significant reduction was already present after 1 month of treatment. In the remaining patient (no. 5), no information about FZT after 1 month of treatment was available but he already showed a FZT reduction of 10% and 6% after 12 days of treatment. The FZT reduction persisted over a median treatment interval of 10.1 months (range, 7–16) in eight eyes of the five patients. In two eyes, the right eye of patient no. 2 and the left eye of patient no. 8, a rebound effect occurred where the macular cysts returned to at least baseline levels. This happened after dose reduction of oral acetazolamide from 125 mg three times a day to daily 250 mg with sustained release in patient no. 2. In patient no. 8, the rebound effect occurred after cessation of additional topical brinzolamide eight times a day. After restarting brinzolamide six times a day, FZT again decreased significantly. Overall mean FZT decreased from 409.1 μm at baseline to 332.8 μm at the most recent visit during treatment (P=0.024). In the 5 patients
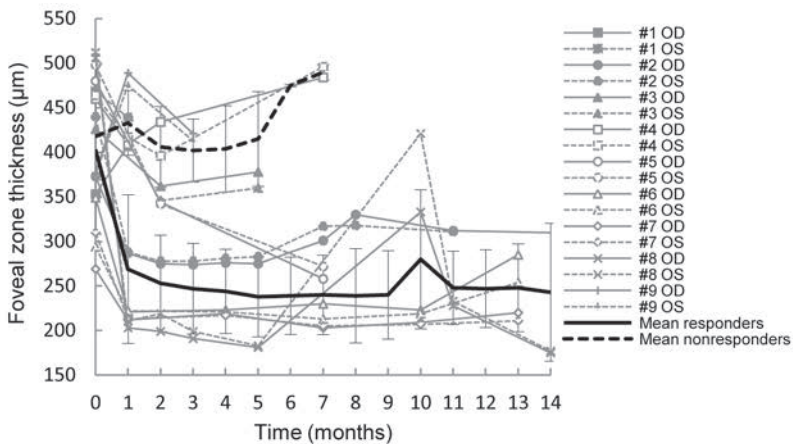

Figure 1. Change in FZT over time. The solid black line indicates the mean FZT of the five XLRS patients with a significant reduction of FZT, and the dotted black line indicates the mean FZT of the patients without a significant reduction. Vertical lines are the standard deviation of the mean responder and mean nonresponder lines.

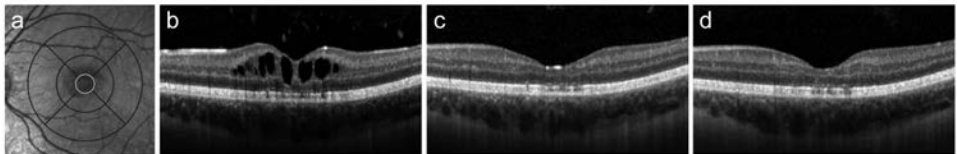**Figure 2.** Infrared and horizontal spectral domain optical coherence tomography (SD-OCT) images (30°) from the left eye of patient #7 showing the response to oral acetazolamide. Near infrared image with a projection of the ETDRS grid (A). The highlighted most inner circle of the grid was used to measure foveal zone thickness (FZT). SD-OCT image at baseline (B), after one month of treatment (C) and after 13 months of treatment (D).

Table 1. Clinical characteristics of XLRS patients at baseline and during acetazolamide treatment.

Patient	Age, y*	Gender	Family	Duration, mo†	VA, logMAR		FZT, µm (% Change)		Acetazolamide dose	Topical therapy (times a day)	Side effects
					OD	OS	OD	OS			
No. 1	6	Male	1	Baseline	0.60	0.45	353	469	125 mg b.i.d.	-	Absent
				1	0.70	0.68	407 (+15)	439 (-6)	125 mg b.i.d.¶	-	
No. 2	11	Male	1	Baseline	0.38	0.45	373	440	250 mg b.i.d.	-	Paresthesia
				1	0.35	0.33	**287 (-23)**	**288 (-35)**	125 mg b.i.d.	-	
				5	**0.15**	**0.15**	**275 (-26)**	**283 (-36)**	250 mg SR‡ b.i.d.	Dorzolamide (8)	
				23	**0.13**	**0.08**	376 (+1)	391 (-11)	250 mg SR‡ daily	Dorzolamide (8)	
No. 3	6	Male	1	Baseline	0.18	0.25	426	Poor quality	125 mg b.i.d.	-	Absent
				2	0.18	0.35	362 (-15)	346	125 mg b.i.d.	-	
				4	0.08	0.13	378 (-11)	360	250 mg SR‡ daily¶	-	
No. 4	15	Male		Baseline	0.28	0.38	460	464	250 mg b.i.d.	-	Paresthesia
				1	0.38	0.53	409 (-11)	417 (-10)	250 mg t.i.d.	-	
				7	0.28	0.45	484 (+5)	496 (+7)	250 mg b.i.d.+ 125 mg daily	Dorzolamide (6)	
No. 5	13	Male		Baseline	0.10	0.28	480	498	125 mg t.i.d.	-	Absent
				2	0.15	0.15	**344 (-28)**	**342 (-30)**	250 mg b.i.d. + 125 mg daily	-	
				7	0.08	0.15	**258 (-46)**	**272 (-45)**	250 mg b.i.d. + 125 mg daily	-	
No. 6	12	Male	2	Baseline	0.40	0.45	349	294	125 mg t.i.d.	-	
				1	0.40	0.38	**214 (-39)**	**209 (-29)**	125 mg daily	Brinzolamide (6)	Paresthesia
				7	0.35	0.35	**230 (-34)**	**213 (-28)**	250 mg daily + 125 mg daily	Brinzolamide (2)	Fatigue§
				13	0.40	0.38	285 (-18)	254 (-14)	250 mg b.i.d.	-	

No.	Age	Sex	FZT	Timepoint	VA	VA	Foveal thickness	Foveal thickness	Dosage	Switch	Side effects
No. 7	15	Male	2	Baseline	0.38	0.33	269	310	125 mg t.i.d.	-	Fatigue
				1	0.33	0.30	**201 (-25)**	**205 (-34)**	125 mg daily	Brinzolamide (6)	
				7	0.30	0.30	**203 (-25)**	**205 (-34)**	250 mg daily + 125 mg daily	Brinzolamide (2)	
				13	0.43	0.43	220 (-18)	**211 (-32)**	250 mg daily + 125 mg daily	-	
No. 8	16	Male		Baseline	0.65	0.35	506	512	250 mg t.i.d.	Brinzolamide (8)	Paresthesia
				1	**0.34**	0.28	**203 (-60)**	**211 (-59)**	250 mg t.i.d.	Brinzolamide (8)	
				5	**0.35**	0.35	**181 (-64)**	**183 (-64)**	125 mg b.i.d. + 250 mg daily	Brinzolamide (8)	
				14	**0.40**	0.35	**175 (-65)**	**177 (-65)**	250 mg b.i.d.	Brinzolamide (6)	
No. 9	13	Male		Baseline	0.63	0.55	377	375	250 mg b.i.d.	-	
				1	0.53	0.40	489 (+30)	475 (+27)	250 mg SR† daily	-	Paresthesia||
				3	**0.38**	**0.30**	421 (+12)	413 (+10)	250 mg SR† daily	Brinzolamide (6)	

(-), Decrease in FZT; (+), increase in FZT; b.i.d., two times a day; t.i.d., three times a day. Visual acuity printed in bold indicate a significant improvement of at least 0.14 logMAR. Foveal zone thickness values printed in bold indicate a significant reduction, which was defined as a reduction in foveal zone thickness of 22.4%. * Age at start of acetazolamide treatment. † Total duration of treatment (in months) calculated from the baseline. ‡ Acetazolamide with sustained release. § Side effects disappeared over time. || Side effects disappeared after switching to oral acetazolamide with sustained release. ¶ Therapy discontinued due to lack of effect.
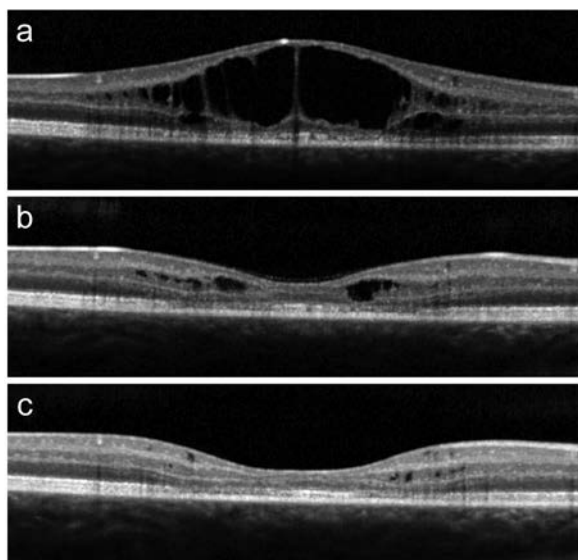
Chapter 5.1

Figure 3. Horizontal spectral domain optical coherence tomography (SD-OCT) images (30°) from the right eye of patient #8 showing the response to oral acetazolamide. SD-OCT image at baseline (A), after one month of treatment (B) and after 14 months of treatment (C).

with a significant reduction, mean FZT decreased from 403.1 μm at baseline to 261.9 μm at the most recent visit during treatment (*P*=0.006). Age at baseline (p=0.111) or mean FZT at baseline (*P*=0.531) did not predict the response to CAIs.

Visual acuity improved significantly (≥0.14 logMAR) from baseline value in at least one eye in 3 out of 9 (33.3%) XLRS patients. Two patients (22.2%) showed a significant improvement of visual acuity in both eyes (Table 1 and Figure 4). Overall, mean visual acuity at baseline (0.39 ± 0.15 logMAR) and mean visual acuity at the most recent visit (0.32 ± 0.19 logMAR) were not statistically different (*P*=0.078). Only one patient showed both a visual improvement and a significant reduction in FZT at the most recent visit during CAI treatment. Improvement of visual acuity was therefore not correlated with a reduction in FZT as well as not correlated with patients age. Six patients (66.6%) experienced minor side effects during treatment such as digital and/or perioral paresthesia (55.6%) and fatigue (22.2%) (Table 1). In patient no. 9, the paresthesias disappeared after switching from oral acetazolamide 250 mg two times a day to oral acetazolamide with sustained release 250 mg daily.

Discussion

We investigated the therapeutic effect of CAIs in the management of cystic macular lesions in children with XLRS. Five of nine patients showed a significant reduction of FZT in both eyes that was observed within 1 month in the majority of patients. Judged by the treatment effect in our patients, the response to CAIs can be assessed after only 1 month in most patients. This treatment response was quicker than the effect described in XLRS patients by Apushkin and
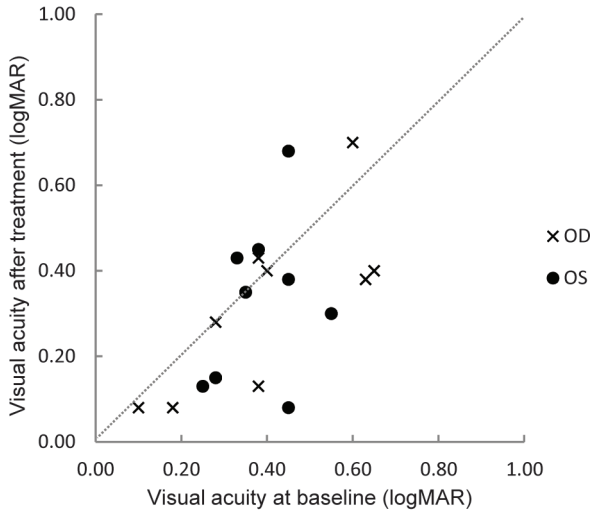
Figure 4. Changes in visual acuity from baseline to the most recent visit during acetazolamide treatment.

Fishman, though they used only topical CAIs with notable lower doses.[12] The difference in treatment response might consequently be explained by the dose differences between both studies as dose dependency was previously described in patients with XLRS or other retinal dystrophies who were treated with CAIs.[11,20,21] This is supported by the return of macular cysts after reduction of the CAI dose in patient no. 2 and no. 8 that may, at least in part, be dose dependent and not solely a rebound effect.

In this study we defined FZT changes of more than 22.4% as statistically significant. This percentage is slightly higher compared to the 17.1% used in other studies.[10-12] This difference may be explained by the higher variation in thickness in younger patients on which our calculation was based. Not all patients could be included in the intervisit percent difference calculations because of the lack of SD-OCT scans made within 6 months prior to the baseline measurement. By using 22.4% as cut off point, we might have underestimated the CAI effect compared to other studies.

No prognostic factors for response to CAIs were found in this study. Age at baseline and greater initial FZT did not affect treatment response, although such influences were previously described in patients with retinitis pigmentosa (RP).[22]

Improvement of visual acuity in at least one eye occurred in three patients (33.3%). In accordance with previous studies, improvement of visual acuity was not correlated with age nor with reduction of central retinal thickness on OCT.[10,19,23] To our knowledge, the natural course of visual acuity in children with XLRS has not been described previously. To be comparable with studies performed in adults, we used 0.14 logMAR as cut-off point for improvement in visual acuity, keeping in mind that the results may be over- or underestimated.[11,12]

No patient discontinued CAI treatment due to the side effects. However, one patient was

Chapter 5.1

243

excluded from the study because he discontinued treatment due to paresthesias in the second week of treatment. The disappearance of the side effects in patient no. 9 can be caused by the switch to oral acetazolamide with sustained release, but at the same time patients' total daily CAI dose was reduced. Consequently, we cannot conclude that sustained release treatment shows fewer side effects. Limitations of our study include its retrospective nature, the inherent small cohort size of rare diseases and the variation in dosage of CAIs, partly by the selective use of topical CAIs. Because of these limitations and the different follow-up intervals, conclusions should be interpreted cautiously.

Despite the side effects and the little improvement in visual acuity, there may also be a long-term benefit in restoring normal retinal anatomy. In patients with XLRS, treatment of the cystoid macular lesions may decrease the occurrence of later-onset atrophic lesions and the associated visual loss.[24]

With upcoming treatments such as gene therapy, CAIs may play a role in preserving and restoring retinal anatomy to create optimal circumstances. Retinal pretreatment with CAIs shortly before subretinal injection with transgene vectors may reduce the risk of traumatic damage to the central retina caused by the subretinal injection. The long term benefits of CAI treatment, especially in relation to the side effects, will have to be studied further.

In conclusion, reduction of central retinal thickness occurred in more than half of the children treated with CAIs, but only three patients experienced visual improvement over a median treatment interval of 6.8 months. Evaluation of treatment effect is possible after only 1 month in the majority of patients. Restoration of macular architecture with CAI treatment may delay functional retinal loss and could be important in the creation of more optimal circumstances for gene therapy.

References

1. Mooy CM, Van Den Born LI, Baarsma S, et al. Hereditary X-linked juvenile retinoschisis: a review of the role of Muller cells. *Arch Ophthalmol.* 2002;120(7):979-984.
2. Tantri A, Vrabec TR, Cu-Unjieng A, Frost A, Annesley WH, Jr., Donoso LA. X-linked retinoschisis: a clinical and molecular genetic review. *Surv Ophthalmol.* 2004;49(2):214-230.
3. Molday RS, Kellner U, Weber BH. X-linked juvenile retinoschisis: clinical diagnosis, genetic analysis, and molecular mechanisms. *Prog Retin Eye Res.* 2012;31(3):195-212.
4. Salvatore S, Fishman GA, Genead MA. Treatment of cystic macular lesions in hereditary retinal dystrophies. *Surv Ophthalmol.* 2013;58(6):560-584.
5. Wolfensberger TJ, Dmitriev AV, Govardovskii VI. Inhibition of membrane-bound carbonic anhydrase decreases subretinal pH and volume. *Doc Ophthalmol.* 1999;97(3-4):261-271.
6. Wistrand PJ, Schenholm M, Lonnerholm G. Carbonic anhydrase isoenzymes CA I and CA II in the human eye. *Invest Ophthalmol Vis Sci.* 1986;27(3):419-428.
7. Wolfensberger TJ. The role of carbonic anhydrase inhibitors in the management of macular edema. *Doc Ophthalmol.* 1999;97(3-4):387-397.
8. Zhang L, Reyes R, Lee W, et al. Rapid resolution of retinoschisis with acetazolamide. *Doc Ophthalmol.* 2015;131(1):63-70.
9. Ali S, Seth R. X-linked juvenile retinoschisis in females and response to carbonic anhydrase inhibitors: case report and review of the literature. *Semin Ophthalmol.* 2013;28(1):50-54.
10. Thobani A, Fishman GA. The use of carbonic anhydrase inhibitors in the retreatment of cystic macular lesions in retinitis pigmentosa and X-linked retinoschisis. *Retina.* 2011;31(2):312-315.
11. Genead MA, Fishman GA, Walia S. Efficacy of sustained topical dorzolamide therapy for cystic macular lesions in patients with X-linked retinoschisis. *Arch Ophthalmol.* 2010;128(2):190-197.
12. Apushkin MA, Fishman GA. Use of dorzolamide for patients with X-linked retinoschisis. *Retina.* 2006;26(7):741-745.
13. Khandhadia S, Trump D, Menon G, Lotery AJ. X-linked retinoschisis maculopathy treated with topical dorzolamide, and relationship to genotype. *Eye (Lond).* 2011;25(7):922-928.
14. Bastos AL, Freitas Bde P, Villas Boas O, Ramiro AC. Use of topical dorzolamide for patients with X-linked juvenile retinoschisis: case report. *Arq Bras Oftalmol.* 2008;71(2):286-290.
15. Yang FP, Willyasti K, Leo SW. Topical brinzolamide for foveal schisis in juvenile retinoschisis. *J AAPOS.* 2013;17(2):225-227.
16. Rocha Cabrera P, Pareja Rios AC, Cordoves Dorta L, Mantolan Sarmiento C, Serrano Garcia MA. A combination of topical and systemic carbonic anhydrase in the treatment of chromosome X-linked retinoschisis. *Arch Soc Esp Oftalmol.* 2014;89(8):320-323.
17. Gurbaxani A, Wei M, Succar T, McCluskey PJ, Jamieson RV, Grigg JR. Acetazolamide in retinoschisis: a prospective study. *Ophthalmology.* 2014;121(3):802-803.e803.
18. Ghajarnia M, Gorin MB. Acetazolamide in the treatment of X-linked retinoschisis maculopathy. *Arch Ophthalmol.* 2007;125(4):571-573.
19. Grover S, Apushkin MA, Fishman GA. Topical dorzolamide for the treatment of cystoid macular edema in patients with retinitis pigmentosa. *Am J Ophthalmol.* 2006;141(5):850-858.
20. Fishman GA, Gilbert LD, Fiscella RG, Kimura AE, Jampol LM. Acetazolamide for treatment of chronic macular edema in retinitis pigmentosa. *Arch Ophthalmol.* 1989;107(10):1445-1452.
21. Boon CJ, van den Born LI, Visser L, et al. Autosomal recessive bestrophinopathy: differential diagnosis and treatment options. *Ophthalmology.* 2013;120(4):809-820.
22. Liew G, Moore AT, Webster AR, Michaelides M. Efficacy and prognostic factors of response to carbonic anhydrase inhibitors in management of cystoid macular edema in retinitis pigmentosa. *Invest Ophthalmol Vis Sci.* 2015;56(3):1531-1536.
23. Ikeda Y, Hisatomi T, Yoshida N, et al. The clinical efficacy of a topical dorzolamide in the management of cystoid macular edema in patients with retinitis pigmentosa. *Graefes Arch Clin Exp Ophthalmol.* 2012;250(6):809-814.

Chapter 5.1

General discussion

This thesis contains a comprehensive overview of our current understanding of the genotype, phenotype and therapeutic options for retinitis pigmentosa. This thesis also adds to this knowledge with studies on the phenotypic and molecular characteristics of *IMPG1*, *KIAA1549*, *RP1* and *TULP1*-associated retinal dystrophies. We discuss genotype-phenotype correlations and evaluate the effect of the treatment of cystic macular lesions in children with XLRS with oral and topical acetazolamide. In this section, the knowledge gained from these studies will be placed in a wider context.

Merely 20 years ago, the ophthalmologist could do little more than monitor the relentless progression of inherited retinal diseases. Besides a watchful eye for other associated ocular abnormalities that might be treated, such as cataract and CME, their pallet of therapeutic options was limited. Currently, our knowledge of the underlying disease mechanisms has expanded tremendously and although the actual treatment of inherited retinal disorders is still at a very early stage, we are at the verge of a breakthrough with emerging therapeutics like gene augmentation therapy and small molecules aimed at interfering the visual cycle, lipofuscin accumulation or splicing. Genetic tests have become widely available to differentiate genetic subtypes of dystrophies, the first gene augmentation therapy for patients with *RPE65*-associated retinal disease recently became clinically available, and several other treatments for retinal diseases are being developed (https://clinicaltrials.gov).

Nomenclature of retinal dystrophies

An optimal disease nomenclature is simple, unambiguous and comprehensible for both ophthalmologists and patients. Unfortunately, the current nomenclature of retinal dystrophies that has gradually expanded over almost a century and a half, has become complicated, illogical, insufficient for the heterogeneous nature of these disorders and without enough consideration for the underlying genetic defect. Historically, in the era prior to genetic and electrophysiological testing, the nomenclature of retinal dystrophies was entirely based on clinical observations and the topographic arrangement of morphological alterations in the retina. This resulted in differentiation between disorders confined to a specific area of the retina such as macular dystrophies, or generalized diseases including LCA and RP (formerly known as tapeto-retinal degeneration (TRD), which is derived from the tapetum nigrum, an ancient term for the RPE). Additionally, phenotypes with distinctive characteristics and/or a particular geographical area of occurrence often received an own name; for example, vitelliform macular dystrophy (characteristic yellow lesions in the macula resembling the yolk of an egg), Stargardt disease (pisciform yellow-white fundus flecks in the posterior pole), or North Caroline macular dystrophy (congenital macular drusen and/or macular coloboma, named after a large kindred from North Caroline in which it was first described). The invention of electrophysiological testing provided some refinement and enabled a further differentiation based on the primary site of retinal dysfunction. Generalized diseases in which rod involvement precedes cone involvement are generally labeled retinitis pigmentosa or rod-cone dystrophy. However, as described in Chapter 2.1, choroideremia (patchy chorioretinal atrophy and normal appearing retinal vessels), gyrate

atrophy (well demarcated circular chorioretinal atrophy with elevated ornithine levels), and late-onset retinal degeneration (perimacular drusen-like lesions and long anterior lens zonules) definitely share features with RP and although they could be considered RP subtypes, historically, these highly specific phenotypes have been differentiated from RP.[1,2]

Improvements in investigative techniques and better understanding of the natural course have expanded our knowledge of these disorders significantly, often leaving the original names confusing or even misleading and almost always incomplete. A fine example is the disease 'benign concentric annular macular dystrophy' that we discuss in Chapter 4.2. The visual acuity in these patients eventually deteriorates to light perception and the periphery is involved as well. Hence, this disease is certainly not 'benign' and neither is the disease process confined to the macular region. Consequently, we have suggested to revise this diagnosis to retinitis pigmentosa with relative early macular involvement. Interestingly, RP is a term that itself can also be considered a misnomer since this dystrophy is not caused by inflammation.

There is also significant overlap between phenotypes that are currently separated through nomenclature. For example the large clinical and genetic overlap between LCA and RP. The distinction between LCA and RP is solely determined by the patient's age at onset, and rather arbitrarily as well, instead of the retinal characteristics and even more important, the underlying genetic defect. In Chapter 3.2 we described two patients with *TULP1*-associated early-onset RP, of whom the youngest patient had an age of onset of one year. If the disease would have been detected a few months earlier, the formal diagnosis would have been LCA instead of RP. Remarkably, since the age of onset in these disorder in general is more 'an age of detection' and highly dependent on the alertness of parents in such small infants. Since LCA and RP share large clinical and genetic overlap, they should be considered a continuum of retinal dystrophies. The current nomenclature also does not consider patients who represent two phenotype categories. For example, patients with *IMPG1*-(Chapter 4.2) and *IMPG2*-associated RP are diagnosed as RP with relative early onset macular atrophy. Therefore, they basically have a combination of a macular dystrophy and RP, though they are classified as patients with RP.

The effect of time should not be underestimated. The current classification may result in a two or more separate labels during the course of the disease. For example, a macular dystrophy phenotype may become more generalized and progress to a cone-rod phenotype, as might be the case in the patients with *RP1*-associated macular dystrophy described in Chapter 4.1. In turn, this might lead to an all-out loss of photoreceptor signal on ERG examination that is associated with RP. Since the underlying pathophysiological mechanism is not subject to change, it seems illogical to adjust the diagnosis depending on the phase of the disease. A change in diagnosis can also be very confusing to the patient. It is therefore essential to consider the entire disease course when classifying retinal dystrophies.

The emergence of genetic testing has resulted in a further subdivision of disease. Genetic testing has already identified 87 non-syndromic RP-subtypes and well over 250 genes have been associated with retinal dystrophies in general (RetNet, available at https://sph.uth.edu/retnet/. Chapter 2.1 illustrates that the genetic subtypes explain part of RP's heterogeneity. Therefore,

a nomenclature based on the molecular diagnosis has been suggested for obvious reasons. However, a subdivision based on the genotype alone into the daily clinical practice has its drawbacks, considering the vast number of genes, in view of the fact that gene names are meaningless for the majority of patients and general ophthalmologists, and the large clinical heterogeneity of retinal dystrophies illustrated by a single gene that may cause remarkably different forms of retinal dystrophies. *RP1*-associated phenotypes for example, can range from RP to macular/cone-rod dystrophy (Chapter 4.1) and pathogenic variants in the *IMPG1* gene have been associated with vitelliform macular dystrophy and a generalized dystrophy such as RP (Chapter 4.2). Expansion to the specific alteration within a gene would only solve part of the problem. Nevertheless, the identification of a molecular diagnosis is extremely valuable to optimally counsel patients and is required to identify patients eligible for upcoming genetic therapies.

Aforementioned arguments highlight the complexity of creating a comprehensive nomenclature for retinal dystrophies. In this light, a more descriptive nomenclature that contains additional information on clinical findings, including the age of onset, and genetic features is perhaps the best compromise. This way, we could preserve generally accepted terms that are present throughout every textbook, such as RP, even though these are theoretically incorrect. Secondly, LCA and RP share large clinical and genetic overlap and could be considered a continuum of disease. LCA could be referred to as early-onset RP. LCA and RP patients with an onset before the age of five could be named early-onset RP. In general, an indication of the age of onset should be included, perhaps differentiating between early and late onset variants, since this often provides a crude estimation of the disease severity, as previously shown in Stargardt disease.[3,4] Finally, it is vital to include the causal gene in the diagnosis, to explain as much clinical variability as possible, provide accurate counseling, and to be able to select the patients eligible for upcoming genetic treatment. Describing the causative genetic defect is also the first step towards a potential situation, somewhere in the distant future, in which only the gene involved might be important as the consequent ophthalmic characteristics can be prevented with the appropriate treatment.

Clinical heterogeneity/modifiers

Retinal dystrophies are generally considered monogenetic disease, and large phenotypic differences in patients with the same causative gene can be explained by allelic heterogeneity caused by the type of mutation, its location and/or the amount of residual function. However, even patients with the same molecular alteration in a specific gene, for instance in family members, can display large variation. This is illustrated by the substantial variation in the age at onset of vision loss (range: 12–63 years) in a large family with autosomal dominant central areolar choroidal dystrophy caused by mutations in the *PRPH2* gene,[5] as well as the large clinical heterogeneity in a Dutch family with autosomal dominant RP caused by the p.Leu579Pro variant in *IMPG1* (Chapter 4.2) or the heterogeneity in patients with the same combination of autosomal recessive variants in *RP1* (Chapter 4.1). This variation may indicate the involvement of other

genetic and/or environmental modifying factors that exert their effect on the final phenotype. However, in contrast to the progress in identifying disease causing genes, little information is known about potential modifiers.

Genetic modifying factors could affect the causal gene itself, for example by altering gene expression levels. A single nucleotide polymorphisms (SNP) is a relatively common variant in the human genome that in itself does not induce pathology. However, a SNP in *cis* or *trans* with a mutation could affect gene expression levels, gene splicing or transcription factor binding and thereby affect the phenotype. This might explain the clinical heterogeneity in patients with the same mutation, particularly in autosomal dominant families.[6] Genetic modifiers could also exert their effect on genes in the same pathway. In Chapter 2.1, we described several vital processes within the neuroretinal and/or RPE and the genes that play a role in these processes. An alteration in the function of a particular protein may affect the entire pathway. For example, SNPs or mutations in a gene that is involved in the same pathway as the causative gene might affect the protein interaction and therefore influence the eventual phenotype. Modifying variants in *AHI1*, *CCDC28B, CEP290* and *RPGRIP1L1* have been shown in patients with syndromic RP,[7-9] and *CNOT3* and *MERTK* have been reported to be a modifiers of *PRPF31*-associated RP and *CEP290*-associated LCA, respectively.[10,11] In rare cases, it may even be that heterozygous variants in two different genes together result in retinal dystrophy, whereas haploinsufficiency at each of these loci is insufficient to cause retinal degeneration. We then speak of a digenic inheritance instead of a monogenetic disease. Putative digenic inheritance patterns have been described in patient with non-syndromic RP and pathogenic variants in the *ROM1* and *PRPH2* gene,[12,13] as well as in syndromic RP patients.[14-16] Finally, environmental factors might also exert their effect on the final phenotype, although their potential effect on inherited retinal disease is probably very limited, in contrast to typical multifactorial disorders such as age-related macular degeneration where these can attribute to approximately 30% of a patients risk score.[17] However, we yet cannot exclude that a person's overall health has an effect on the retina's vulnerability and that good nutrition with, for example, antioxidants has a positive effect on the development of retinal dystrophies. These environmental factors may have a small influence on the age of onset or progression rate.

Generally, retinal dystrophies affect both eyes and display large symmetry. However, inter-eye asymmetry has been reported in patients with autosomal dominant disease such as patients with Best disease or central areolar choroidal dystrophy and autosomal recessive disease such as Stargardt disease or *RP1*-associated retinal dystrophy (Chapter 4.1).[5,18,19] Yet how certain are we that both eyes have the same genetic and environmental background? In X-linked disorders, a difference in gene expression levels might be explained by nonrandom X-inactivation in retinal cells (Lyonization). However, an influence of potential X-linked modifiers on genes not located on the sex chromosomes is less likely considering that both males and females display inter-eye asymmetry. In the patients with Stargardt disease, the discordance was the highest in older patients, suggesting that small initial differences could eventually result in significant differences between both eyes.[18] Perhaps small anatomical differences could affect the vulnerability of the retina, although pure coincidence cannot be excluded.

Chapter 6

Knowledge about modifiers is not only crucial to explain the clinical heterogeneity and predict the disease course but could also play a key role in predicting treatment response. In Chapter 5.1 we showed that more than half of the children with XLRS responded to treatment with carbonic anhydrase inhibitors. However, treatment was only effective in one of two brothers (patient number 2 and 3). Although it is uncertain whether a modifying effect is at play here, knowledge about potential modifiers can become important when considering treatment options.

The identification of modifiers is limited by their small effect and sample size and the consequent lack of power. To gain more knowledge concerning modifying factors, we first need an accurate description of patients' phenotype to be able to explain phenotypic differences, which requires extensive clinical evaluation and follow-up studies. Secondly, and probably the most difficult, larger sample sizes are required. Large genome-wide association studies in patients with age-related macular degeneration containing over 16,000 patients and 17,000 controls have identified new common variants to be independent risk factors.[20] These patient numbers are not attainable for retinal dystrophies, but international collaborations are necessary to increase the sample size and gather large, homogeneous cohorts. Additionally, not only patients with the same pathogenic variants, but also patients with comparable variants (e.g., nonsense mutations leading to nonsense-mediated decay) could be included, and one might consider starting with studying the most extreme subgroups. Eventually, the diagnosis retinal dystrophy might also contain information regarding the modifiers involved in addition to the causal gene. For now, further research is essential to identify modifiers of retinal dystrophies.

Molecular diagnosis

Obtaining a molecular diagnosis is valuable in the optimal counseling of patients and is a necessity to identify patients eligible for upcoming genetic therapies. The extent, speed and costs of molecular diagnostic techniques have improved tremendously over the last decade. The implementation of whole exome sequencing (WES) in the field of retinal dystrophies in 2011 has led to the discovery of over 50 novel retinal dystrophy-associated genes.[21-25] Today, WES provides a genetic diagnosis in approximately two-thirds of the patients with a retinal dystrophy.[26-28] In all likelihood, the genes with the highest prevalence in RP have already been identified. In the remaining one third of the patients, the variant may be located in a gene that has not yet been associated with inherited retinal diseases, such as the recently described *KIAA1549* gene (Chapter 3.1). In most cases, the genetic defect will concern an unknown variant in genes that have already been associated with RP. It may not have been detected using WES when the defect resides in a noncoding region, a GC-rich region, concerns a structural variant or was not covered for another reason. For example, the variant may be located in the near-exon splice region and affects the process of splicing, as described for *TULP1* in Chapter 3.2. WES does not only facilitate in the identification of novel retinal dystrophy-associated genes, also multiple new genotype-phenotype correlations have been reported, among which macular/cone-rod dystrophy in patients with variants in the *RP1* gene and an RP phenotype in patients with pathogenic variants in the *IMPG1* gene (Chapter 4.1 and 4.2).

WGS is an attractive successor to identify the molecular cause in the remaining genetically unsolved patients. In general, WGS provides full coverage of the genome and its non-coding regions, and is more reliable for detecting copy-number variants.[29,30] The costs of WGS have declined rapidly over the years from approximately several hundred million euro's at the beginning of this century (before next-generation sequencing became available in the research setting), to less than 600 euro's today,[31] and the costs are expected to decrease even further. Nevertheless, implementation to a diagnostic setting is hampered due to a requirement of an immense data storage capacity since one genome sample has a size of approximately 150–300 gigabytes. In addition, data processing requires high computational capacity, though new technological innovations will likely support these challenges. Where WES results in approximately 40,000 variants, WGS generally identifies 3–5 million variants which cannot be assessed without setting initial criteria for putative pathogenic variants.[32,33] Analysis of these variants is time consuming, and most importantly, functional consequences of intronic variants identified by WGS often remain difficult to interpret. Although the growth of public databases such as ExAC and GnomAD, which contain a growing number of genomic variants in the healthy population, will facilitate a better prediction of candidate variants based on their allele frequency, functional analysis is paramount to assess their pathogenicity.

A new sequencing method that is currently being developed is third-generation sequencing or long-read sequencing. This method may further improve the field of sequencing since it may be able to generate reads with an average size larger than 10,000 bp of high-molecular weight DNA, and thereby enables covering of GC-rich regions, detection of large rearrangements and structural variants, and improves haplotype mapping.[34] However, before this technique can be implemented in the clinical practice, the error rates and high costs of this technique have to be reduced.

Functional analysis

Intronic or non-coding variants may display a pathological effect at the RNA level by either altering correct-mRNA splicing or reducing or enhancing transcript expression levels.[35] Their effect on canonical or alternative splice sites can be predicted by multiple *in silico* prediction programs, including SpliceSiteFinder-like, MaxEntScan, NNSPLICE, GeneSplicer and Human Splicing Finder.[36-39] However, as we illustrate in Chapter 3.2, the sequence context should also be included in the prediction of the effect, e.g., the strengths of nearby splice acceptor and donor sites, the size of flanking exons, and the presence of exonic splice enhancers and splice silencer motifs.[40,41] The actual effect can be assessed at the level of RNA. Since retinal cells of patients are difficult to access purely for practical reasons, other methods should be used. For example, mRNA obtained from patient's blood cells (e.g., lymphoblast or fibroblast cells) can be assessed by performing reverse transcriptase PCR. However, this requires expression of the gene of interest in these blood cells, which is only the case in approximately two third of the inherited retinal disease genes.[25,42] For the genes that are not ubiquitously expressed or when blood cells cannot be obtained, splice assays have proven to be a sound alternative. In short,

a wildtype and mutant midigene that contain, if possible, multiple exons and introns of the same gene can be transfected in human embryonic kidney 293 cells that express the SV40 large T antigen (i.e., HEK293T cells) to study the effect of variants on the transcript. We employed this technique in Chapter 3.2 for a variant in *TULP1*.[40] A disadvantage of this method is that the cells splicing machinery may be tissue–specific and therefore when variants appear to not have an effect one should consider that HEK293T cells may not represent the actual splicing in human photoreceptor cells.[43,44] An alternative well-established method to study the functional effect of a pathogenic variant or localization of proteins is to make use of the hTERT-immortalized RPE cell line (i.e., hTERT-RPE1 cells). In Chapter 3.1 we used these cells to study the effect of KIAA1549, encoding for a gene associated a with inherited retinal disease, on ciliogenesis by knockdown of KIAA1549 in vitro using small interfering RNAs (i.e., siRNAs).

To more closely study the *in vivo* effect of putative pathogenic variants and/or their effect on splicing, variants can be analyzed by generating induced pluripotent stem cells (iPSC)–derived photoreceptor progenitor cells (PPCs) and/or RPE cells. Generating these cells is an expensive (approximately €6.000–€8.000), labor-intensive and time-consuming process that takes several months depending on the research questions as well as the expression of the gene of interest. Nevertheless, iPSC-derived PPCs and/or RPE cells have been successfully used to identify splice defects and study the preclinical efficacy of novel therapeutic interventions in multiple genes including the *ABCA4*, *CEP290*, *MAK* and *USH2A* genes.[44-48] The development of iPSC-derived PPCs to study the pathophysiology of retinal disease represents an important alternative to *in vivo* animal studies, particularly for genes of interest that are not present in the genome of animal species. An important example is the *EYS* gene, which is not present in the rodent genome even though it is an important gene in RP (Chapter 2.1).[49] In such cases it may be unavoidable to use a larger animal model. A naturally occurring model already exists for over 20 retinal dystrophies.[49,50] Probably the most well-known animal model for retinal disease is the Briard dog. In particular Lancelot, a Briard dog with naturally occurring *RPE65*-associated blindness who was treated with gene augmentation therapy after which his vision improved significantly.[51] Subsequent trials in humans eventually resulted in the clinical approval of the first gene therapy for retinal disease.[52]

Management

Ultimately, research into retinal dystrophies is aimed at finding a curative treatment for patients with a retinal dystrophy. If not for themselves, patients hope for a treatment for their family members or peers. Luckily, the eye, and particularly the retina, has been at the forefront of advances in innovative therapies such as gene- and cell-based therapies and retinal implants, due to its limited size, accessibility and immune-privileged status.

Current therapies

Two retinal implants, the Argus II epiretinal implant and the Alpha AMS subretinal implant, are currently available on the market for patients with a retinal dystrophy (mostly RP) with intact

inner retinal architecture and very little to no light perception, as described in Chapter 2.1. These retinal implants can restore basic visual function and increase the daily mobility of patients.[53-55] Visual acuity assessed with Landolt C-rings improved from light perception without projection to 20/546 in a patient with an Alpha AMS implant.[53] However, despite these promising results, several challenges have to be overcome including adverse effects, improving the surgical procedure, device longevity, resolution and bilateral implantation.[55-57] In addition, the economic feasibility of high-cost, low-volume devices dampens research and development.

As already discussed in Chapter 2.1, gene augmentation therapy for LCA and RP patients with *RPE65*-associated retinal dystrophy has become clinically available after the phase III clinical trial confirmed treatment safety and efficacy.[52] Multiple trials for other retinal dystrophies are already ongoing, including phase III trials for choroideremia and Leber Hereditary Optic Neuropathy (https://clinicaltrials.gov).[58] The genetic cargo can be delivered to the retina via intravitreal or subretinal injection. Delivery of the gene to the posterior retina is less effective after intravitreal injection, although the newest generation AAV vectors have been shown to deliver the gene from the anterior surface of the retina to the outer retina.[59] In addition, intravitreal injection results in a greater systemic distribution and is therefore more likely to induce an immunological response.[60,61] In contrast, subretinal injections are effective for targeting the photoreceptors and RPE cells. However, they are more invasive, require a vitrectomy, only work at the location of administration, and are less suited for repeated injections. Subretinal administration is an even higher risk in patients with a pre-existent vulnerable retina, such as in patients with XLRS. In these patients, a intravitreal injection is desired, although pretreatment of patients with carbonic anhydrase inhibitors to reduce the cystoid macular lesions may reduce the vulnerability of the retina (Chapter 5.1).

In addition to the delivery method, other challenges must be overcome before gene augmentation therapy can be widely implemented. For example, the delivery capacity of adeno-associated virus (AAV) vectors that are generally used to deliver the genetic cargo to the target cells in the retina is limited to ~4.7 kb. As a result, these vectors are not suitable for large genes such as *ABCA4*, *EYS* and *USH2A* and dual AAV vectors or other vectors (e.g., viruses with larger cargo capacity such as the lentivirus that can contain approximately 9 kb, or nanoparticles) should be considered.[62] Second, it is also unclear whether one-time administration of a therapeutic vector can provide long-term, long-lasting clinical benefits. Third, gene augmentation therapy is not suitable for autosomal dominant mutations with a gain-of-function effect, since the affected allele remains present in the cells. Other challenges include controlled expression levels and the costs of this gene-specific treatment, particularly considering the relatively small number of patients per genetic subtype.

Future therapies

A therapeutic strategy that is currently being developed involves antisense oligonucleotides (AONs), which are small and versatile RNA molecules that can be used in two ways. First, they can modulate the splicing process, by specifically binding to their target region in the pre-mRNA

CRISPR/Cas9

Although nucleases that can specifically cut genomic DNA at a desired locus (e.g. zinc-finger nucleases, and transcription activation-like effector nucleases) have been discovered decades ago, the discovery of the CRISPR (clustered regularly interspaced short palindromic repeats)/Cas9 (Crispr associated protein 9) system has enormously boosted the field of genome editing.[74-76] The CRISPR-Cas system is originally part of the adaptive immune system of many bacteria and archaea.[77] However, it can also be used as genome-editing system to induce a double strand break. Since RNA molecules are used as a guide to direct the Cas9 nuclease to its genomic target, virtually every locus in an organisms genome can be cut with high precision.
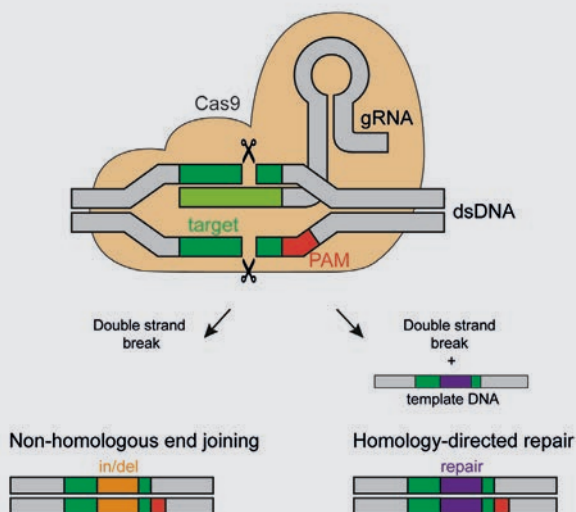
Here, a schematic overview of the CRISPR/Cas9 complex bound to DNA provided. The Cas9 endonuclease that can induce a double strand break into the DNA, is indicated in light orange. This endonuclease is directed to the target DNA (in green) by a guide RNA that is complementary to the target DNA. Additionally, the protospacer adjacent motif (PAM, indicated in red) is required for Cas9 to bind and cleave the targeted DNA sequence. Subsequently, the cell employs one of its two major DNA repair mechanisms to repair the double-stranded DNA break. Non-homologous end joining directly joins the two DNA ends and potentially results in the introduction of small insertions/deletions (in/del). In contrast, homology-directed repair uses a donor sequence as template to precisely repair the DNA break. This template DNA sequence can be present on the second allele or supplemented to the CRISPR/Cas9 components.[78]

Adapted from: https://commons.wikimedia.org/wiki/File:GRNA-Cas9.png and Slijkerman et al.[79]

and thereby interfering with the binding of small nuclear ribonucleoprotein (snRNP) complexes and other splice-promoting factors.[63] The efficacy of this approach in several different cellular and animal models has been demonstrated for a number of deep-intronic mutations underlying retinal disease, including *CEP290*-associated LCA, *USH2A*-associated RP and optic atrophy.[44,64-68] Additionally, a recent clinical trial by Cideciyan et al. reported an improvement in visual acuity and no serious adverse effects in patients with CEP290-associated LCA.[69] Second, AONs can also be used to degrade transcripts upon binding mRNA, even in an allele-specific manner.[63] In a transgenic rat model, AON delivery led to the specific degradation of mutant *RHO* transcripts encoding for the p.Pro23His rhodopsin protein which exerts a dominant-negative effect on the wild-type protein.[70] AON treatment for Duchene muscular dystrophy and spinal muscular dystrophy has already been clinically approved in the U.S.A. and Europe,[71-73] and additional clinical trials for retinal dystrophies employing this strategy will be initiated soon. An advantage of AONs is that these molecules are small and thus relatively easy to deliver to the retinal target cells. Yet their drawbacks include the necessity for repetitive administration, which can be very invasive and undesirable particularly in children, and to design tailor-made and clinical trial evaluated approaches for each pathogenic variant.

Another gene specific strategy that has gained a lot of attention over the last few years is genome editing. The CRISPR/Cas9 technology can be used to generate animal models by mutagenesis or for clinical purposes (e.g., the use of CRISPR/Cas9 for creating corrected iPSCs for autologous cell replacement or genome editing). In therapeutic genome editing, cutting at the site of the mutation and providing an exogenous corresponding wild-type donor template would allow the removal of the primary genetic defect from the patient's genome. In contrast to gene augmentation therapy, this approach can also be used in case of large genes or dominant negative mutations. CRISPR/Cas9 can be applied either *ex vivo* or *in vivo*, and several successful examples of both approaches have been reported.[80,81] CRISPR/Cas9-based genome editing on patient-derived pluripotent stem cells was used to demonstrate the potential of a non-homologous end-joining approach to remove an intronic region harboring a deep-intronic mutation in *CEP290*,[82] an homology-directed repair approach to correct a mutation in *MAK, MERTK* or *RPGR*,[82-84] and an allele-specific degradation approach for a common autosomal dominant *RHO* mutation.[82] Others have shown the *in vivo* potential of therapeutic genome editing, by delivering CRISPR and Cas9 molecules to the retina via AAV injections, in a rat model for *RHO*- or *MERTK*-associated RP,[85,86] and a mouse model for *RHO*- or *CEP290*-associated LCA.[87,88] Despite its obvious and enormous potential, there are still a number of challenges to overcome in order to allow therapeutic genome editing to become widely implemented in humans. First, better insight into and control of potential off-target cleavage has to be gained. Second, similar to gene augmentation therapy, the choice of an optimal vector system is crucial.[89] Although the vector does not need to contain entire gene, the currently used Streptococcus pyogenes Cas9 is too large (4.2 kb) to be transported together with its guide RNA and promoter sequence by one AAV vector alone.[78] However, the smaller Staphylococcus aureus Cas9 fits into a single AAV

Chapter 6

vector. The third major challenge includes finding means to activate the homology-direct repair pathway instead of the non-homologous end-joining repair mechanism in post-mitotic cells such as the retinal photoreceptors in order to correctly alter the patient's DNA.[78]

Gene editing and gene replacement therapy can also be combined, for example in the 'ablate and replace' approach, which has recently been described by Tsai et al. and is particularly suitable for autosomal dominant disease.[90] In a dominant *RHO*-associated RP mouse model, the *RHO* gene was ablated using CRISPR/Cas9 with double guide RNAs with subsequent gene augmentation therapy to provide the wild-type *RHO* cDNA. Although multiple challenges of CRISPR/Cas9 and gene augmentation also apply to this technique, this strategy is mutation-independent and does not require design and optimization for every mutation.

Cell replacement therapy involves the administration of stem-cell–derived retinal cells into the subretinal space to replenish the RPE and/or photoreceptor cells that have degenerated. The different types of stem cells and their origin have been described in Chapter 2.1. To date, RPE cells can be administered in a solution or, as a monolayered sheet, which appears to be a superior method.[91] The first phase 1 clinical trials in a handful of patients with age-related macular degeneration using a sheet of iPSC-derived RPE cells or a bioengineered patch containing human ESC-derived RPE cells provided the first evidence for graft survival of at least one year, and have illustrated a potential improvement in visual acuity.[92,93] Life-long immunosuppressive therapy in the often young patients, with retinal dystrophies, which is necessary in case of human ESC-derived cells, is undesirable. The emergence of iPSC-derived retinal cells has allowed autologous transplantation, thus avoiding life-long (local) immunosuppressive therapy. However, in patients with a retinal dystrophy this individualized treatment requires a correction of the genetic defect prior to transplantation and is therefore labor intensive and expensive. Since RPE cells are not sensitive to light, photoreceptors need to be present to restore vision. Transplantation of photoreceptors is highly challenging, since it requires the formation of synaptic connections. Although synapse formation between donor photoreceptors and host bipolar cells has been reported in animal models, the recent finding of material transfer between donor and host photoreceptors demands further evaluation of the actual synapse formation and potential donor-host cell fusion before transplantation of photoreceptors can proceed to clinical trials.[94] In conclusion, additional trials are necessary to assess the graft safety, graft survival, immunological issues and tumorgenicity of cell replacement therapy.[94,95]

Therapeutic window

The best treatment depends on the stage of the disease. To be effective, gene-specific and/or mutation-specific approaches require the presence of the living cells as a target. As a result, these approaches are most successful in the early stages of the disease, before cell degeneration sets in. In contrast, stem cell treatment and retinal implants respectively replace the cells that have been lost or their function and are therefore suitable for more advanced stage of the disease.

Gene augmentation therapy, even if successful, may not halt the retinal degeneration. A study on gene therapy for patients with *RPE65*-associated LCA showed a progressive decline in the number of photoreceptor cells, despite a functional improvement.[96,97] The ongoing degeneration might be explained by the fact that not all photoreceptor cells were reached by the viral vectors cells, or the cells had already reached the threshold for apoptosis. In contrast, a canine model indicated that early treatment in a stage with only dysfunction and no degeneration may be associated with preservation of the remaining photoreceptors, and highlights the importance of an early diagnosis and consequent treatment.[97]

Aside from the therapeutic options, multiple preventive strategies can be offered in families in which the genetic defect is known. For example, partners of genetically solved patients can be screened for variants in the causative gene. If partners coincidentally carry a variant in the same gene or in case of autosomal dominant inheritance, patients are potentially eligible for prenatal testing or preimplantation genetic diagnosis. These options should be considered since they are less expensive and already clinically available.

Social consequences and challenges

The development of these new therapeutic approaches has resulted in legal and ethical challenges. CRISPR/Cas9-based genome editing is the only therapy which aims at correcting the causative mutation. Yet, this permanent alteration of the DNA raises ethical questions. To date, gene therapy that affects the germline (i.e., in which gene alterations would be passed to future generation) is prohibited by legislation or guidelines.[98] Although germline alterations could eradicate a mutation from a family, this treatment should only be initiated until the long-term side effects are known and there is social consensus about the use of such treatments. Another challenge is the costs of these treatments for orphan diseases. The development of a treatment from the proof-of-principle studies to the completion of a phase 3 trial that leads to governmental approval is very expensive. Orphan drugs legislations have been created in the European Union, USA and other countries to encourage development of drugs for orphan diseases such as retinal dystrophies by providing fast drug approval, tax benefits (in USA) and offering longer patents that guarantee extended exclusivity in the market.[99] However, the limited number of patients eligible for treatments and the lack of competition in the market increases the prices. The costs of new therapies also resulted in heated discussions about the maximum costs of a treatment. According to the Dutch National Health Institute, the maximum willingness-to-pay threshold for a treatment is €80,000 per QALY.[100] The cost-effectiveness of the epiretinal Argus retinal implant, which itself costs approximately €100,000,[101] has been estimated at ~€50,000/QALY assuming a 10 year device life span.[102] A shorter device longevity, such as the estimated median operating life of 3.3 years for the subretinal Alpha AMS device, will result in a considerable decrease in the cost-effectiveness and is a major challenge.[103] In contrast, the price of gene augmentation therapy is currently estimated at approximately €400.000 per injection. Currently, the direct visual gain seems limited as only an increased sensitivity to dim light is reported.[104,105] In the future, this treatment might prevent the deterioration of visual acuity

Quality adjusted life years (QALYs)

The effect of a particular treatment is often expressed in quality adjusted life years (QALYs, i.e., years lived in perfect health). Although a retinal dystrophy does not affect mortality, it severely affects patients' quality of life. However, the effect of vision on the quality of life is difficult to quantify. A regularly used method is the use of utility scores (utility scores vary from 1 to 0, with 1 indication a perfect health state, and the closer to 0 the poorer the quality of life) to calculate the QALYs gained from treatment. For example, the utility score of patients with age-related macular degeneration is ~0.59 for legal blindness (≤0.1) in the better-seeing eye, and ~0.71 for moderate visual acuity loss (0.4–0.1).106 Hence, a treatment that can prevent or delay the deterioration of the visual acuity to legal blindness for at least 10 years yields approximately 1 QALY. Utility scores based on the visual field have also been determined in patients with glaucoma.107 To the best of our knowledge, reliable utility scores for patients with both visual acuity and visual field loss, such as various RP patients, have not been established and should be determined to accurately calculate QALYs for cost-effectiveness scores.

if administered before the onset of retinal degeneration and may prove to be cost-effective, assuming the effect from a single injection lasts at least several years. Finally, we should not assess the cost-effectiveness of such therapies solely on visual gain. A much broader and perhaps better alternative is to determine how these therapies improve patients' capabilities. Accurate treatment might enable patients to visit regular schools, improve daily life activities and enable the patient to work, which also benefits society as a whole.

Universal therapies, which are not limited to a select group of patients, have the advantage of a larger market. For example, retinal implants and stem cell treatment could also be used in patients with a more common disease such as advanced age-related macular degeneration (although their visual gain should be improved and exceed the visual acuity that can be obtained from the peripheral retina). Ideally, therapy should be installed much earlier in the disease process and aimed at maintaining the visual function that is still present. This means that in the long term genome editing and gene augmentation therapy seem the most promising, although challenges such as vector size, off-target effects and repair mechanisms should be accounted for. In an ideal situation, an universal mold is created so only the concerning gene or guide RNA has to be adjusted according to the gene or mutation involved. Nevertheless, it will take some time before genome editing is accessible and gene augmentation therapy becomes available for the majority of genes. Therefore, research and developments on retinal implants and AON treatment, the treatments for the near future, is also highly encouraged.

Concluding remarks

In the last decade, we have witnessed considerable developments in the field of retinal dystrophies. The emergence of whole exome and whole genome sequencing have enabled the identification of the genetic defect in most patients, and has shifted the attention to the individual genetic subtypes of disease. New RP genes, such as *KIAA1549*, and new genotype-phenotype correlations of *RP1*- and *IMPG*-associated dystrophies have been described. Since the majority of variants in the protein-coding regions have already been discovered, the search for new causal variants will be expanded to the non-coding regions. On the other hand, we need a better understanding of the modifying factors that affect the phenotype and are responsible for the large clinical heterogeneity of retinal dystrophies. More insight in the natural history of gene-specific phenotypes in necessary, if only to better assess the efficacy of future therapies. The advances in genetic testing have been paralleled by the development of such treatment strategies, of which retinal implants and gene augmentation therapy for *RPE65*-associated disease have become commercially available. Hopefully, in the next decades, these developments will continue to increase our knowledge about the pathophysiology of retinal diseases, and will pave the way for new therapeutic options for these high impact diseases.

Chapter 6

References

1. Borooah S, Collins C, Wright A, Dhillon B. Late-onset retinal macular degeneration: clinical insights into an inherited retinal degeneration. Br J Ophthalmol 2009;93(3):284-9.
2. Mauthner L. Ein Fall von Choroideremia. Berl Natur-med Ver Innsbruck 1872;2:191.
3. Lambertus S, van Huet RA, Bax NM, et al. Early-onset stargardt disease: phenotypic and genotypic characteristics. Ophthalmology 2015;122(2):335-44.
4. Westeneng-van Haaften SC, Boon CJ, Cremers FP, et al. Clinical and genetic characteristics of late-onset Stargardt's disease. Ophthalmology 2012;119(6):1199-210.
5. Boon CJ, Klevering BJ, Cremers FP, et al. Central areolar choroidal dystrophy. Ophthalmology 2009;116(4):771-82, 82.e1.
6. Shankar SP, Hughbanks-Wheaton DK, Birch DG, et al. Autosomal Dominant Retinal Dystrophies Caused by a Founder Splice Site Mutation, c.828+3A>T, in PRPH2 and Protein Haplotypes in trans as Modifiers. Invest Ophthalmol Vis Sci 2016;57(2):349-59.
7. Khanna H, Davis EE, Murga-Zamalloa CA, et al. A common allele in RPGRIP1L is a modifier of retinal degeneration in ciliopathies. Nat Genet 2009;41(6):739-45.
8. Badano JL, Leitch CC, Ansley SJ, et al. Dissection of epistasis in oligogenic Bardet-Biedl syndrome. Nature 2006;439(7074):326-30.
9. Tory K, Lacoste T, Burglen L, et al. High NPHP1 and NPHP6 mutation rate in patients with Joubert syndrome and nephronophthisis: potential epistatic effect of NPHP6 and AHI1 mutations in patients with NPHP1 mutations. J Am Soc Nephrol 2007;18(5):1566-75.
10. Venturini G, Rose AM, Shah AZ, et al. CNOT3 is a modifier of PRPF31 mutations in retinitis pigmentosa with incomplete penetrance. PLoS Genet 2012;8(11):e1003040.
11. Littink KW, Pott JW, Collin RW, et al. A novel nonsense mutation in CEP290 induces exon skipping and leads to a relatively mild retinal phenotype. Invest Ophthalmol Vis Sci 2010;51(7):3646-52.
12. Conley SM, Stuck MW, Watson JN, Naash MI. Rom1 converts Y141C-Prph2-associated pattern dystrophy to retinitis pigmentosa. Hum Mol Genet 2017;26(3):509-18.
13. Dryja TP, Hahn LB, Kajiwara K, Berson EL. Dominant and digenic mutations in the peripherin/RDS and ROM1 genes in retinitis pigmentosa. Invest Ophthalmol Vis Sci 1997;38(10):1972-82.
14. Liu YP, Bosch DG, Siemiatkowska AM, et al. Putative digenic inheritance of heterozygous RP1L1 and C2orf71 null mutations in syndromic retinal dystrophy. Ophthalmic Genet 2016:1-6.
15. Fauser S, Munz M, Besch D. Further support for digenic inheritance in Bardet-Biedl syndrome. J Med Genet 2003;40(8):e104.
16. Beales PL, Badano JL, Ross AJ, et al. Genetic interaction of BBS1 mutations with alleles at other BBS loci can result in non-Mendelian Bardet-Biedl syndrome. Am J Hum Genet 2003;72(5):1187-99.
17. Seddon JM, Cote J, Page WF, et al. The US twin study of age-related macular degeneration: relative roles of genetic and environmental influences. Arch Ophthalmol 2005;123(3):321-7.
18. Lambertus S, Bax NM, Groenewoud JM, et al. Asymmetric Inter-Eye Progression in Stargardt Disease. Invest Ophthalmol Vis Sci 2016;57(15):6824-30.
19. Kaden TR, Tan AC, Feiner L, Freund KB. Unilateral Best Disease: A Case Report. Retin Cases Brief Rep 2017;11 Suppl 1:S191-S6.
20. Fritsche LG, Igl W, Bailey JN, et al. A large genome-wide association study of age-related macular degeneration highlights contributions of rare and common variants. Nat Genet 2016;48(2):134-43.
21. Sergouniotis PI, Davidson AE, Mackay DS, et al. Recessive mutations in KCNJ13, encoding an inwardly rectifying potassium channel subunit, cause leber congenital amaurosis. Am J Hum Genet 2011;89(1):183-90.
22. Ozgul RK, Siemiatkowska AM, Yucel D, et al. Exome sequencing and cis-regulatory mapping identify mutations in MAK, a gene encoding a regulator of ciliary length, as a cause of retinitis pigmentosa. Am J Hum Genet 2011;89(2):253-64.
23. Bowne SJ, Humphries MM, Sullivan LS, et al. A dominant mutation in RPE65 identified by whole-exome sequencing causes retinitis pigmentosa with choroidal involvement. Eur J Hum Genet 2011;19:1074.
24. Zuchner S, Dallman J, Wen R, et al. Whole-exome sequencing links a variant in DHDDS to retinitis pigmentosa. Am J Hum Genet 2011;88(2):201-6.
25. Astuti GD. Molecular genetic elucidation of inherited retinal dystrphies. Hum Genet: Radboud univerity Nijmegen, 2017.
26. Haer-Wigman L, van Zelst-Stams WA, Pfundt R, et al. Diagnostic exome sequencing in 266 Dutch patients with visual impairment. Eur J Hum Genet 2017;25(5):591-9.
27. Tiwari A, Bahr A, Bahr L, et al. Next generation sequencing based identification of disease-associated mutations in Swiss patients with retinal dystrophies. Sci Rep 2016;6:28755.
28. Abu-Safieh L, Alrashed M, Anazi S, et al. Autozygome-guided exome sequencing in retinal dystrophy patients reveals pathogenetic mutations and novel candidate disease genes. Genome Res 2013;23(2):236-47.
29. Lelieveld SH, Spielmann M, Mundlos S, et al. Comparison of Exome and Genome Sequencing Technologies for the Complete Capture of Protein-Coding Regions. Hum Mutat 2015;36(8):815-22.
30. Carss KJ, Arno G, Erwood M, et al. Comprehensive Rare Variant Analysis via Whole-Genome Sequencing to Determine the Molecular Pathology of Inherited Retinal Disease. Am J Hum Genet 2017;100(1):75-90.
31. The Cost of Sequencing a Human Genome. 2016.
32. Biesecker LG, Nussbaum RL, Rehm HL. Distinguishing variant pathogenicity from genetic diagnosis: How to know whether a variant causes a condition. JAMA 2018;320(18):1929-30.

33. Genomes Project C, Auton A, Brooks LD, et al. A global reference for human genetic variation. Nature 2015;526(7571):68-74.
34. Nakano K, Shiroma A, Shimoji M, et al. Advantages of genome sequencing by long-read sequencer using SMRT technology in medical area. Hum Cell 2017;30(3):149-61.
35. Spielmann M, Mundlos S. Looking beyond the genes: the role of non-coding variants in human disease. Hum Mol Genet 2016;25(R2):R157-R65.
36. Zhang MQ. Statistical features of human exons and their flanking regions. Hum Mol Genet 1998;7(5):919-32.
37. Yeo G, Burge CB. Maximum entropy modeling of short sequence motifs with applications to RNA splicing signals. J Comput Biol 2004;11(2-3):377-94.
38. Desmet FO, Hamroun D, Lalande M, et al. Human Splicing Finder: an online bioinformatics tool to predict splicing signals. Nucleic Acids Res 2009;37(9):e67.
39. Pertea M, Lin X, Salzberg SL. GeneSplicer: a new computational method for splice site prediction. Nucleic Acids Res 2001;29(5):1185-90.
40. Sangermano R, Khan M, Cornelis SS, et al. ABCA4 midigenes reveal the full splice spectrum of all reported noncanonical splice site variants in Stargardt disease. Genome Res 2018;28(1):100-10.
41. Cartegni L, Chew SL, Krainer AR. Listening to silence and understanding nonsense: exonic mutations that affect splicing. Nat Rev Genet 2002;3(4):285-98.
42. Kim MS, Pinto SM, Getnet D, et al. A draft map of the human proteome. Nature 2014;509(7502):575-81.
43. Garanto A, Duijkers L, Collin RW. Species-dependent splice recognition of a cryptic exon resulting from a recurrent intronic CEP290 mutation that causes congenital blindness. Int J Mol Sci 2015;16(3):5285-98.
44. Parfitt DA, Lane A, Ramsden CM, et al. Identification and Correction of Mechanisms Underlying Inherited Blindness in Human iPSC-Derived Optic Cups. Cell Stem Cell 2016;18(6):769-81.
45. Sangermano R, Bax NM, Bauwens M, et al. Photoreceptor Progenitor mRNA Analysis Reveals Exon Skipping Resulting from the ABCA4 c.5461-10T-->C Mutation in Stargardt Disease. Ophthalmology 2016;123(6):1375-85.
46. Albert S, Garanto A, Sangermano R, et al. Identification and Rescue of Splice Defects Caused by Two Neighboring Deep-Intronic ABCA4 Mutations Underlying Stargardt Disease. Am J Hum Genet 2018;102(4):517-27.
47. Tucker BA, Mullins RF, Streb LM, et al. Patient-specific iPSC-derived photoreceptor precursor cells as a means to investigate retinitis pigmentosa. Elife 2013;2:e00824.
48. Tucker BA, Scheetz TE, Mullins RF, et al. Exome sequencing and analysis of induced pluripotent stem cells identify the cilia-related gene male germ cell-associated kinase (MAK) as a cause of retinitis pigmentosa. Proc Natl Acad Sci U S A 2011;108(34):E569-76.
49. Slijkerman RW, Song F, Astuti GD, et al. The pros and cons of vertebrate animal models for functional and therapeutic research on inherited retinal dystrophies. Prog Retin Eye Res 2015;48:137-59.
50. Veleri S, Lazar CH, Chang B, et al. Biology and therapy of inherited retinal degenerative disease: insights from mouse models. Dis Model Mech 2015;8(2):109-29.
51. Acland GM, Aguirre GD, Ray J, et al. Gene therapy restores vision in a canine model of childhood blindness. Nat Genet 2001;28(1):92-5.
52. Russell S, Bennett J, Wellman JA, et al. Efficacy and safety of voretigene neparvovec (AAV2-hRPE65v2) in patients with RPE65-mediated inherited retinal dystrophy: a randomised, controlled, open-label, phase 3 trial. Lancet 2017;390(10097):849-60.
53. Stingl K, Schippert R, Bartz-Schmidt KU, et al. Interim Results of a Multicenter Trial with the New Electronic Subretinal Implant Alpha AMS in 15 Patients Blind from Inherited Retinal Degenerations. Front Neurosci 2017;11:445.
54. da Cruz L, Dorn JD, Humayun MS, et al. Five-Year Safety and Performance Results from the Argus II Retinal Prosthesis System Clinical Trial. Ophthalmology 2016;123(10):2248-54.
55. Edwards TL, Cottriall CL, Xue K, et al. Assessment of the Electronic Retinal Implant Alpha AMS in Restoring Vision to Blind Patients with End-Stage Retinitis Pigmentosa. Ophthalmology 2018;125(3):432-43.
56. Zrenner E. Fighting blindness with microelectronics. Science Translational Medicine 2013;5(210):210ps16.
57. Cheng DL, Greenberg PB, Borton DA. Advances in Retinal Prosthetic Research: A Systematic Review of Engineering and Clinical Characteristics of Current Prosthetic Initiatives. Curr Eye Res 2017;42(3):334-47.
58. Jiang DJ, Xu CL, Tsang SH. Revolution in Gene Medicine Therapy and Genome Surgery. Genes (Basel) 2018;9(12).
59. Dalkara D, Byrne LC, Klimczak RR, et al. In vivo-directed evolution of a new adeno-associated virus for therapeutic outer retinal gene delivery from the vitreous. Sci Transl Med 2013;5(189):189ra76.
60. Reichel FF, Dauletbekov DL, Klein R, et al. AAV8 Can Induce Innate and Adaptive Immune Response in the Primate Eye. Mol Ther 2017;25(12):2648-60.
61. Ochakovski GA, Bartz-Schmidt KU, Fischer MD. Retinal Gene Therapy: Surgical Vector Delivery in the Translation to Clinical Trials. Front Neurosci 2017;11:174.
62. Adijanto J, Naash MI. Nanoparticle-based technologies for retinal gene therapy. Eur J Pharm Biopharm 2015;95(Pt B):353-67.
63. Collin RW, Garanto A. Applications of antisense oligonucleotides for the treatment of inherited retinal diseases. Curr Opin Ophthalmol 2017;28(3):260-6.
64. Garanto A, Chung DC, Duijkers L, et al. In vitro and in vivo rescue of aberrant splicing in CEP290-associated LCA by antisense oligonucleotide delivery. Hum Mol Genet 2016;25(12):2552-63.
65. Collin RW, den Hollander AI, van der Velde-Visser SD, et al. Antisense Oligonucleotide (AON)-based Therapy for Leber

Congenital Amaurosis Caused by a Frequent Mutation in CEP290. Mol Ther Nucleic Acids 2012;1:e14.

66. Gerard X, Perrault I, Hanein S, et al. AON-mediated Exon Skipping Restores Ciliation in Fibroblasts Harboring the Common Leber Congenital Amaurosis CEP290 Mutation. Mol Ther Nucleic Acids 2012;1:e29.

67. Slijkerman RW, Vache C, Dona M, et al. Antisense Oligonucleotide-based Splice Correction for USH2A-associated Retinal Degeneration Caused by a Frequent Deep-intronic Mutation. Mol Ther Nucleic Acids 2016;5(10):e381.

68. Bonifert T, Gonzalez Menendez I, Battke F, et al. Antisense Oligonucleotide Mediated Splice Correction of a Deep Intronic Mutation in OPA1. Mol Ther Nucleic Acids 2016;5(11):e390.

69. Cideciyan AV, Jacobson SG, Drack AV, et al. Effect of an intravitreal antisense oligonucleotide on vision in Leber congenital amaurosis due to a photoreceptor cilium defect. Nat Med 2019;25(2):225-8.

70. Murray SF, Jazayeri A, Matthes MT, et al. Allele-Specific Inhibition of Rhodopsin With an Antisense Oligonucleotide Slows Photoreceptor Cell Degeneration. Invest Ophthalmol Vis Sci 2015;56(11):6362-75.

71. Lim KR, Maruyama R, Yokota T. Eteplirsen in the treatment of Duchenne muscular dystrophy. Drug Des Devel Ther 2017;11:533-45.

72. Aartsma-Rus A, Krieg AM. FDA Approves Eteplirsen for Duchenne Muscular Dystrophy: The Next Chapter in the Eteplirsen Saga. Nucleic Acid Ther 2017;27(1):1-3.

73. Ottesen EW. ISS-N1 makes the First FDA-approved Drug for Spinal Muscular Atrophy. Transl Neurosci 2017;8:1-6.

74. Jinek M, East A, Cheng A, et al. RNA-programmed genome editing in human cells. Elife 2013;2:e00471.

75. Cho SW, Kim S, Kim JM, Kim JS. Targeted genome engineering in human cells with the Cas9 RNA-guided endonuclease. Nat Biotechnol 2013;31(3):230-2.

76. Cong L, Ran FA, Cox D, et al. Multiplex genome engineering using CRISPR/Cas systems. Science 2013;339(6121):819-23.

77. Barrangou R, Fremaux C, Deveau H, et al. CRISPR provides acquired resistance against viruses in prokaryotes. Science 2007;315(5819):1709-12.

78. Yanik M, Muller B, Song F, et al. In vivo genome editing as a potential treatment strategy for inherited retinal dystrophies. Prog Retin Eye Res 2017;56:1-18.

79. Slijkerman RW. Splice modulation as potential therapy for Usher syndrome IIa. Genetics. Rotterdam: Radboud University Nijmegen, 2019.

80. Bakondi B. In vivo versus ex vivo CRISPR therapies for retinal dystrophy. Expert Rev Ophthalmol 2016;11(6):397-400.

81. Burnight ER, Giacalone JC, Cooke JA, et al. CRISPR-Cas9 genome engineering: Treating inherited retinal degeneration. Prog Retin Eye Res 2018;65:28-49.

82. Burnight ER, Gupta M, Wiley LA, et al. Using CRISPR-Cas9 to Generate Gene-Corrected Autologous iPSCs for the Treatment of Inherited Retinal Degeneration. Mol Ther 2017.

83. Artero Castro A, Long K, Bassett A, et al. Generation of gene-corrected human induced pluripotent stem cell lines derived from retinitis pigmentosa patient with Ser331Cysfs*5 mutation in MERTK. Stem Cell Res 2018;34:101341.

84. Bassuk AG, Zheng A, Li Y, et al. Precision Medicine: Genetic Repair of Retinitis Pigmentosa in Patient-Derived Stem Cells. Sci Rep 2016;6:19969.

85. Bakondi B, Lv W, Lu B, et al. In Vivo CRISPR/Cas9 Gene Editing Corrects Retinal Dystrophy in the S334ter-3 Rat Model of Autosomal Dominant Retinitis Pigmentosa. Mol Ther 2016;24(3):556-63.

86. Suzuki K, Tsunekawa Y, Hernandez-Benitez R, et al. In vivo genome editing via CRISPR/Cas9 mediated homology-independent targeted integration. Nature 2016.

87. Ruan GX, Barry E, Yu D, et al. CRISPR/Cas9-Mediated Genome Editing as a Therapeutic Approach for Leber Congenital Amaurosis 10. Mol Ther 2017;25(2):331-41.

88. Latella MC, Di Salvo MT, Cocchiarella F, et al. In vivo Editing of the Human Mutant Rhodopsin Gene by Electroporation of Plasmid-based CRISPR/Cas9 in the Mouse Retina. Mol Ther Nucleic Acids 2016;5(11):e389.

89. Sanjurjo-Soriano C, Kalatzis V. Guiding Lights in Genome Editing for Inherited Retinal Disorders: Implications for Gene and Cell Therapy. Neural Plast 2018;2018:5056279.

90. Tsai YT, Wu WH, Lee TT, et al. Clustered Regularly Interspaced Short Palindromic Repeats-Based Genome Surgery for the Treatment of Autosomal Dominant Retinitis Pigmentosa. Ophthalmology 2018;125(9):1421-30.

91. Diniz B, Thomas P, Thomas B, et al. Subretinal implantation of retinal pigment epithelial cells derived from human embryonic stem cells: improved survival when implanted as a monolayer. Invest Ophthalmol Vis Sci 2013;54(7):5087-96.

92. da Cruz L, Fynes K, Georgiadis O, et al. Phase 1 clinical study of an embryonic stem cell-derived retinal pigment epithelium patch in age-related macular degeneration. Nat Biotechnol 2018;36(4):328-37.

93. Mandai M, Watanabe A, Kurimoto Y, et al. Autologous Induced Stem-Cell-Derived Retinal Cells for Macular Degeneration. N Engl J Med 2017;376(11):1038-46.

94. Gasparini SJ, Llonch S, Borsch O, Ader M. Transplantation of photoreceptors into the degenerative retina: Current state and future perspectives. Prog Retin Eye Res 2018.

95. Rao RC, Dedania VS, Johnson MW. Stem Cells for Retinal Disease: A Perspective on the Promise and Perils. Am J Ophthalmol 2017;179:32-8.

96. Jacobson SG, Cideciyan AV, Roman AJ, et al. Improvement and decline in vision with gene therapy in childhood blindness. N Engl J Med 2015;372(20):1920-6.

97. Cideciyan AV, Jacobson SG, Beltran WA, et al. Human retinal gene therapy for Leber congenital amaurosis shows advancing

retinal degeneration despite enduring visual improvement. Proc Natl Acad Sci U S A 2013;110(6):E517-25.

98. Araki M, Ishii T. International regulatory landscape and integration of corrective genome editing into in vitro fertilization. Reprod Biol Endocrinol 2014;12:108.

99. Hall AK, Carlson MR. The current status of orphan drug development in Europe and the US. Intractable Rare Dis Res 2014;3(1):1-7.

100. Zwaap J, Knies S, Van der Meijden C, et al. Kosteneffectiviteit in de praktijk. Diemen: Zorginstituut Nederland 2015.

101. Miller A. Retinal implant system delivers limited sight to some blind people. CMAJ 2013;185(14):E659-60.

102. Vaidya A, Borgonovi E, Taylor RS, et al. The cost-effectiveness of the Argus II retinal prosthesis in Retinitis Pigmentosa patients. BMC Ophthalmol 2014;14:49.

103. Daschner R, Greppmaier U, Kokelmann M, et al. Laboratory and clinical reliability of conformally coated subretinal implants. Biomed Microdevices 2017;19(1):7.

104. Le Meur G, Lebranchu P, Billaud F, et al. Safety and Long-Term Efficacy of AAV4 Gene Therapy in Patients with RPE65 Leber Congenital Amaurosis. Mol Ther 2018;26(1):256-68.

105. Bennett J, Wellman J, Marshall KA, et al. Safety and durability of effect of contralateral-eye administration of AAV2 gene therapy in patients with childhood-onset blindness caused by RPE65 mutations: a follow-on phase 1 trial. Lancet 2016;388(10045):661-72.

106. Brown MM, Brown GC, Sharma S, et al. Quality of life with visual acuity loss from diabetic retinopathy and age-related macular degeneration. Arch Ophthalmol 2002;120(4):481-4.

107. Gothwal VK, Bagga DK, Rao HL, et al. Is utility-based quality of life in adults affected by glaucoma? Invest Ophthalmol Vis Sci 2014;55(3):1361-9.

Chapter 6

Summary

Inherited retinal diseases encompass a clinically and genetically heterogeneous group of rare disorders, which together account for more than 3 million affected individuals worldwide. Much remains to be elucidated about these disorders with regard to the (molecular) pathogenesis and the large variation in clinical presentation. This knowledge is important to accurately counsel patients and their families, to select patients for upcoming therapies and to evaluate the effects of these novel treatments. The aim of this thesis is to provide a synthesis of all the clinical, genetic and therapeutic information available for a group of inherited retinal diseases entitled retinitis pigmentosa (RP). In addition, the goal is to increase knowledge of three genetic RP subtypes and evaluate the effect of treatment with carbonic anhydrase inhibitors (CAIs) in children with X-linked retinoschisis (XLRS).

Chapter 1 serves to familiarize the reader with the normal retinal anatomy, retinal imaging and molecular genetics. This chapter is also an introduction on inherited retinal diseases and addresses the general clinical characteristics, genetic principles and large heterogeneity.

Chapter 2 provides a detailed overview of the clinical, genetic and therapeutic aspects of non-syndromic RP, as well as the specific features of all genetically defined RP subtypes. This chapter contains a unique atlas that contains images of 75 genetic subtypes that have been published over the years. This information can help the clinician identify the clinical RP entity and better predict the disease course, ultimately providing the patient with the best possible information regarding prognosis and genetic counseling. Additionally, this chapter shows a schematic representation of human photoreceptor cells, the RPE and the interphotoreceptor matrix, and demonstrates the vital processes affected in RP (e.g. the phototransduction cascade, the visual cycle, etc.), as well as the location and function of the proteins involved, thereby revealing high genetic and clinical similarity between RP and other inherited retinal diseases, including Leber congenital amaurosis (LCA) and cone-rod dystrophies. Finally, we discuss current and future therapeutic options such as gene- and cell-based therapies, retinal implants and transplantation. The eventual therapy should be individualized and determined based on the molecular pathogenesis and the extent of the degeneration in the individual patient.

In **Chapter 3** we describe two new genetic associations. **Chapter 3.1** provides additional evidence supporting the hypothesis that variants in the *KIAA1549* gene are associated with autosomal recessive RP. By performing whole exome sequencing we identified homozygous frameshift or missense variants in *KIAA1549* in two families diagnosed with RP. Two isoforms of *KIAA1549* exist, a long and a short isoform. We demonstrated retina-specific expression of the short isoform and provide evidence that these damaging variants positioned in the long transcript may cause RP by reducing the expression of the short retina-specific transcript. Additionally, we showed that KIAA1549 is located in the connecting cilium of the mouse retina,

thereby providing supporting evidence that KIAA1549 might act as an essential photoreceptor protein.

Chapter 3.2 describes the identification of a near exon aberrant RNA splice (NEAR) variant that is present outside the general consensus splice site sequence in *TULP1*. The variant was identified in two siblings with early-onset RP in whom a single pathogenic variant in *TULP1* was found previously. We provide proof of causality for this splice variant by performing an *in vitro* midigene splice assay. This chapter highlights the importance of analysis of noncoding regions beyond the noncanonical splice sites in patients with inherited retinal diseases.

The emphasis in **Chapter 4** is on the phenotypic characteristics of two inherited retinal dystrophy genes. In **Chapter 4.1** we describe the clinical spectrum of diseases caused by pathogenic variants in the *RP1* gene. In this international collaborative study, we included 22 patients with *RP1*-associated retinal dystrophies from 19 families, who were clinically examined in detail. Besides the previously described autosomal recessive and autosomal dominant RP phenotypes, our study provides further evidence that autosomal recessive macular dystrophy and cone-rod dystrophy are also included in the *RP1*-disease spectrum, and could be distinguished based on the clinical findings, inheritance pattern, age of onset and disease course. All patients with autosomal recessive macular dystrophy or cone-rod dystrophy carried a variant with predicted residual function, in combination with a likely deleterious frameshift or nonsense pathogenic variant. The macular involvement in patients with a hypomorphic *RP1* variant suggests that macular function may remain compromised if expression levels of RP1 do not reach adequate levels after treatment with for example gene augmentation therapy. In addition, with the advent of novel therapeutic options, recognition of the entire clinical spectrum associated with *RP1* mutations is essential to aid the selection of patients eligible for treatment, and to evaluate the effect of the treatment provided.

Chapter 4.2 describes a large Dutch family previously diagnosed with benign concentric annular macular dystrophy (BCAMD). Since the peripheral photoreceptors are already involved in early disease stages, we propose to revise the inaccurate, descriptive term BCAMD to *IMPG1*-associated retinitis pigmentosa with relative early macular involvement. We also provide additional evidence on the causal role of the autosomal dominant p.Leu579Pro missense change in *IMPG1* in this family. This enlarges the clinical spectrum of disorders caused by pathogenic variants in *IMPG1* that previously consisted of dominant and recessive forms of vitelliform macular dystrophy. Therefore, the *IMPG1* gene should be added to the list of genes that, when mutated, can cause autosomal dominant forms of RP.

X-linked juvenile retinoschisis (XLRS) is the leading cause of hereditary juvenile macular degeneration in males, with cystic macular lesions as the hallmark feature in the early stage of the disease. Both oral and topical CAIs have been successfully used in the management of these cystic macular lesions. However, the vast majority of previous studies investigated the effect of CAI treatment in adults, despite the fact that this disease often manifests during childhood.

Chapter 7

Therefore, **Chapter 5** evaluates the effect of treatment with CAIs on the best-corrected visual acuity and foveal zone thickness in nine children with XLRS. A reduction of central retinal thickness occurred in more than half of the children treated with CAIs, but only three patients experienced visual improvement over a median treatment interval of 6.8 months. In 80 percent of patients the effect was already visible within 1 month. Therefore, evaluation of treatment effect is possible after only 1 month in the majority of patients. We hypothesize that restoration of the macular architecture with CAI treatment may delay functional retinal loss and may contribute to creating more optimal circumstances for gene therapy.

Finally, **Chapter 6** places the aforementioned results in a broader and future perspective. The general discussion describes the complicated and insufficient nomenclature of retinal dystrophies and attempts to shed light on the large clinical heterogeneity of retinal dystrophies by discussing possible genetic modifiers. In addition, this chapter describes the current challenges and limitations in providing patients with a molecular diagnosis. Lastly, this chapter discusses the main therapeutic approaches that are currently evaluated, as well as their expected potential and ethical challenges.

Samenvatting

Retinale dystrofieën omvatten een klinisch en genetisch heterogene groep van zeldzame erfelijke netvliesaandoeningen, die wereldwijd gezamenlijk meer dan drie miljoen mensen treffen. Er moet nog veel opgehelderd worden over deze ziekten met betrekking tot de (moleculaire) pathogenese en de bijbehorende grote variatie in klinische presentatie. Deze kennis is noodzakelijk om patiënten en hun familieleden nauwkeurig te kunnen begeleiden, de juiste patiënten te selecteren voor aankomende therapieën en de effecten van deze nieuwe behandelopties te evalueren. The doel van dit proefschrift is om een overzicht te geven van alle beschikbare informatie omtrent klinische, genetische en therapeutische aspecten van de groep van erfelijke retinale dystrofieën genaamd retinitis pigmentosa (RP). Daarnaast vergroot dit proefschrift de kennis over drie genetische RP subtypen en wordt het effect van behandeling met koolzuuranhydraseremmers (CAIs) bij kinderen met X-gebonden retinoschisis (XLRS) geëvalueerd.

Hoofdstuk 1 dient om de lezer vertrouwd te maken met de normale anatomie van de retina, retinale beeldvorming en genetica. Dit hoofdstuk is tevens een inleiding in erfelijke retinale dystrofieën en behandelt de algemene klinische kenmerken, genetische principes en de grote heterogeniciteit van deze groep ziektebeelden.

Hoofdstuk 2 geeft een gedetailleerd overzicht van de klinische, genetische en therapeutische aspecten van niet-syndromale RP, evenals de specifieke kenmerken van alle genetisch bevestigde RP subtypes. Dit hoofdstuk bevat een unieke atlas met afbeeldingen van 75 genetische subtypes van RP. Deze kennis kan de oogarts helpen bij het identificeren van het juiste klinische RP subtype en het nauwkeuriger voorspellen van het beloop van de ziekte, om de patiënt uiteindelijk te voorzien van zo accuraat mogelijke kennisoverdracht met betrekking tot de prognose. Daarnaast toont dit hoofdstuk een schematische weergave van menselijke fotoreceptorcellen, het retina pigment epitheel (RPE) en de interfotoreceptormatrix, en toont het de vitale processen die zijn aangetast in RP (bijvoorbeeld de fototransductiecascade, de visuele cyclus etc.), evenals de localisatie en functie van de betrokken eiwitten. Hierbij wordt er een hoge genetische en klinische gelijkenis onthuld tussen RP en andere erfelijke retinale dystrofieën, waaronder Leber congenitale amaurosis (LCA) en kegel-staafdystrofieën. Tot slot bespreken we de huidige en toekomstige therapeutische opties, waaronder gen- en cel-gebaseerde therapieën, retinale implantaten en transplantaties. De uiteindelijk therapie dient te worden gepersonaliseerd en bepaald op basis van de moleculaire pathogenese en mate van degeneratie bij de individuele patiënt.

In **hoofdstuk 3** beschrijven we twee nieuwe genetische associaties. **Hoofdstuk 3.1** levert aanvullend bewijs en ondersteunt de hypothese dat oorzakelijke varianten in het *KIAA1549*-gen geassocieerd zijn met autosomaal recessief RP. Middels exoom sequencing hebben we in twee

271

families vastgesteld dat homozygote frameshift- of missense varianten in *KIAA1549* geassocieerd zijn met RP. Er bestaan twee isovormen van KIAA1549, een lange en een korte isovorm. In deze studie laten we zien dat de korte isovorm tot expressie komt in de retina en illustreren we dat oorzakelijke varianten aanwezig in het lange transcript RP kunnen veroorzaken door de expressie van het korte transcript te beïnvloeden. Bovendien toonden we aan dat KIAA1549 verblijft in het connecting cilium van het muizennetvlies, hetgeen ondersteunt dat KIAA1549 zou kunnen fungeren als een essentieel fotoreceptoreiwit.

Hoofdstuk 3.2 beschrijft de identificatie van een genetische variant gelokaliseerd net buiten de consensus splice site, in een broer en zus met RP bij wie eerder slechts één pathogene variant in *TULP1* was gevonden. Tevens illustreren we de pathogeniciteit van deze splice variant door een *in vitro* midigene splice assay uit te voeren. Dit hoofdstuk benadert het belang van analyse van niet-voor-eiwit-coderende varianten buiten de consensus splice sites in patiënten met een erfelijke retinale dystrofie.

De nadruk in **hoofdstuk 4** ligt op de klinische kenmerken van twee genen die geassocieerd zijn met erfelijke retinale dystrofieën. In **hoofdstuk 4.1** beschrijven we het klinisch spectrum van ziekten veroorzaakt door mutaties in het *RP1* gen. In deze internationale studie hebben we 22 patiënten geïncludeerd met een *RP1*-geassocieerde retinadystrofie afkomstig uit 19 families. Deze patiënten ondergingen een uitgebreid klinisch onderzoek. Naast de eerder beschreven autosomaal recessieve en autosomaal dominante RP-fenotypen bevestigt ons onderzoek dat autosomaal recessieve maculadystrofie en kegel-staafdystrofie ook deel uitmaken van het *RP1*-spectrum en onderscheiden kunnen worden op basis van de klinische bevindingen, het overervingspatroon, de beginleeftijd en het ziektebeloop. Bij alle patiënten met autosomaal recessieve maculadystrofie of kegel-staafdystrofie werd een oorzakelijke genetische variant gevonden met voorspelde restfunctie, in combinatie met een mogelijk schadelijke frameshift of nonsense mutatie. De macula betrokkenheid bij patiënten met een hypomorfe *RP1* variant suggereert dat de functie van de macula nog steeds gevaar loopt als de expressieniveaus van het *RP1* gen niet het juiste niveau bereiken na behandeling met gentherapie. Met de komst van nieuwe therapeutische opties is het bovendien essentieel om het volledige klinische spectrum dat geassocieerd is met *RP1*-mutaties te herkennen om de patiënten te kunnen selecteren die in aanmerking komen voor therapie en het effect van de geboden behandeling te evalueren.

Hoofdstuk 4.2 beschrijft een grote Nederlandse familie die in het verleden is gediagnosticeerd met benigne concentrische annulaire maculadystrofie (BCAMD). Aangezien de fotoreceptoren bij deze patiënten al vroeg in het ziektebeeld aangedaan zijn, stellen we voor om deze onjuiste en beschrijvende term BCAMD te herzien en te veranderen naar RP met relatief vroege macula betrokkenheid. Daarnaast levert dit hoofdstuk aanvullend bewijsmateriaal voor een causale rol van de autosomaal dominante p.Leu579Pro missense verandering in het *IMPG1* gen in deze familie. Dit vergroot het klinisch spectrum van aandoeningen veroorzaakt door een pathogene variant in het *IMPG1* gen, een spectrum dat voorheen enkel bestond uit autosomaal dominant

en recessieve vormen van vitelliforme maculadystrofie. Tevens dient *IMPG1* te worden toegevoegd aan de lijst met genen die, wanneer gemuteerd, autosomaal dominanten vormen van RP kunnen veroorzaken.

X-gebonden juveniele retinoschisis (XLRS) is de belangrijkste oorzaak van erfelijke juveniele maculadegeneratie bij mannen, met cysteuze afwijkingen in de macula als karakteristiek kenmerk in een vroeg stadium van de ziekte. Zowel orale als topicale CAIs zijn met succes toegepast bij het behandelen van deze cysteuze afwijkingen. De overgrote meerderheid van de eerdere studies onderzocht echter het effect van CAI-behandeling bij volwassenen, ondanks het feit dat deze ziekte zich vaak al tijdens de kindertijd manifesteert. **Hoofdstuk 5** evalueert daarom het effect van behandeling met CAIs op de gezichtsscherpte en de dikte van de foveale zone bij negen kinderen met XLRS. Een reductie van de centrale retinadikte trad op bij meer dan de helft van de kinderen die met CAIs werden behandeld, maar slechts drie patiënten hadden een visuele verbetering na een mediane behandelduur van 6,8 maanden. Bij 80% van de patiënten die reageeden op de behandeling was dit effect al zichtbaar binnen 1 maand. Evaluatie van het behandeleffect is daarom al mogelijk na slechts 1 maand in de meerderheid van de patiënten. We suggereren dat herstel van de architectuur van de macula door middel van CAI-behandeling het functieverlies van het netvlies mogelijk kan vertragen en kan bijdragen aan het optimaliseren van de omstandigheden voor genetische therapie.

Tot slot worden in **hoofdstuk 6** de bovengenoemde resultaten in een bredere context geplaatst. De algemene discussie beschrijft de gecompliceerde en incomplete nomenclatuur van retinale dystrofieën en probeert de grote klinische heterogeniteit van retinale dystrofieën te verklaren door mogelijke genetische modifiers aan te dragen. Daarnaast beschrijft dit hoofdstuk de huidige beperkingen en uitdagingen bij het stellen van een genetische diagnose bij patiënten. De belangrijkste toekomstige therapeutische benaderingen worden geëvalueerd, evenals hun verwachte potentiële en ethische uitdagingen.

Chapter 7

Data management page

Type of data	Subject to privacy (yes/no)	Way of anonymization	Storage
Informed consent of patients included in the RD5000 database*	Yes	A study-ID number has been assigned to all patients and the key is stored in a password protected file	Written informed consents of patients included at the Ophthalmology department in Nijmegen are stored in a locked archive. The key file can be found on the Ophthalmology H-drive: H:\Onderzoek\6 Key Files, and is stewarded by the database manager.
Clinical data of the patients included in the RD5000 database*	Yes	A study-ID number has been assigned to all patients and data is stored by study-ID	The clinical data can be found on Ophthalmology H-drive: H:\Onderzoek\1 Personal folders\Sanne Verbakel\Projecten The data from Chapter 3.1, 3.2 and 4.2 is also stored on the Genetics I-drive: I:\GR Theme groups\05 PI Group Frans Cremers\06 Manuscripts
DNA of patients included in the RD5000 database*	Yes	A DNA number has been assigned to each patient by the diagnostics facility of the Department of Human Genetics	The key is stored in the helix database and is accessible by clinicians and members of the cell culture facility. DNA samples are stored at the department of Human Genetics. Contact person for the DNA samples is Saskia van der Velde-Visser; Saskia.vanderVelde@radboudumc.nl
Genotyping and exome sequencing data	No	Data has already been anonymized	Genotype and exome sequencing data can be found in the following folder on the Human Genetics T-drive: T:\PIgroup-Frans-Cremers\NAS\03 NGSdata\Exome NGS\ or in the project specific folder on the Ophthalmology H-drive: H:\Onderzoek\1 Personal folders\Sanne Verbakel\Projecten
Files for publications presented in this thesis	No	Not applicable	All files can be found on the H-drive of Ophthalmology: H:\Onderzoek\1 Personal folders\Sanne Verbakel\Projecten

* All patients included in this thesis are included in the RD5000 database.

List of publications

IMPG1 variant causes autosomal dominant retinitis pigmentosa; revision of the benign concentric annular macular dystrophy phenotype.
Verbakel SK, Hoyng CB, Venselaar H, Klevering BJ, Roosing S.
Submitted

The identification of a RNA splice variant in TULP1 in two siblings with early-onset photoreceptor dystrophy.
Verbakel SK, Fadaie Z, Klevering BJ, van Genderen MM, Feenstra I, Cremers FPM, Hoyng CB, Roosing S.
Mol Genet Genomic Med. 2019;7:e660.

Macular Dystrophy and Cone-Rod Dystrophy Caused by Mutations in the RP1 Gene: Extending the RP1 Disease Spectrum.
Verbakel SK, van Huet RAC, den Hollander AI, Geerlings MJ, Kersten E, Klevering BJ, Klaver CCW, Plomp AS, Wesseling NL, Bergen AAB, Nikopoulos K, Rivola C, Ikeda Y, Sonoda KH, Wada Y, Boon CJF, Nakazawa T, Hoyng CB, Nishiguchi KM.
Invest Ophthalmol Vis Sci. 2019;60(4):1192-1203.

Homozygous variants in KIAA1549, encoding a ciliary protein, are associated with autosomal recessive retinitis pigmentosa.
de Bruijn SE, Verbakel SK, de Vrieze E, Kremer H, Cremers FPM, Hoyng CB, van den Born LI, Roosing S.
J Med Genet. 2018;55(10):705-712.

Non-syndromic retinitis pigmentosa.
Verbakel SK, van Huet RAC, Boon CJF, den Hollander AI, Collin RWJ, Klaver CCW, Hoyng CB, Roepman R, Klevering BJ.
Prog Retin Eye Res. 2018;66:157-186.

Carbonic Anhydrase Inhibitors for the Treatment of Cystic Macular Lesions in Children With X-Linked Juvenile Retinoschisis.
Verbakel SK, van de Ven JP, Le Blanc LM, Groenewoud JM, de Jong EK, Klevering BJ, Hoyng CB.
Invest Ophthalmol Vis Sci. 2016;57(13):5143-5147.

Analysis of Risk Alleles and Complement Activation Levels in Familial and Non-Familial Age-Related Macular Degeneration.
Saksens NT, Lechanteur YT, Verbakel SK, Groenewoud JM, Daha MR, Schick T, Fauser S, Boon CJF, Hoyng CB, den Hollander AI.
PLoS One. 2016;11(6):e0144367

Chapter 7

Curriculum Vitae

Sanne Kirsten Verbakel was born on the seventh of March 1991 in Tilburg, the Netherlands. She completed secondary school at the 'Theresialyceum' in Tilburg. In 2009, she started her medical studies at the Radboud University Nijmegen, where she graduated in November 2015. Her interest in Ophthalmology developed after an elective course at the department of Ophthalmology during her medical studies, and was further amplified after her research internship at the Radboud university medical center on familial age-related macular degeneration.

After finishing her medical studies, she continued research in a PhD project on the clinical and genetic aspects of inherited retinal dystrophies at the Department of Ophthalmology at the Radboud university medical center in Nijmegen, which resulted in this thesis.

In June 2019, she started a residency in Ophthalmology in the same institute.

Dankwoord

Na enkele jaren van hard werken is het dan tijd om dit laatste, maar zeker niet onbelangrijke, hoofdstuk te schrijven. Mijn hele promotietraject zou ik willen vergelijken met een hike in de bergen; een route met onderweg een aantal flinke beklimmingen waarbij het einde lange tijd niet in zicht is en je jezelf soms afvraagt waar je aan begonnen bent, maar eenmaal aangekomen op de top is het uitzicht fantastisch en geeft het een voldaan gevoel! Deze tocht was echter niet gelukt zonder het juiste materiaal, de nodige duwtjes in de rug en afleiding onderweg. Ik wil dan ook van de gelegenheid gebruik maken om hieronder al deze mensen te bedanken die het voor mij mogelijk hebben gemaakt om dit proefschrift te voltooien.

Om te beginnen de vele patiënten want zonder hun inzet en toestemming was er geen wetenschappelijk onderzoek mogelijk.

Geachte professor Klevering, beste Jeroen, jouw deur stond altijd open. Bewonderingswaardig hoe jij altijd precies voor ogen had wat de boodschap van een artikel moest zijn en tot in de details meedacht over hoe dat doel bereikt moest worden. Jouw suggesties hebben de artikelen naar een hoger level getild. Ik wil je dan ook bedanken voor alle moeite en mails op de meest onmogelijke tijdstippen.

Geachte professor Hoyng, beste Carel, bedankt dat je me, ondanks mijn Brabantse accent, vertrouwen hebt gegeven en ik deel uit mocht maken van jouw onderzoeksteam. Jouw out of the box ideeën en liefde voor onderzoek zijn een enorme inspiratie.

Geachte dr. Van Huet, beste Ramon, wat was het fijn om terug te kunnen vallen op iemand die het promotieproces nog redelijk vers in het geheugen heeft zitten. Jouw proefschrift was de aanleiding voor het mooie review. Bedankt voor je openheid, enthousiasme en de avonden dat jij mij met een kopje thee en chocolade op het werk vergezeld hebt, want daardoor had ik toch een stuk minder zelfmedelijden.

Geachte dr. Roosing, beste Susanne, pas in de laatste fase ben jij officieel lid geworden van mijn promotieteam, maar al veel eerder was je betrokken en heb jij mij de basis van de genetica bijgebracht. Je hebt er mede voor gezorgd dat ik de genetica steeds interessanter ben gaan vinden en ik zelfs dagelijks aan 'next generation sequencing' denk bij het passeren van de letters 'NGS' die met graffiti geschreven staan op het Landhoofd bij de spoorbrug op weg naar Lent.

Lieve Vivian en Merel, wat ben ik blij dat jullie mijn paranimfen willen zijn! Vivian, wij zijn op precies dezelfde datum gestart aan ons promotietraject. Het was fijn om een maatje te hebben tijdens deze periode! Ik wil je dan ook heel erg bedanken voor je gezelligheid, luisterende oor en alle mooie herinneringen aan onze reizen naar het ARVO congres in Seattle en Baltimore en de aansluitende tripjes naar Canada en New York.

Chapter 7

Merel, wij kennen elkaar al vanaf het begin van de studie geneeskunde maar ook tijdens mijn promotie bleef jij mijn trouwe hardloop en tennismaatje. Je staat altijd voor iedereen klaar. Bedankt voor alle afleiding en gezelligheid!

Graag wil ik bovendien mijn dank uitspreken naar alle coauteurs die betrokken zijn geweest bij de verschillende artikelen opgenomen in dit proefschrift. In het bijzonder noem ik hierbij professor Anneke den Hollander, professor Caroline Klaver, Hans Groenewoud, John van de Ven, Linda Le Blanc, professor Ronald Roepman, Rob Collin, en professor Camiel Boon.
Dear dr. Nishiguchi, dear Koji, despite the large time difference between Japan and the Netherlands I don't know anyone who responds faster to emails. Thank you for the excellent collaboration.

Collega's van de afdeling Genetica:
Geachte professor Cremers, beste Frans. Bedankt dat ik ruim 2 maanden mee mocht lopen op jouw afdeling om een beter beeld te krijgen van de speurtocht naar nieuwe genetische varianten.
Dear Zeinab, Suzanne, Mubeen, Galuh, Bjorn and Saskia. Thank you for your time and patience while teaching me to perform a PCR reaction or make an Agarose gel for electrophoresis, answering my questions or run certain tests.
Beste Dorien, Lonneke, Wendy en Anneke, door jullie heb ik inzicht gekregen in het proces voorafgaand aan de DNA uitslag die uiteindelijk bij de (oog)arts aankomt. Ik wil jullie bedanken voor het delen van jullie kijk op de soms ethische problemen die voortkomen uit genetisch onderzoek en de interessante discussies tijdens het maandelijkse multidisciplinaire overleg.

Geachte dr. Eggink, beste Cathrien, jij hebt mij er tijdens mijn onderzoeksperiode aan herinnert dat het oog uit meer onderdelen bestaat dan alleen de retina. Het was een gezellige afleiding om samen de patiënten voor de serumdruppelstudie te onderzoeken.

Het zien van alle onderzoekspatiënten was niet mogelijk zonder hulp van alle dames en heren van de administratie, de verpleegpost, het trialcentrum en de optometrie. Jullie ben ik dan ook veel dank verschuldigd. In het bijzonder wil ik Berna, Francis, Laura en Jacqueline bedanken voor het inplannen van alle, soms onmogelijke, afspraken en natuurlijk de gezelligheid op het stafsecretariaat. Anne en Maria bedanken voor het plannen van alle patiënten van de serumdruppelstudie. Mara en Iris, dankjewel voor het vele werk dat jullie verzet hebben voor de RD5000 database en Roel bedankt voor alle hulp die je tijdens je onderzoeksstage hebt geboden.

DOPS2017 organisatie (Wouter, Elon en Vivian); Leiden en Nijmegen vormde een goed team en we hebben samen een geslaagde editie van DOPS neergezet! Het was erg leuk om dit met jullie te organiseren en ik zou het zo weer over doen, hoewel dan misschien gewoon dineren met het licht aan.

Constantin, Laura, Maartje, Nathalie, Stanley, Roos, Vivian, Dyon, Tom, Esmée, Anita, Patty, Birgit, Timo, Bart, Freerk, Susette, Erkin, en Sarah, natuurlijk wil ik jullie als collega promovendi enorm bedanken voor de leuke tijd! Wat is het fijn om even met iemand te kunnen sparren als je vastloopt.

Stanley bedankt voor de goede start van de dag met onze squashpartijen en je hulp bij technische problemen. Leuk dat jij nu officieel mijn 'mentor' bent tijdens de opleiding. Dyon, ook wij zijn slechts enkele maanden na elkaar gestart. Bedankt voor alle gezellige gesprekken en het feit dat je nooit te beroerd bent om iemand te helpen. Esmée bedankt dat je mij wat meer tijd voor mijn projecten gaf door de overname van de werkzaamheden omtrent de RD5000 database en DNA diagnostiek. Maar bovenal wil ik jullie bedanken voor de gezelligheid en mooie herinneringen, van de gesprekken tijdens de pauzes tot de spelletjesavonden, culinaire hoogstandjes (lees frikandellentaart), congressen en onvergetelijke reizen naar Vancouver en New York achteraf!

Mijn bureau op de promovendikamer heb ik ondertussen ingeruild voor de polikliniek. Alle AIOS, stafartsen, verpleegkundigen, orthoptisten, optometristen, OK-medewerkers, en medewerken van het planbureau en de administratie wil ik bedanken dat ik me meteen thuis voelde en we gaan er een mooie tijd van maken samen!

Lieve Theresianen, onze vriendschap gaat helemaal terug naar de middelbare school. Hoewel we tegenwoordig door heel Nederland wonen en even spontaan iets afspreken niet zo makkelijk meer gaat, waardeer ik onze jaarlijkse BBQ's, kerstdiners en dagjes uit des te meer! Bedankt voor alle afleiding en ontspanning de afgelopen jaren en hopelijk kunnen we deze traditie nog jaren voortzetten.

Lieve Merel, Joëlle, Nadieh, Annemieke en Suzanne, dank dat jullie al vanaf het eerste jaar van de studie mijn vriendinnen zijn, bedankt voor alle mooie herinneringen aan onze etentjes, dagjes uit maar ook een luisterend indien nodig op z'n tijd. Ons jaarlijkse weekendje weg houden we er zeker in!

Lieve Flabberdepoepsies (wie heeft deze naam ook alweer bedacht?!), bedankt voor alle gezelligheid, leuke feestjes en vooral het feit dat jullie er altijd voor Brian zijn als ik weer eens moet werken.

Lieve Carla en Joep, al meer dan 10 jaar kom ik bij jullie over de vloer. Vanaf moment één voelde ik me direct welkom. Bedankt dat jullie deur altijd openstaat!

Lieve opa's en oma's, helaas kan opa Henk dit eindresultaat niet meer meemaken, maar ik wil jullie bedanken voor het feit dat jullie altijd geïnteresseerd zijn en me vol trots volgen.

Lieve Jeroen en Esmée, Jeroen wij zijn beiden niet van die praters (daar hebben we Esmée voor), maar ik ga proberen wat meer tijd vrij te maken om samen leuke dingen te doen, om te beginnen een wintersport met ons vieren!

Lieve Papa en Mama, jullie staan altijd voor me klaar. Ik kan jullie niet genoeg bedanken voor alle kansen die jullie me hebben gegeven, jullie onvoorwaardelijke steun en alle leuke momenten samen met als een van de hoogtepunten toch wel onze recente avonturen in Afrika.

Lieve Brian, last maar zeker niet least, bedankt dat je voor mij naar Lent verhuisd bent, me steunde als ik weer eens ging werken in plaats van gezellig iets samen doen, maar me ook afremde als het nodig was. Zonder jouw support was dit nooit gelukt!